

Long-term radiocaesium cycling in forest ecosystems

Thawatchai Itthipoonthanakorn

Agricultural and Environmental Sciences

School of Biosciences

Thesis submitted to the University of Nottingham

For the degree of Doctor of Philosophy

September 2017

Acknowledgement

I would like to thank George Shaw and Neil Crout for their superb supervision throughout the term of my PhD study. Thanks are due to John Corrie, Saul Vazquez Reina, Laura Holt and James Verran for their technical assistance. Thanks also to Maria Izquierdo for helping during the field trips. I would like to acknowledge Scot Young for ICP-MS analysis, Sergey Gaschak (Chernobyl Centre for Nuclear Safety, Ukraine) for managing the field trip at Chernobyl and Sandie Dann (Department of Chemistry, Loughborough University) for clay mineral analysis. I am also would like to thank UK Forestry Commission and Wat Chan Royal Project Development Center for granting entry to sampling in the forest sites.

In terms of non-academic support I would like to express my gratitude to my family for their support, encouragement and understanding.

Finally, I would like to thank the Thai government and Office of Atoms for Peace for financial assistance provided during my PhD study.

ABSTRACT

This study focused on the long-term cycling of radiocaesium in pine forests at Boundary Plantation (Sherwood Forest, England), Chernobyl (Ukraine) and Wat Ban Chan in northern Thailand, each of which received markedly different levels of contamination due to radiocaesium deposition from the atmosphere under different circumstances. Systematic studies were made of stable and radiocaesium, potassium and rubidium in soil horizons, tree stems, needles and throughfall (the latter only at Boundary Plantation). Measurements of total concentrations were complemented with determinations of exchangeable fractions as well as the isotopic exchangeability of radio- and stable caesium. Data from Boundary Plantation and Wat Ban Chan were used to test, validate and calibrate the RIFE (Radionuclides in Forest Ecosystems) model for long-term forecasts of radiocaesium behaviour in forest ecosystems. Finally, modelling of ^{137}Cs migration in forest soils was carried out to describe the relationship between the depth of the forest soil profile and the year of litterfall, to better understand the migration of fallout ^{137}Cs.

Boundary Plantation, a forest of semi-natural Corsican pine (*Pinus nigra*), receives chronic atmospheric fallout from nuclear weapons tests in the 1960s. Forest samples were collected every three months from June 2014 to March 2015 at a 24 randomly located sampling sites. The forest soil has a well-developed surface organic horizon while the mineral soil is composed almost entirely of quartz with no identifiable clay minerals. About 65% of nuclear-weapons fallout ^{137}Cs is distributed within the organic layer (upper 9 cm) and maximum of vertical distribution is 12.9% at 8 cm depth. The accumulation of well-decomposed organic matter in the middle of the organic layer is strongly related to the migration of ^{137}Cs in the soil; modelling describes the relationship between the depth of organic matter accumulating in the upper part of the forest soil profile and the year of litterfall indicates that fallout ^{137}Cs deposited in 1963 has migrated in tandem with organic matter at the same rate of migration from the surface. Soil pH also appears to play a key role in controlling the mobility of Cs isotopes, with the most acidic layers within the soil organic horizons holding the highest ^{137}Cs activity concentrations and having the highest exchangeable ^{133}Cs concentrations.

Wat Ban Chan in Thailand is a native tropical forest of *Pinus kesiya* (or Three-needled pine) which received chronic distribution of atmospheric fallout from nuclear weapons tests in the 1960s. Samples were taken from this site in late February 2016 at six randomly located co-ordinates. The forest soil is typical of similar forest soils in the tropical zone. The organic matter, even at the surface, is much less

abundant than in temperate forest soils while the mineral soil is composed almost entirely of quartz with no identifiable clay minerals. About 84% of nuclear weapons fallout ^{137}Cs is distributed within the upper 3 cm and the maximal distribution is 37.6% at 2 cm depth. Even though the organic matter content in the upper 2 – 3 cm of the soil profile is low it probably still plays an important role in the vertical distribution of ^{137}Cs. The variation of soil pH throughout the upper 13 cm of the soil profile is less than 1 pH unit and thus is unlikely to influence the vertical distributions of ^{137}Cs and ^{133}Cs in the soil.

K and Rb are strong competitors of Cs during cycling within the forest ecosystems at Boundary Plantation and Wat Ban Chan. K is present in the exchangeable fraction in soil at much higher concentration than Rb and especially Cs. The overall degree of translocation from soil to needles is in the order of ^{39}K > ^{85}Rb > ^{133}Cs.

Forest sites surrounding the Chernobyl nuclear power plant in Ukraine received acute and localised deposition of nuclear fallout during the Chernobyl reactor accident in April and May 1986. Samples were taken from four Scots pine (*Pinus sylvestris L.*) plantations close to Chernobyl in early September 2015. Tree cores were taken at all four sites (Red Forest, North Trace, Kopachi and Bourakovka). Soil cores were also collected at Kopachi where ^{137}Cs behaviour appears similar to ^{133}Cs as indicated by T_{ag} values of ^{133}Cs and ^{137}Cs.

Scots pine at the Red Forest and the North Trace sites were exposed to extremely high and acute radiation doses (more than 5.0 mGy/h) in the very early stages of the Chernobyl accident. The surviving Scots pine trees sampled in 2015 show a transient decrease in growth rate for several years after 1986, and then show signs of accelerated growth possibly due to a reduction in competition from surrounding trees (an effect known to foresters as 'growth release').

Calculations of present day ^{137}Cs distributions using the RIFE model for Boundary Plantation and Wat Ban Chan calibrated with inter-compartmental half-times from seven European ('SEMINAT') forest sites proved surprisingly accurate, although the model consistently under- and over-predicted the percentage of the total ^{137}Cs inventories retained in the organic and mineral soil layers, respectively.

Site-specific calibrations of the RIFE model were made using newly acquired data for nuclear weapons ^{137}Cs deposited in 1963 at Boundary Plantation and Wat Ban Chan. It is considered that these calibrations are more applicable for long-term predictions of radiocaesium cycling in forests than the SEMINAT calibrations which were based on measurements made less than 10 years after the Chernobyl accident in 1986.

Finally, measured unsupported ^{210}Pb activities in forest soil profiles were modelled to describe the relationship between the accumulating depth of organic matter in the forest soil profile and the year of litterfall, to improve understanding of the migration of fallout ^{137}Cs at Boundary Plantation (Sherwood Forest, UK) and in the relatively organic-poor soil at Wat Ban Chan in Thailand.

CONTENT

Chapter 1: Introduction **1**

1.1 General aims of the study 2

1.2 Literature review 2

1.2.1 Source of global nuclear-fallout 2

1.2.2 Source of fallout caesium 4

1.2.3 Transport of radiocaesium from forests to humans 5

1.2.4 Radiocaesium in local fallout within forest soil 9

1.2.5 Factors influencing radiocaesium behaviour in forest ecosystems 9

1.2.6 Correlation of ^{137}Cs and ^{133}Cs distributions in forest ecosystems 13

1.2.7 Distribution of radiocaesium in tropical forests 14

1.2.8 Prediction of long-term migration of ^{137}Cs in forest ecosystems 15

1.3 Specific objectives of the study 22

1.3.1 Boundary Plantation and Wat Ban Chan 22

1.3.2 Chernobyl nearby forest 22

1.3.3 Modelling work 22

Chapter 2: Materials and methods **23**

2.1 Research locations 23

2.2 Sampling methods 23

2.3 Preparation of samples 25

2.4 Analysis of samples 26

2.4.1 Organic matter content of soil samples 26

2.4.2 Soil pH measurement 27

2.4.3 Mineralogy of soil 27

2.4.4 Determination of total concentrations of stable caesium (^{133}Cs) and its competitive elements 28

2.4.5 Determination of exchangeable (available) concentrations of stable caesium (^{133}Cs) and its competitive nutrients in soil samples 29

2.4.6 Determination of ^{137}Cs, ^{40}K and ^{210}Pb 30

2.4.7 Measuring annual tree growth ring width 37

2.4.8 Isotopic exchange of caesium 38

Chapter 3: Boundary Plantation, Sherwood Forest 39

3.1 Introduction 39

3.1.1 Objectives 39

3.1.2 Sample collection sites 39

3.2 Results 42

3.2.1 Soil properties 42

3.2.2 Vertical distributions of ^{133}Cs, ^{39}K, ^{85}Rb and ^{137}Cs in forest soil 48

3.2.3 Exchangeable fractions of ^{133}Cs, ^{39}K and ^{85}Rb 56

3.2.4 Correlation of forest soil properties with ^{133}Cs, ^{39}K, ^{85}Rb and ^{137}Cs in the soil profile 58

3.2.5 Correlation between fractions of ^{133}Cs and ^{137}Cs within forest soil 71

3.2.6 Isotopic exchange of ^{133}Cs and ^{134}Cs 75

3.2.7 Bio-availabilities of ^{133}Cs, ^{39}K and ^{85}Rb in above-ground compartments 78

3.2.8 Competition between ^{133}Cs, ^{39}K and ^{85}Rb in recirculation processes within forest ecosystems 81

3.3 Discussion 87

3.4 Conclusions 94

Chapter 4: Chernobyl forest **96**

4.1 Introduction 96

4.1.1 Objectives 96

4.1.2 Sampling locations 96

4.2 Results 99

4.2.1 Vertical distribution of ^{137}Cs within Chernobyl forest soil 99

4.2.2 Distribution of ^{137}Cs in Scots pine 101

4.2.3 Distribution of ^{137}Cs in forest inventory 103

4.2.4 Impact of acute high dose radiation on the growth of Scots pine 105

4.3 discussion 107

Comparison of findings of Kopachi to Boundary Plantation 108

4.4 Conclusions 110

Chapter 5: Wat Ban Chan forest, Thailand **111**

5.1 Introduction 111

5.1.1 Objectives 111

5.1.2 Sampling locations 112

5.2 Results 114

5.2.1 Soil properties 114

5.2.2 Vertical distribution of total of stable caesium (^{133}Cs), potassium (^{39}K) and rubidium (^{85}Rb) 118

5.2.3 Exchangeable fractions of ^{133}Cs, ^{39}K and ^{85}Rb 126

5.2.4 Correlations of forest soil properties with ^{133}Cs, ^{39}K, ^{85}Rb and ^{137}Cs in the soil cores 128

5.2.5 Correlation between fractions of ^{133}Cs and ^{137}Cs within forest soil 140

5.2.6 Isotopic exchange of ^{133}Cs and ^{134}Cs 143

5.2.7 Accumulation of ^{133}Cs, ^{39}K and ^{85}Rb in above-ground biological compartments 146

5.2.8 Comparison of ^{133}Cs, ^{39}K and ^{85}Rb in recirculation processes within forest ecosystems 149

5.3 Discussion 154

Comparison of findings of Wat Ban Chan to Boundary Plantation 157

5.4 Conclusions 158

Chapter 6: Validation and calibration of long-term predictions using the RIFE model 160

6.1 Objectives 160

6.2 RIFE1 model 160

6.3 Parameters used for RIFE model calculations 162

6.3.1 Density of standing biomass calculation 162

6.3.2 Initial deposition of ^{137}Cs 167

6.4 Validation of The RIFE model 170

6.4.1 Boundary Plantation 175

6.4.2 Wat Ban Chan 180

6.5 Calibration of RIFE model 184

6.5.1 Boundary Plantation 184

6.5.2 Wat Ban Chan 187

6.6 Conclusions 189

Chapter 7: Modelling ^{137}Cs migration in forest soils 191

7.1 Application of ^{210}Pb dating technique 191

7.2 Concept of modelling 193

7.3 Model description 195

7.3.1 Adjusting depth of soil due to organic decomposition 195

7.3.2 Input of ^{137}Cs and ^{210}Pb 195

7.3.3 Binning annual activities of ^{137}Cs and ^{210}Pb into soil profile 196

7.4 Model parameterisation 200

7.5 Model Results 201

7.6 Discussion 206

7.7 Conclusion 207

Chapter 8: General Conclusions **209**

Future studies **212**

Annex 1 Comparison of findings of boundary plantation, kopachi and wat ban chan **213**

Annex 2 Model script of ^{137}Cs migration in forest soils **217**

References **221**

CHAPTER 1: INTRODUCTION

Forests are important receptors of atmospheric pollutants, including fallout from nuclear explosions and nuclear facility accidents (Bunzl and Kracke, 1988). Major radioactive contamination of forest ecosystems occurred after the Kyshtym accident (1957), during the era of atmospheric nuclear weapons testing which peaked in 1962, and following the accidents at the Chernobyl and Fukushima nuclear power plants in 1986 and 2011, respectively (IAEA, 2013). The area designated as the Chernobyl Exclusion Zone comprised approximately 40% forest at the time of the accident (Shaw, 2007). In the case of the Fukushima accident, the majority of the Fukushima prefecture is covered with forest which is currently contaminated with ^{137}Cs (Hashimoto et al., 2012).

Radionuclides in the atmosphere are initially intercepted by tree canopies but rapidly move to the forest floor where they migrate to the organic and mineral layers of the forest soil. At the same time, they are transferred to tree tissues and a range of edible and non-edible forest products. Human exposure to radionuclides in forests is possible at all stages of biogeochemical recycling following the initial deposition. ^{137}Cs is among the most important dose-forming radionuclides in forests due to its biogeochemical behaviour and its long (~30 year) physical half-life.

Predictive models are needed to quantify the radiation dose which humans receive from forest ecosystem pathways as well as to explore and evaluate any proposed remedial and abatement strategies. A number of existing models have been developed to estimate the migration of radionuclide contamination in forests. The results of the IAEA's BIOMASS Forest Working Group showed large conceptual discrepancies between models developed in response to the Chernobyl accident, associated with high uncertainty for predictions of radio-caesium behaviour after 1986 (Shaw et al., 2005). Very few of these models have been rigorously tested against independent site data over the long term (Shaw et al., 2005).

The RIFE model (Radionuclides in Forest Ecosystems) was one of the models developed to forecast radiocaesium contamination in forest ecosystems following the Chernobyl accident (Shaw and Belli, 1999). It has been calibrated using data obtained in several European countries up to 1996 and has recently been

used to make predictions of radiocaesium dynamics in forests of the Fukushima prefecture from 2011 to 2031 (Hashimoto et al., 2013). However, to have greater predictive reliability models such as RIFE need to be validated against longer-term data.

1.1 GENERAL AIMS OF THE STUDY

The research presented in this thesis aims to provide data to improve our understanding of the long-term cycling of radiocaesium in forest ecosystems. The data can be used to develop and validate models such as RIFE in order to make forecasts of radiocaesium behaviour over 50 or more years following a contamination event. As well as seeking data relevant to northern hemisphere coniferous forests it is also important to obtain data for tropical forests in countries such as Thailand. Southeast Asia received less atmospheric fallout than Europe during the peak period of nuclear weapons testing in the early 1960s. However, countries such as Thailand and Vietnam are developing civil nuclear power programmes and are in need of assessment capabilities for potential nuclear releases in the future.

To achieve the broad aim of this thesis, systematic studies have been made of stable and radiocaesium, and competitive elements, in soil horizons, tree stems and needles in both temperate and tropical pine forests. Measurements of total concentrations have been complemented with determinations of exchangeable fractions as well as the isotopic exchangeability of radio- and stable caesium.

1.2 LITERATURE REVIEW

1.2.1 Source of global nuclear-fallout

Nuclear fallout is residual radioactive dust that is entered into the atmosphere following nuclear weapon explosions and nuclear accidents which may involve non-nuclear explosions. Following explosions involving nuclear materials, radioactive aerosols are dispersed into the atmosphere and remain suspended for days, weeks or months depending on the magnitude of the explosion and prevailing climatic conditions. Radionuclides such as ^{137}Cs, ^{90}Sr, ^{131}I and ^{241}Am are produced by fission and activation reactions during nuclear explosions and

can condense onto suspended aerosol particles which are distributed into the Stratosphere up to several thousand kilometres downwind. Up to the present day, several significant sources of nuclear fallout have been distributed in the world's atmosphere due to the following major events.

1.2.1.1 Nuclear accidents

- *Kyshtym accident*

The Kyshtym accident occurred in 1957 at a plutonium production facility in the former Soviet Union and resulted in the large scale contamination of part of the Ural Mountains, near Chelyabinsk. About 74 PBq of radioactive substances were released into the atmosphere following a chemical explosion in a waste storage pond (Karavaeva et al., 1994). Approximately 20 % of the contaminated area surrounding the accident site was forested. Death of vegetation up to 3-4 years after initial contamination was evident in areas which received greater than 18 MBq m^{-2} and some of the earliest observed biological impacts were defects in pine growth in 1958 (NRPA, 2007).

- *Chernobyl accident*

The Chernobyl accident occurred on 26th April 1986 as a result of a steam explosion at a nuclear power plant in the north of Ukraine. The radioactivity released was at least 100 times more than was released by the atomic bombs in Hiroshima and Nagasaki. Around 8 x 10^{16} Bq of ^{137}Cs deposited in Europe resulting in 6% of the continental area being contaminated with more than 20 kBq m^{-2} ^{137}Cs (IAEA, 1996). Moreover, within a 30 km radius of the reactor the so-called 'exclusion zone' received very high level contamination with reactor fuel particles or 'hot particles' of uranium oxide and other condensed particles (Chesser et al., 2004; Shaw, 2007).

About 45% of the area surrounding the Chernobyl nuclear power plant is forest which has been contaminated with various radionuclides after the accident but the majority of ^{137}Cs is still found to be distributed within the surface organic (AoF and AoH) soil layers (Shaw, 2007).

- *Fukushima Daiichi accident*

On 11th March 2011 an earthquake of magnitude 9 (the 'Great East Japan Earthquake') happened off the east coast of Japan resulting in a catastrophic

tsunami across the Fukushima and Miyagi Prefectures. The Fukushima Daiichi Nuclear Power Plant, situated on the Pacific coast of Japan, was inundated with sea water which ultimately led to loss of reactor and waste cooling and a series of hydrogen explosions. Consequently, radionuclides including ^{131}I, ^{134}Cs and ^{137}Cs were released into the sea and the atmosphere. Extremely low, but detectable, levels of radioactivity were dispersed as far away as Europe and North America (IAEA, 2015).

Nuclear fallout from the Fukushima Daiichi accident became widely deposited on forests which cover about 70% of the Fukushima prefecture. Eighty percent of accident-generated fallout in the contaminated area is associated with either agriculture or forests (Sawai et al., 2015).

1.2.1.2 Testing of nuclear weapons in the atmosphere

The atmospheric tests of nuclear weapons that continued from 1945 to 1980 were the most significant man-made source of radiation exposure of the world's population. The average annual effective dose of the world population reached a peak of 110 micro Sieverts in 1963 and has since reduce to approximately 5 - 6 micro Sieverts in 1999. The average annual dose in the northern hemisphere, where the majority of testing took place, was 10% higher than in the southern hemisphere (UNSCEAR, 2000).

1.2.2 Source of fallout caesium

Caesium is a volatile element which, following explosions involving nuclear materials, can be dispersed in the atmosphere up to several thousand kilometres from the source, depending on meteorological conditions and the effective height at which it is ejected into the atmosphere (UNSCEAR, 2000).

^{133}Cs is the stable isotope which occurs naturally in soils at a global average concentration of approximately 4 mg kg^{-1} (Bowen, 1979; FOREGS, 2005). It is mainly associated with mineral soil and additional ^{133}Cs from atmospheric deposition is negligible (Yoshida et al., 2002). Radiocaesium fallout can be made up of ^{137}Cs, ^{135}Cs and ^{134}Cs depending on the source. ^{137}Cs and ^{135}Cs are fission products generated by the decay of fission-produced ^{137}I and ^{135}I via the intermediate radionuclides ^{137}Xe and ^{135}Xe, respectively, as shown in Figure 1-1. In contrast, ^{134}Cs is produced via neutron activation of ^{133}Cs which is a fission product; the production rate of ^{134}Cs is slow so appreciable activities of ^{134}Cs are

only produced in nuclear reactors. Therefore, ^{134}Cs is released only by reactor accidents whilst ^{137}Cs and ^{135}Cs are produced by both reactor accidents and nuclear weapons (Snyder et al., 2012).

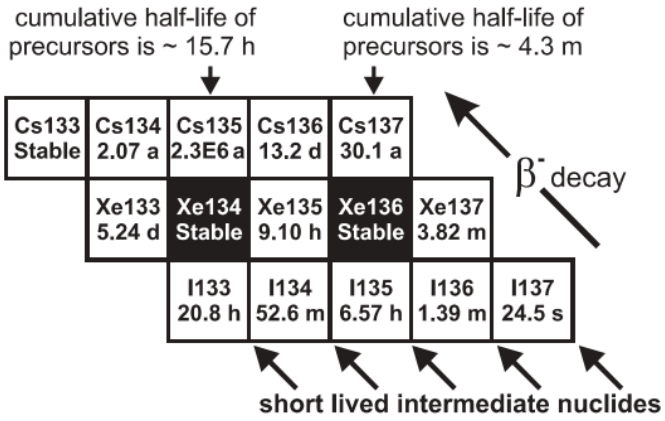


Figure 1-1 A part of nuclide chart (133 – 137 mass range) shows the precursor nuclides of ^{137}Cs, ^{135}Cs and ^{134}Cs and their cumulative half-lives (Snyder et al., 2012).

1.2.3 Transport of radiocaesium from forests to humans

^{137}Cs and ^{134}Cs are both associated with contamination of forests after nuclear fallout events. However, over a period of 5 - 50 years, radiation doses in forest ecosystems are likely to be dominated by only ^{137}Cs because of its relatively long physical half-life (30 years). In contrast, ^{134}Cs may be an important dose former in the first five years after deposition, but is quite quickly removed by radioactive decay due to its 2.06 year physical half-life (Shaw, 2007).

1.2.3.1 Interception of radiocaesium deposition by forest canopies

About 31% of the world's land area is covered by forest which acts as an important receptor of atmospheric pollutants of all kinds. Interception of nuclear fallout by tree canopies is known to result in elevated radioactive contamination of forest ecosystems when compared with other ecosystem types such as grassland (Bunzl and Kracke, 1988).

The effectiveness of pollutant interception varies according to the type of forest, the age of trees and the type of deposition (wet or dry). Coniferous forest is a highly effective interceptor of atmospheric fallout. Over the first few days of fallout dispersed from the Chernobyl accident, around 70 – 80% of nuclear fallout was retained by above-ground parts of tree. Coniferous forest intercepted 2 or 3 times more radioactivity from the atmosphere than deciduous forest and 7 to 10 times more than any other natural and semi-natural ecosystems (IAEA, 2010) including grassland and arable land (Bunzl and Kracke,

1988). Approximate half of the initial deposition on coniferous forest canopies is associated with needles (Shcheglov et al., 2001). Younger forest has a lower interception efficiency for nuclear fallout due to a lower leaf or needle density (leaf area index).

1.2.3.2 ^{137}Cs within forest soils

- *Migration from forest crown to floor*

Following interception by the tree canopy, a small fraction of radionuclide is adsorbed into leaves or needles whilst the majority is removed to the forest floor by litterfall, throughfall and stemflow (Shaw, 2007). ^{137}Cs movement by throughfall is greater than by stemflow while ^{137}Cs concentration in litterfall differs among the litter components (Endo et al., 2015). The rate of removal by these processes depends on the period after deposition, the type of forest as well as seasonality (Endo et al., 2015). During the early period after initial canopy interception, radiocaesium is removed quickly to the forest floor. One year following the Chernobyl and Fukushima accidents, respectively, more than 90% and 35 – 55% of ^{137}Cs was leached from the tree crown to the forest floor (Smith, 2005; Loffredo et al., 2015).

- *Distribution in forest soil*

The soil is the major ecological storage compartment for nutrients such as potassium as well as radiocaesium following deposition on the forest floor. After deposition from the atmosphere, ^{137}Cs is often observed to accumulate within the surface layers of forest soil, commonly remaining largely within the organic soil layer (Varskog et al., 1994; Yoshida et al., 2002; Konopleva et al., 2009; Pumpanen et al., 2016; Yoshida et al., 2004; Rühm et al., 1999).

^{137}Cs is known to be a generally strongly-bound radionuclide within most soils and downward migration is strongly controlled by sorption and desorption processes (Pröhl et al., 2012). The migration rate of ^{137}Cs in forest soils is between 0.19 – 1.07 cm per year, depending on the properties of individual soils (IAEA, 2010). In particular, soils with high clay mineral contents can substantially slow down migration of ^{137}Cs to deeper soil layers (Kirchner et al., 2009).

Mobility of ^{137}Cs in forest soil is controlled by various transport mechanism such as convective transport by flowing water, dispersion caused by spatial variations

of convection velocities within the soil matrix, diffusive movement within the liquid phase and physico-chemical interactions (ie. sorption-desorption) within the soil matrix.

^{137}Cs in the soil exists in four physico-chemical forms:

- aqueous form in soil solution

Radiocaesium in this form can be taken up by plant roots and microbes and is the most subject to leaching by rainwater.

- exchangeable or absorbed forms on exchange sites of soil particles

Exchangeable radiocaesium is the fraction that is electrostatically bound to the surfaces of humus and clay particles. This fraction is readily exchanged with other cations and readily available for plant uptake as well.

- fixed or non-exchangeable forms

Radiocaesium becomes fixed between adjacent tetrahedral layers of di-octahedral and tri-octahedral micas, vermiculites and intergrade clay minerals such as chloritized vermiculite because the binding forces between caesium and the clay surfaces are greater than the hydration forces between individual cations of caesium (Sparks, 2001). Non-exchangeable radiocaesium is moderately to sparingly available to plants.

- structural or mineral forms (including compounds of sulphides, phosphates, silicates etc.)

Transfers between caesium forms in soil are controlled by equilibrium and kinetic reactions between them. The order of availability of caesium for plant uptake is solution > exchangeable > fixed > mineral form.

Wyttenbach et al. (1995) suggested that the uptake (as measured by concentration ratios, CRs) of the alkali metals (K, Rb and Cs) by spruce needles should be similar, but large differences are observed due to their different sorption behaviour in the soil. CRs for ^{137}Cs should be closer to those for exchangeable ^{133}Cs than for total ^{133}Cs, which is largely in insoluble mineral forms in most soils. Consequently, fallout ^{137}Cs and exchangeable ^{133}Cs are more available for plant uptake than total native ^{133}Cs (Varskog et al., 1994).

The uptake of ^{137}Cs from soil is known to reduce with time due to the processes of adsorption, fixation and redistribution throughout the rooting zone (IAEA,

2010). The processes of adsorption and fixation are particularly prevalent in soils with high clay mineral contents. Pine needles collected in 1995 have higher decay-corrected activity concentrations of ^{137}Cs than in 2013 after the Chernobyl accident (Pumpanen et al., 2016). However, 27 years after the Chernobyl accident, ^{137}Cs in pine needles in Finland was at steady state though ^{137}Cs in surface layers of forest soil remained mobile (Pumpanen et al., 2016).

Numerous studies have shown that most ^{137}Cs accumulates in the organic layer of forest soils where the bioavailable fraction is higher than in the deeper mineral soil layers (Comans et al., 1998). Thus, it is generally concluded that ^{137}Cs uptake by trees is directly related to ^{137}Cs activity concentrations in the organic soil layer (Varskog et al., 1994).

The age of trees at the time of initial deposition also affects uptake of ^{137}Cs with younger trees being more obviously susceptible to contamination with ^{137}Cs than older trees as a result of more active nutrient uptake (Shaw, 2007). Furthermore, activity concentration of ^{137}Cs within trees varies strongly in different tissues. In coniferous trees, the activity concentration of ^{137}Cs is highest in needles and reduces in bark, sapwood and heartwood, respectively (Pumpanen et al., 2016).

^{137}Cs is probably transported from non-growing parts of trees to actively growing tissues together with essential nutrients, especially potassium. Migration of ^{137}Cs occurs from heartwood, composed of non-living cells, to sapwood where cells predominantly carry water. This results in higher activity concentrations of ^{137}Cs in sapwood than in heartwood (IAEA, 2010).

1.2.3.3 Human exposure to radiation from forest products

Following contamination of forests, radionuclides are transferred to tree tissues and a range of edible and non-edible forest products. Human exposure to radionuclides in forests is possible at all stages of biogeochemical recycling following the initial distribution. ^{137}Cs is concentrated in the edible part of some fruits (Eslava-Gomes and Brown, 2013) including the berries of forest plants such as blackberry and bilberry. In response to concern in several countries, especially after large-scale nuclear dispersion and fallout from the Chernobyl accident, there has been considerable research on radioactive contamination in forest products, including human dose estimation (Hus et al., 2001). Work specifically related to contaminated forests includes the development of generic methodology for determination of public dose including the calculation of dose

conversion coefficients for timber used in the wood industries and in household applications (IAEA, 2003).

1.2.4 Radiocaesium in local fallout within forest soil

Atmospheric transportation of nuclear fallout is related to the size and density of particulate material released either by weapons or reactors. Relatively large particles were found within several kilometres of the Chernobyl reactor, some of which were identified as uranium oxide 'hot particles' in surface soil on the line of the western trace at Shepelichi but also to the immediate south of the reactor at Kopachi (Shaw, 2007), as shown in Figure 4-1.

Uranium oxide fuel particles found in local fallout close to Chernobyl differ from the 'condensed particles' which were smaller and therefore subject to much longer distance atmospheric transport. These two types of particle also differed in their physico-chemical properties after deposition to forest soils (IAEA, 2006). Very low solubility of fuel particles deposited in forests in the vicinity of the Chernobyl power plant resulted in vertical migration of ^{137}Cs which was much slower than water-soluble forms of ^{137}Cs within global fallout (Boulyga et al., 2003).

1.2.5 Factors influencing radiocaesium behaviour in forest ecosystems

Bioavailability of radiocaesium is strongly dependent on soil pH, organic matter, clay content and competitive cations, especially potassium. Collectively, these factors can be used to predict radiocaesium uptake by plants (Absalom et al., 2001).

1.2.5.1 Soil pH

In acid soils caesium sorption is reduced due to competition for cation exchange sites with excess hydrogen ions in soil solution which, in very acidic soils, can occupy most of the negatively charged sites on clay and organic matter. Adsorption of caesium has been found to be at a maximum at soil pH about 8.0 (Giannakopoulou et al., 2007).

Transfer of caesium from soil to plant is also affected by soil pH although Van Bergeijk et al. (1992) determined that, when other soil factors were taken into

account, pH had little influence on the transfer of caesium from soil to plant within a range between 3.9 and 8.7.

1.2.5.2 Cation exchange capacity (CEC)

Cation exchange capacity (CEC) is a measure of the holding capacity of cations within a soil. This capacity to hold cations is conferred through electrostatic charge which is dominated by the negative charge at the surfaces of organic matter and clay minerals. CEC in soil can be high or low depending on the type and amount of clay minerals and organic matter.

The CEC of organic matter can be 4 – 50 times higher than that of clay minerals for a given mass. However, CEC of organic matter is pH-dependent because negative charge on organic molecules such as humic and fulvic acids results from dissociation of acidic functional groups, a process which depends on soil pH. Soils with low pH have higher H^+ activities in solution which reduce CEC by preferentially replacing other cations at exchange sites.

Soils with high CEC have a high capacity to adsorb nutrient and other cations such as Cs^+ (Giannakopoulou et al., 2007). These cations are simply exchangeable with other cations in soil solution and, as a result, they are available for plant uptake. Cation exchange is one of the adsorption mechanisms which can decrease the leaching of caesium through the soil profile.

1.2.5.3 Soil organic matter

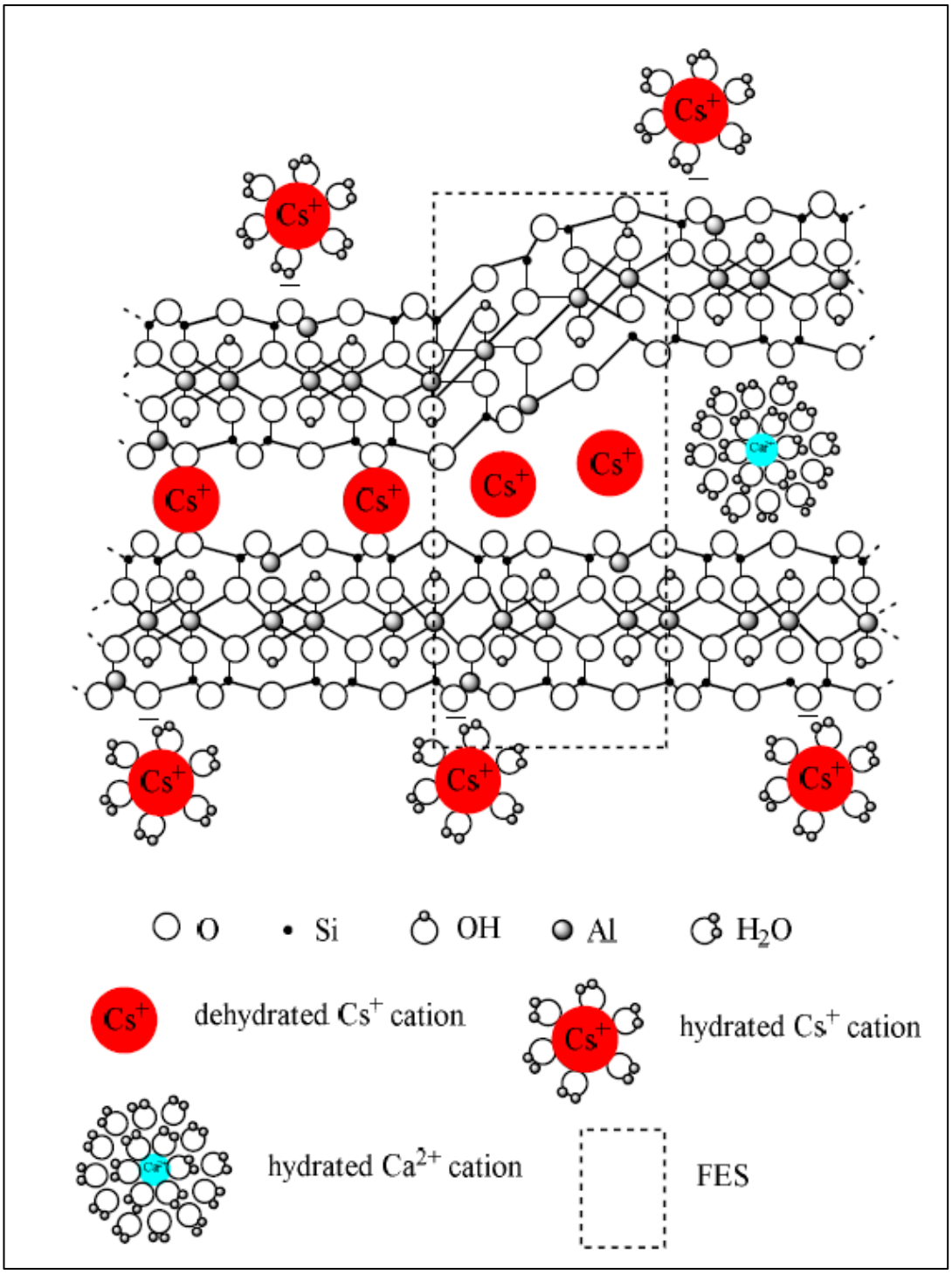
Soil organic matter is composed of residual plant and animal materials at various stages of decomposition. Decomposed organic matter is an important determinant of caesium mobility and availability. Net negative charge on the surfaces of humus attracts and holds cations resulting in a positive correlation between organic matter and the cation exchange capacity of soils.

Organic horizons within soils possess large cation exchange capacities which can reduce Cs mobility and bioavailability. However, distribution of organic matter around clay particles can reduce adsorption and subsequent fixation on clay minerals, thereby increasing potential caesium uptake by plants (Van Bergeijk et al., 1992; Thammavech, 2007). Furthermore, organic matter is not able to 'fix' adsorbed radiocaesium in the same way that clays do (Absalom et al., 2001).

1.2.5.4 Clay minerals

Clay minerals have a negative charge on their outer planar surfaces which electrostatically attract and hold cations including nutrients and trace elements such as caesium, as shown in Figure 1-2.

Figure 1-2 Diagram of general structure of a 2:1 clay mineral such as illite to illustrate the different sorption sites for Cs (Söderlund et al., 2016).



Due to its low hydration energy, the caesium cation is able to lose its hydration shell and thus penetrate the frayed edges of clays, eventually causing collapse of alumninosilicate sheets in the clay mineral, trapping or 'fixing' Cs ions. Thus, increasing the clay mineral content within a soil can strongly increase caesium adsorption by soil particles (Giannakopoulou et al., 2007). Soil to plant transfer of caesium in clay or loam soils is 5 - 3 times lower than in sandy soils in which clay content is minimal or absent (Van Bergeijk et al., 1992). Illite is a non-expanding layer silicate which has been identified as being mainly responsible for the specific sorption of caesium when present in soils, a property which can measured using the Radiocaesium Interception Potential (see section 1.2.8.3) (Absalom et al. 1995).

1.2.5.5 Aluminium in soil

Aluminium is the third most abundant element in soil, most commonly present as amorphous sesquioxides and structured aluminosilicate minerals. Aluminium solubility increases in acidic soils and, under strongly acidic conditions, it exists in the form of Al^{3+} in the soil solution (Kidd et al., 2001; Krstic, 2012). Under acidic conditions, soluble Al can penetrate the interlayers of some 2:1 clay minerals, forming aluminium hydroxyl interlayers, thus displacing interlayer cations such as Ca^{2+}, K^{+} and Cs^{+} and reducing the cation exchange capacities of the clay minerals (Tate, 1997).

1.2.5.6 Competitive elements

Potassium, rubidium and caesium are all Group I alkali metals which, due to their physico-chemical similarities, act as mutual competitors during sorption and biological uptake.

- *Within forest soils*

Theoretically, the size of a hydrated cation is directly related to the capacity of replacement between the cation on exchange sites within soil particles. Cations with smaller hydrated radii have greater replacement power so, for the alkali metals, the general order of replacement on exchange sites within soil particles is $K^{+} < Rb^{+} < Cs^{+}$ (Israelachvili, 2011).

In the soil compartment, cations which are competitive with caesium, notably K^{+}, are rapidly released from leaf litter then subject to sorption on organic

matter, clay minerals and sesquioxides, all of which possess cation exchange properties.

Some soils possess very large reserves of potassium within soil minerals. In British soils, the amount of exchangeable K^+ is between 10 - 100 times larger than the amount in solution which it effectively buffers (Rowell, 1994). Compared with Cs, there are potentially massive stores of stable potassium within soil minerals and potassium is therefore an important competitor for Cs within forest ecosystems.

Norway spruce has concentration ratios in the order of K > Rb > Cs which suggests that the adsorption properties of the soil strongly affect the uptake of these elements (Wyttenbach et al., 1995).

- *Uptake by plants*

Potassium is an essential macronutrient for plant growth; it is taken up by and redistributed in plants via K^+ transporter channels within the outer and inner cell membranes. Because of the similarity of their physico-chemical properties to those of potassium, caesium and rubidium are transported into and throughout plants via the potassium transport system (White and Broadley, 2000).

The relative uptake of caesium, rubidium and potassium by plants depends on their respective concentrations in soil solution at the surface of root hairs. Potassium is much more abundant in soils and is therefore taken up by plants in much greater quantities due to the much higher concentrations of K^+ in the root zone which easily exceed Cs^+ and Rb^+. Furthermore, due to the selectivity of potassium transporter channels in favour of K^+, it is commonly observed that plants preferentially absorb the alkali metals in the order K > Rb > Cs. For example, this has been observed for Norway spruce (*Picea abies*) in Switzerland by Wyttenbach et al. (1995). However, the interaction between caesium and potassium uptake is strongly concentration-dependent; at low concentrations of K, plant roots are able to absorb Cs at a faster rate than when K is present at higher concentrations (Shaw and Bell, 1991).

1.2.6 Correlation of ^{137}Cs and ^{133}Cs distributions in forest ecosystems

Due to the expected similarity in physico-chemical forms of the stable isotope of caesium (^{133}Cs) and radiocaesium isotopes, various attempts have been made to

determine whether the former can be used as a reliable indicator for ^{137}Cs distribution behaviour in forest ecosystems.

Theoretically, ^{137}Cs fallout should behave in a similar manner to native ^{133}Cs after sufficient time has elapsed for the two isotopes to equilibrate. However, as ^{133}Cs is held strongly inside the crystal structure of soil minerals, isotopic equilibrium with ^{137}Cs is only likely over long timescales.

Over a period of 1 – 3 years following deposition of Chernobyl fallout, equilibrium between ^{137}Cs and ^{133}Cs in subalpine ecosystems was not found, with ^{137}Cs being more readily available for plant uptake than ^{133}Cs (Varskog et al., 1994). However, Uchida and Tagami (2007a) found that the plant uptake of the bioavailable fraction of ^{133}Cs could be correlated with ^{137}Cs. So, in forest ecosystems it might be expected that the exchangeable fraction of ^{133}Cs can be used to understand the likely behaviour of ^{137}Cs.

In humus rich soil with low mineral content the equilibrium between ^{137}Cs and ^{133}Cs is more expected because of the higher exchangeable fractions for both isotopes. Moreover, equilibrium between exchangeable fractions of ^{137}Cs and ^{133}Cs is expected to occur in plant tissues growing in organic soils due to the relationship between their exchangeable forms (Yoshida et al., 2004; Yoshida et al., 2002; Rühm et al., 1999; Karadeniz and Yaprak, 2007; Uchida and Tagami, 2007a).

^{133}Cs has been suggested and used as an indicator of the long-term migration of ^{137}Cs in forest ecosystems (Cook et al., 2007; Sawai et al., 2015;, Yoshida et al., 2002). It has thus been suggested that ^{133}Cs can be used to verify predictions of radioecological models in forest ecosystem over the long-term (Rühm et al., 1999).

1.2.7 Distribution of radiocaesium in tropical forests

Tropical forests are located in the tropical geographical zone, roughly within 23.5° N and S from the equator. In tropical forests the water content of surface soil is strongly affected by extreme high temperatures during day time, with the humidity of surface soil rapidly decreasing under strong sunlight. High annual rainfall is also an important factor in the development of specific properties of tropical soils.

The major characteristics differentiating tropical forest ecosystems from temperate forests include specific circumstances such as the distinct dry and wet

periods in tropical forests and high rates of organic matter decomposition and weathering, all of which can modify radionuclide behaviour when compared with temperate ecosystems. Rapid degradation of organic matter and advanced decomposition of clay minerals lead to low cation exchange capacities for macro-nutrients including potassium, which are held weakly in the soil. Nutrients are available for uptake by plants but are also susceptible to being leached down the soil profile by rainwater. According to Pröhl et al. (2012) the leaching rate of nutrients and radionuclides is directly correlated with their soil-to-plant transfer factors. However, because ^{137}Cs is a generally strongly bound radionuclide, the effect of the tropical climate and associated conditions is perhaps lower than for other elements and its downward migration is still likely to be mainly due to sorption and desorption processes with soil particles (Pröhl et al., 2012).

Rapid decomposition of litter in tropical soil minimises the accumulation of organic matter in surface soil and consequently leads to rapid recycling of nutrients and trace contaminant such as ^{137}Cs (Payne and Edis, 2012).

Leaf area indices in tropical forest tend to be higher than in temperate systems, hence relative transfer factors (TF) for caesium are likely to be higher in tropical forests (Tagami et al., 2012). Thammavech (2007) estimated soil-to-plant transfer factors in Thailand and found that they decreased when soil pH, clay content and exchangeable potassium increased and when organic matter and NH_4^+ decreased.

1.2.8 Prediction of long-term migration of ^{137}Cs in forest ecosystems

1.2.8.1 Predictive models of ^{137}Cs in forest ecosystems

Understanding the natural recirculation of radionuclides is key to understanding and predicting the long-term behaviour of radionuclides in forest ecosystems. However, the transportation of ^{137}Cs in forests is difficult to forecast because of the complex and interacting nature of the ecological compartments which, together, make up the forest ecosystem. Reliable predictive models are needed to quantify the radiation dose which humans receive from forest ecosystem pathways as well as to explore and evaluate any proposed remedial and abatement strategies. A number of existing models have been developed to estimate the migration of radionuclide contamination in forest.

In 1996, the International Atomic Energy Agency (IAEA) established the BIOMASS Forest Working Group. One of the objectives of this group was to

compare and test the accuracy of models which had been developed to predict the behaviour of ^{137}Cs in forest ecosystems, up to a period of 20 years. The results showed large conceptual discrepancies between these models, associated with high uncertainty for predictions of radio-caesium behaviour after 1986, especially within organic soil layers in which radiocaesium derived from nuclear tests and the Chernobyl accident is persistently retained. Very few of these models had previously been rigorously tested against independent site data (IAEA, 2002; Shaw et al., 2005).

1.2.8.2 Validation of long-term model forecasts

An important parameter that has been used in quantifying and modelling radionuclide contamination of forest trees is the aggregated transfer factor (section 1.2.8.5). It has been used for quick evaluations of radionuclide uptake by trees and other forest vegetation after acute deposition and is especially applicable to multi-layer soils which are typical of temperate forests. However, aggregated transfer factors usually exhibit wide ranges of values as well as time-dependence, both of which have been reported to lead to high deviations of model predictions (IAEA, 2002).

Validation of forest models is needed to provide the capability to make reliable predictions over periods longer than two decades, during which ^{137}Cs contamination remains important (Shaw et al., 2005; Yoshida et al., 2004). Finally, reliable prediction is needed to support improvement of estimations of doses to humans and other organisms received during long-term cycling of ^{137}Cs in forest ecosystems.

1.2.8.3 Parameters used in predicting radiocaesium cycling in forest ecosystems

The accuracy of model predictions ultimately depends on the quality of data used to represent radionuclide distributions in forest compartments. Ideally, such data should be obtained by direct measurement of forest samples. The following parameters can be derived from such measurements and are commonly used in models to describe and predict radionuclide behaviour in forest ecosystems.

- *The solid-liquid distribution coefficient (K_d)*

The solid-liquid distribution coefficient (K_d) (IAEA, 2010) is used to quantify the degree of sorption of radionuclides on the solid (particle) phase of the soil with

respect to the liquid (solution) phase. The K_d is often used in the assessment of radionuclide mobility and residence time in soil. The concept of the K_d assumes that equilibrium exists between radionuclides on the solid phase and in the liquid phase, without considering sorption and desorption mechanisms. The K_d is calculated using the following equation.

$$K_d = A_S/A_L \quad (1.1)$$

Where K_d = solid-liquid distribution coefficient (L kg^{-1})

A_S = activity concentration in solid phase (Bq kg^{-1})

A_L = activity concentration in liquid phase (Bq L^{-1})

The K_d value is controlled by the chemical forms and speciation of radionuclides as well as soil properties. Recommended values for the K_d of radiocaesium, classified on the basis of soil group, are provided in Table 1-1.

- *Radiocaesium interception potential (RIP)*

Radiocaesium interception potential (RIP) is generally accepted as the standard indicator to quantify the retention of radiocaesium in soil (Cremers et al., 1988). It is measured under standardised experimental conditions and expressed as the product of frayed edge site (FES) pool capacity and the value of the trace selectivity coefficient (with respect to potassium or ammonium) of the FES (Madruga et al., 1996). RIP is determined using the following equation (Vandebroek et al., 2012).

$$RIP = K_C*[FES] = K_D^{Cs} \times [K^+] \quad (1.2)$$

Where RIP = Radiocaesium interception potential (mmol.kg^{-1})

K_C = ^{137}Cs-K selectivity coefficient

[FES] = capacity of Frayed Edge Sites with high adsorption selectivity for Cs^+

K_D^{Cs} = ^{137}Cs solid-liquid distribution coefficient

$[K^+]$ = concentration of K in solution

RIP is related to K_d as shown in Table 1-1.

Table 1-1 The K_d value of radiocaesium in soils grouped according to texture/organic matter criteria and the interception potential of radiocaesium (L kg^{-1}), GSD = geometric standard derivation (IAEA, 2010).

Criterion	Soil group	N	Mean	GSD	Minimum	Maximum
Texture and organic matter	All soils	255	52	5.9	0.4	6,500
	Sand	65	22	6.4	0.4	2,400
	Loam + clay +organic	176	69	5.4	2.0	6,500
Radiocaesium interception potential (RIP, $mmol.kg^{-1}$)	RIP<50	47	74	2.4	10	730
	150<RIP<1000	78	320	5.6	10	34,000
	1000<RIP<2500	72	2,400	4.1	62	95,000
	RIP>2500	60	7,200	4.0	220	380,000

- *Concentration ratio (transfer factor) of ^{133}Cs, ^{39}K and ^{85}Rb*

Transfer of elements or radionuclides between forest soils and trees (and other forest plants) is affected by various factors. The concentration ratio (CR) or soil-to-plant transfer factor (TF) provides a simplified measure of this uptake from soils, which can be statistically related to variations in soil- and plant-related factors. A fundamental assumption of the CR is that transfer of an element or radionuclide from soil to vegetation is at equilibrium. The concentration ratio (*CR*) for a radionuclide is generally calculated using the following equation.

$$CR = M_P/M_S \quad (1.3)$$

Where CR = Concentration ratio

M_P = Mass concentration in plant (Bq kg^{-1} dry or fresh weight)

M_S = Mass concentration in soil (Bq kg^{-1} dry weight)

Calculation of CRs has been applied using different definitions of radionuclide distribution in soil layers, as follows.

- *Standardised soil depth*

The standardised soil layer is usually the uppermost layer with a defined thickness, often 10 – 20 cm representing the 'ploughed layer'. This definition has been used widely in agricultural ecosystems in which, due to tillage, radionuclides are distributed homogeneously within the rooting soil depth (IAEA, 2002).

- *Specific soil horizon*

Sometimes a specific soil layer is used to calculate the CR, for example one in which fungal mycelia or plant root systems are known to be located. It is appropriate for use with fungal fruiting bodies ('mushrooms') or green plants (IAEA, 2002).

- *Soil solution-plant*

Some definitions of the CR refer to the radionuclide activity concentration in soil solution which is directly available for plant uptake. This concentration ratio is suitable for long-term predictions of radionuclide uptake by fungi and green plants (IAEA, 2002). However, at present no experimental data on the soluble fractions of radionuclides specifically in forest soils are generally available in the literature, though soluble concentrations can be estimated using the K_d, as described above.

CR implies that transfer process proportional to nuclide content in the soil therefore, in the equilibrium of soil-plant system achieved concentration of nuclide in soil is not affected to CR calculation (Guillén et al., 2017, IAEA, 2010).

- *The aggregated transfer factor (T_{ag})*

Concentration ratios are not applicable for the determination of radionuclide transfer from multilayered soils which are often typical of semi-natural or natural forest ecosystems, in which redistribution of a radionuclide in the soil profile can occur rapidly after acute deposition. For this situation the aggregated transfer factor (T_{ag}) has been devised as a more appropriate measure of soil-to-plant transfer (IAEA, 2002). The T_{ag} is defined according to the following relationship.

$$T_{ag}\ (m^2\ kg^{-1}) = A_P/T_D \qquad (1.4)$$

Where T_{ag} = Aggregated transfer factor ($m^2\ kg^{-1}$)

A_P = activity conc. in forest vegetation compartment (Bq kg^{-1})

T_D = Total deposition to forest floor (Bq m^{-2})

A major shortcoming of the T_{ag} is the fact that it can be strongly time-dependent. Uptake of a radionuclide from soil to tree, for example, is affected by soil fixation processes and migration of radionuclides into and out of the rooting zone, which both result in a change, with time, of activity concentration to which the plant or tree root is exposed.

T_{ag} values for ^{137}Cs transfer into wood and needles of coniferous trees under apparent steady state conditions (IAEA, 2010) are shown in Table 1-2.

Table 1-2 The aggregated transfer factor (T_{ag}, m^2 kg^{-1} dry weight) of ^{137}Cs under apparent steady state conditions to wood and needles/leaves of trees, measured under apparent steady state conditions. N = number of samples, GM = geometric mean (IAEA, 2010).

Species	Wood		Needle/leaf		*N*
	GM	Range	GM	Range	
Spruce	1.5×10^{-3}	2.8×10^{-4} – 3.9×10^{-3}	8.6×10^{-3}	5.7×10^{-4} – 5.2×10^{-2}	7
Fir tree	1.2×10^{-4}	-	-	-	1
Pine	1.7×10^{-3}	1.1×10^{-4} – 2.1×10^{-2}	1.0×10^{-2}	2.4×10^{-4} – 9.2×10^{-2}	22
Oak	8.6×10^{-4}	1.1×10^{-4} – 3.8×10^{-3}	1.0×10^{-2}	1.1×10^{-2} – 1.2×10^{-2}	3
Beech	7.2×10^{-4}	1.8×10^{-4} – 1.6×10^{-3}	2.5×10^{-3}	2.3×10^{-3} – 2.7×10^{-3}	3
Birch	9.4×10^{-4}	2.4×10^{-4} – 3.8×10^{-3}	8.7×10^{-3}	2.8×10^{-3} – 3.0×10^{-2}	3
Willow	2.5×10^{-5}	1.0×10^{-5} – 6.8×10^{-5}	2×10^{-2}	-	4

1.3 SPECIFIC OBJECTIVES OF THE STUDY

1.3.1 Boundary Plantation and Wat Ban Chan

The research presented here has examined stable and radiocaesium (and competitive elements) in forest compartments over the long-term following initial deposition. Specifically, data have been obtained to test the following hypotheses.

- ^{137}Cs largely and preferentially accumulates within the surface organic layers of forest soil
- Clay minerals (if present) and organic matter content both play an important role in the long-term behaviour of ^{137}Cs in forest soils
- Organic matter and soil pH both affect the circulation of ^{137}Cs and ^{133}Cs in forest ecosystems, particularly related to their exchangeabilities in forest soils
- Stable potassium and rubidium are the important competitors during circulation of ^{137}Cs and ^{133}Cs in forest ecosystems
- Stable caesium is a suitable indicator of the long-term behaviour of radiocaesium within forest ecosystems.

1.3.2 Forests in the Chernobyl Exclusion Zone

- ^{137}Cs largely and preferentially accumulates within the surface organic layers of forest soil
- Acute and high radiation doses have impacted the growth of Scots Pine.

1.3.3 Modelling work

Modelling work was carried out using data obtained from Boundary Plantation and Wat Ban Chan sites as follows:

- calibration and validation of an existing model (RIFE1)
- development of a new model of radiocaesium and ^{210}Pb accumulation in forest soils

CHAPTER 2: MATERIALS AND METHODS

2.1 RESEARCH LOCATIONS

Coniferous (pine) forest was sampled in three locations, each of which received markedly different levels of contamination due to radiocaesium deposition from the atmosphere under different circumstances, as shown in Table 2-1.

Table 2-1 Sample collection sites and their circumstances

Forest site	Location	Forest zone	Nuclear fallout deposition
Boundary Plantation, Sherwood Forest	England 53° 12'N 1° 6'W	Temperate (*Pinus nigra*)	Chronic deposition from atmospheric weapons testing (peak deposition in 1963)
Kopachi forest, Chernobyl	Ukraine 51° 21'N 30° 7'E	Temperate (*Pinus sylvestris*)	Acute deposition from the Chernobyl accident (deposition in 1986)
Wat Ban Chan forest	Thailand 19° 3'N 98° 18'E	Tropical (*Pinus kesiya*)	Chronic deposition from atmospheric weapons testing (peak deposition in 1963)

2.2 SAMPLING METHODS

Coordinates of collecting points were randomly selected within each forest sampling site. At Boundary Plantation, samples were taken on four separate occasions, in June, September and December of 2014 and March 2015. Before each visit the coordinates of six sampling points were identified using a stratified random sampling strategy. These coordinates were generated using random numbers and converted into 10-figure Ordnance Survey coordinates which were located in the field using GPS. A total of 24 samples were taken across an area

of approximately 25 hectares of forest. Soil core samples collected at each point in Boundary Plantation were taken using plastic tubes (6.2 cm diameter, 20 and 10 cm lengths; Figure 2-1) which were hammered vertically into the soil. Soil core samples were collected on one sampling trip to Kopachi and Wat Ban Chan forests. Kopachi was visited in September 2015. Due to the radiation dose rate at this site only two soil cores were collected; these were located by walking randomly off a nearby road into the forest for a distance of approximately 100 m. Wat Ban Chan was visited in February 2016. Six sampling points were located randomly by walking across an area of approximately 1 hectare of forest. Soil cores at Wat Ban Chan and Kopachi were taken using steel soil corers which were available at each sampling site and suitable for the local soil conditions, as shown in Figure 2-2 and Figure 2-3, respectively. Cross contamination between soil samples was completely avoided at Boundary Plantation by using new plastic tubes at each sampling point. The steel corers were re-used at individual sampling points at Wat Ban Chan and Kopachi, but were thoroughly cleaned between samples. Any differences between the quality and quantity of soil samples obtained using each type of corer are very small and can be neglected.

A screw-type increment tree corer, as shown in Figure 2-4, was used to take two narrow (5 mm diameter) cores of wood across one half of the width of a representative pine tree at each site as close as possible to the corresponding soil sampling point. The tree cores were taken approximately 40 and 60 cm above ground level. Tree cores collected in Ukraine were sampled at Kopachi, Bourakovka, the 'Red Forest' and the 'North Trace'. At Boundary plantation, throughfall (rainwater) samples were taken under *Pinus nigra* using light-proof plastic bottles with collecting funnels, left for a period of three months. Finally, living (green) and dead (dry) pine needles were collected as near as possible to each soil sampling point at all three sampling sites.

Figure 2-1 *Plastic pipe used for collecting soil cores at Boundary Plantation (6.2 cm diameter, 20 and 10 cm lengths).*



Figure 2-2 *Soil corer used for collecting soil cores at Kopachi forest (6.4 cm diameter, 20 cm length).*



Figure 2-3 *Soil corer used for collecting soil cores at Wat Ban Chan forest (6.8 cm diameter, 15 cm length).*



Figure 2-4 *Increment tree corer, manufactured by Haglöf (Sweden).*



2.3 PREPARATION OF SAMPLES

Soil cores were pushed out from the sampling tubes and cut into 0.01 m thick layers. NB. for samples collected from Boundary Plantation in plastic pipes, the cores were pushed from the sampling tubes and cut into depth increments in the laboratory. For samples collected at Kopachi and Wat Ban Chan, the cores were pushed from the sampling tubes and cut into depth increments in the field. Cross contamination between depths within soil core was less and neglected. Stones, pebbles and roots were removed prior to sample processing. In order to obtain sufficient sample mass for analysis, 4, 2 and 2 of soil cores were collected (beside each other for same sampling site) at Boundary Plantation, Kopachi and Wat Ban Chan respectively. Soil samples from the same depth had to be

combined and mixed together. All soil samples after pebble and stone removed were weighed to allow bulk density to be calculated, then stored in plastic bags in a cold store (4°C) to maintain their original moisture content. These moist soil samples were subsequently used for analysis of exchangeable and isotopically exchange fractions of elements and pH.

A sub-sample of each field-moist soil sample (the rest was for analysis of exchangeable and isotopically exchange fractions of elements and pH) was weighed and oven dried overnight at 105°C then weighed before grinding using a mortar and pestle. Ground soil samples were passed through a 1 mm soil sieve and collected in a clean sample bag. These dried soil samples were subsequently used for analysis of stable elemental concentrations and organic matter content.

Needle samples were dried overnight at 105°C in an oven then ground to a fine powder in a ultra-centrifugal mill (ZM200; Retsch®).

Annual growth ring widths in tree cores were measured using a low-power binocular microscope as soon as possible after collection, then the cores were dried overnight in an oven at 105°C.

Canopy throughfall water (rainwater) samples were kept in clean plastic bottles without acidification and left in a cold store at 4°C prior to analysis.

2.4 ANALYSIS OF SAMPLES

2.4.1 Organic matter content of soil samples

The loss on ignition method was used to determine organic matter content in this research. It is an approximate measure of organic matter content in sandy soil but can be an overestimate when applied to high-clay mineral soil (Rowell, 1994).

Approximately 5 g of pulverised oven-dried soil were placed overnight in ceramic crucibles in a furnace at 550°C to combust any organic material in the soil samples.

After combustion and cooling, the contents (ash) of crucibles were weighed and the organic matter content of the original soil samples calculated using equation 2.1.

$$\%LOI = (W1-W2) \times 100/W1 \quad (2.1)$$

When %LOI = Loss on ignition (%)

W1 = Weight of oven dried soil (g)

W2 = Weight of ignited soil (g)

2.4.2 Soil pH measurement

A bench-top pH meter (pH 209; Hanna Instrument) used for soil pH measurement was calibrated using buffer solutions at pH 7.01 and 4.01. Rinsed and immersed the pH electrode in buffer solution, shook briefly and waited for 1 – 2 minutes for the reading to stabilise. Adjusted offset and slope knobs (for pH 7.01 and 4.01 respectively) until the reading is accurate.

Approximately 5 g of moist soil and 12.5 ml of deionised water were put into an Oak Ridge centrifuge tube. Samples were shaken for 30 minutes then the pH electrode was immersed in the soil suspension. The soil pH reading was recorded after a short period of stabilisation.

2.4.3 Mineralogy of soil

Mineralogy analysis and result investigation were carried out by Department of Chemistry, Loughborough University. Approximately 2 g of dried soil sample was analysed to investigate changes in mineralogy down the soil profile using powder X-Ray Diffraction (XRD). Diffraction patterns were collected on each sample using a Bruker D8 powder diffractometer operating with monochromated CuKÎ±1 radiation in reflection mode over the 2-θ range 10-90° using a 0.014° 2-θ step over a period of 3h in a flat plate sample holder. The resulting diffractograms were investigated using standard reference patterns to identify the major crystalline forms within the original samples.

2.4.4 Determination of total concentrations of stable caesium (^{133}Cs) and its competitive elements

Only rainwater was directly measured by Inductively Coupled Plasma Mass Spectroscopy (icapQ; Thermo Scientific). All other samples were acid-digested before elemental analysis by ICP-MS. The acid digestion methods used differed, depending on type of sample, as described below. All measurement conducted using ICP-MS was calculated after remove of measurement value of blank samples (average of 3 – 5 of blank samples).

2.4.4.1 Aqua Regia digestion of soil samples

Approximately 2 g of dried soil sample was weighed out and digested in 5 ml of concentrated nitric acid and 15 ml of concentrated hydrochloric acid. The *Aqua Regia* solutions plus soil samples were heated on a hot plate over its boiling point (108^{o}C) in a fume cupboard until 5 ml remained. The digest was then filtered through a quantitative filter paper (9 mm diameter) and the filtrate was diluted to 50 ml with ultra-pure ('Milli-Q') deionised water (~1.70 % of nitric acid remain). Finally, it was 10 times re-diluted with ultra-pure ('Milli-Q') deionised water before analysis by ICP-MS. Final sample for ICP-MS analysis was about 0.17 % of nitric acid.

2.4.4.2 Nitric acid digestion of pine needle samples

Approximately 1 g of ground pine needles was digested in 20 ml of concentrated nitric acid on a hot plate over its boiling point (83^{o}C) in a fume cupboard until the acid volume was reduced to approximately 5 ml. The digest was filtered through a quantitative filter paper (9 mm diameter) and the filtrate was then diluted to 50 ml with ultra-pure ('Milli-Q') deionised water (~6.80 % of nitric acid remain). Sample solution was 10 times re-diluted with ultra-pure ('Milli-Q') deionised water before analysis by ICP-MS. Final sample for ICP-MS analysis was about 0.68 % of nitric acid.

2.4.4.3 Nitric acid digestion of tree core samples

After measuring the widths of annual growth rings in the tree cores, sub-samples consisting of five adjacent growth rings (representing growth periods of five years) were cut from each core and dried in an oven at 105^{o}C for 8 hr. The dried tree core sub-samples were ashed in individual ceramic crucibles within a furnace for 4 hr. The temperature of the furnace was programmed to increase from laboratory temperature at a rate of 14°C per minute, reaching a peak

temperature of 550°C. The ash of each sub-sample was extracted at laboratory temperature with 0.5 ml of conc. HNO_3 until the solution became clear. The acid extract was then diluted with ultra-pure ('Milli-Q') deionising water to a final volume of 10 ml (~3.40 % of nitric acid remain). Sample solution was 10 times re-diluted with ultra-pure ('Milli-Q') deionised water before analysis by ICP-MS. Final sample for ICP-MS analysis was about 0.34 % of nitric acid.

2.4.5 Determination of exchangeable (available) concentrations of stable caesium (^{133}Cs) and its competitive nutrients in soil samples

Exchangeable fractions of stable caesium and other elements in the forest soil samples were extracted using 1M ammonium nitrate. The following procedure is adapted from Rowell (1994).

Approximately 2 g of moist soil sample were weighed into an Oak Ridge centrifuge tube containing 10 ml of 1M ammonium nitrate. After shaking on an end-over-end shaker for 1 hour, the suspension was filtered through a quantitative filter paper (9 mm diameter). The filtrate (~5 ml) was kept in a cold room at 4°C awaiting analysis of stable caesium and its competitive elements by ICP-MS. The filtrate was 10 times diluted with 2% of nitric acid before analysis by ICP-MS.

The exchangeable fractions of stable caesium and competitive elements were calculated using equation 2.2 below.

$$\alpha_{Ex} = (A_{Ex}/A_S) \times 100 \qquad (2.2)$$

When α_{Ex} = Exchangeable fraction (%)

A_{Ex} = Concentration of caesium extracted from soil using 1M NH_4NO_3 (mg kg^{-1})

A_S = Total concentration of caesium extracted from soil using *Aqua Regia* (mg kg^{-1})

2.4.6 Determination of ^{137}Cs, ^{40}K and ^{210}Pb

A high resolution gamma-ray spectrometry system with a high-purity germanium (HP-Ge) detector (suitable for <50 – ~2,000 keV) wide range measuring of gamma energy) was used to determine the activity concentrations of ^{137}Cs (661.7 keV), ^{40}K (1,460 keV), and ^{210}Pb (59.5 keV), in soil samples. The analytical procedure was as follows.

2.4.6.1 Preparation of samples

Before counting by gamma-ray spectrometry samples were prepared using different methods, as appropriate to the type of sample.

Dried and ground soil samples were packed into plastic Petri dishes of two different sizes (5.4 cm and 3.5 cm diameter). The internal volume of the Petri dish was completely filled with sample and the dish plus loose-fitting lid were sealed using Parafilm®. The 5.4 cm diameter Petri dishes were used for Boundary Plantation soil samples while 3.5 cm Petri dishes were used for Thai forest soil samples, for which less mass of sample was available. Chernobyl forest soil samples were analysed at the Chornobyl Center for Nuclear Safety, Radioactive Waste and Radioecology in Slavutych (Ukraine) by using their own method by their staff.

Only pine needles collected at Kopachi (Chernobyl) were sufficiently radioactive of ^{137}Cs to be measured by gamma-ray spectrometry (pine needles collected at Boundary Plantation and Wat Ban Chan were very low radioactivity of ^{137}Cs and undetectable by gamma-ray spectrometry. For this analysis, pine needles were air dried and milled then packed into a 3.5 cm diameter Petri dish, completely filling the dish. Radioactivity of ^{137}Cs calculated using efficiency of milled litter prepared in same geometry (T004.6) and nearly density as explained in section 2.4.6.2.

As with the pine needles, only the tree cores collected at Kopachi (Chernobyl) forest were sufficiently radioactive of ^{137}Cs to be measured by gamma-ray spectrometry (tree cores collected at Boundary Plantation and Wat Ban Chan were very low radioactivity of ^{137}Cs and undetectable by gamma-ray spectrometry). They were air dried and cut into lengths representing growth periods of ten years. Each ten-year piece was then analysed separately by gamma-ray spectrometry.

2.4.6.2 Efficiency calibration of gamma-ray spectrometry system for forest soil samples

An accurate efficiency calibration is needed to convert gamma-ray counts obtained by the gamma-ray spectrometry system to nuclear disintegrations per second (i.e. becquerels). To achieve this, a standard sample (or samples) of known radioactivity is needed, which matches the samples to be counted as closely as possible in size and shape (geometry) and density. As described above, plastic Petri dishes of two different sizes (5.4 cm and 3.5 cm diameter) were used to provide standard sample geometries in this study. The forest soils sampled ranged in characteristics from almost purely organic matter to almost purely sand so, to represent this range, standards in each geometry were made up using sand (sulfuric acid washed), homogenised garden compost and homogenised deciduous leaf litter, representing mineral soil, organic soil and litter, respectively. All media used to make up standards were oven dried and sieved at 1 mm to remove any unwanted material such as stones and large pieces of organic matter. Pre-weighed masses of the homogenised media were mixed in plastic containers with a solution of a certified mixed gamma standard obtained from the National Physical Laboratory (NPL, Teddington, UK) (R08-01-2016040167-1; radionuclides and activity concentrations are shown in Table 2-2). This standard is accompanied by a non-radioactive carrier solution containing stable isotopic salts of each of the radionuclides in the mixed gamma solution. An equivalent volume of this solution was also added to the standards to reduce localise sorption of the radionuclides which would lead to inhomogeneous mixing of the radionuclides in the standard matrix. The exact masses of sieved media, mixed gamma standard and carrier solution were recorded.

Table 2-2 List of radionuclides and their activities in the NPL mixed gamma standard solution on the reference date (1st June 2016)

Nuclide/Activity (Bq kg^{-1})											
^{57}Co	^{139}Ce	^{113}Sn	^{85}Sr	^{241}Am	^{88}Y	^{54}Mn	^{137}Cs	^{60}Co	^{65}Zn	^{51}Cr	^{109}Cd
110	137	348	429	526	519	541	587	627	1,125	2,216	2,920

After mixing, each standard was left open to the atmosphere for up to one week in a stream of air in a fume cupboard until completely dry. Each standard was

then homogenised and used to fill completely one 5.4 cm Petri dish and one 3.5 cm Petri dish. All mixed gamma standards were coded as shown in Figure 2-5 and Table 2-3.

The radioactivity of each radionuclide (*Bq*) was corrected to the date of counting using equation 2.3.

$$A = A_0 e^{-\lambda t} \qquad (2.3)$$

Where A = Radioactivity of radionuclide at counting date (Bq)

A_0 = Radioactivity of radionuclide at reference date (1st June 2016) (Bq)

λ = Decay constant of radionuclide (y^{-1})

(= [ln2]/half live of radionuclide)

t = time between reference date and counting date (y)

Figure 2-5 Mixed gamma standards prepared homogeneously with milled litter, compost and sand in 3.5 and 5.4 cm diameter Petri dishes.



All mixed gamma standards were counted for at least 24 hours on a gamma-ray spectrometry system consisting of two high purity germanium detectors (Canberra). Using Canberra's Genie 2000® gamma acquisition and analysis software, individual peak areas associated with the multiple radionuclides in the standards were recorded and expressed as gamma-ray counts per second. The efficiency of collection of these counts can be calculated using equation 2.4.

$$\varepsilon = \frac{cps}{Bq(1/\gamma)} \qquad (2.4)$$

Where ε = Efficiency of gamma counting system at specific energy

cps = Counting rate of specific gamma peak (cps)

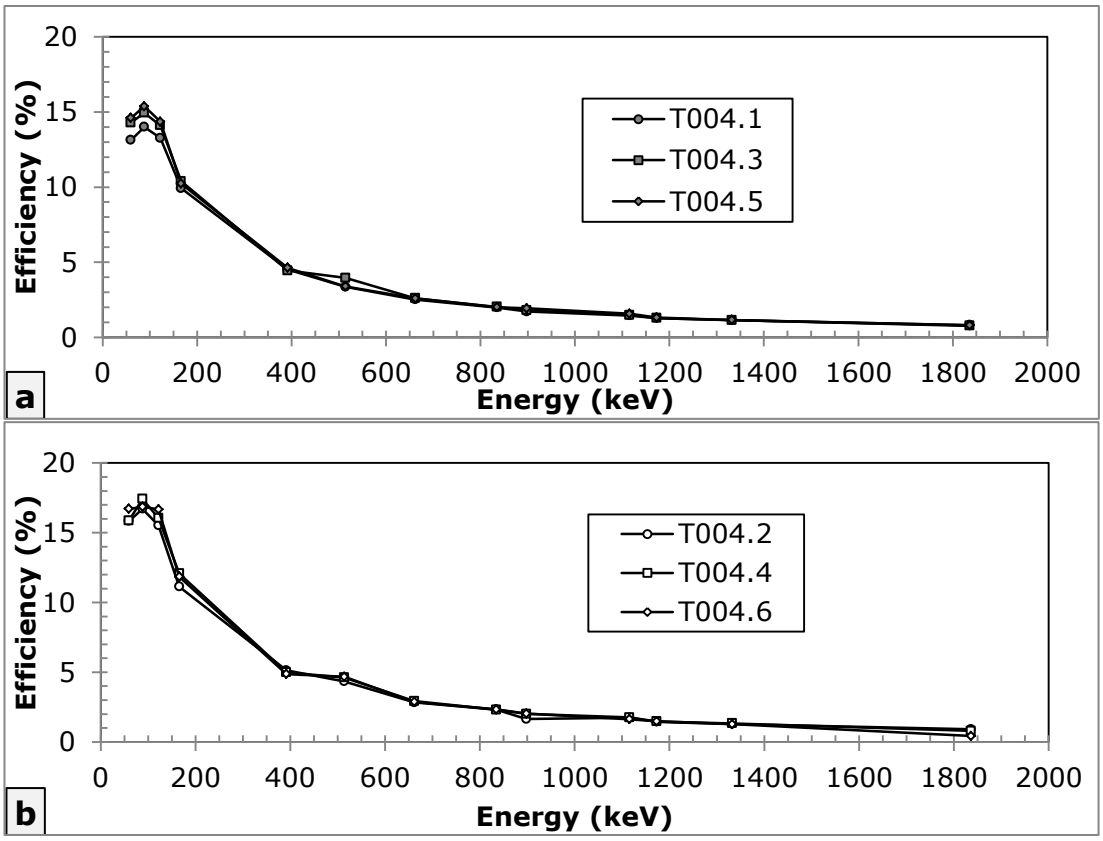
Bq = Radioactivity of specific radionuclide (Bq)

γ = Gamma-ray emission intensity

Idealised gamma energy vs. counting efficiency curves were calculated for each geometry/standard medium combination using Canberra's Genie 2000® software, as shown in Figure 2-6.

Radionuclides measured in this research were ^{137}Cs, ^{40}K and ^{210}Pb. However, only the counting efficiency of ^{137}Cs could be calculated directly from the counts obtained for the 661.67 keV photopeak obtained from each standard. ^{40}K and ^{210}Pb were not included in the mixed gamma standard so their efficiencies could not be calculated directly from their photopeaks. The counting efficiency of ^{40}K for its 1,460.83 keV photopeak was obtained by extrapolation between the efficiencies obtained for the 1,332.5 keV photopeak of ^{60}Co and the 1,836.1 keV photopeak of ^{88}Y. The counting efficiency of ^{210}Pb was obtained by counting the reference material IAEA-447 ('moss soil' containing 0.42 x 10^3 Bq kg^{-1} of ^{210}Pb on reference date 15/11/2009) in Petri dishes with 5.4 and 3.5 cm diameter and determining the area of the photopeak at 46.59 keV. The counting efficiencies of these three radionuclides in different sample matrices in 5.4 and 3.5 cm diameter Petri dishes are summarised in Table 2-3.

Figure 2-6 Optimised efficiency calibration curves for 5.4 cm (a) and 3.5 cm (b) diameter Petri dishes with NPL mixed gamma standards in three matrices of different densities (see Table 2-3 for sample codes).



Disregarding other factors, gamma-ray counting efficiency is negatively correlated with the size of a sample (Harb et al., 2009). Table 2-3 shows that counting efficiencies for ^{137}Cs, ^{40}K and ^{210}Pb were higher for the smaller Petri dish diameter.

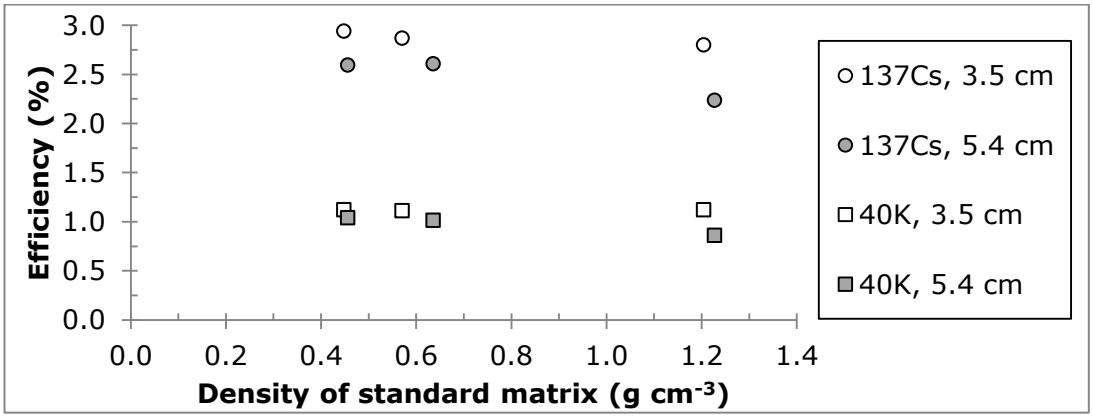
As well as geometry, the density of a standard or sample is also an important factor influencing counting efficiency. Figure 2-7 indicates that the density of each standard was negatively correlated with counting efficiency which is consistent with Harb et al. (2009) and Metzger et al. (2016).

These results confirm that different sample geometries and densities both significantly change the counting efficiencies for ^{137}Cs and ^{40}K using a high resolution gamma spectrometry system. The efficiencies obtained from this experiment were reasonable and applicable for calculation of sample activity concentrations in this research.

Table 2-3 Calculated counting efficiencies for ^{210}Pb (46.59 keV), ^{137}Cs (661.67 keV) and ^{40}K (1,460.83 keV) in different sample matrices in 5.4 and 3.5 cm diameter Petri dishes.

Code	Medium type	Density (g cm^{-3})	Petri dish diameter (cm)	Efficiency (%)		
				^{137}Cs	^{40}K	^{210}Pb
T004.1	sand	1.43	5.4	2.53	0.86	13.03
T004.2	sand	1.39	3.5	2.84	1.12	16.90
T004.3	compost	0.60	5.4	2.61	1.01	13.03
T004.4	compost	0.55	3.5	2.94	1.11	16.90
T004.5	leaf litter	0.54	5.4	2.61	1.04	13.03
T004.6	leaf litter	0.50	3.5	2.87	1.12	16.90

Figure 2-7 Correlations of the counting efficiencies of ^{137}Cs and ^{40}K with density of the standard matrix.



2.4.6.3 Calculation of ^{137}Cs, ^{40}K and unsupported ^{210}Pb

^{137}Cs and ^{40}K activity concentrations were directly calculated using equation 2.5.

$$\boldsymbol{Bq(\gamma) = \frac{cps}{\varepsilon I W}} \qquad (2.5)$$

Where Bq = calculated activity concentration of sample (Bq kg^{-1})

Cps = counts per second obtained from the area of the peak of interest (661.67 keV for ^{137}Cs; 1,460 keV for ^{40}K, cps)

I = gamma ray intensity of the peak of interest (0.85 for ^{137}Cs; 0.11 for ^{40}K)

W = weight of sample (kg)

$\boldsymbol{\varepsilon}$ = efficiency of detection of the peak of interest

Activity concentrations of unsupported ^{210}Pb were calculated by subtracting the activity of supported ^{210}Pb (obtained from the average activities of ^{214}Pb and ^{214}Bi) from total ^{210}Pb.

$$^{210}Pb_{UN} = {}^{210}Pb_T - {}^{210}Pb_{SU} = {}^{210}Pb_T - [(^{214}Pb + {}^{214}Bi)/2] \qquad (2.6)$$

Where $^{210}Pb_{UN}$ = activity concentration of unsupported ^{210}Pb (Bq kg^{-1})

$^{210}Pb_T$ = activity concentration of total ^{210}Pb (Bq kg^{-1})

$^{210}Pb_{SU}$ = activity concentration of supported ^{210}Pb (Bq kg^{-1})

^{214}Pb = activity concentration of ^{214}Pb (Bq kg^{-1})

^{214}Bi = activity concentration of ^{214}Bi (Bq kg^{-1})

$^{210}Pb_T$, ^{214}Pb and ^{214}Bi were calculated using equation 2.5.

2.4.6.4 Decay correction for ^{137}Cs

Deposition of ^{137}Cs in Boundary Plantation and Wat Ban Chan Pine forests was from atomic weapons fallout which peaked in 1963 (Cambray, 1989) whilst in Chernobyl forests measurable deposition was from the Chernobyl accident in 1986. Radioactivity of ^{137}Cs reported in this research was corrected to the initial year of deposition using the following equation.

$$A_0 = A \times exp(k \times t) \qquad (2.7)$$

Where A = Radioactivity of ^{137}Cs at counting time (Bq)

A_0 = Initial radioactivity of ^{137}Cs (Bq)

t = time between counting and initial deposition time (y)

k = $\ln(2) / t_{1/2}$

$t_{1/2}$ = half-life of ^{137}Cs = 30.05 (y)

2.4.6.5 Quality Assurance for ^{137}Cs and ^{40}K

IAEA reference material IAEA-447 ('moss soil') was used to check the accuracy and repeatability of measurements of ^{137}Cs and ^{40}K activity concentrations in soil and tree samples. The certified activity concentrations for ^{137}Cs and ^{40}K are 425 ($\pm$10) Bq kg^{-1} and 550 ($\pm$20) Bq kg^{-1}, respectively. Random checks of gamma-ray spectra were made to verify the accuracy of the data collected from two high purity germanium detectors.

2.4.7 Measuring annual tree growth ring width

Every year the seasonal cycle of tree growth in spring and summer, followed by dormancy in winter, results in the formation of clearly identifiable 'early' and 'late' growth rings in the trunk of the tree. These provide a record of tree growth which can be quantified by measuring the width of the tree's annual rings. Tree cores, taken as described in section, 2.2, provide convenient samples for this type of tree growth analysis.

Having obtained tree cores from each of the sampling sites, the widths of annual growth rings were measured using a low power binocular microscope. An eye-piece graticule was calibrated against a millimetre scale placed on the microscope stage and subsequently used to measure growth ring widths in millimetres.

2.4.8 Isotopic exchange of caesium

Isotopic exchange of ^{133}Cs with ^{134}Cs was investigated using an approach which was an extension of the method to determine exchangeable (available) concentrations of stable caesium, previously described in section 2.4.5. The resulting E-value gives an indication of the concentration of ^{133}Cs which may be labile (ie. chemically and/or biologically reactive) but not immediately exchangeable (Hamon et al., 2008).

A mass of field moist soil which was equivalent to 2 g of dry soil was weighed into a 50 ml 'Falcon' tube and 20 ml of 1M NH_4NO_3 then added. Next, a 391 Bq 'spike' of ^{134}Cs tracer was injected, the tube was capped and shaken end-over-end for 1, 24 or 168 hrs. After shaking, the tubes were centrifuged for 15 minutes at 3,000 RPM then an aliquot of the supernatant was passed through a 0.22 µm syringe filter. An aliquot of ^{134}Cs tracer in 10 ml of 1M NH_4NO_3 was prepared as a blank (final activity of ^{134}Cs is 19.5 Bq ml^{-1}). Finally, the filtered and blank solutions were directly counted by gamma ray spectrometry to determine the ^{134}Cs activity concentration using the procedure described in sections 2.4.7.3 and 2.4.7.4 (10 ml filtered and blank samples were prepared in Universal tubes and counted for 1 hour).

The isotopic exchange (E-value) was calculated using the following equation.

$$E\text{-}value = \frac{^{133}Cs_{Ex} \times {}^{134}Cs_{B}}{^{134}Cs_{S}} \qquad (2.8)$$

Where E-value = Isotopically exchangeable ^{133}Cs (mg kg^{-1})

$^{133}Cs_{Ex}$ = Concentration of NH_4-exchangeable ^{133}Cs (mg kg^{-1}) in soil (A_{Ex} in section 2.4.6)

$^{134}Cs_{B}$ = Activity of ^{134}Cs in blank (cps or Bq)

$^{134}Cs_{S}$ = Activity of ^{134}Cs in soil solution (cps or Bq)

CHAPTER 3: BOUNDARY PLANTATION, SHERWOOD FOREST

3.1 INTRODUCTION

3.1.1 Objectives

The long-term migration and recirculation behaviour of caesium in Boundary Plantation (Sherwood Forest) and possible related factors were investigated to test the hypotheses as follows.

- Within rich-organic layer of temperate-forest soil ^{137}Cs largely accumulated within the organic layer, clay mineral (if any) and organic matter content play important role on fixation of ^{137}Cs and supporting such fixation.
- Organic matter and soil pH effect on circulation of ^{137}Cs and ^{133}Cs in forest ecosystems particularly related to their exchangeabilities in forest soil.
- Stable potassium and rubidium are the important competitors on circulation of ^{137}Cs and ^{133}Cs in the forest ecosystems.
- Stable caesium is the suitable indicator of radiocaesium within the forest ecosystems.

3.1.2 Sample collection sites

Boundary Plantation (Sherwood Forest) is a plantation of Corsican pine (*Pinus nigra)* managed by the Forestry Commission. The plantation was the primary sampling site for this study, adjacent to Budby Heath, Nottinghamshire, UK. This area received chronic distribution of atmospheric fallout from nuclear weapon tests in the 1960s. The soil is podzolic, similar to many other coniferous forests in the temperate zone, comprising a thick organic layer with sand (derived from Sherwood sandstone) underneath.

Forest samples were collected every three months from June 2014 to March 2015. The random co-ordinates of each sampling point are presented in Figure 3-1 and Table 3-1. Soil cores and tree cores were collected at all sampling

points but, due to inaccessibility, fresh needles were not collected at sites 8, 10 – 12 whilst dry needles were collected only at site 13 – 24.



Figure 3-1 The 24 sampling points at Boundary plantation (Sherwood Forest), United Kingdom (picture captured from Google Earth).

Table 3-1 Random coordinates of 24 sampling points visited during four field trips to Boundary Plantation, Sherwood Forest (coordinates are shown in the Ordnance Survey GB system).

26th June 2014		*30th September 2014*		*18th December 2014*		*19th March 2015*	
Site no.	*Coordinates*	*Site no.*	*Coordinates*	*Site no.*	*Coordinates*	*Site no.*	*Coordinates*
1	*SK59997 68944*	*7*	*SK60178 69065*	*13*	*SK60187 68809*	*19*	*SK60368 69191*
2	*SK60086 68873*	*8*	*SK60111 69111*	*14*	*SK60059 68807*	*20*	*SK60153 69132*
3	*SK60087 68802*	*9*	*SK60060 69113*	*15*	*SK60108 68879*	*21*	*SK60129 68988*
4	*SK60210 68754*	*10*	*SK60372 68851*	*16*	*SK60377 68659*	*22*	*SK55982 68829*
5	*SK60372 68904*	*11*	*SK60116 68816*	*17*	*SK60294 68636*	*23*	*SK60281 68683*
6	*SK60279 68834*	*12*	*SK60041 68837*	*18*	*SK60043 68858*	*24*	*SK60386 69049*

3.2 RESULTS

3.2.1 Soil properties

Soil cores were taken to a depth of 18 cm at Boundary Plantation. The fundamental soil properties investigated were soil pH, organic matter content and clay mineralogy, as described below.

3.2.1.1 Organic matter and identification of organic and mineral soil layers

Organic matter content in soil profiles was measured using loss on ignition (LOI - see section 2.4.1 for details of methods); the results are shown in Figure 3-2.

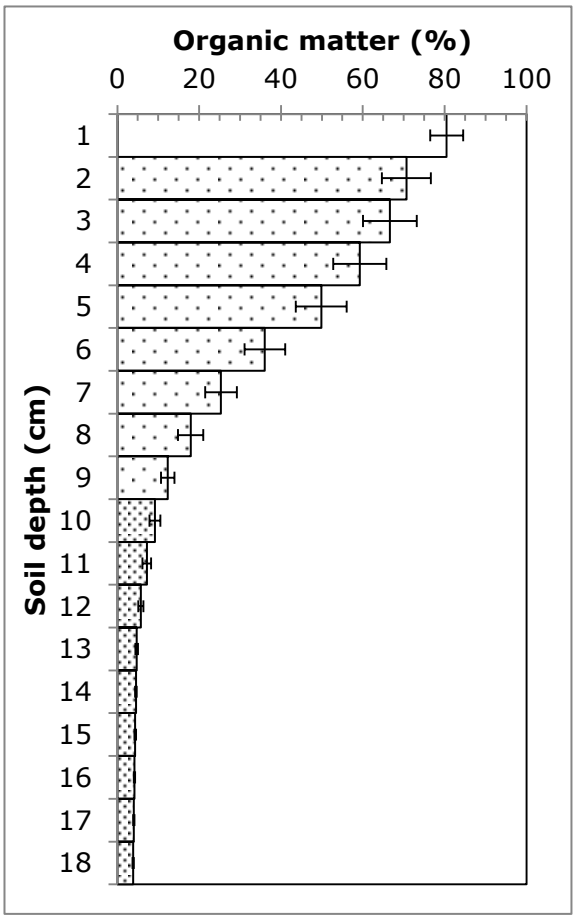


Figure 3-2 Depth profile of average organic matter content of soil collected at Boundary Plantation (24 replicates, the horizontal bars show standard errors of means).

The organic matter content of the soil was highest in the upper part of the soil profile, corresponding to the litter layer on the forest floor, decreasing

systematically with soil depth. The maximum average organic matter content was 81% in the litter layer and the minimum was 4% in the deepest part of the soil cores (18 cm depth). The variability of organic matter, as measured by the standard deviation, was generally greater in the upper part of the soil cores than lower down. The photograph of a typical soil core in Figure 3-3 shows that macroscopic remains of tree litter were identifiable to a depth of 4 - 5 cm and that dark staining of incorporated humic matter was visible down to a depth of 10 - 11 cm.

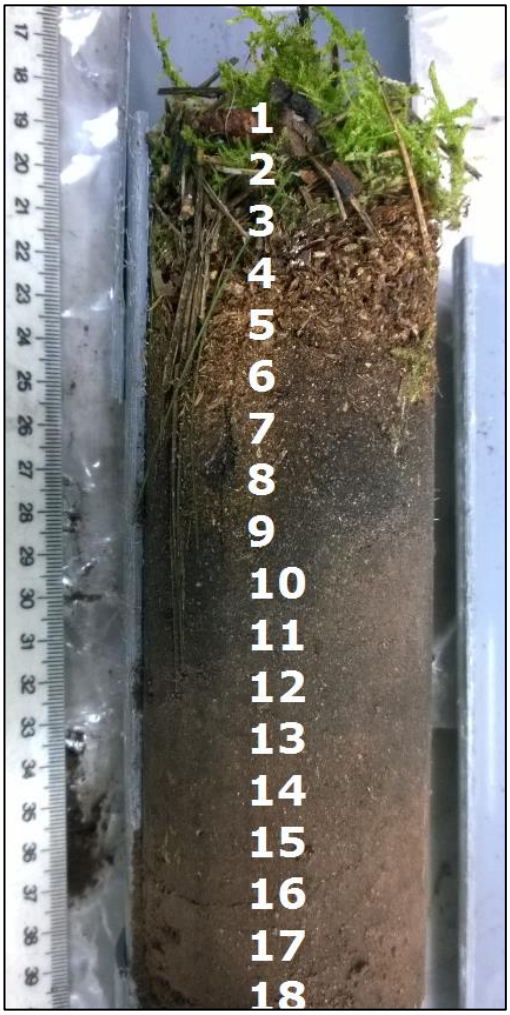


Figure 3-3 A typical soil core taken at Boundary Plantation; the numbers 1 to 18 show the depth of soil layers in centimetres.

The boundary between organic and mineral layers in the soil profile is highly variable, but identifying where this boundary occurs is necessary for the analysis of stable and radiocaesium in the forest soil. This is because the behaviour of stable and radiocaesium in organic and mineral parts of the soil profile are

expected to differ due to differences in their interaction with organic and mineral soil components.

To identify the boundary between organic and mineral layers in the soil horizon a LOI value of 12% was used, based on the United States Department of Agriculture and the Food and Agriculture Organisation of the United Nations (USDA, 1999; FAO, 1998) definitions of 'organic soil'. On this basis the upper 9 cm of the soil profile at Boundary Plantation was considered to be 'organic soil'.

In addition to the simple classification based on 12% LOI, one-way ANOVA, with Tukey's 95% confidence *post hoc* comparisons, was applied to investigation the effect of soil depth on organic matter content; the results are shown in Table 3-2.

Table 3-2 Result of one-way ANOVA with Tukey 95% confidence post hoc comparisons using Minitab Software (n=24) to investigate the effect of soil depth on organic matter content in soil cores collected at Boundary Plantation (means that do not share a common letter are significantly different).

Factor	Type	Levels	Values
Depth (cm)	fixed	18	1, 2, 3, 4, 5, 6, 7, 8, 9, 10, 11, 12, 13, 14, 15, 16, 17, 18

Grouping Information Using Tukey Method and 95.0% Confidence

Depth (cm)	N	Mean	Grouping
1	24	80.503	A
2	24	70.666	A B
3	24	66.629	A B
4	24	59.243	B C
5	24	49.845	C D
6	24	36.050	D E
7	24	25.324	E F
8	24	17.927	F G
9	24	12.319	F G
10	24	9.202	F G
11	24	7.215	G
12	24	5.771	G
13	24	4.761	G
14	24	4.540	G
15	24	4.351	G
16	24	4.162	G
17	24	4.014	G
18	24	3.851	G

The results of the ANOVA indicate that the boundary between organic and mineral soil layers is in the region of 8 – 10 cm depth which confirms the identification of an organic-mineral boundary depth of 9 cm based on USDA / FAO criteria.

For all subsequent analyses of soils from Boundary Plantation it was assumed that the upper 9 cm of the soil profile was 'organic' soil and that deeper layers (> 9 cm depth) were 'mineral' in composition.

3.2.1.2 Soil pH

Soil pH is another factor which is likely to exert a significant effect on stable and radiocaesium behaviour in forest soil. Soil pH of the soil cores collected at Boundary Plantation was measured layer-by-layer (see section 2.4.2 for details of methods) as illustrated in Figure 3-4.

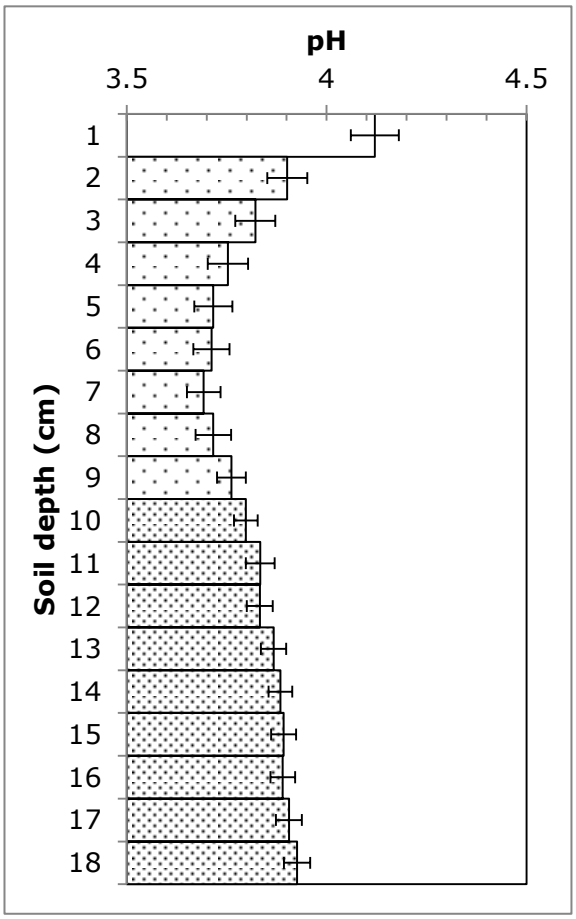


Figure 3-4 Depth profile of average of soil pH of organic (1 – 9 cm depth) and mineral layers (deeper than 9 cm depth) of soil cores collected at Boundary Plantation (24 replicates, the horizontal bars show standard errors of means).

Soil pH at Boundary Plantation ranged between 3.69 in the middle of the organic soil (7 cm depth) to 4.12 in the litter layer. Associated H^+ produces by

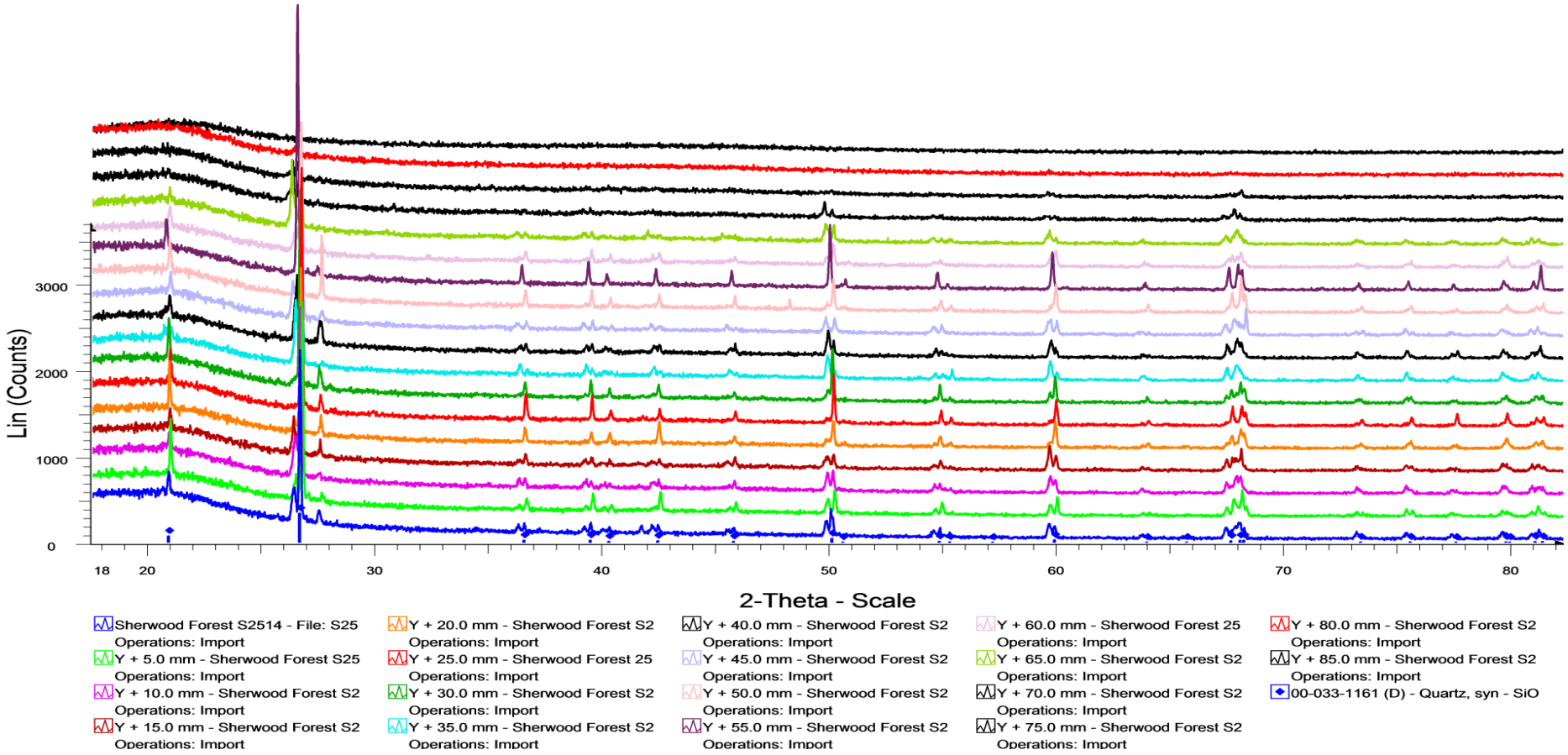
decomposition process of organic matter, resulting in lower soil pH suggests that the decomposition of organic matter was complete at 7 cm depth and no undecomposed organic matter was likely to remain below this depth.

3.2.1.3 Mineralogy

Samples from each 1 cm layer within the Boundary Plantation soil cores were analysed to investigate changes in mineralogy down the soil profile using X-Ray Diffraction (XRD - see section 2.4.3 for details of methods). The diffraction patterns (diffractograms) of all 18 depth samples of the soil profile are shown in Figure 3-5.

The XRD results suggest that the upper 2 cm depth of soil (litter layer) contained amorphous, non-crystalline material (ie. only organic matter) whilst, below 2 cm depth, quartz was the only major crystalline phase. At some depths there was evidence of a second phase with reflections around the major quartz reflections. This is typical of the plagioclase group feldspars e.g. labradorite, albite, microcline ($M(AlSi)_4O_8$). Significantly, there was no indication of low-angled reflections belonging to any layered clay minerals which might be implicated in the specific sorption of caesium isotopes (Dann, pers. comm.). The intensity of the quartz signal increased steadily from 2 cm to 7 cm depth, indicating a progressively larger sand content with depth within the organic part of the soil profile.

Figure 3-5 Overlaid XRD diffractograms of 18 soil samples representing 1 to 18 cm depths (from uppermost to lowermost samples) of the soil profile at Boundary Plantation. The Y axis represents intensity (related to only the lowermost spectrum of the 18 cm depth sample), the X axis is 2Theta (2Θ, degree of diffraction) of the Bragg equation.



3.2.2 Vertical distributions of ^{133}Cs, ^{39}K, ^{85}Rb and ^{137}Cs in forest soil

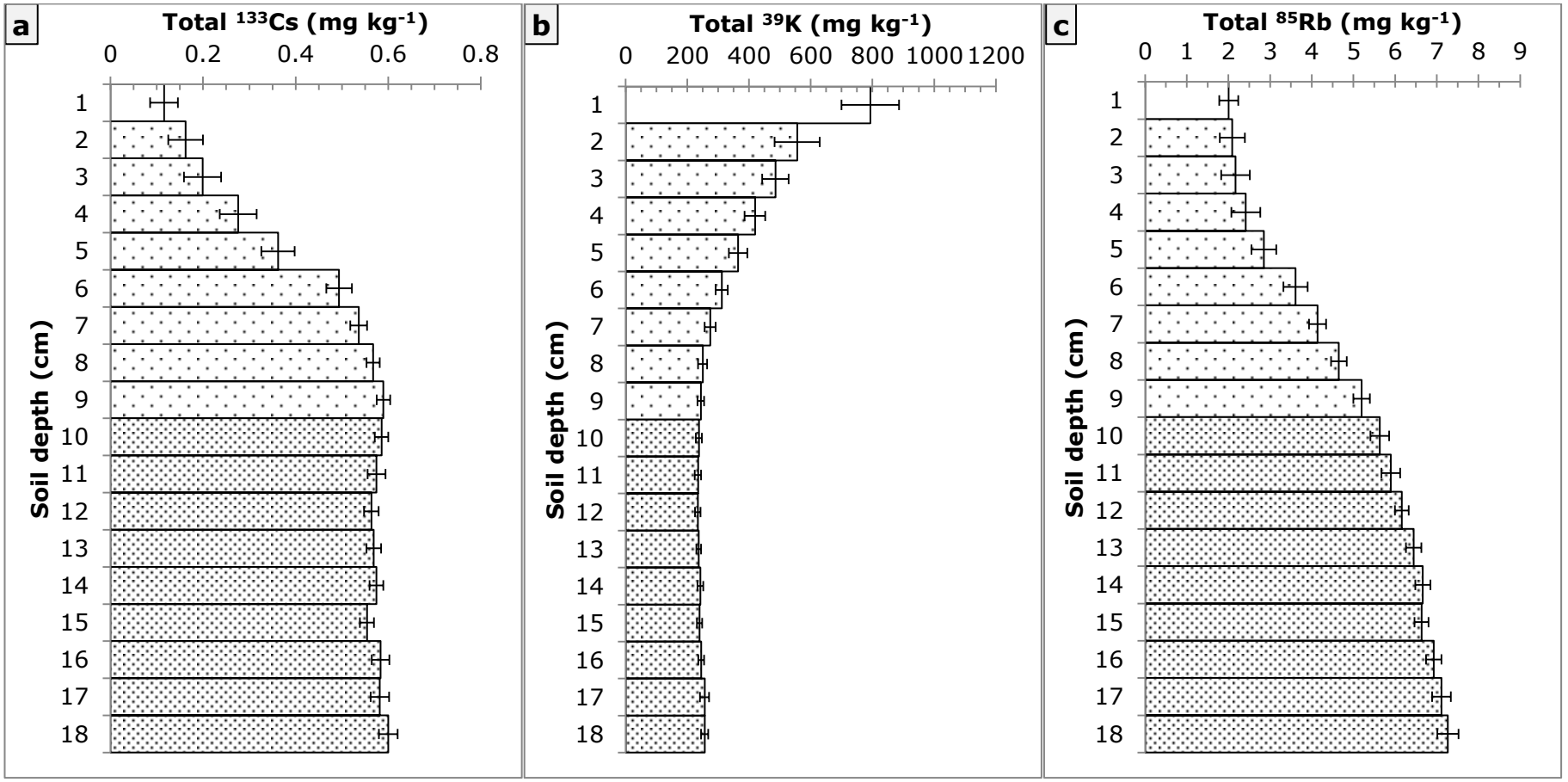
Vertical distributions of total, exchangeable and fixed concentrations of ^{133}Cs, ^{39}K and ^{85}Rb including activity concentration of ^{137}Cs were measured throughout the 18 cm soil cores collected at Boundary Plantation; the results are presented below.

3.2.2.1 Total ^{133}Cs, ^{39}K and ^{85}Rb

Vertical distributions of average total concentrations of ^{133}Cs, ^{39}K and ^{85}Rb throughout the upper 18 cm of the Boundary Plantation soil profile are shown in Figure 3-6.

The results illustrate that total ^{133}Cs and ^{85}Rb concentrations were minimal at 0.12 and 2.01 mg kg^{-1}, respectively, in the litter layer (1 cm depth). In contrast, total ^{39}K concentration was at its maximum (793 mg kg^{-1}) in this layer. Maximal ^{133}Cs and ^{85}Rb concentrations were both found within the mineral soil layers (10 - 18 cm depth; ranging from 0.55 - 0.60 mg kg^{-1} and 5.63 - 7.27 mg kg^{-1} respectively) where total average ^{39}K concentrations (234 - 256 mg kg^{-1}) were minimal. Total concentrations of ^{133}Cs, ^{85}Rb and ^{39}K were in the ranges of UK soil (Rawlins et al., 2012)

Figure 3-6 Depth profiles of average total concentrations of ^{133}Cs (a), ^{39}K (b) and ^{85}Rb (c) within organic (1 – 9 cm depth) and mineral layers (deeper than 9 cm depth) of soil collected at Boundary Plantation (24 replicates, the horizontal bars are standard errors of means).



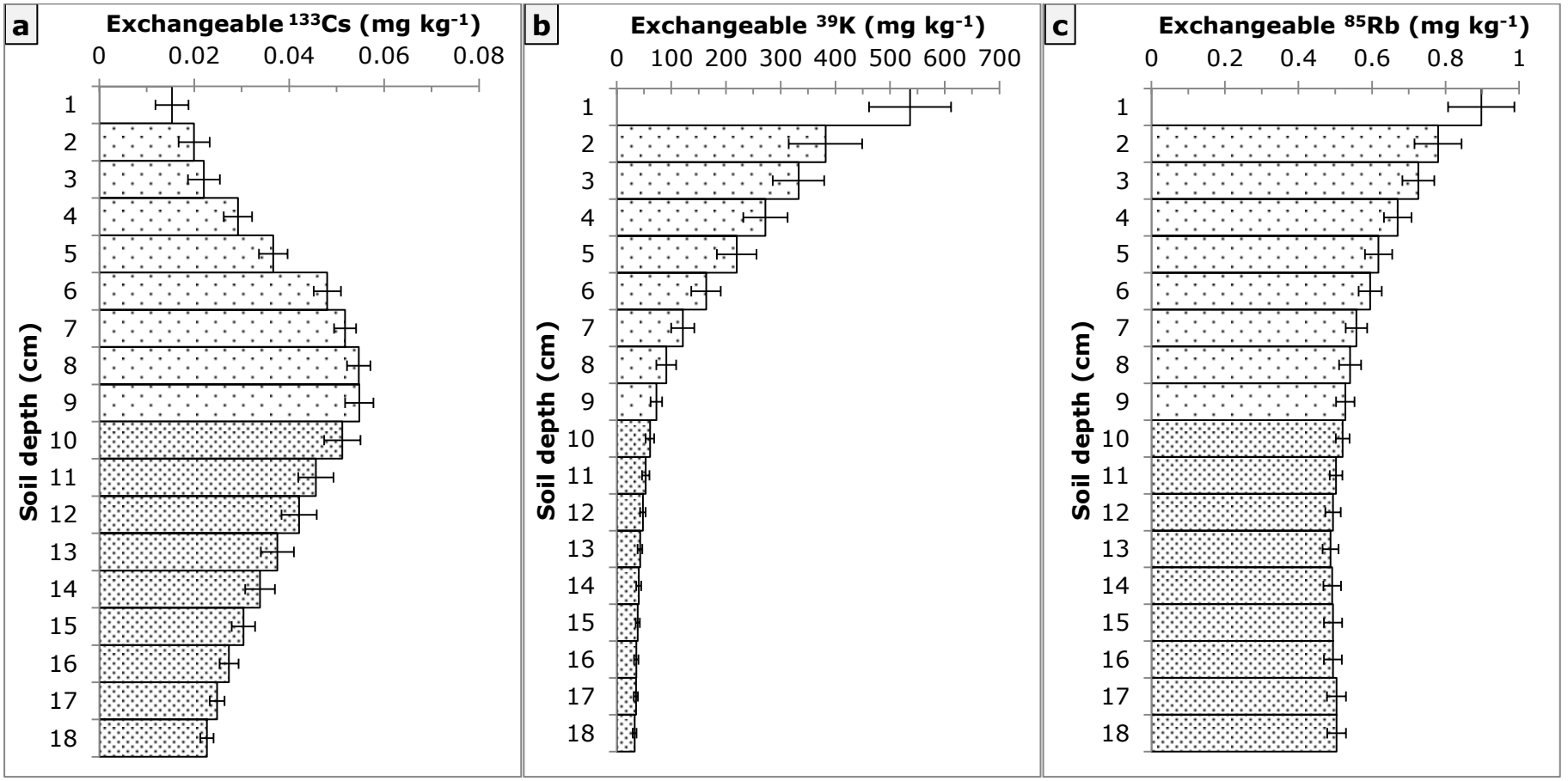
3.2.2.2 Exchangeable ^{133}Cs, ^{39}K and ^{85}Rb

Vertical distributions of exchangeable concentrations of ^{133}Cs, ^{39}K and ^{85}Rb throughout the Boundary Plantation soil profile are shown in Figure 3-7.

The distribution of exchangeable ^{133}Cs was symmetrical between the upper (organic) and lower (mineral) parts of the soil profile, with the maximum exchangeable concentration (0.055 mg kg^{-1}) at the centre of the distribution at 9 cm depth. Minimum exchangeable concentrations were in the uppermost (litter) and lowermost (18 cm depth) layers at 0.015 and 0.023 mg kg^{-1}, respectively.

The vertical distributions of exchangeable ^{39}K and ^{85}Rb were similar, with the highest concentrations in the litter layer at 536 and 0.9 mg kg^{-1}, respectively, and the minimum concentrations in the mineral soil (35.2 and 0.49 mg kg^{-1}, respectively).

Figure 3-7 Depth profiles of average exchangeable concentrations of ^{133}Cs (a), ^{39}K (b) and ^{85}Rb (c) within organic (1 – 9 cm depth) and mineral layers (deeper than 9 cm depth) of soil cores collected at Boundary Plantation (24 replicates, the horizontal bars are standard errors of means).

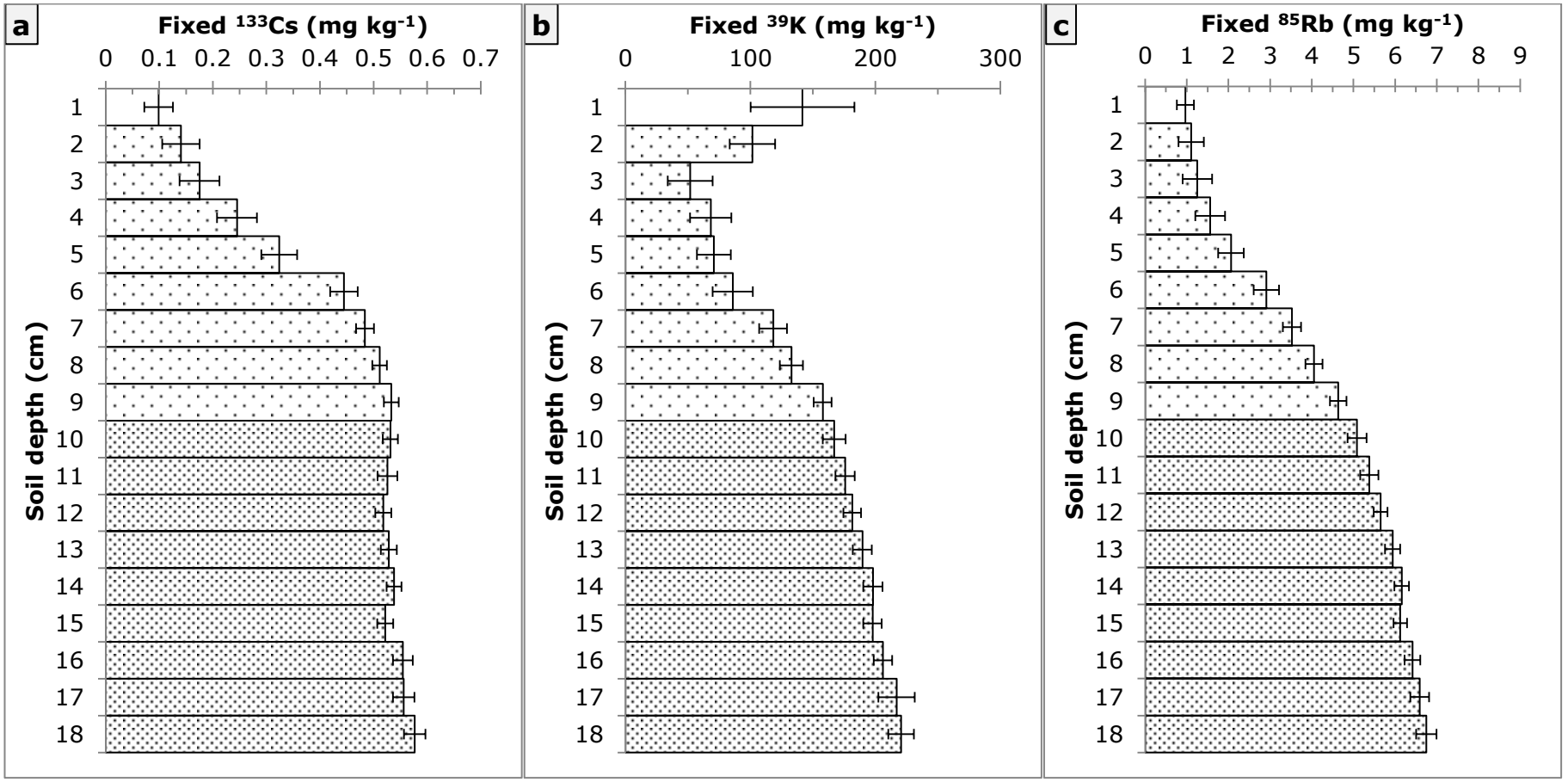


3.2.2.3 Fixed ^{133}Cs, ^{39}K and ^{85}Rb

'Unavailable' or 'fixed' concentrations of ^{133}Cs, ^{39}K and ^{85}Rb were calculated by subtraction of exchangeable from total concentrations. The vertical distributions of unavailable concentrations throughout the 18 cm depth of the soil cores are shown in Figure 3-8.

As with the total concentrations, the fixed fraction of ^{39}K was much higher in absolute concentration units than for ^{133}Cs and ^{85}Rb throughout the soil profile. The vertical distribution of fixed ^{133}Cs was qualitatively very similar to its total concentration, with minimum fixed ^{133}Cs (0.10 mg kg^{-1}) in the uppermost layer, maximum fixed ^{133}Cs (0.48 – 0.58 mg kg^{-1}) in the lower part of the organic soil (7 - 9 cm) and throughout the mineral soil (below 9 cm depth). Fixed ^{85}Rb also showed a qualitatively very similar distribution to its total concentration. Fixed ^{39}K, however, was minimal (51.9 mg kg^{-1}) in the middle of the organic layer (3 - 5 cm) with higher values in the upper and lower parts of the organic soil. The maximum fixed ^{39}K (221 mg kg^{-1}) was in the mineral lower part of the soil profile.

Figure 3-8 Depth profiles of average 'unavailable' concentrations of ^{133}Cs (a), ^{39}K (b) and ^{85}Rb (c) of organic (1 – 9 cm depth) and mineral layers (deeper than 9 cm depth) of soil collected at Boundary Plantation (24 replicates, the horizontal bars are standard errors of means).



3.2.2.4 ^{137}Cs

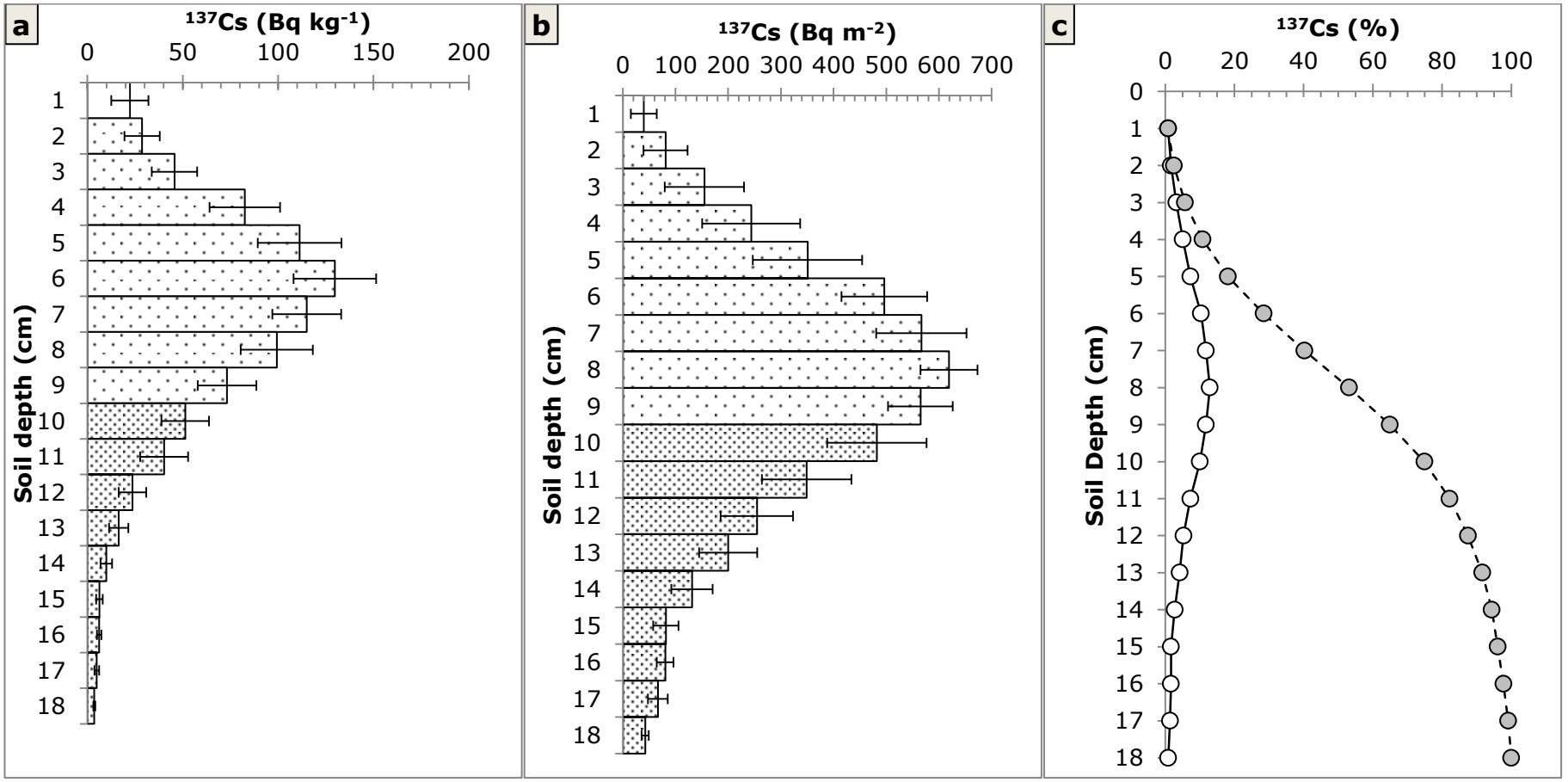
Activity concentrations of ^{137}Cs in the soil profile were measured and decay corrected to 1963 as the assumed year of peak atmospheric deposition at Boundary Plantation. The results are shown in Figure 3-9a.

The results clearly show accumulation of ^{137}Cs in the middle of the organic soil layer (130 Bq kg^{-1} at 6 cm depth) with a systematic decrease in activity concentrations in each successive layer above and below the layer of maximum accumulation. Minimum activity concentrations were found at 18 cm depth in the mineral soil and at 1 cm depth (ie. the litter layer) in the organic soil.

The deposition of radionuclides from the atmosphere to the ground surface is usually measured and expressed as an inventory – ie. a total activity per unit ground area (usually Bq m^{-2}). This is relatively straightforward immediately after deposition because almost all of the deposited activity lies in the upper 1 or 2 cm of the soil profile. As time progresses, however, the radionuclide migrates through the soil profile and the detailed vertical distribution must be evaluated before a full inventory can be calculated.

For Boundary Plantation, a full depth distribution of ^{137}Cs activity concentrations (Bq kg^{-1}) is available (Figure 3-9a). By multiplying the activity concentration in each soil layer by the bulk density for that layer a layer-by-layer activity inventory can be constructed, as shown in Figure 3-9b. These inventories were decay corrected to 1963 and summed to provide a total soil profile inventory of 4,800 Bq m^{-2}. The percentage distribution of ^{137}Cs in soil cores is shown in Figure 3-9c; from the cumulative percentage data it can be seen that 65% of ^{137}Cs was located within the organic soil layer, to a depth of 9 cm, even though deposition occurred 52 years prior to sampling in 2015.

Figure 3-9 Depth profile of average ^{137}Cs activity concentration (a), inventory (b) and percentage inventory (white circle) and accumulated percentage inventory (dark circle) (c), decay corrected to 1963 in organic (1 – 9 cm depth) and mineral layers (deeper than 9 cm depth) of soil collected at Boundary Plantation (24 replicates, the horizontal bars are standard errors of mean).



3.2.3 Exchangeable fractions of ^{133}Cs, ^{39}K and ^{85}Rb

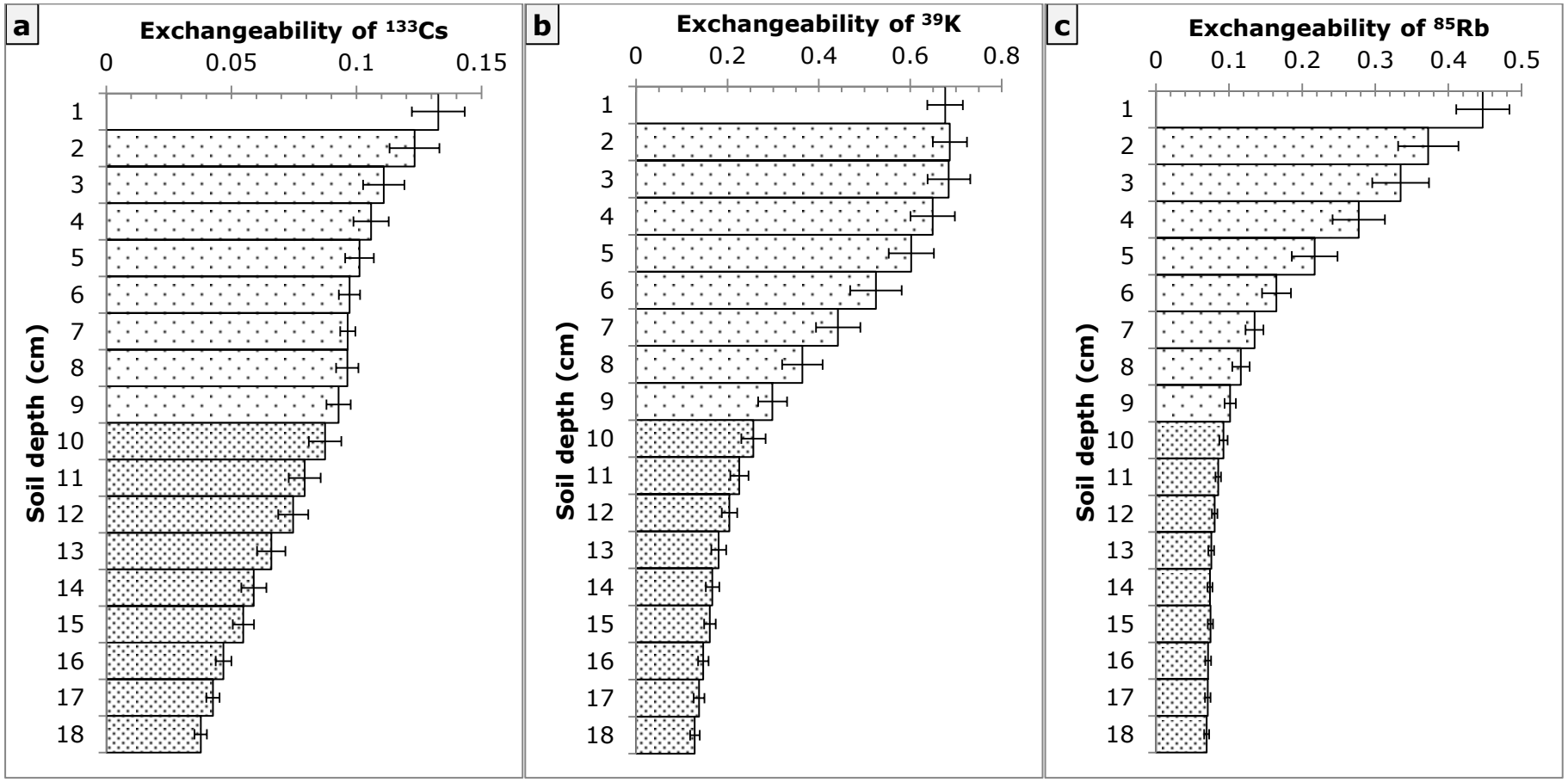
The exchangeable fractions ('exchangeability') of ^{133}Cs, ^{39}K and ^{85}Rb within the soil profile were calculated using equation 3.1 and the results are shown in Figure 3-10.

$$Exchangeability = \frac{Exchangeable\ concentration\ (mg\ kg^{-1})}{Total\ concentration\ (mg\ kg^{-1})} \qquad (3.1)$$

Results suggest that exchangeability of ^{133}Cs (4 – 13%) was least whilst exchangeability of ^{39}K (13 – 69%) was highest among the three alkali metals. The exchangeability of ^{133}Cs, ^{39}K and ^{85}Rb generally decreased with soil depth. However, the decrease in exchangeability of ^{85}Rb throughout the soil profile was the steepest, while the exchangeability of ^{39}K was almost constant in the upper 4 cm of the organic soil layer. The exchangeability of ^{133}Cs in the organic layer decreased less steeply than it did for ^{39}K and ^{85}Rb.

One-way ANOVA with Tukey 95% confidence *post hoc* comparisons suggested that the exchangeability of ^{133}Cs between 6 – 9 cm depth did not vary significantly.

Figure 3-10 Depth profiles of average exchangeabilities of ^{133}Cs (a), ^{39}K (b) and ^{85}Rb (c) in organic (1 – 9 cm depth) and mineral layers (deeper than 9 cm depth) within soil cores collected at Boundary Plantation (24 replicates, the horizontal bars are standard errors of means).



3.2.4 Correlation of forest soil properties with ^{133}Cs, ^{39}K, ^{85}Rb and ^{137}Cs in the soil profile

Relationships of soil pH and organic matter with total, exchangeable and fixed concentrations of ^{133}Cs, ^{39}K, ^{85}Rb and ^{137}Cs were investigated by examining correlations between these variables.

3.2.4.1 Soil pH

Theoretically, soil pH is directly related to H^+ activity in soil solution. Since the H^+ is a strong competitor for available cation exchange sites in soils correlations between exchangeable ^{133}Cs, ^{39}K and ^{85}Rb with soil pH were investigated. In the case of ^{137}Cs, soil sample was not enough to analysis therefore, no exchangeable concentrations were available so the correlation of total ^{137}Cs with soil pH was investigated.

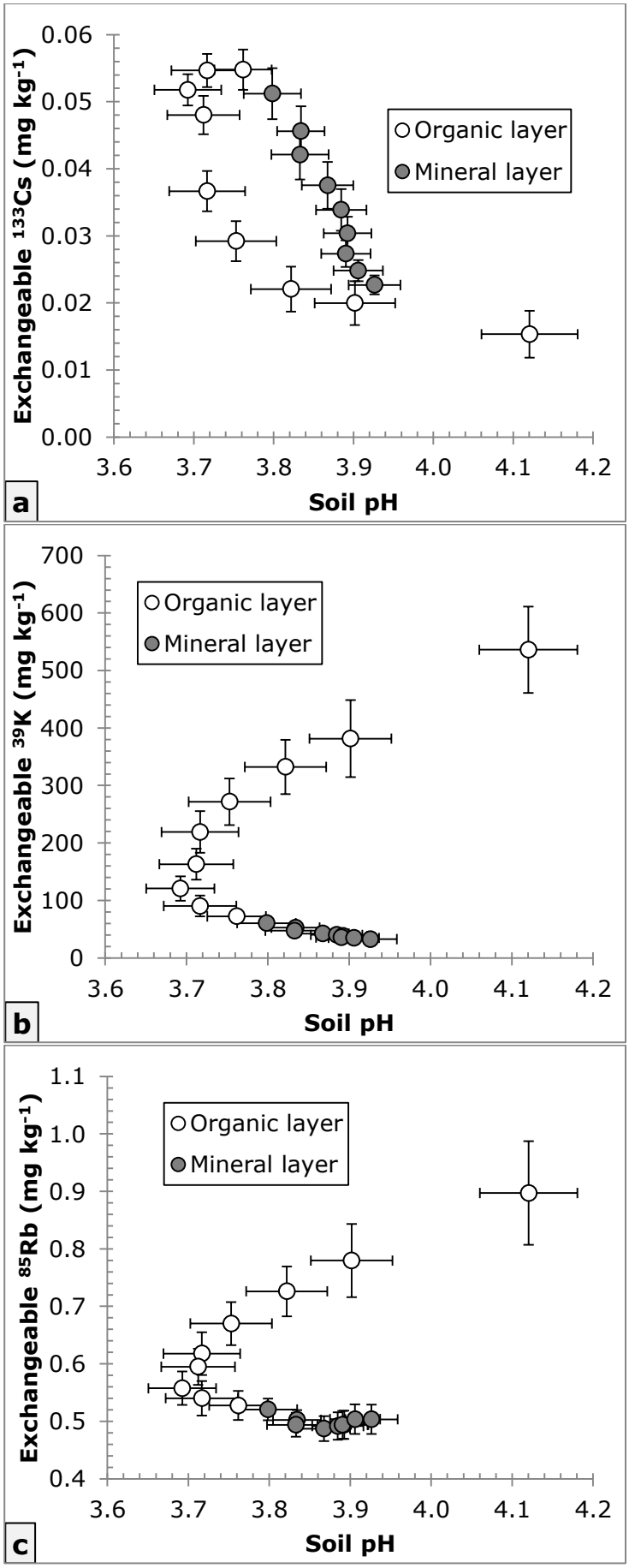
- *Correlations of soil pH with exchangeable concentrations of ^{133}Cs, ^{39}K and ^{85}Rb*

Correlations between average soil pH and exchangeable concentrations of ^{133}Cs, ^{39}K and ^{85}Rb within the soil profile are shown in Figure 3-11.

Correlation patterns of soil pH with exchangeable concentrations of ^{39}K and ^{85}Rb were similar, but somewhat different for ^{133}Cs. However, for all three alkali metals there were distinct correlations for the organic and mineral parts of the soil profile.

The lowest soil pH (3.69) was measured at 7 cm depth (Figure 3-4). Increasing distance upwards or downwards from this point resulted in higher pH values. This increase in pH was accompanied by a general decrease in the exchangeable concentration of ^{133}Cs in both organic and mineral parts of the soil. However, for ^{39}K and ^{85}Rb an increase in soil pH was associated with a reduction in the exchangeable concentrations in the mineral soil but with a general increase in the exchangeable concentrations in the organic soil.

Figure 3-11 *Correlations of average soil pH with average exchangeable concentrations of ^{133}Cs (a), ^{39}K (b) and ^{85}Rb (c) within organic (light circles) and mineral (dark circles) layers collected at Boundary Plantation (24 replicates, the bars are standard errors of means).*



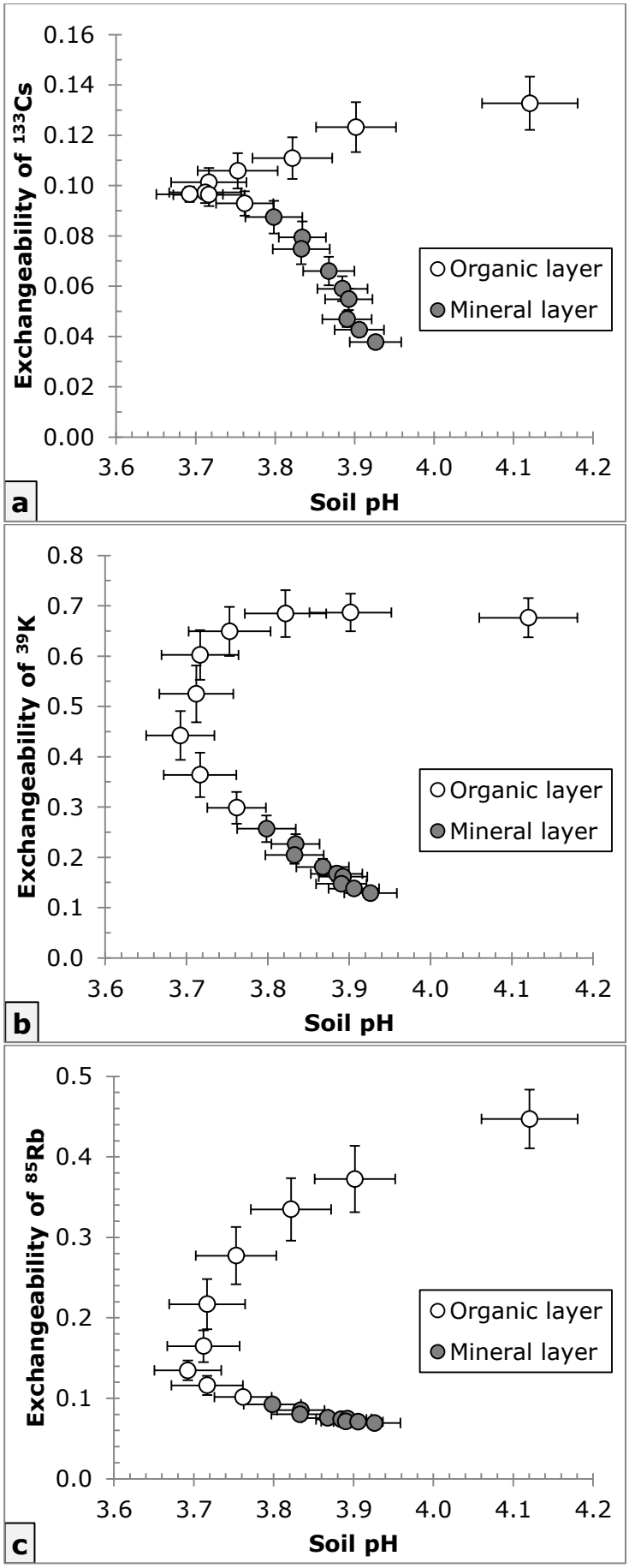
- *Correlations with exchangeabilities of ^{133}Cs, ^{39}K and ^{85}Rb*

Correlations between average soil pH and exchangeable fractions of ^{133}Cs, ^{39}K and ^{85}Rb within the soil profile are shown in Figure 3-12.

As for the exchangeable concentrations, correlations of soil pH with exchangeable fractions of ^{133}Cs, ^{39}K and ^{85}Rb were not obviously separated by the boundary between organic and mineral layers, but there were distinct correlations for the organic and mineral parts of the soil profile. Unlike the exchangeable concentrations, the correlations of soil pH with exchangeable fractions of all three alkali metals were qualitatively similar.

From 7 cm depth (soil pH 3.69) downward, increasing soil pH was associated with reductions in exchangeability of ^{133}Cs, ^{39}K and ^{85}Rb. This trend was reversed for the soil layers above 7 cm – ie. there was a positive correlation between soil pH and exchangeability of ^{133}Cs, ^{39}K and ^{85}Rb in the upper 7 cm of the soil (organic layer).

There was an almost constant exchangeability of ^{133}Cs between 6 – 9 cm depths where the pH range was extremely acidic (3.69 – 3.76). An almost constant exchangeability of ^{39}K was seen in the upper 4 cm depth over a pH range of 3.75 – 4.12.

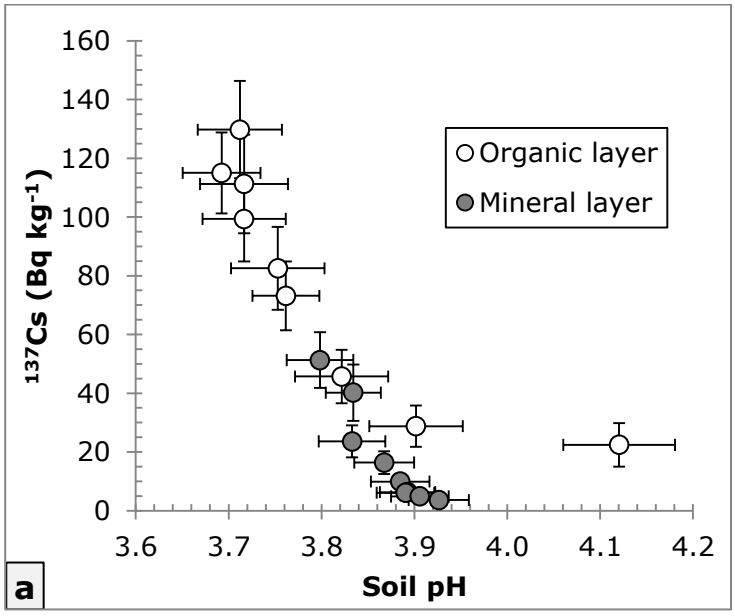


<u>Figure 3-12</u> Correlations of average soil pH with average exchangeable fractions of ^{133}Cs (a), ^{39}K (b) and ^{85}Rb (c) within organic (light circles) and mineral (dark circles) layers collected at Boundary Plantation (24 replicates, the bars are standard errors of means).

- *Correlation of soil pH with total ^{137}Cs*

The systematically negative correlation between soil pH and total ^{137}Cs activity concentration within the soil profile is shown in Figure 3-13. This shows that radiocaesium from atmospheric weapons testing, deposited in 1963, has accumulated predominantly in the most acidic part of the soil profile (6 cm depth, pH 3.71, 129.7 Bq kg^{-1} ^{137}Cs).

Figure 3-13 Correlation of average soil pH with average activity concentration of ^{137}Cs within organic (light circles) and mineral (dark circles) layers collected at Boundary Plantation (7 replicates, the bars are standard errors of means).

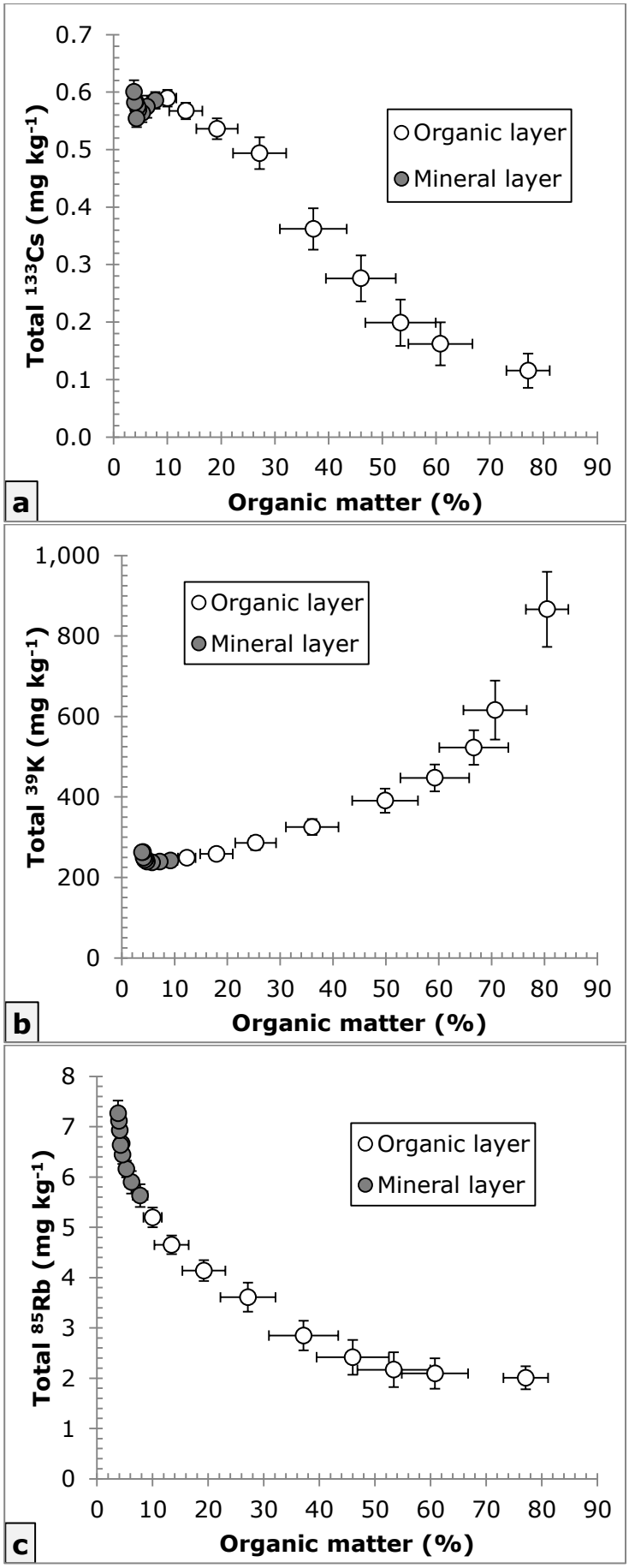


3.2.4.2 Soil organic matter

- *Correlations of soil organic matter with total concentrations of ^{133}Cs, ^{39}K and ^{85}Rb*

Correlations between soil organic matter (as measured by LOI) and total ^{133}Cs, ^{39}K and ^{85}Rb within organic and mineral layers are shown in Figure 3-14.

Unlike the correlations between soil pH and total ^{133}Cs, ^{39}K and ^{85}Rb, the correlations between the alkali metal concentrations and organic matter were all monotonic. However, while the correlations were negative for ^{133}Cs and ^{85}Rb, ^{39}K was positively correlated with soil organic matter.

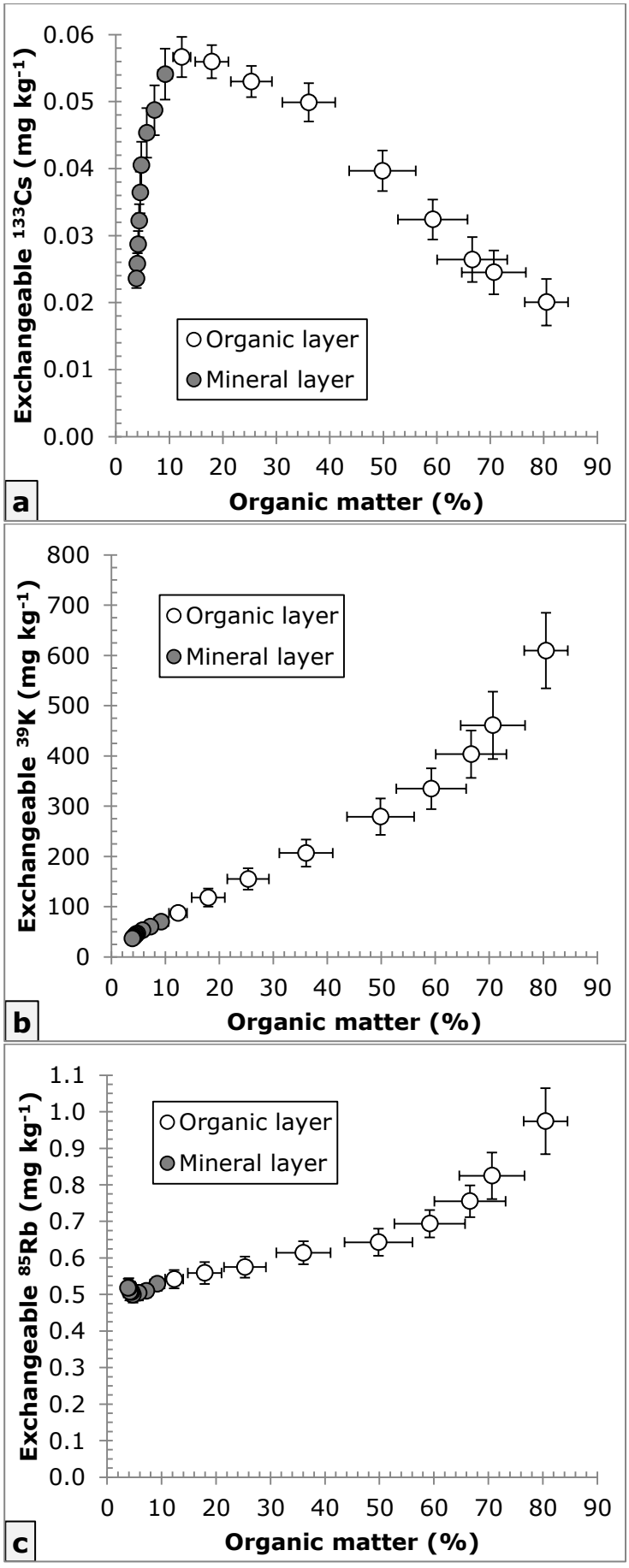


<u>Figure 3-14</u> Correlations of average soil organic matter with average total concentrations of ^{133}Cs (a), ^{39}K (b) and ^{85}Rb (c) within organic (light circles) and mineral (dark circles) layers collected at Boundary Plantation (24 replicates, the bars are standard errors of means).

- *Correlations of soil organic matter with exchangeable concentrations of ^{133}Cs, ^{39}K and ^{85}Rb*

Correlations between soil organic matter (as measured by LOI) and exchangeable ^{133}Cs, ^{39}K and ^{85}Rb are shown in Figure 3-15.

Correlations of organic matter with exchangeable ^{39}K and ^{85}Rb were qualitatively similar, following a monotonically positive trend within all (organic and mineral) soil layers. In contrast, the correlations between organic matter and exchangeable ^{133}Cs were distinct for the organic and mineral layers (negative and positive correlations, respectively).



<u>Figure 3-15</u> Correlations of average soil organic matter with average exchangeable concentrations of ^{133}Cs (a), ^{39}K (b) and ^{85}Rb (c) within organic (light circles) and mineral (dark circles) layers collected at Boundary Plantation (24 replicates, the bars are standard errors of means).

- *Correlations of soil organic matter with 'fixed' concentrations of ^{133}Cs, ^{39}K and ^{85}Rb*

Correlations between organic matter (as measured by LOI) and 'fixed' ^{133}Cs, ^{39}K and ^{85}Rb concentrations are shown in Figure 3-16.

Correlations of organic matter with fixed ^{133}Cs and ^{85}Rb were qualitatively similar, following a negative trend within all (organic and mineral) soil layers.

Within the upper 3 cm depth of the organic layer, a decrease in organic matter was accompanied by a decrease in fixed ^{39}K concentration. However, at all other soil depths organic matter and fixed ^{39}K concentrations were negatively correlated.

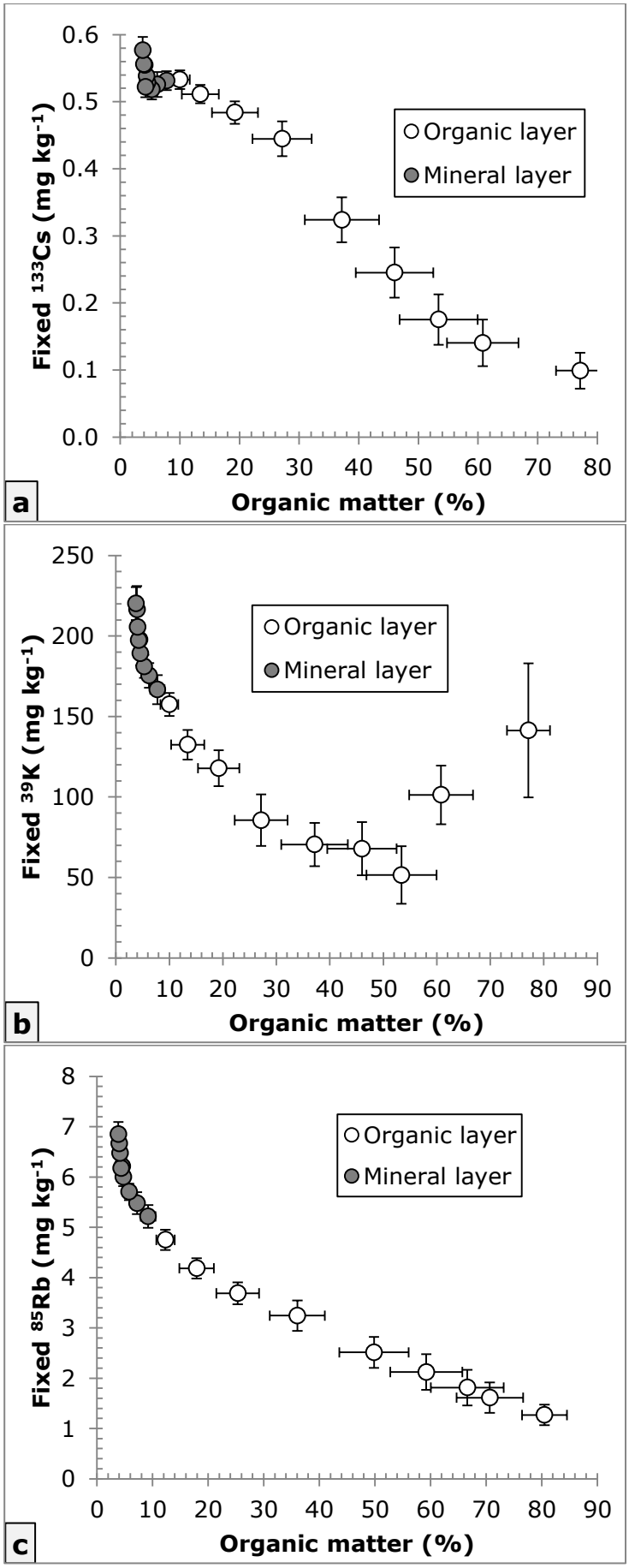


Figure 3-16 Correlations of average soil organic matter with average 'fixed' concentrations of ^{133}Cs (a), ^{39}K (b) and ^{85}Rb (c) within organic (light circles) and mineral (dark circles) layers collected at Boundary Plantation (24 replicates, the bars are standard errors of means).

- *Correlations of soil organic matter with exchangeable fractions of ^{133}Cs, ^{39}K and ^{85}Rb*

Correlations between soil organic matter (as measured by LOI) and exchangeable fractions of ^{133}Cs, ^{39}K and ^{85}Rb are shown in Figure 3-17. The correlations were all positive. However, while the relationships between organic matter and exchangeable fractions of ^{39}K and ^{85}Rb were monotonic, the relationship between organic matter and exchangeable fraction of ^{133}Cs was more complex, taking the form of a quadratic polynomial regression. The relationship shows an almost constant exchangeability of ^{133}Cs between 6 – 9 cm depth in soil with 12.3 – 36.1% organic matter.

For ^{39}K, there was an almost constant exchangeability in the upper 4 cm depth in soil with 59.2 – 80.5% organic matter.

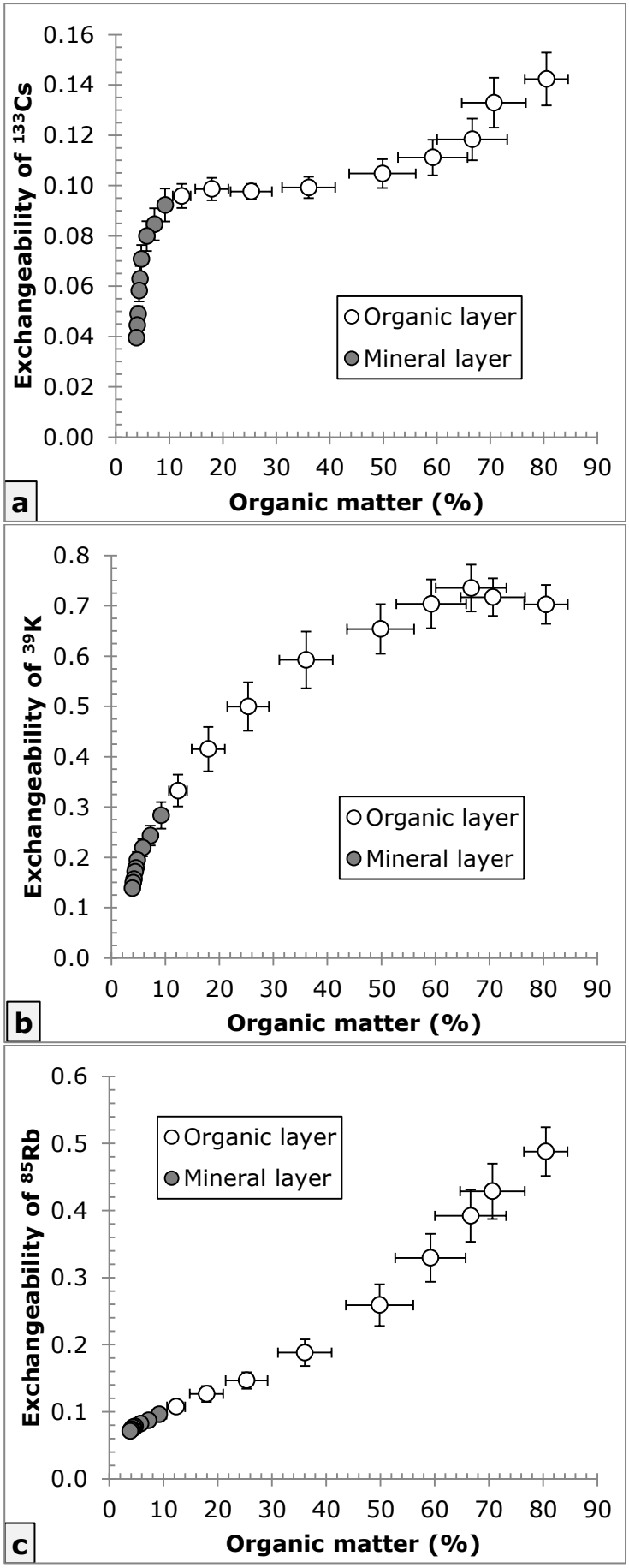
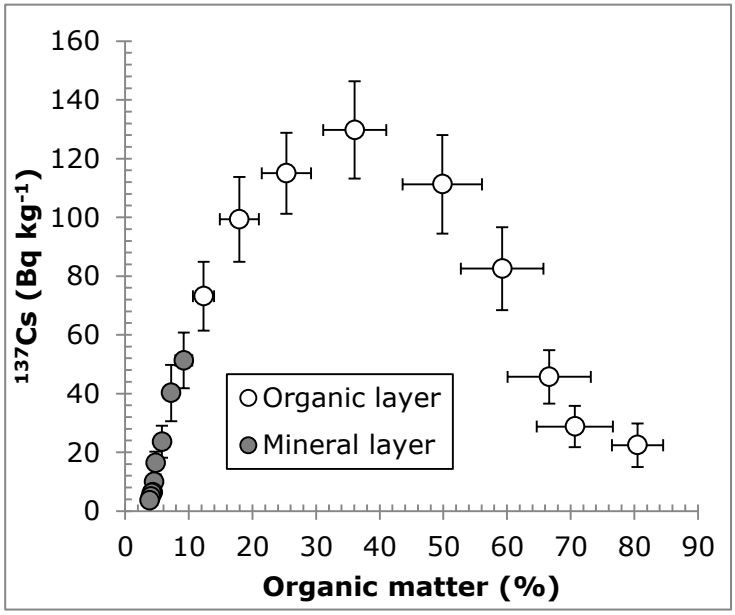


Figure 3-17 Correlations of average of soil organic matter with average of exchangeabilities of ^{133}Cs (a), ^{39}K (b) and ^{85}Rb (c) within organic (light circles) and mineral (dark circles) layers collected at Boundary Plantation (24 replicates, the bars are standard errors of means).

- *Correlation or soil organic matter with ^{137}Cs*

The correlation between soil organic matter (as measured by LOI) and total activity concentrations of ^{137}Cs is shown in Figure 3-18.

Figure 3-18 Correlations of average soil organic matter with average activity concentrations of ^{137}Cs within organic (light circles) and mineral (dark circles) layers collected at Boundary Plantation (7 replicates, the bars are standard errors of means).



The graph shows that the maximum ^{137}Cs activity concentration (129.7 Bq kg^{-1}) was associated with an organic matter content of 36.1 % (at a depth of 6 cm within the soil profile). The overall shape of the correlation emphasises the successive decrease in ^{137}Cs activity concentrations away from the point of peak contamination, with successively higher organic matter contents above this point and lower organic matter contents below.

3.2.5 Correlation between fractions of ^{133}Cs and ^{137}Cs within forest soil

3.2.5.1 Total ^{133}Cs versus exchangeable and fixed ^{133}Cs

Correlations between total ^{133}Cs and exchangeable and fixed concentrations were investigated, as shown in Figure 3-19.

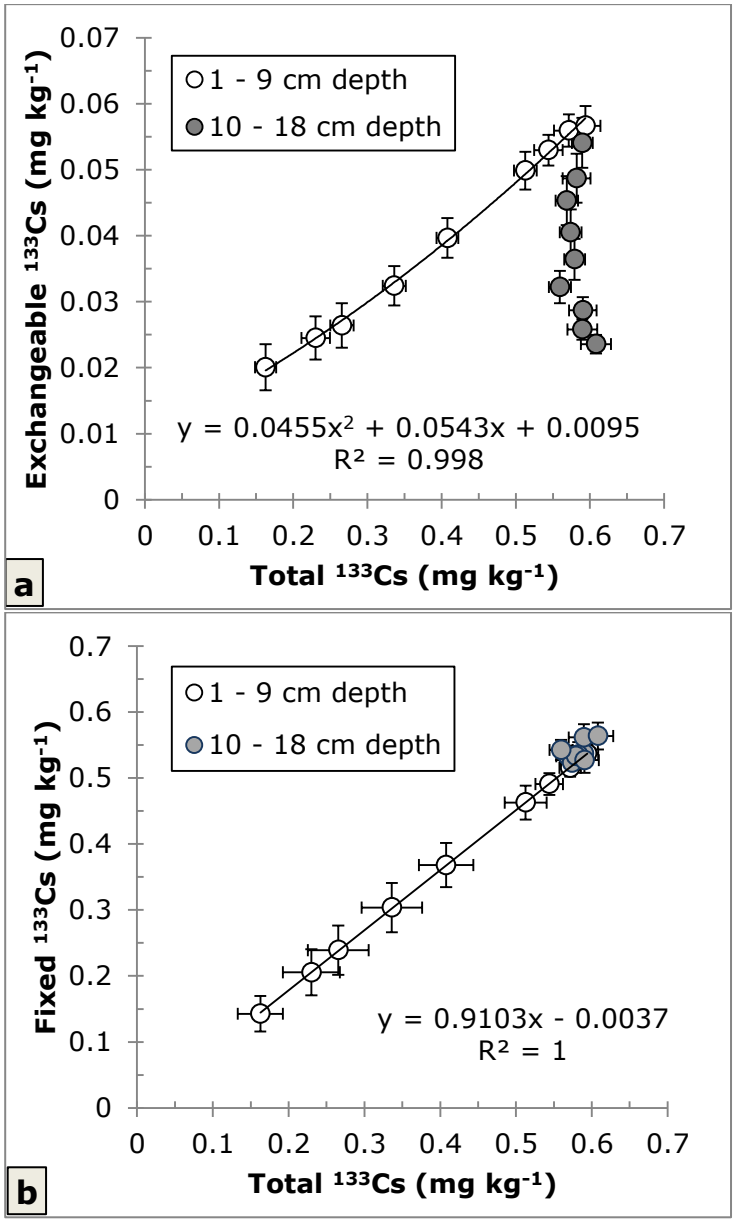


Figure 3-19 Correlations of average total ^{133}Cs with average exchangeable concentration (a) and fixed concentration (b) of ^{133}Cs within the organic layer (light circles) and the mineral (dark circles) layer collected at Boundary Plantation (24 replicates, the bars are standard errors of means).

Total ^{133}Cs was strongly correlated with the 'fixed' fraction of ^{133}Cs throughout the soil profile. The exchangeable concentration was strongly positively correlated with total ^{133}Cs in the organic soil layers, but there was no clear

correlation between exchangeable and total ^{133}Cs concentrations in the mineral layers.

3.2.5.2 ^{137}Cs with total, exchangeable and fixed ^{133}Cs

Correlations of ^{137}Cs with total, exchangeable and fixed concentrations of ^{133}Cs were investigated, as shown in Figure 3-20.

When examining the correlations of ^{137}Cs with total, exchangeable and fixed fractions of ^{133}Cs the data were separated into groups according to soil depth, viz. 1 - 5 (upper organic), 6 - 9 (lower organic) and 10 - 18 cm (mineral) depths.

Within the upper and lower organic layers ^{137}Cs was correlated positively and negatively, respectively, with total, exchangeable and fixed fractions of ^{133}Cs. However, within the mineral soil ^{137}Cs was correlated only with exchangeable ^{133}Cs.

Correlations of ^{137}Cs with total, exchangeable and fixed fraction of ^{133}Cs between soil depths were also investigated using their isotopic ratios within the soil profile as shown in Figure 3-21.

The depth profile of each of the isotopic ratios calculated for ^{137}Cs (with total, exchangeable and fixed ^{133}Cs) broadly reflected the shape of the ^{137}Cs depth distribution previously shown in Figure 3-9, though with maximum values at 5 cm depth.

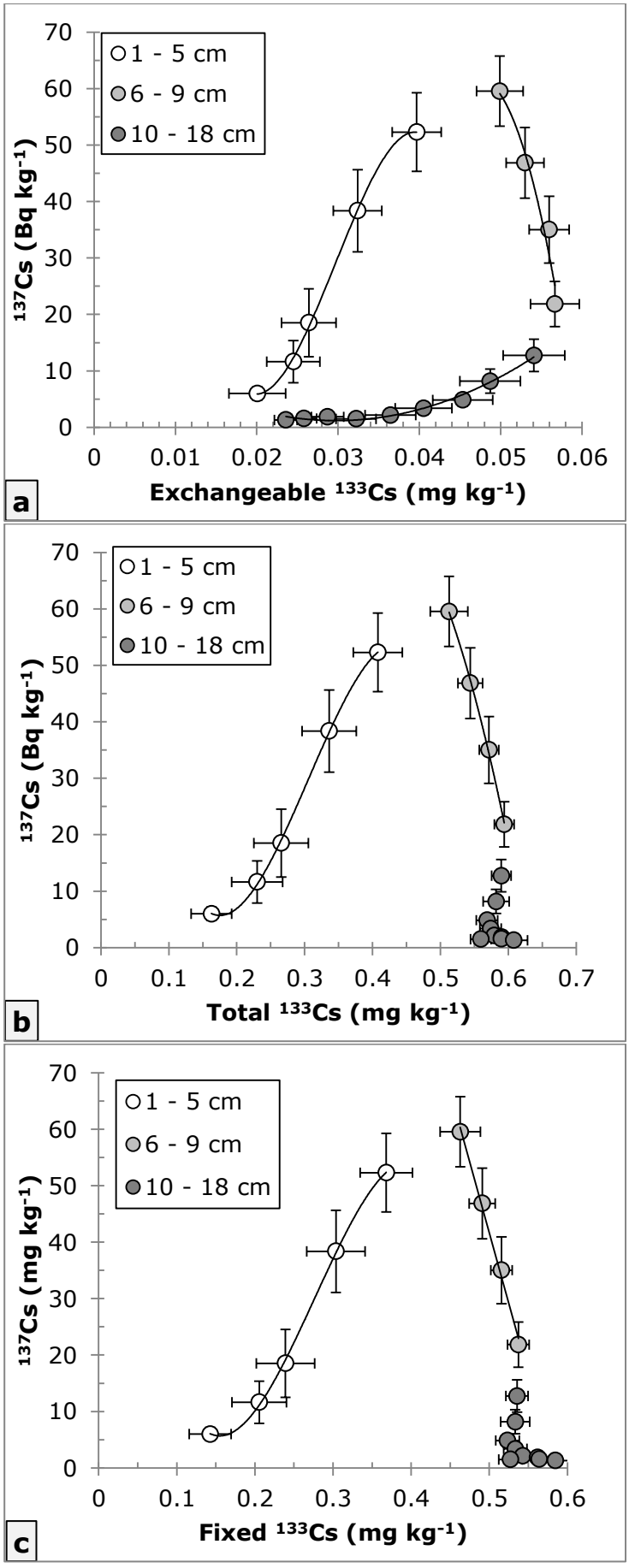
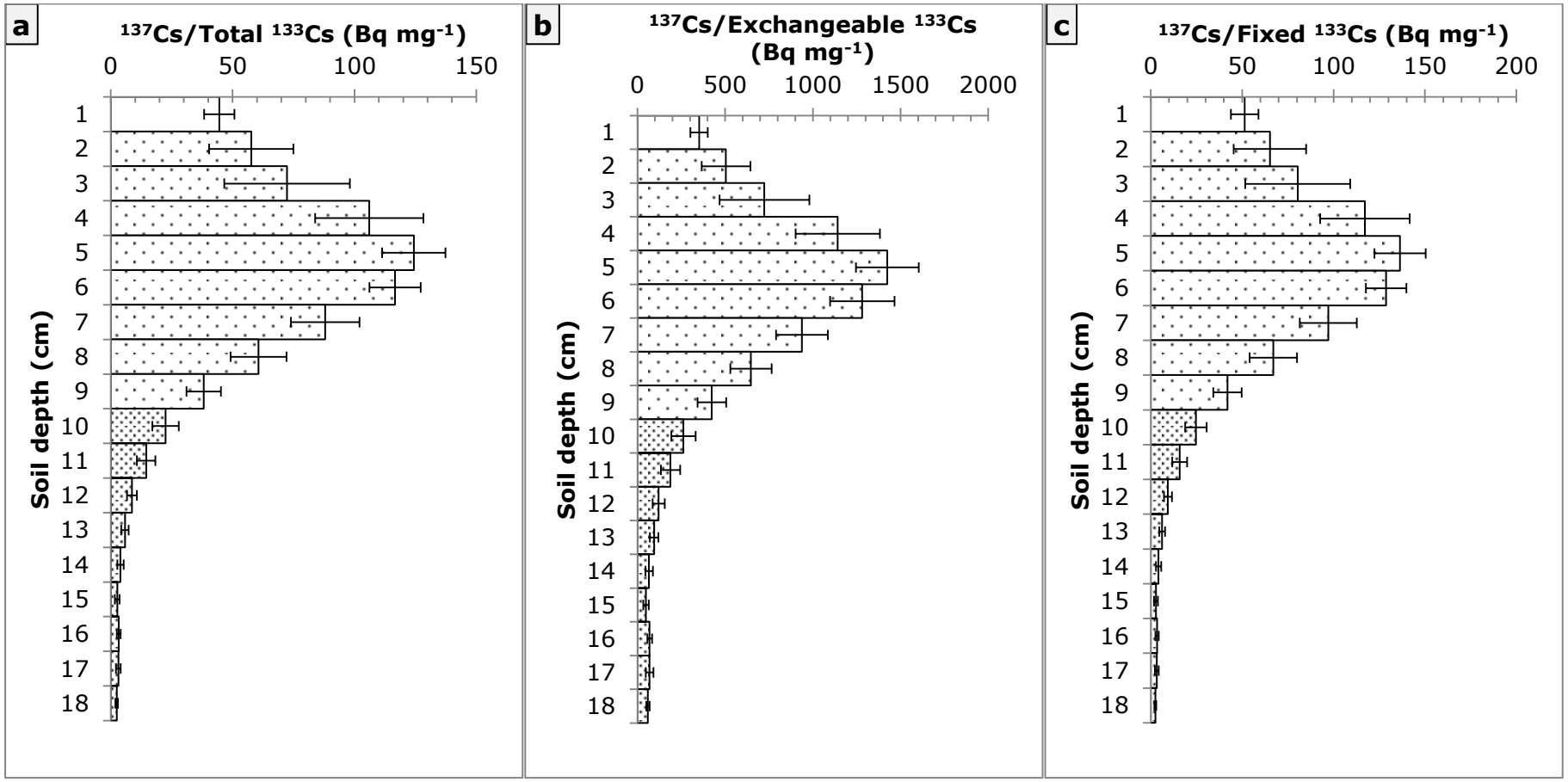


Figure 3-20 Correlations of average activity concentrations of ^{137}Cs with average exchangeable (a), total (b) and fixed (c) concentrations of ^{133}Cs within organic (light circles) and mineral (dark circles) layers collected at Boundary Plantation (7 replicates, the bars are standard errors of means).

Figure 3-21 Depth profiles of average isotopic ratios of ^{137}Cs (n = 5) with average ^{133}Cs in total concentration (a, n = 24), exchangeable fraction (b, n = 24) and fixed fraction (c, n = 24) within organic (1 – 9 cm depth) and mineral layers (deeper than 9 cm depth) of soil collected at Boundary Plantation (horizontal bars are standard errors of means).



3.2.6 Isotopic exchange of ^{133}Cs and ^{134}Cs

^{134}Cs was used to investigate the isotopic exchangeability of ^{133}Cs throughout the Boundary Plantation soil profile (site 20 only). Isotopically exchangeable ^{133}Cs (E-value) was calculated using equation 2.8. The results of data obtained from this experiment are shown in Table 3-3 and Figure 3-22 for selected soil depths (1, 3, 5, 7, 9, 11, 13, 15 and 17 cm) and for equilibration (shaking) times of 1 h, 24 h (1 day) and 168 h (1 week). Finally, the progression of E-values for the three equilibration (shaking) times at each soil depth is shown in Figure 3-23.

Isotopic exchangeability of ^{133}Cs with ^{134}Cs in soil collected at Boundary Plantation was higher (103 – 145%) than the exchangeable concentrations of ^{133}Cs, especially in the 1 cm (143 % average) and 2 cm (131 % average) depths. Except for the litter layer (1 cm) increasing the shaking time from one hour to one week increased the E-value by less than 2-fold. Longer-term shaking may increase the E-value further, although the rate of increase of the E-value was much more rapid at the beginning of the experiment (from one hour to one day) than during the following 6 days. For the litter layer, increasing the shaking time from one day to one week decreased the E-value and longer term shaking may decrease the E-value further.

Isotopic exchangeability of ^{133}Cs with ^{134}Cs was low in the litter layer but high in the middle part of the organic layer (5 and 7 cm) (Figure 3-22), while in the other depths the calculated E-values were rather constant.

Table 3-3 Concentrations of ^{134}Cs and exchangeable ^{133}Cs, and E-values obtained for soil samples collected at Boundary Plantation, site 20.

Depth (cm)	^{134}Cs (Bq ml^{-1})			Exchangeable ^{133}Cs (mg kg^{-1})			E-value (mg kg^{-1})		
	Shaking time (hours)			Shaking time (hours)			Shaking time (hours) (% of exchangeable concentration)		
	1	24	168	1	24	168	1	24	168
1	13.2	13.2	12.8	0.018	0.019	0.015	0.025 (141)	0.027 (142)	0.021 (145)
3	14.3	14.2	14.2	0.050	0.057	0.060	0.065 (130)	0.074 (131)	0.079 (132)
5	15.2	15.0	15.5	0.088	0.110	0.116	0.107 (122)	0.136 (124)	0.140 (120)
7	16.8	16.7	17.0	0.104	0.127	0.143	0.115 (111)	0.142 (112)	0.156 (110)
9	16.8	17.1	17.9	0.068	0.081	0.095	0.076 (111)	0.089 (109)	0.099 (104)
11	16.8	17.7	17.2	0.051	0.063	0.075	0.057 (111)	0.067 (105)	0.081 (109)
13	17.4	17.9	17.8	0.049	0.059	0.076	0.052 (107)	0.062 (104)	0.079 (105)
15	18.1	17.5	17.1	0.052	0.063	0.079	0.054 (103)	0.067 (106)	0.086 (109)
17	18.1	16.8	17.2	0.029	0.040	0.051	0.030 (103)	0.044 (111)	0.055 (108)

Figure 3-22 Depth profiles of E-values for ^{133}Cs after equilibration for 1 hour (a), 1 day (b) and 1 week (c) within organic (1 – 9 cm depth) and mineral layers (deeper than 9 cm depth) of soil collected at Boundary Plantation, site 20.

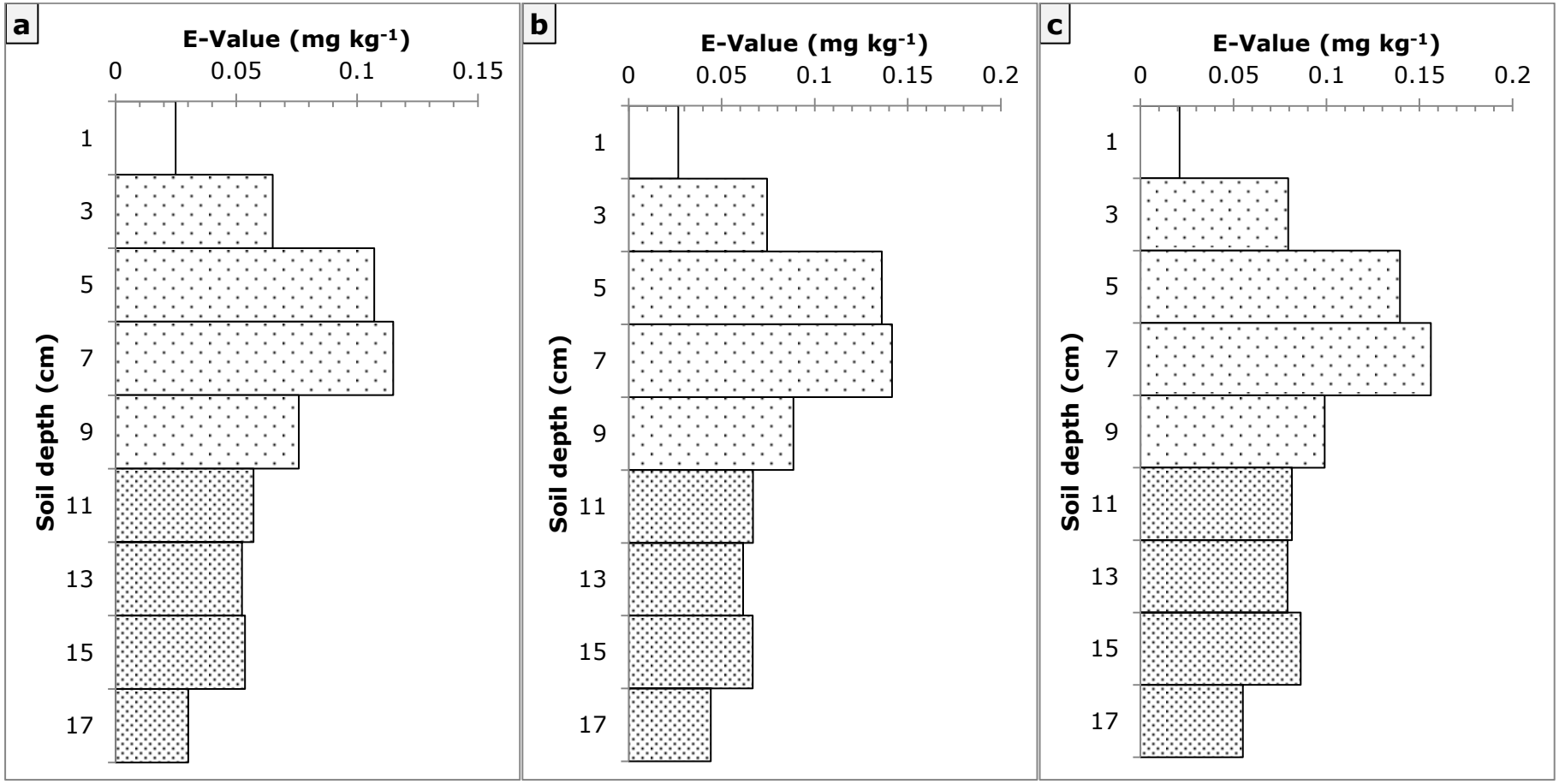
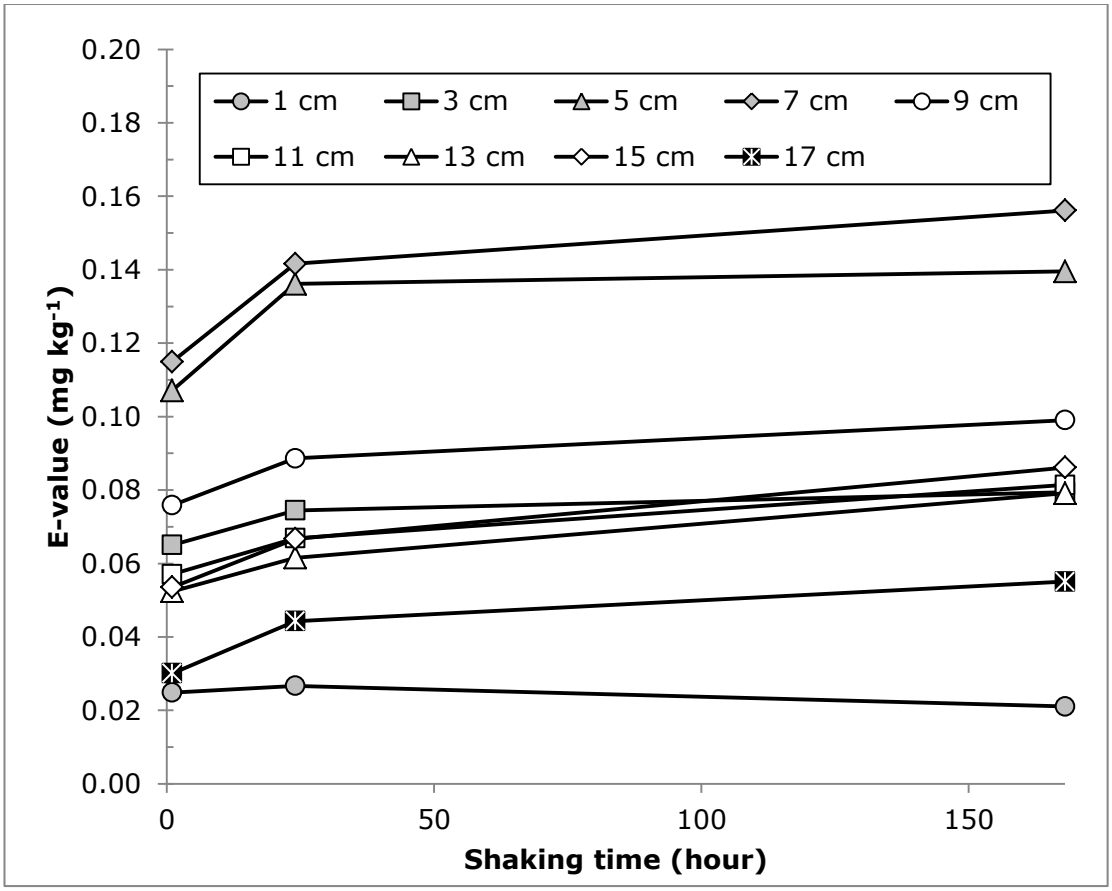


Figure 3-23 Progression of E-value with equilibration (shaking) time for 1, 3, 5, 7, 9, 11, 13, 15 and 17 cm depths of soil collected at Boundary Plantation, site 20.

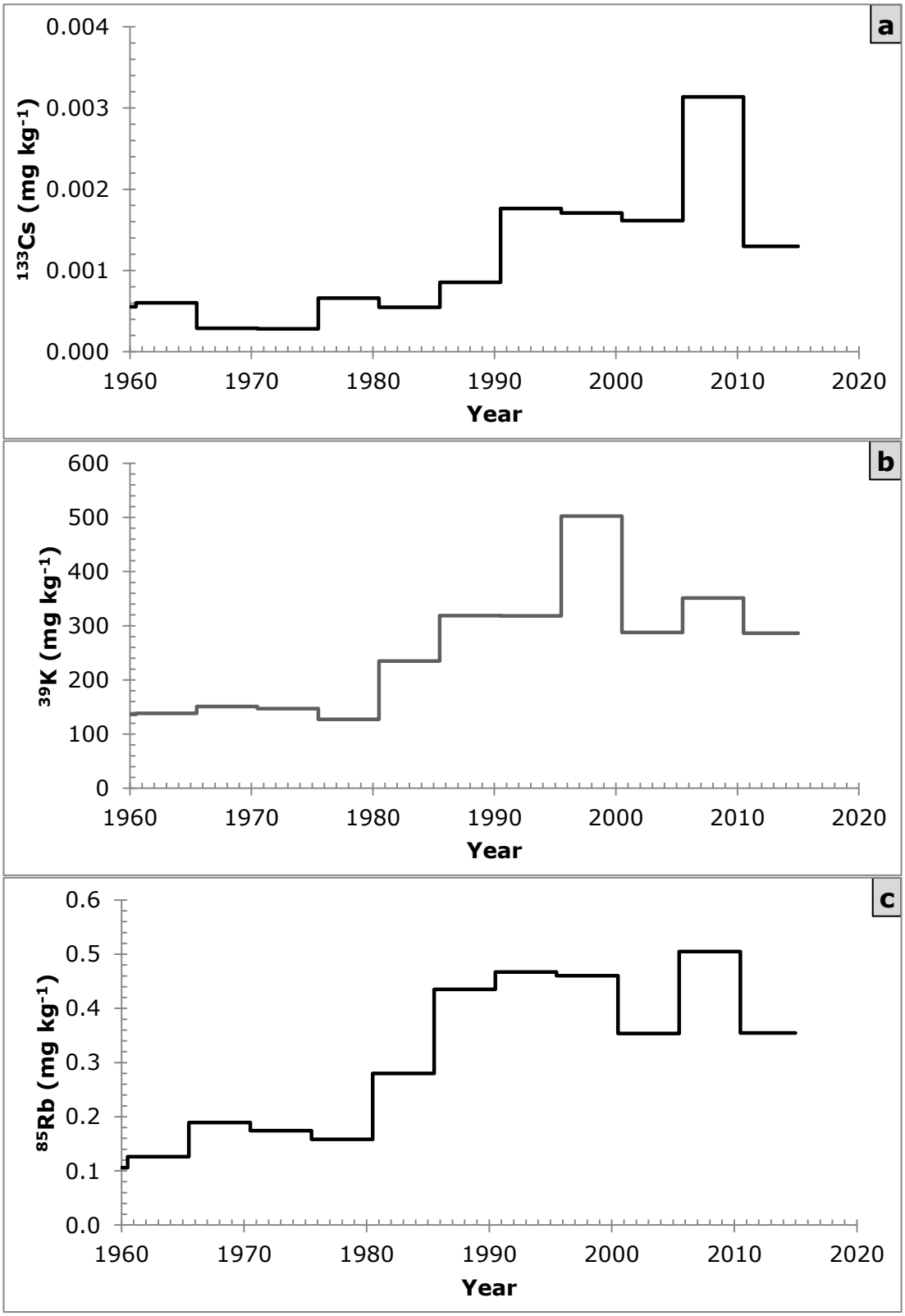


3.2.7 Bio-availabilities of ^{133}Cs, ^{39}K and ^{85}Rb in above-ground compartments

3.2.7.1 ^{133}Cs, ^{39}K and ^{85}Rb concentrations in stem wood and bark of Corsican pine

Tree cores of Corsican pine collected at Boundary Plantation were analysed to investigate concentrations of ^{133}Cs, ^{39}K and ^{85}Rb; the results are shown in Table 3-4. Sub-samples of tree cores consisting of five adjacent annual growth rings were also analysed and the results are shown in Figure 3-24 a, b and c, respectively.

Figure 3-24 Concentrations of ^{133}Cs (a), ^{40}K (b) and ^{85}Rb (c) in tree ring samples, collected on February 2016 (1 replicate).



Analysis of tree rings of Corsican pine from Boundary plantation indicates that they were planted around 1958. Concentrations of ^{133}Cs in tree cores from the first experiment had large errors, therefore a second set of measurements using a larger mass of wood was carried out. The results of both experiments show that younger tree rings (after about 1980) contained higher concentrations of ^{133}Cs, ^{39}K and ^{85}Rb than older rings.

The bark of Corsican pine was also analysed. The results are shown in Table 3-4 which shows that bark contained higher concentrations of ^{133}Cs, ^{39}K and ^{85}Rb than stem wood.

Table 3-4 Average concentrations of ^{133}Cs, ^{39}K and ^{85}Rb in fresh needles (20 replicates) and dry needles (12 replicates) collected during June 2014 to March 2015, throughfall (6 replicates) collected during December 2015 to March 2016, wood (1 replicate) and bark (1 replicate) collected in 2016 at Boundary Plantation (SEM is standard errors of means).

Sample type	^{133}Cs (mg kg^{-1})		^{39}K (mg kg^{-1})		^{85}Rb (mg kg^{-1})	
	Conc.	SEM	Conc.	SEM	Conc.	SEM
Wood	1.16 x 10^{-3}	-	261	-	3.14 x10^{-1}	-
Fresh needle	1.20 x 10^{-2}	2.22 x 10^{-3}	7,620	552	8.12	0.83
Dry needle	1.18 x 10^{-2}	0.17 x 10^{-2}	1,060	104	1.13	0.18
Bark	5.00 x 10^{-3}	-	700	-	1.25	-
Throughfall	3.00 x 10^{-5}	3.15 x 10^{-6}	5.21	1.63	5.94 x10^{-3}	1.71 x10^{-3}

3.2.7.2 ^{133}Cs, ^{39}K and ^{85}Rb concentrations in needles of Corsican pine

Fresh and dry needles were collected and analysed for ^{133}Cs, ^{39}K and ^{85}Rb. The results are shown in Table 3-4.

^{133}Cs concentrations in fresh and dry needles were very low and lower than those of ^{39}K and ^{85}Rb by about 5 and 2 orders of magnitude, respectively.

The results also indicate that ^{39}K and ^{85}Rb concentrations in dry needles were much lower than in fresh needles by about 7 – 8 times. In contrast, ^{133}Cs concentrations in dry and fresh needles were not significantly different (using a paired-T-test: t stat = 0.541, P(T<=t) two-tail = 0.599).

3.2.7.3 ^{133}Cs, ^{39}K and ^{85}Rb in throughfall (rainwater)

Throughfall (rainwater) was collected under the canopy of the Corsican pine plantation during December 2013 to March 2014 and analysed for ^{133}Cs, ^{39}K and ^{85}Rb. The results are shown in Table 3-4.

^{133}Cs concentration in throughfall (rainwater) was very low and less than ^{39}K and ^{85}Rb by about 5 and 2 orders of magnitude, respectively.

3.2.8 Competition between ^{133}Cs, ^{39}K and ^{85}Rb in recirculation processes within forest ecosystems

3.2.8.1 Uptake of alkali metals by Corsican pine

Uptake of ^{133}Cs, ^{39}K and ^{85}Rb by Corsican pine was investigated by examining their concentration ratios and aggregated transfer factors as follows.

- *Concentration ratio (CR)*

Concentration ratios for ^{133}Cs, ^{39}K and ^{85}Rb of wood and needles of Corsican pine were calculated using equation 1.3 (section 1.2.8.3), assuming that root absorption takes place from the organic layer (0 - 9 cm) within the soil. The results are shown in Table 3-5.

Calculated *CRs* of ^{133}Cs, ^{85}Rb and ^{39}K in wood are consistent with *CRs* calculated by Uchida and Tagami (2007b) and IAEA (2010).

Table 3-5 Concentration ratios (CR) of ^{133}Cs, ^{39}K and ^{85}Rb in wood (n = 24) and fresh needles (n = 20) calculated on a dry weight basis for wood and needles using total and exchangeable concentrations in the organic soil layer (n = 24).

Nuclide	*CR* (dry weight basis of organic soil)			
	Total concentration		Exchangeable concentration	
	Wood	Fresh needle	Wood	Fresh needle
^{133}Cs	2.24×10^{-3}	2.32×10^{-2}	2.18×10^{-2}	2.27×10^{-1}
^{39}K	7.47×10^{-1}	21.8	1.22	35.6
^{85}Rb	8.03×10^{-2}	2.08	5.07×10^{-1}	13.1

- *Aggregated transfer factor (T_{ag})*

Aggregated transfer factors (T_{ag}) for ^{133}Cs, ^{39}K and ^{85}Rb in Corsican pine wood and needles were calculated using equation 1.4 (section 1.2.8.3) in which the elemental inventory within the upper 18 cm of soil profile was used as the denominator. The results are shown in Table 3-6.

For both *CR* and T_{ag} the lowest values for ^{133}Cs, ^{85}Rb and ^{39}K were found in wood and the highest values in fresh needles, with consistent order of magnitude differences between these two tissue types.

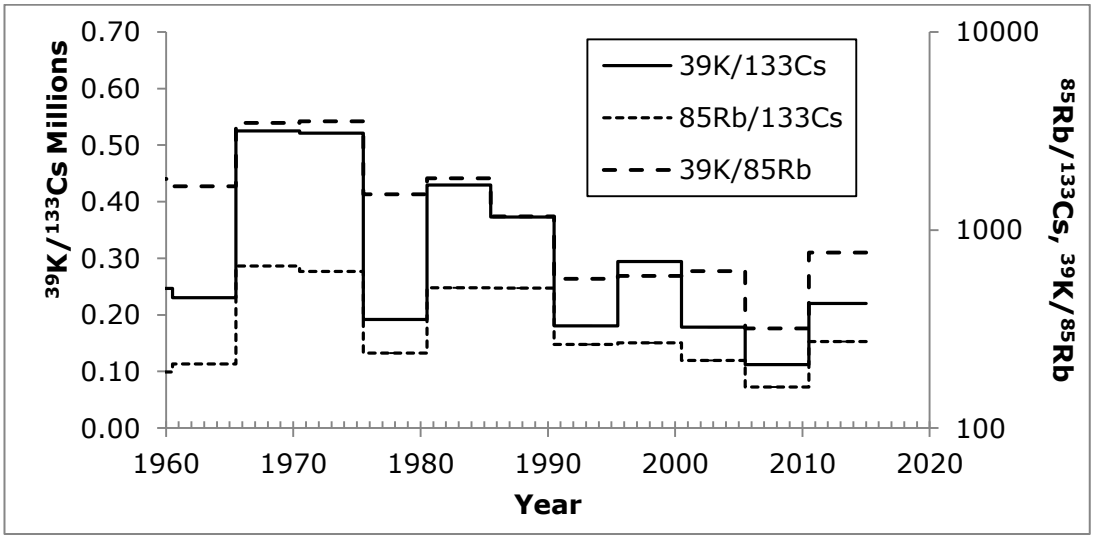
Table 3-6 Aggregated transfer factors (T_{ag}) of ^{133}Cs, ^{39}K and ^{85}Rb in wood (n = 24) and fresh needles (n = 20) of Corsican pine calculated on a dry weight basis for wood, needles and soil (n = 24).

Nuclide	T_{ag} (m^2 kg^{-1} dry weight basis)			
	Total concentration		Exchangeable concentration	
	Wood	Fresh needle	Wood	Fresh needle
^{133}Cs	1.34×10^{-5}	1.39×10^{-4}	1.90×10^{-4}	1.97×10^{-3}
^{39}K	6.42×10^{-3}	1.87×10^{-1}	2.19×10^{-2}	6.40×10^{-1}
^{85}Rb	3.37×10^{-4}	8.72×10^{-3}	3.83×10^{-3}	9.93×10^{-2}

3.2.8.2 Translocation within wood of Corsican pine

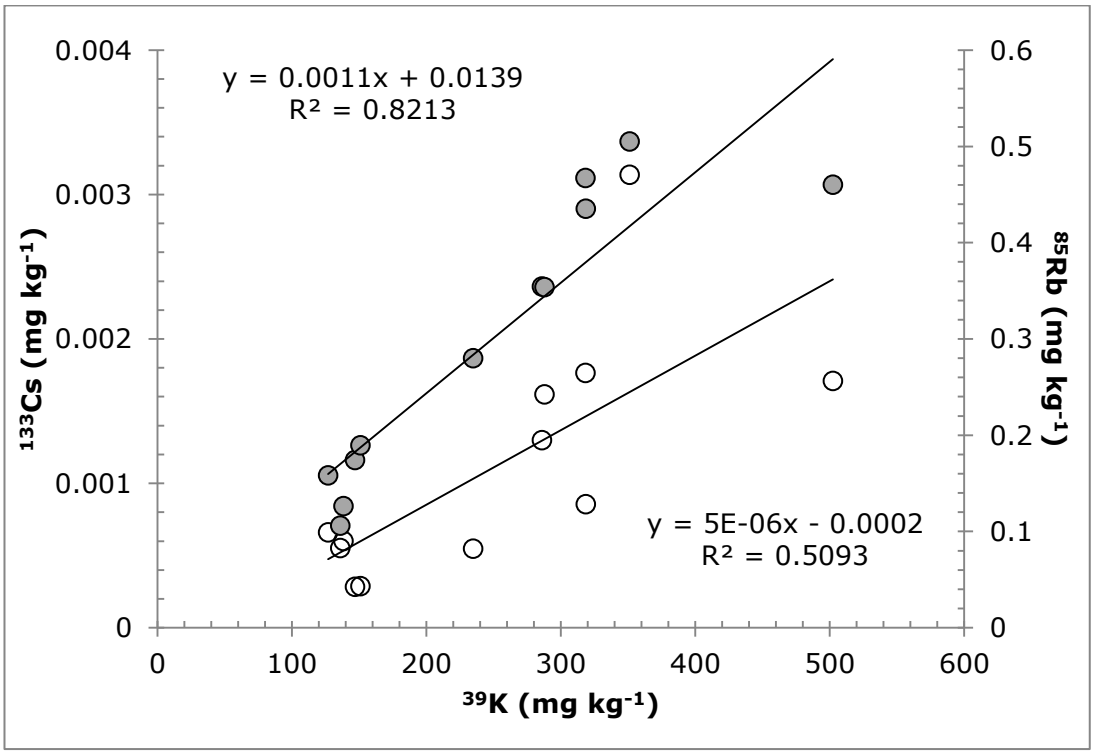
Concentration ratios of $^{39}K/^{133}Cs$, $^{85}Rb/^{133}Cs$ and $^{39}K/^{85}Rb$ in annual growth rings of wood are shown in Figure 3-25.

Figure 3-25 Concentration ratios of $^{39}K/^{133}Cs$, $^{85}Rb/^{133}Cs$ and $^{39}K/^{85}Rb$ in annual growth rings of Corsican pine collected at Boundary Plantation (1 replicate).



Concentration ratios of ^{39}K and ^{85}Rb to ^{133}Cs in wood decreased from older to younger annual rings suggesting that ^{39}K and ^{85}Rb are less mobile than ^{133}Cs towards the cambial region in wood of Corsican pine. Moreover, the trends of $^{39}K/^{133}Cs$ and $^{85}Rb/^{133}Cs$ were very similar which suggests that ^{85}Rb behaves in a more similar manner to ^{39}K than to ^{133}Cs, as confirmed by the correlations of ^{39}K with ^{133}Cs and ^{85}Rb in Figure 3-26.

Figure 3-26 Scatter plots of average concentration of ^{39}K versus ^{133}Cs (light circle) and ^{85}Rb (dark circle) in stem wood of Corsican pine collected at Boundary Plantation (n = 1).



3.2.8.3 Translocation from timber to needles of Corsican pine

The relative magnitude of translocation of ^{39}K, ^{85}Rb and ^{133}Cs from wood to needles was investigated using the following ratios.

- *Concentration ratios of $^{39}K/^{133}Cs$, $^{85}Rb/^{133}Cs$ and $^{39}K/^{85}Rb$*

Concentration ratios of $^{39}K/^{133}Cs$, $^{85}Rb/^{133}Cs$ and $^{39}K/^{85}Rb$ in tree cores and needles were calculated, as shown in Table 3-7.

Table 3-7 Ratios of $^{39}K/^{133}Cs$, $^{85}Rb/^{133}Cs$ and $^{39}K/^{85}Rb$ in organic soil layer (total and exchangeable concentrations, n = 24) wood (n = 1), bark (n =1), fresh needles (n = 20), dry needles (n = 6), throughfall (n = 6) and litter (n = 24) calculated on a dry weight basis.

Ratio	$^{39}K/^{133}Cs$	$^{85}Rb/^{133}Cs$	$^{39}K/^{85}Rb$
Total concentration (organic layer)	473 ± 21.0	10.8 ± 0.23	43.8 ± 1.65
Exchangeable concentration (organic layer)	3,480 ± 471	12.1 ± 0.65	275 ± 26.5
Wood	2.25×10^5	270.81	832
Bark	1.39×10^5	249	559
Fresh needle	$9.51 \times 10^5 \pm 1.58 \times 10^5$	914 ± 139	1,060 ± 91.3
Dry needle	$1.04 \times 10^5 \pm 1.39 \times 10^4$	98.7 ± 9.95	1,070 ± 108
Throughfall (rainwater)	$1.84 \times 10^5 \pm 5.9 \times 10^4$	209 ± 62.7	853 ± 60.4
Litter	$1.00 \times 10^4 \pm 1.73 \times 10^3$	19.8 ± 2.45	448 ± 39.0

The results show that concentration ratios of $^{39}K/^{133}Cs$ were higher than $^{85}Rb/^{133}Cs$ and $^{39}K/^{85}Rb$ these ratios were higher in fresh needles than in wood. This indicates that K is transported to needles in preference to both ^{85}Rb and ^{133}Cs and that this preference is particularly exerted against ^{133}Cs. Similarly,

^{85}Rb is transported to needles in preference to ^{133}Cs. This is further examined using wood to needle translocation factors.

- *Translocation factor*

Wood to needle translocation factors (f_{tr}) were calculated using equation 3.2 to compare the degree of transfer of ^{133}Cs, ^{39}K and ^{85}Rb from wood to fresh needles. The results are shown in Table 3-8.

$$f_{tr} = \frac{\text{Mass concentration in needle (mg kg}^{-1}\text{ dry weight)}}{\text{Mass concentration in wood (mg kg}^{-1}\text{ dry weight)}} \quad (3.2)$$

Table 3-8 Translocation factors (f_{tr}) of ^{133}Cs, ^{39}K and ^{85}Rb from wood to fresh needles of Corsican pine calculated on a dry weight basis.

Translocation factor (f_{tr}, dry weight basis)		
^{133}Cs	^{39}K	^{85}Rb
10.4	29.2	25.9

The results suggest the translocation factors of ^{133}Cs, ^{39}K and ^{85}Rb are in the same order of magnitude but that the tendency for translocation of ^{39}K and ^{85}Rb from wood to needles is higher (2.81 and 2.50 times, respectively) than for ^{133}Cs.

3.2.8.4 Transport of alkali metals from the tree canopy in throughfall

Concentration ratios of ^{39}K/^{133}Cs, ^{85}Rb/^{133}Cs and ^{39}K/^{85}Rb in throughfall water collected at Boundary Plantation were calculated and compared with their ratios in fresh needles to determine the relative degrees to which the alkali metals are transported from the tree canopy to the forest floor by this mechanism.

Results in Table 3-7 indicate that concentration ratios of ^{39}K/^{133}Cs and ^{85}Rb/^{133}Cs for dry needles and throughfall were lower than for fresh needles.

3.3 DISCUSSION

The Boundary Plantation soil is acidic which is a consequence of the freely-draining, acidic sandy substrate (Sherwood Sandstone) in which the soil is developed and the thick accumulation of organic matter at the surface. The pH range (3.69 – 4.12) is consistent with the database of the UK soil observatory (UKSO, 2006) for this type of soil and, on this basis, the Boundary Plantation soil can be classified as being extremely acid (USDA, 1999).

From the XRD analyses, no evidence of clay minerals was found even in the mineral layer of the soil profile which was dominantly composed of quartz particles, consistent with the Sherwood Sandstone parent material. The Boundary Plantation soil is a weakly-developed podzol overlying the Sherwood Sandstone (Ambrose et al., 2014), an acidic and quartz-rich substrate which is typically associated with free-draining, nutrient-poor soils. XRD analyses also indicated the absence of clays in the Boundary Plantation soil. As a result of their lamellar structure, clay minerals give strong reflections even when the phase fraction is low so, if present, would be expected to be seen clearly in the XRD diffractograms (Dann, personal communication).

The boundary of the organic and mineral layers was identified at 9 – 10 cm depth (section 3.2.1.1) using the criterion of 12% organic matter proposed by the USDA (1998) and FAO (1998). Statistical analysis (one-way ANOVA with 95% confidence *post hoc* Tukey comparison of means) of the variation of LOI in the soil profile confirmed this distinction between organic and mineral soil layers. This identification proved useful in analysing the distributions of stable and radiocaesium and the interrelationships of these isotopes with soil pH and organic matter content.

Humus or decomposed organic matter is different to undecomposed organic matter with respect to its properties of cation adsorption and release. The decomposition of organic matter releases cations such as the alkali metals whilst humus has a substantial capacity to absorb cations within and at the surface of organic particles.

The layer-by-layer decrease of LOI with increasing depth from the litter layer is evidence of the decomposition process which produces humus and associated H^+ ions, resulting in lower soil pH. The minimum pH (3.69) within the Boundary Plantation soil profile was at 7 cm depth (section 3.2.1.2) which suggests that

the decomposition of organic matter was complete at this depth and no undecomposed organic matter was likely to remain below this point. Furthermore, peak intensities of the dominant quartz reflection in XRD diffractograms (Figure 3-5) increased steadily from zero in the surface litter layer to a maximum at 7 cm. It is likely, therefore, that a significant physico-chemical boundary exists at 7 cm depth above and below which caesium behaviour could be expected to vary.

^{133}Cs has previously been observed to accumulate in the lower part of organic soil layers according to Rühm et al. (1999) and Yoshida et al. (2002). However, the majority of ^{133}Cs in the soil of Boundary Plantation is to be found in mineral soil layers which suggests it is mainly bound in the lattices of native soil mineral particles which do not originate from atmospheric fallout ^{133}Cs (Varskog et al., 1994, Yoshida et al., 2004). The profile of ^{133}Cs in the soil (Figure 3-6) shows a minimum concentration in the surface litter layer increasing with depth throughout the organic layer to a more or less constant concentration in the mineral part of the soil. Since the source of ^{133}Cs is within the mineral grains below the organic-mineral boundary this implies there is a mechanism by which ^{133}Cs is transported upwards into the organic layer. This probably involves the uptake of low concentrations of ^{133}Cs by trees (section 3.2.8.1) which are returned in the form of litter fall to the forest floor. Decomposition of litter results in a concentration of ^{133}Cs within humified organic matter, reaching a maximum at the organic-mineral boundary which is close to the concentration in the mineral soil. Some degree of mixing of humified organic matter with mineral particles at this boundary would also be expected as a result of bioturbation, which would 'smooth' any differences in ^{133}Cs concentrations between organic and mineral layers.

In contrast, at Boundary Plantation ^{137}Cs has accumulated in the mid-depth (8 cm) of the organic soil layer whilst a minority of ^{137}Cs has migrated deeper into the mineral to a depth of 18 cm and, presumably, deeper than this (ie. below the depth of sampling in this study). If it is assumed that the major deposition of ^{137}Cs at this site occurred in 1963, this would imply a mean long-term vertical migration rate of 1.54 mm per year. The total measured inventory of ^{137}Cs in the soil, decay corrected to 1963, was 4,800 Bq m^{-2} down to a depth of 18 cm. This value is compared to the relevant literature values in section 6.3.2.2.

Throughout the soil profile the exchangeable fraction of ^{133}Cs (4 – 13%) was low in comparison with that of K (13 - 69%) (section 3.2.3). This confirms that ^{133}Cs was mainly in a 'fixed' form, especially in the mineral soil (4 - 9%

exchangeable ^{133}Cs). In the organic part of the soil, exchangeability of ^{133}Cs decreased systematically with depth from 13% in the litter layer to 9% in the lowermost organic layer (9 cm deep). This pattern probably results from the introduction of ^{133}Cs in a more labile form in tree litter at the soil surface, which gradually becomes less labile as decomposition of the litter takes place.

Isotopic exchangeability has been proposed as a better measure of the 'available' portion of an element within a soil than the 'exchangeable' concentration which is measured by displacing readily exchangeable ions using a salt solution such as 1M ammonium nitrate. In this study the isotopic exchangeability (E-Value) of ^{133}Cs with ^{134}Cs was higher (103 – 145%) than the exchangeable concentrations of ^{133}Cs (Table 3-3). This suggests that the exchangeable fraction of Cs isotopes in soil at Boundary Plantation probably does not provide an adequate measure of Cs lability and potential availability for biological uptake. At 5 and 7 cm depth, where ^{137}Cs accumulated (peaking at 6 cm), the exchangeable concentrations and the isotopic exchangeability (E-Value) of ^{133}Cs were both higher in the rest of the soil core. So, by both measures, the 'availability' of ^{133}Cs, was highest in the middle portion of the organic layer of the soil at Boundary Plantation where pH was lowest. E-Values were strongly negatively correlated with pH (R^2 = -0.9) which suggests that increased proton activity increases the reactivity of ^{133}Cs held on exchange sites or more specific binding sites, thus increasing availability. In studies of isotopic exchangeability of metals in soils, an equilibration period of at least 24 hours (Midwood, 2007) and usually 2 – 3 days (Ahmed et al., 2006) is usually considered sufficient. In the present study an equilibration period of 7 days (168 hours) was used as there was no prior information to suggest a longer or shorter time might be appropriate. Adsorption of ^{134}Cs increased rapidly between 1 hour and 1 day but slowed considerably between 1 day and 1 week (NB. desorption of ^{134}Cs occurred between 1 day and 1 week in the litter layer sample, 0 – 1 cm depth). This pattern of time-dependency indicates that adsorption of ^{134}Cs is kinetically limited, perhaps as a result of diffusion of ^{134}Cs into reactive sites in the soil solid phase. Careful scrutiny of Table 3-3 shows that the increase of E-values from 1 hour to 1 day and eventually to 1 week was greater in the mineral part of the soil. This shows that reaction of ^{134}Cs with soil solids is slower here than in the organic surface layers and suggests that longer equilibration times may be needed to achieve truly representative E-values. It would be useful to investigate the exchangeability and E-values of ^{137}Cs in the layers of peak accumulation, but this was not possible in this study due to restrictions on

counting time and detection limits for the low-level gamma-emissions from dilute liquid soil extracts.

Soil pH was negatively correlated with exchangeable ^{133}Cs and total ^{137}Cs within both organic and mineral soil layers (section 3.2.4.1). The peak ^{137}Cs activity concentration was found at a depth of 6 cm, just above the most acidic part of the soil profile (7 cm). Soil pH increased layer-by-layer above and below this depth, as did ^{137}Cs activity concentration, leading to the strongly negative correlation between pH and ^{137}Cs in Figure 3-13. This might be a coincidence resulting from the relative vertical distributions of pH and ^{137}Cs activity concentrations, or it may indicate that the highly decomposed and most acidic organic matter has a particularly high affinity for Cs. Native ^{133}Cs was more evenly distributed through the soil profile than ^{137}Cs, yet exchangeable ^{133}Cs concentration was also negatively correlated with pH. Interestingly, this overall negative correlation could be broken down into clearly distinct organic and mineral soil components, suggesting that the effects of pH on exchangeable ^{133}Cs was different in organic and mineral parts of the soil profile.

The distinction between mineral and organic parts of the soil was even stronger when the relationship between pH and the exchangeable fraction of ^{133}Cs was examined (Figure 3-12a). In this case there was positive correlation with pH in the organic soil, but a negative correlation with pH in the mineral soil. This pattern was also evident for ^{39}K and ^{85}Rb, suggesting a fundamental difference in the behaviour of all three alkali metals in organic and mineral parts of the soil.

The non-monotonic relationship between ^{137}Cs activity concentration and soil organic matter (Figure 3-18) was clearly strongly influenced by the relative vertical distributions of these two variables within the soil profile.

Total ^{133}Cs was systematically negatively correlated with soil organic matter, reflecting the fact that the major source of total native ^{133}Cs in the soil lies within the mineral component where organic matter is lowest (Figure 3-14a). Interestingly, this correlation was completely reversed for ^{39}K which is much more strongly incorporated into biological tissues and thus is much more concentrated in forest litter and organic matter than ^{133}Cs (Figure 3-14b).

The relationship between exchangeable concentrations of ^{133}Cs and soil organic matter was non-monotonic and indicated very different behaviour of exchangeable ^{133}Cs in organic and mineral parts of the soil profile. In organic soil above 9 cm depth, exchangeable ^{133}Cs decreased as organic matter increased, indicating that organic matter is involved in binding ^{133}Cs in this part

of the soil. The reverse correlation in the mineral soil suggests that the relatively small amounts of organic matter below 9 cm depth can increase the exchangeability of ^{133}Cs.

Total ^{133}Cs was very strongly correlated with its exchangeable and fixed fractions within the organic soil layer but the almost perfect linear correlation with the fixed fraction (Figure 3-19b) confirmed that most ^{133}Cs is present in an unavailable form.

Correlations of ^{137}Cs with total, exchangeable and fixed fractions of ^{133}Cs in the organic layer (section 3.2.5.2) were very similar whilst within the mineral layer ^{137}Cs was positively correlated with exchangeable ^{133}Cs. Negative correlations of ^{137}Cs with fixed and exchangeable ^{133}Cs occurred between 6 – 9 cm depth suggesting that ^{133}Cs has accumulated within the humidified part of the organic layer whilst ^{137}Cs was impeded from deeper migration though no clay minerals could be identified in the soil by XRD.

Potassium and rubidium both have strong physico-chemical similarities to caesium but generally (especially potassium) occur at much higher concentrations than caesium in soils. In the Boundary Plantation soil ^{39}K (237 – 866 mg kg^{-1}) and ^{85}Rb (2.24 – 7.37 mg kg^{-1}) were at much higher total concentrations than ^{133}Cs (0.16 – 0.61 mg kg^{-1}) (section 3.2.2.1). Depth profiles of the exchangeable fractions of ^{39}K and ^{85}Rb (Figure 3-10) show that exchangeabilities of ^{39}K (13.8 – 73.5%, 39.4% average) and ^{85}Rb (7.13 – 48.8%, 17.7% average) were 4.48 and 2.01 times greater than the exchangeability of ^{133}Cs (3.78 – 13.3%, 8.79% average). Within the organic layer the exchangeabilities of ^{133}Cs, ^{39}K and ^{85}Rb all increased with increasing organic matter content; however, exchangeabilities of ^{39}K (range 33.3 – 73.5%, average 59.5%) and ^{85}Rb (range 10.7 – 48.8%, average 27.4%) were greater than the average for the entire soil core (average 39.4% of ^{39}K and 17.7% of ^{85}Rb) for 51.0 and 55.1%, respectively. In contrast, the exchangeability of ^{133}Cs within the organic layer (range 9.59 – 14.2%, average 11.12%) was greater than the average of the entire soil profile (average 8.79%) for only 26.5%. This suggests that the 'available' concentrations of potassium, especially, dominated over exchangeable ^{133}Cs in the cation exchange sites within the Boundary Plantation soil. Thus, potassium availability, as a fraction of total soil potassium, for uptake by Corsican pine is much greater than that of caesium.

Generally, the aggregated transfer factor is more appropriate than a concentration ratio for evaluating radionuclide uptake by plants from multi-

layered forest soils. Corsican pine at Boundary Plantation favours uptake of ^{39}K and ^{85}Rb over ^{133}Cs, as indicated by the comparative concentration ratios (*CR*) and aggregated transfer factor (T_{ag}) of these elements in section 3.2.8.1. The *CR* and T_{ag} values for ^{39}K and ^{85}Rb in wood were greater than those of ^{133}Cs by 2 and 1 orders of magnitude whilst in fresh needles the differences were 3 and 2 orders of magnitude, respectively.

Corsican pine at Boundary Plantation absorbed both ^{39}K and ^{85}Rb in preference to ^{133}Cs, as indicated by the comparative concentration ratios (*CR*) of these elements in Table 3-7. The ratios of the $^{39}K/^{133}Cs$ CRs in wood and needles were 225,000 and 951,000, respectively, while the $^{85}Rb/^{133}Cs$ CRs in wood and needles were 271 and 914, respectively. Thus, of these three alkali metals Cs is not only the least abundant, it is also the least available within the soil and the least preferred during biological uptake from the available soil pool.

Despite the availability and biological uptake of K, Rb and Cs being quantitatively very different, the patterns of distribution of all three elements in trees appear similar (section 3.2.7.1). The radial distributions of ^{39}K, ^{85}Rb and ^{133}Cs concentrations across annual growth rings of Corsican pine were particularly similar in qualitative terms, with higher concentration of tree rings after around 1985 (344 and 156 mg kg^{-1} of ^{39}K, 0.43 and 0.17 mg kg^{-1} of ^{85}Rb, 1.73×10^{-3} and 4.92×10^{-4} mg kg^{-1} of ^{133}Cs for average concentration of tree rings after and before 1985, respectively). This probably reflects the demand for potassium, in particular, at the physiologically active cambial layer just beneath the bark, from which point secondary growth (trunk expansion) is initiated. It is likely that both ^{85}Rb and ^{133}Cs 'piggy back' on the movement of ^{39}K, since neither Rb or Cs are known to be essential for plant metabolism.

Translocation factors (f_{tr}) for ^{39}K, ^{85}Rb and ^{133}Cs from timber to needles in Corsican pine also indicate that transport of ^{39}K and ^{85}Rb are favoured over ^{133}Cs (f_{tr} = 29.2, 25.9 and 10.4 for ^{39}K, ^{85}Rb and ^{133}Cs, respectively). In addition, the ratios of $^{39}K/^{133}Cs$, $^{39}K/^{85}Rb$ and $^{85}Rb/^{133}Cs$ in wood (2.25×10^5, 8.32×10^2 and 2.71×10^2, respectively) are lower than in needles (6.34×10^5, 9.38×10^2 and 6.76×10^2, respectively), indicating that discrimination in favour of K is particularly high in needles where physiological activity is high.

All calculated factors related to the relative uptake and transport of ^{39}K, ^{85}Rb and ^{133}Cs from soil to wood and needles of Corsican pine indicate a strong biological preference in the order $^{39}K > ^{85}Rb > ^{133}Cs$ in Corsican pine.

The water solubilities of ^{39}K, ^{85}Rb and ^{133}Cs are directly related to their potential for leaching from Corsican pine needles as rainwater passes through the tree canopy. Ratios of $^{39}K/^{133}Cs$, $^{85}Rb/^{133}Cs$ in fresh needles (951,000 and 914, respectively) as shown in Table 3-7 were higher than in dry needles (104,000 and 987, respectively) suggesting a greater potential for loss of ^{39}K and ^{85}Rb by rainwater leaching than ^{133}Cs. However, ratios of $^{39}K/^{133}Cs$ and $^{85}Rb/^{133}Cs$ measured in throughfall water (184,000 and 209, respectively; Table 3-7) were somewhat lower than in fresh needles indicating that, in relation to the needle concentrations, proportionately less ^{39}K and ^{85}Rb is leached from needles than ^{133}Cs.

Interestingly, there was almost no difference in the $^{39}K/^{85}Rb$ ratios in fresh (1,060) and dry needles (1,070), which confirms the greater physiological similarity between these two elements than with Cs.

3.4 CONCLUSIONS

The soil at Boundary Plantation is typical of coniferous forests in the temperate zone. With an underlying geology of Sherwood Sandstone it has a well-developed surface organic horizon while the mineral part of the soil is composed almost entirely of quartz with no identifiable clay minerals which might 'fix' caesium originating from atmospheric fallout. Despite this lack of clay minerals, 52 years following deposition of nuclear weapons fallout, almost all the ^{137}Cs within the soil is distributed within the upper 9 cm of the surface organic layer.

The organic matter content in the soil appears to play an important role in the vertical distribution of ^{137}Cs and exchangeable (ie. non-fixed) ^{133}Cs. It increases the exchangeability of ^{133}Cs in the mineral part of the soil but decreases the exchangeable concentrations in the organic soil. Soil pH also appears to play a key role in controlling the mobility of Cs isotopes, with the most acidic layers within the soil organic horizons holding the highest ^{137}Cs activity concentrations and having the highest exchangeable ^{133}Cs concentrations.

The physico-chemical properties of the alkali earth elements K, Rb and Cs are very similar, yet there are distinct differences in their behaviour within soil and trees at Boundary Plantation. As a major nutrient, K is present in tree tissues at much higher concentrations than Rb and especially Cs. The degree of translocation of K from wood to pine needles is also higher than that of Rb and Cs. The vertical profile of K concentrations in the Boundary Plantation soil suggests that there is a substantial input of K at the soil surface in the form of tree litter. This is a quantitatively less important mechanism for Cs, but must still be operating because it accounts for the small concentrations of ^{133}Cs measured in the soil litter layer. Progressive humification of litter added to the soil surface leads to increasing concentrations of ^{133}Cs in the deeper parts of the soil organic horizon. This could be the most plausible mechanism to explain the slow migration of ^{137}Cs deposited in 1963 to a 'peak activity' depth of only 6 cm in 2015.

The soil depth at which maximum accumulation of ^{137}Cs is observed is also the most acidic part of the soil and appears to be the depth of complete humification of organic matter. If the rate of 'burial' of the organic matter at this depth is the same as the apparent rate of downwards migration of ^{137}Cs, it would suggest

that organic matter decomposition is the key process controlling the longevity of ^{137}Cs in the forest ecosystem. This hypothesis is tested in Chapter 7.

CHAPTER 4: CHERNOBYL FOREST

4.1 INTRODUCTION

The accident at the Chernobyl nuclear power plant occurred in April 1986 and released at least 100 times more radioactivity than the atomic weapons dropped on Japan in 1945. Around 8 x 10^{16} Bq of ^{137}Cs was deposited in Europe resulting in 6% of the continental area becoming contaminated with more than 20 kBqm^{-2} (IAEA, 1996; Smith, 2005). Moreover, within a 30 km radius an exclusion zone was established in which high levels of contamination with reactor fuel particles (so-called 'hot particles' of uranium oxide) were deposited (Chesser et al., 2004; Shaw, 2007).

About 45% of the area surrounding the Chernobyl nuclear power plant is covered with forest which was contaminated with various radionuclides after the accident. Within the soils of these forests the majority of ^{137}Cs is still found to be distributed within the surface organic (AoF and AoH) soil layers (Shaw, 2007).

4.1.1 Objectives

The long-term migration and recirculation behaviour of ^{137}Cs in Chernobyl nearby forest and possible impact on growth of Scots pine were investigated to test the hypotheses as follows.

- Long-term after initial deposition of 'hot particles' ^{137}Cs almost water-insoluble fragments of reactor fuel (uranium oxide) is faded and results to deeper migration of ^{137}Cs than AoF and AoH soil layers indicated by previous publications.
- Cycling of ^{137}Cs is comparable with other sites not receiving hot particles.
- Growth of Scots pine is effect by acute and high radiation exposure at duration of Chernobyl accident in 1986.

4.1.2 Sampling locations

Samples were taken in early September 2015 in Scots pine (*Pinus sylvestris L.*) plantations surrounding the Chernobyl nuclear power plant in Ukraine. This area

received acute and localised deposition of nuclear fallout during the Chernobyl reactor accident in April and May 1986.

The four sampling sites are shown in Figure 4-1 and their details are given in Table 4-1.

Figure 4-1 Map of the area surrounding the Chernobyl nuclear power plant showing sampling sites and contour lines of exposure to radiation from local nuclear fallout from the Chernobyl accident in 1986. The outer contour (red thin line) is the area which received radiation at about 0.5 - 2.0 mGy/h, while the middle contour line (red dashed line) covers the area which received radiation between 2.0 - 5.0 mGy/h. The inner contour (red thick line) is the area which received radiation more than 5.0 mGy/h. Within this contour lethal damage to coniferous trees was observed; the red areas within the North Trace and Red Forest are the areas affected by very high radiation doses where forest death occurred.

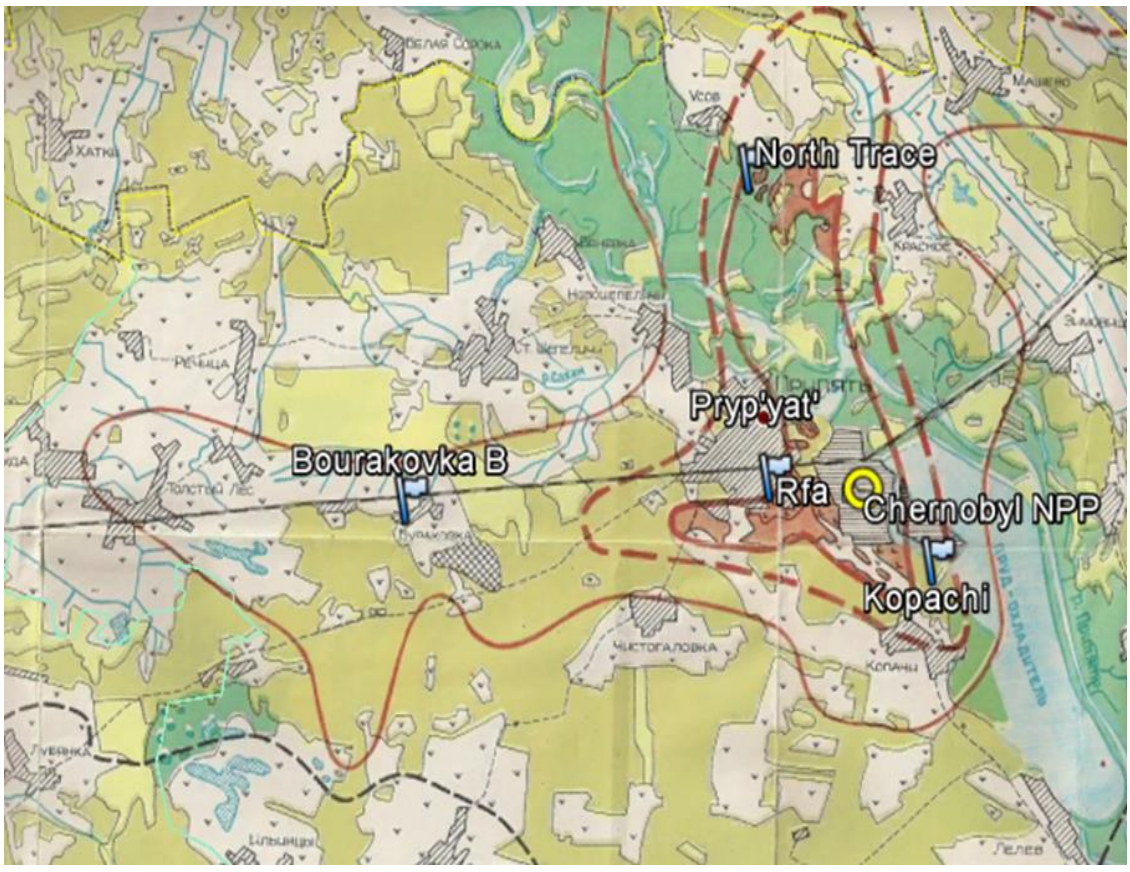


Table 4-1 Coordinates and sample types collected at six sites in the Chernobyl exclusion zone (tree cores and needles were all from Scots pine).

Collecting date	Site	Distance from reactor (km)	Coordination (WGS84 system)	Samples collection
1st September 2015	Kopachi	4 (south)	51°21'54.70"N 30° 7'46.43"E	2 soil cores, 2 tree cores, 1 fresh needle sample
	Bourakovka	13 (west)	51°22'47.49"N 29°54'40.21"E	1 tree core
	Red Forest	3 (west)	51°23'6.49"N 30° 3'43.51"E	2 tree cores
	Red Forest	3 (west)	51°23'12.07"N 30° 3'44.39"E	2 tree cores
2nd September 2015	North trace	7 (north)	51°27'30.69"N 30° 3'12.42"E	3 tree cores
5th September 2015	Bourakovka	13 (west)	51°22'45.28"N 29°54'49.31"E	2 tree cores

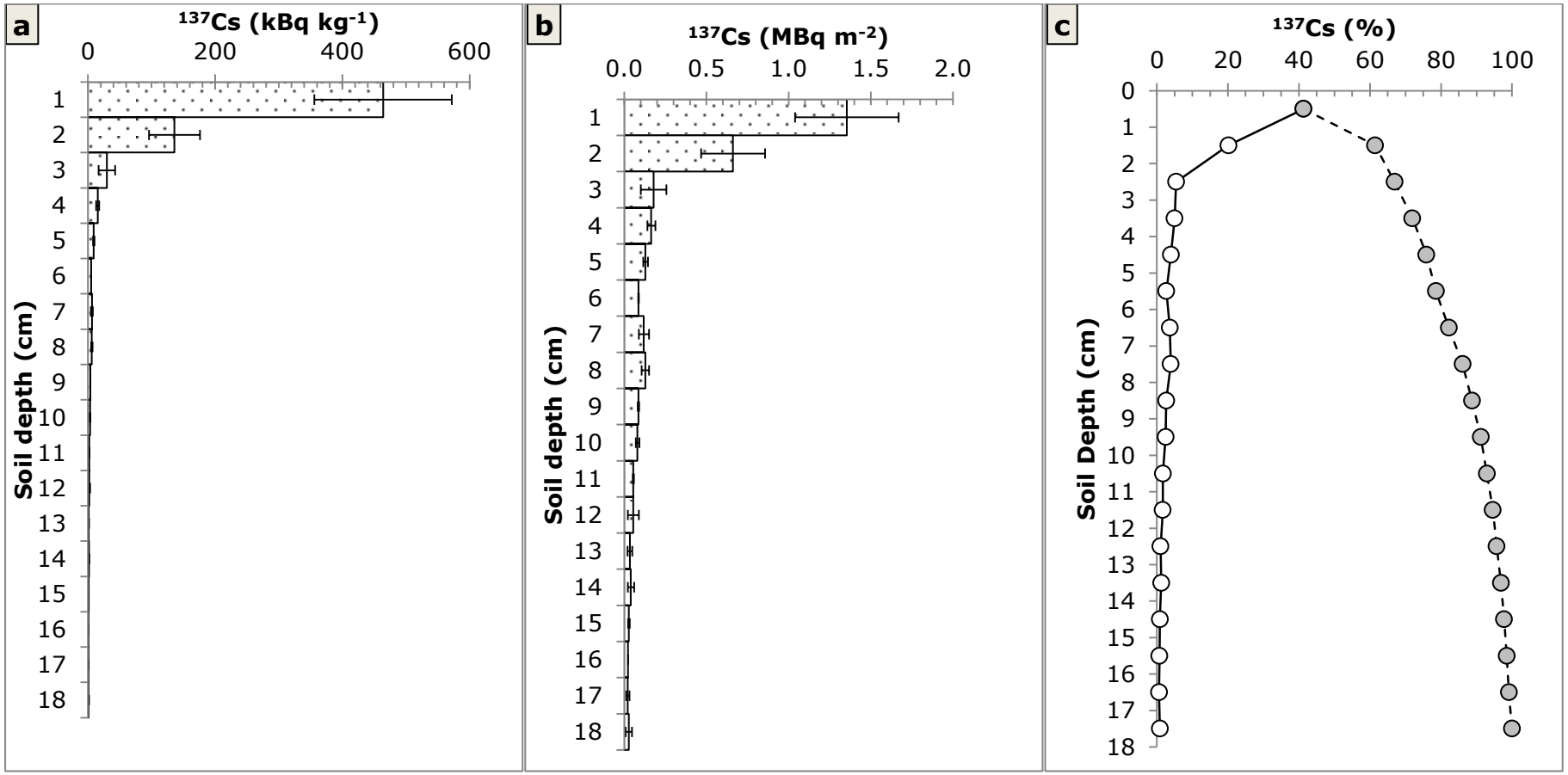
4.2 RESULTS

4.2.1 Vertical distribution of ^{137}Cs within Chernobyl forest soil

The activity concentration of ^{137}Cs within the forest soil profile at Kopachi was measured to investigate its distribution 29 years after deposition, as illustrated in Figure 4-2a. The results show that the activity concentration of ^{137}Cs was highest in the upper 2 - 3 cm of the soil profile, corresponding to the litter and organic layers on the forest floor. These surface layers contained approximately 70% of total ^{137}Cs 29 years after deposition to the forest at Kopachi, as shown in Figure 4-2c.

Total deposition of ^{137}Cs was calculated, as shown in Figure 4-2b. The calculated total deposition of ^{137}Cs at the sampling and deposition times are 1.69 MBq m^{-2} and 3.28 MBq m^{-2}, respectively.

Figure 4-2 Depth profile of average ^{137}Cs (a), ^{137}Cs deposition inventories (b) and percentage ^{137}Cs inventory (white circle) and accumulated percentage ^{137}Cs inventory (dark circle) (c), decay corrected to 1963 of soil collected at Kopachi (6 replicates, the horizontal bars are standard errors of means).



4.2.2 Distribution of ^{137}Cs in Scots pine

4.2.2.1 Bioavailability of ^{137}Cs

The tree rings and needles of Scots pine collected at forest sites within the Chernobyl exclusion zone were measured for ^{137}Cs activity concentration by high resolution gamma ray spectrometry; the results are shown in Table 4-2.

The most contaminated wood was collected at the Red Forest, followed by samples from the North Trace, Kopachi and Bourakovka, respectively. At Kopachi, ^{137}Cs contamination of needles was an order of magnitude higher than wood.

Table 4-2 Average ^{137}Cs in Scots pine wood collected at Red Forest (n = 4), North Trace (n = 3), Kopachi (n = 2) and Bourakovka (n = 5) and in Scots pine needles (n = 1) collected at Kopachi (SEM = standard error of mean).

Collecting site	^{137}Cs in Scots pine (Bq kg^{-1} dry weight)		
	wood		needle
	Average	SEM	Average
Red Forest	8.22×10^{3}	9.75×10^{1}	-
North Trace	5.31×10^{3}	7.38×10^{2}	-
Kopachi	2.93×10^{3}	1.75×10^{3}	2.21×10^{4}
Bourakovka	9.55×10^{2}	4.73×10^{2}	-

4.2.2.2 Uptake of ^{137}Cs

Quantifying the transfer of radionuclides from soils to plants within semi-natural or natural forest ecosystems is complicated due to the multi-layered nature of forest soils. The aggregated transfer factor (T_{ag}) is considered to be more appropriate than conventional concentration ratios in this context (IAEA, 2002). In this study T_{ag} values for ^{137}Cs in pine wood and needles at Kopachi were

calculated using equation 1.4 (section 1.2.8.3) and the results are shown in Table 4-3.

Table 4-3 Average T_{ag} of ^{137}Cs in Scots pine wood (n = 2) and needles (n = 1) collected at Kopachi in 2015 (SEM = standard error of mean).

T_{ag} (m^2 kg^{-1}) of ^{137}Cs in Scots pine at Kopachi		
Wood (n = 2)		Needle (n = 1)
Average	SEM	Average
1.74×10^{-3}	1.04×10^{-3}	1.31×10^{-2}

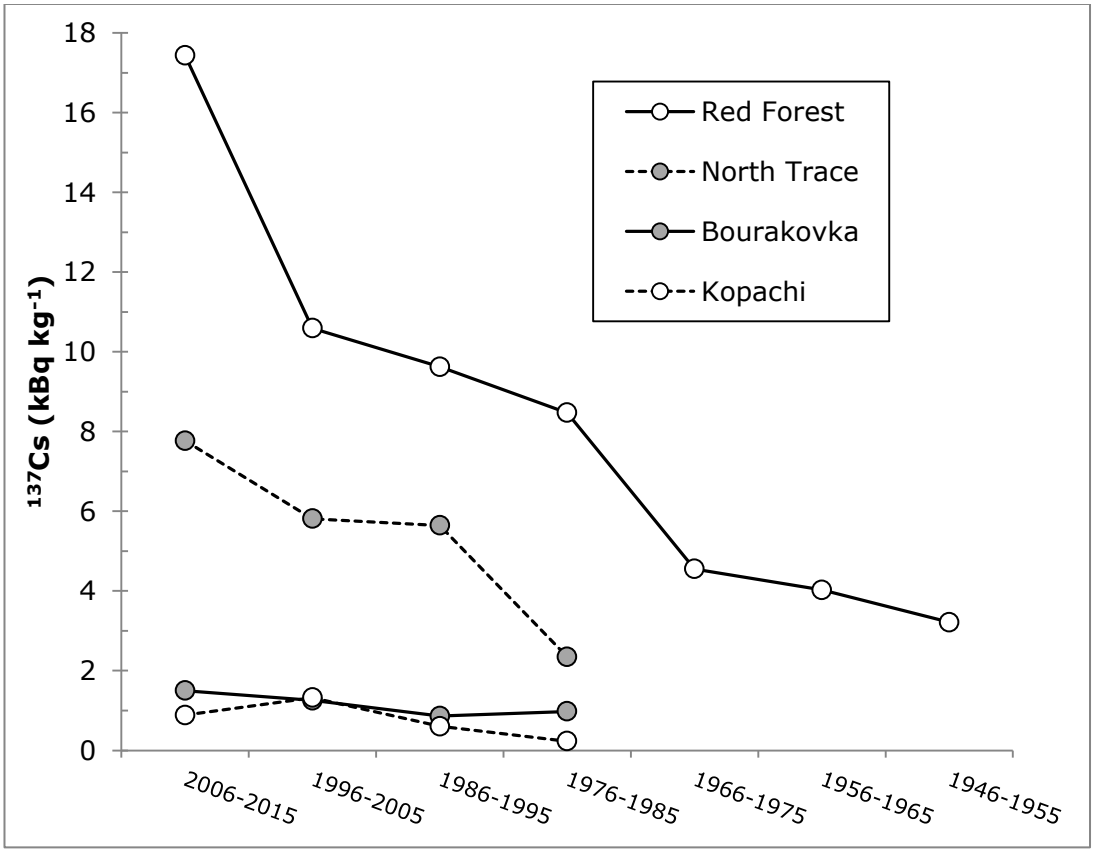
4.2.2.3 Distribution of ^{137}Cs in annual tree rings

Tree rings of Scots pine (in 10 year groups) were investigated for ^{137}Cs activity concentrations and the results are shown in Figure 4-3.

Average ^{137}Cs activity concentrations in tree cores collected at the Red Forest were around 8.60 and 2.81 times higher than those from Bourakovka and Kopachi, respectively. Activity concentrations in tree cores collected at the North Trace were around 5.56 and 1.81 times higher than those from Bourakovka and Kopachi, respectively.

There was a clear and consistent trend of higher ^{137}Cs activity concentrations in younger wood than in the older annual growth rings.

Figure 4-3 Activity concentrations of ^{137}Cs in wood of Scots pine collected at the Red Forest (4 replicates), North Trace (3 replicates), Bourakovka (3 replicates) and Kopachi (2 replicates), in the Chernobyl Exclusion Zone in September 2015.



4.2.2.4 Translocation of ^{137}Cs from timber to needles

A translocation factor (f_{tr}) was calculated using equation 3.2 (section 3.2.8.3) to determine the degree of transfer of ^{137}Cs from the wood of Scots pine to needles; the resulting value of 7.55 indicates a seven- to eight-fold higher activity concentration in needles compared with trunk wood.

4.2.3 Distribution of ^{137}Cs in forest inventory

Initial deposition of ^{137}Cs in soil was calculated in section 4.2.1 while in Scots pine was calculated by multiplying the activity concentration of Scots pine's crown by the biomass then decay corrected to 1963. Biomass of timber and crowns of Scots pine at Kopachi was calculated using forest mensuration tables and the geometric mean of the biomass fraction of needle and branch

compartments of temperate forests in the SEMINAT study (Belli, 2000) (as calculated for biomass of Corsican pine at Boundary Plantation in section 6.3.1).

The results summarised in Table 4-4 suggest about half of the deposited ^{137}Cs was distributed within litter. About 21.2% of ^{137}Cs was distributed in Scots pine, which is higher than about 3% measured for the same site in the 1990s (Shaw, 2007).

Table 4-4 Calculated biomass and distribution inventory of ^{137}Cs of Scots pine at Kopachi in 1986 (Calculated density of stand tree = 2.90 x 10^{-1} m^{-2}, Single timber volume = 6.74 x 10^{-1} m^3; depth of litter, organic layer and mineral layer refer to Boundary Plantation which were 2, 7 and 9 cm, respectively)

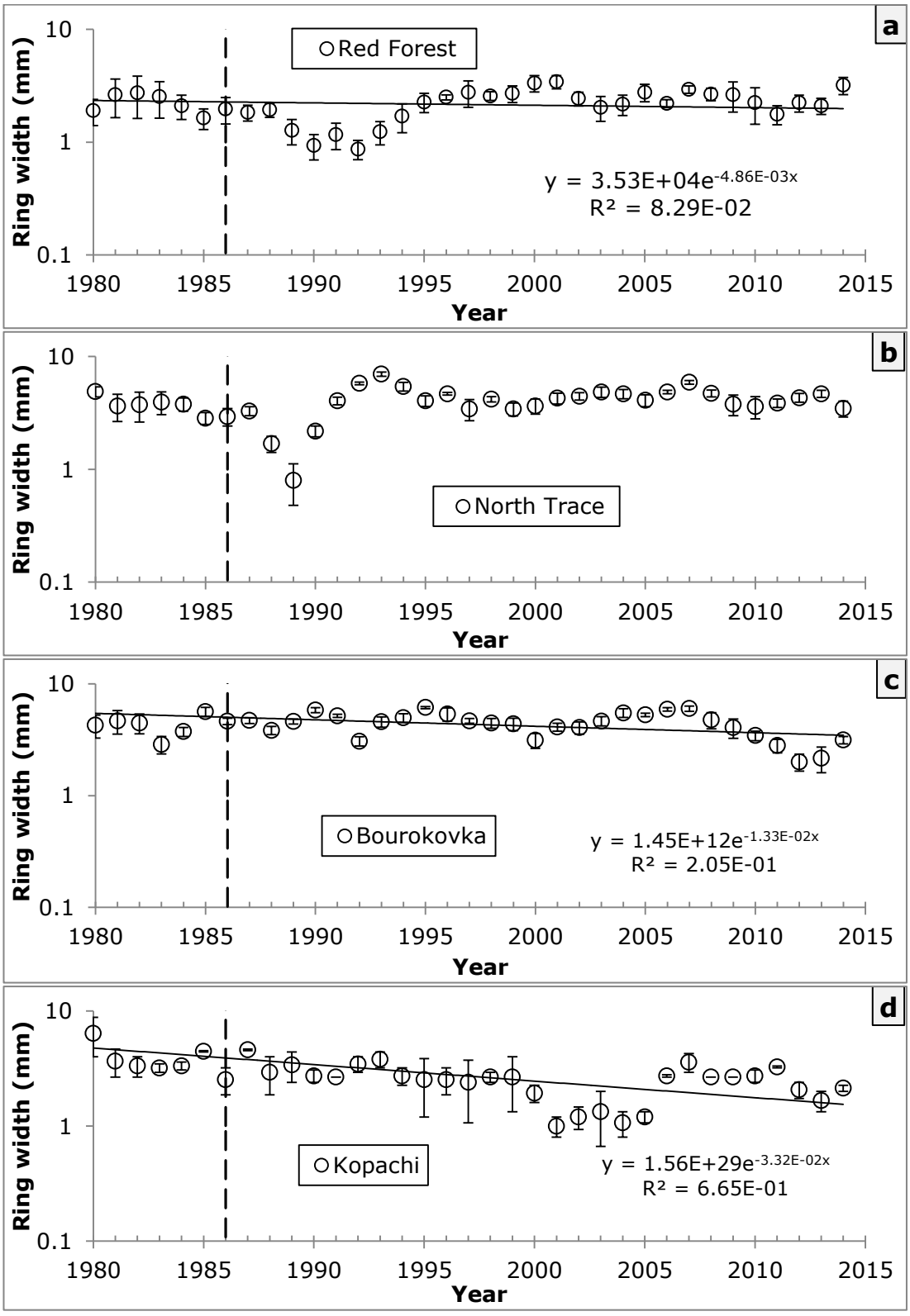
Forest inventory	Biomass (kg m^{-2})	^{137}Cs (Bq m^{-2})	Distribution (%)
Litter	-	2.02 x 10^6	48.4
Organic layer	-	8.95 x 10^5	21.5
Mineral layer	-	3.69 x 10^5	8.86
Timber	97.6 ± 12.6	5.56 x 10^5	13.4
Branch	8.98	5.12 x 10^4	1.23
Twig	3.22	6.95 x 10^4	0.44
Needle	6.00	2.58 x 10^5	6.20
Total	127	5.56 x 10^5	100

4.2.4 Impact of acute high dose radiation on the growth of Scots pine

The impact of acute high dose radiation on the growth of Scots pine was investigated using tree ring measurements obtained from trees in the Chernobyl Exclusion Zone (Figure 4-1 and Table 4-1). The average widths of annual growth rings obtained in this analysis are shown in Figure 4-4.

The results suggest that the growth of Scots Pine in the Red Forest and the North Trace decreased for several years after exposure to radiation in 1986. In the case of the North Trace, the widths of tree rings substantially increased between 1990 and 1993. From 1993 onwards, the widths of tree rings in the Red Forest and the North Trace decreased to continue the trend in tree ring widths measured before 1986. The widths of tree rings of pine stem wood collected at Bourakovka and Kopachi did not show any observable decrease immediately after 1986.

Figure 4-4 Mean annual growth ring widths (mm) of Scots pine collected in the Red Forest (a, n = 4), the North Trace (b, n = 2), Bourakovka (c, n = 2) and Kopachi (d, n = 2); the vertical bars are standard errors of means. NB. the vertical dashed line shows the year of the Chernobyl accident (1986).



4.3 DISCUSSION

The majority of ^{137}Cs was found to have accumulated within the AoF and AoH layers of the forest soil at Kopachi when sampled 7 – 8 years after the initial deposition of Chernobyl fallout (Shaw, 2007). Surprisingly, in 2015, 29 years after the initial deposition, ^{137}Cs in the same forest soil was still predominantly distributed within the organic material in the upper 2 - 3 cm of the soil profile.

This may be partly explained by the physico-chemical form of the fallout at this site which contained small, almost water-insoluble fragments of reactor fuel (uranium oxide), sometimes referred to as 'hot particles'.

However, this explanation is not entirely consistent with results of ^{137}Cs uptake in trees which indicate relatively high T_{ag} values (section 4.2.2.2) suggesting that uptake has been comparable with other sites not receiving hot particles.

Aggregated transfer factors (T_{ag}) of ^{137}Cs for Scots pine collected at Kopachi (1.74×10^{-3} and 1.31×10^{-2} m^2 kg^{-1} for wood and needles, respectively) were two orders of magnitude higher than of ^{133}Cs for wood and needle of Corsican pine at Boundary Plantation (Sherwood Forest - section 3.2.8.1; 1.34×10^{-5} and 1.39×10^{-4} m^2 kg^{-1} for wood and needles, respectively) which indicates that ^{137}Cs was more readily absorbed by pine trees at Kopachi than ^{133}Cs at Boundary Plantation. T_{ag} values for ^{133}Cs were also calculated based on exchangeable concentrations of ^{133}Cs in the organic layer (section 3.2.8.1; 1.90×10^{-4} and 1.97×10^{-3} m^2kg^{-1} for wood and needles, respectively). These are probably more appropriate for evaluation of ^{137}Cs uptake in pine wood and needles, but they are still an order of magnitude lower than the T_{ag} values for ^{137}Cs at Kopachi.

Approximately 21.2% of the total ^{137}Cs at Kopachi was distributed in Scots pine in 2015. This represents an increase from less than 3% in the 1990s, suggesting that ^{137}Cs in the soil at Kopachi had become more available for uptake by pine 10 – 20 years after initial measurements were made. Moreover, calculations using aggregated transfer factors suggest that only 4 – 5% of total deposition of ^{137}Cs is stored in the internal tree tissues at Boundary Plantation in 2015 and at Wat Ban Chan in 2016. This is probably because the estimated biomass of Scots pine at Kopachi (127 kg m^{-2}) is much greater than that of Corsican pine at Boundary Plantation (34.1 kg m^{-2}) and Three-needled pine at Wat Ban Chan (20.9 kg m^{-2}). These comparisons should be treated cautiously since estimates of percentage distributions of total radionuclide inventories in trees are sensitive to both T_{ag} values and estimates of standing biomass.

Figure 4-3 clearly shows that ^{137}Cs was preferentially transferred from older tree rings to younger wood adjacent to the cambial region where secondary growth (trunk expansion) occurs. This pattern of distribution was also seen for ^{133}Cs in the stem wood of Corsican pine at Boundary Plantation. This distribution, and the higher accumulation of both Cs and K in needles compared with stem wood, is probably due to the preferential transport of alkali metal ions to the more physiologically active tissues in trees, particularly to points of active growth including apical and lateral meristems.

The heaviest contamination of pine stem wood with ^{137}Cs was found in samples taken in the Red Forest. Pine stem wood samples from the North Trace had lower contamination than in the Red Forests, but significantly higher than in Kopachi and Bourakovka. The trend in contamination of pine stem wood is consistent with the level of exposure to radiation within the Chernobyl Exclusion Zone shown in Figure 4-1 which indicates that the Red Forest and North Trace were the areas affected by very high radiation doses resulting from very high initial deposition of ^{137}Cs. Kopachi and Bourakovka received lower ^{137}Cs deposition and significantly lower radiation doses between 2.0 – 5.0 and 0.5 – 2.0 mGy/h, respectively.

The growth of Scots Pine in the Red Forest and the North Trace decreased for several years after exposure to high radiation doses in 1986. In the case of the North Trace, there is evidence of a stimulation in growth (growth release) between 1990 and 1993, probably due to reduction in competition for resources as surrounding trees died. From 1993 onwards, tree growth in the Red Forest and the North Trace had returned to 'normal' (ie. it was consistent with the pre-1986 growth curve). Tree cores collected at Bourakovka and Kopachi did not show any signs of reduced or stimulated growth resulting from the acute release of nuclear fallout in 1986.

The impact of high radiation on the growth of Scots Pine is consistent with the level of exposure to radiation within the Chernobyl Exclusion Zone shown in Figure 4-1 as well as concentration of ^{137}Cs in pine stem wood which indicates that the Red Forest and North Trace were the areas affected by lethal of radiation dose.

Comparison of findings at Kopachi and Boundary Plantation

Summary data from Boundary Plantation, Wat Ban Chan and Kopachi are presented in Annex 1.

The shallow migration of ^{137}Cs into the soils at both Boundary Plantation and Kopachi is striking. Using the depth at which the maximum activity of ^{137}Cs was measured at the time of sampling mean migration rates of 1.54 and 0.69 mm y^{-1} can be calculated for Boundary Plantation and Kopachi, respectively. The 2-fold slower migration at Kopachi may be due in large part to the initial 'hot particle' form in which ^{137}Cs was deposited here in 1986, compared with the much finer (~1 μm) particles washed out of the atmosphere by rainfall which formed the bulk of atmospheric weapons fallout. Comparatively low ^{137}Cs migration in the soil at Kopachi might also be due, in part, to the apparently high percentage of the ^{137}Cs inventory (21.2 %) which has been estimated to be incorporated in standing tree tissues. The uptake of ^{137}Cs by Corsican pine at Boundary Plantation was below detection limits. However, the T_{ag} value for ^{137}Cs uptake by Scots pine at Kopachi was greater than the T_{ag} value of ^{133}Cs at Boundary Plantation (and Wat Ban Chan as well) which indicates that ^{137}Cs at Kopachi was more biologically available than ^{133}Cs at Boundary Plantation.

4.4 CONCLUSIONS

Almost 30 years after the Chernobyl nuclear accident the majority of ^{137}Cs appears to have been retained in the upper few centimetres of the forest soil profile at Kopachi, 8 km to the south east of the reactor. Even though this site received significant inputs of uranium oxide 'hot particles' in 1986, significant uptake of ^{137}Cs has occurred into both stem wood and needles of Scots pine. This suggests significant long-term recirculation of ^{137}Cs has occurred in the forest ecosystem at Kopachi since the initial deposition occurred. Uptake and translocation of ^{137}Cs by trees such as Scots pine is effected by the same transport system which delivers nutrients such as K to actively growing tissues, which is evidenced by the relatively high activity concentrations of ^{137}Cs measured in needles and younger tree rings.

Extremely high and acute radiation doses (more than 5.0 mGy/h) occurred in the Red Forest and the North Trace in the very early stages of the Chernobyl accident. Some of the Scots pine trees which were exposed to these doses died within a few weeks; those trees which survived, however, show only a transient decrease in growth rate for several years after 1986, and then show signs of accelerated growth possibly due to a reduction in competition from other surrounding trees. This is an acknowledged phenomenon known as 'growth release' which is observed after catastrophic events such as storms, major pollution episodes such as 'acid rain' or after thinning.

At Kopachi and Bourakovka, both sites that received much lower radiation doses, no effect of radiation on the growth rate of Scots pine trees was observed.

CHAPTER 5: WAT BAN CHAN FOREST, THAILAND

5.1 INTRODUCTION

The tropical forest zone lies roughly within 23.5 N and S from the equator. Data on radiocaesium contamination in tropical forest ecosystems are limited and few papers have been published on this topic (Thammavech, 2007).

Radionuclide transport in all parts of the world is dependent on site-specific climatic and environmental conditions. In tropical forests abundant rainfall plays an important role in the development of soil properties, although the water content of surface soil is strongly affected by extremely high temperatures during day time. Specific circumstances in tropical forest soils, such as dry and wet periods and high rates of weathering, may perhaps modify radionuclide behaviour. Rapid degradation of organic matter and advanced decomposition of clay minerals lead to low exchange capacities for macro-nutrients such as potassium. ^{137}Cs may be held weakly in tropical soils - the leaching rate is directly correlated to soil-to-plant transfer of nutrients such as potassium and ^{137}Cs (Pröhl et al., 2012).

Thammavech (2007) estimated soil-to-plant transfer factors (TF) of soils in Thailand and found that they decreased when soil pH, clay content and exchangeable potassium increased and when organic matter and NH_4^+ decreased.

5.1.1 Objectives

The long-term migration and recirculation behaviour of caesium in Wat Ban Chan and possible related factors were investigated to test the hypotheses as follows.

- Within poor-organic layer of tropical-forest soil surface soil with high clay mineral fixes ^{137}Cs at surface layer whilst surface soil without clay mineral ^{137}Cs is leached down to deeper layer.
- Low organic matter and narrow range pH are no effect on circulation of ^{137}Cs and ^{133}Cs in forest ecosystems.
- Stable potassium and rubidium are the important competitors on circulation of ^{137}Cs and ^{133}Cs in the forest ecosystems

- Stable caesium is the suitable indicator of radiocaesium within the forest ecosystems

5.1.2 Sampling locations

Sample collection was carried out during 25 – 26 February 2016 in a native tropical pine forest of *Pinus kesiya* (or Three-needled pine) at Wat Ban Chan which received chronic nuclear fallout from atmospheric weapons tests but not from the Chernobyl accident. The locations of sample collection points are shown in Figure 5-1.



Figure 5-1 Map showing location of Wat Ban Chan in Thailand and 6 random sampling points in a Three-needled pine forest (picture captured from Google Earth).

Figure 5-2 Photograph of Three-needled pine forest at Wat Ban Chan



The soil taxonomy system of USDA 1938 (USDA, 1977) has been applied to classify soils in Thailand into 20 Great Soil Groups. Figure 5-3 shows a soil map overlaid onto Google Earth showing that the Wat Ban Chan sampling site is in an area of Great Soil Group no. 20, that is 'steep land, intermediate to basic rocks, mainly Red-Yellow podzolic soils and Reddish-Brown Lateritic soils'. Figure 5-4 shows soil colour at the site suggesting it is red-yellow podzolic soil.

Pine forest in this area is tropical coniferous forest, mainly Kesiya pine mixed with some Two-needled pine, teak and palm trees. A general view of this pine forest (Figure 5-2) looks similar to a pine forest in the temperate zone. However, the litter layer and organic matter in soil are much less conspicuous in the tropical pine forest and mineral content is observable even on the surface of the soil.

Six collecting sites were randomly selected as shown in Table 5-1. Three soil samples were collected on 25th February 2016 and another three samples on 26th February 2016 after heavy overnight rainfall.

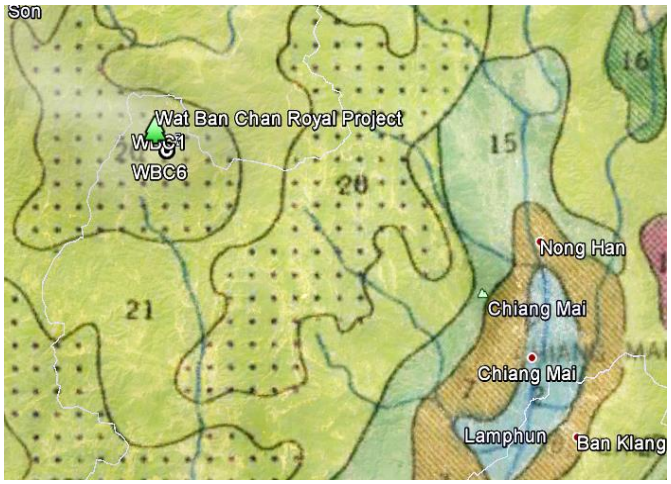


Figure 5-3 Soil classification map overlaid on Google Earth showing the Wat Ban Chan collecting site is in an area of Great Soil Group no. 20, that is 'steep land, intermediate to basic rocks, mainly Red-Yellow podzolic soils and Reddish-Brown Lateritic soils'.



Figure 5-4 Photograph of soil at a Three-needled pine forest at Wat Ban Chan, Chiang Mai, Thailand. It shows the typical red-yellow colour of a podzolic soil.

Table 5-1 Randomly selected geographical coordinates of 6 sampling sites in Wat Ban Chan Pine forest. Soil cores, tree cores and needles of Three-needled pine were collected from all sites.

Collecting date	Site	Coordinates (WGS84*)
25 February 2016	1	19° 3'55.10"N, 98°18'55.96"E
	2	19° 3'54.83"N, 98°18'56.24"E
	3	19° 3'54.51"N, 98°18'55.50"E
26 February 2016	4	19° 3'55.20"N, 98°18'55.59"E
	5	19° 3'53.04"N 98°18'54.57"E
	6	19° 3'52.44"N, 98°18'56.17"E

5.2 RESULTS

5.2.1 Soil properties

Soil cores were taken to a depth of 13 cm at Wat Ban Chan. The fundamental soil properties investigated were soil pH, organic matter and mineralogy, as described below.

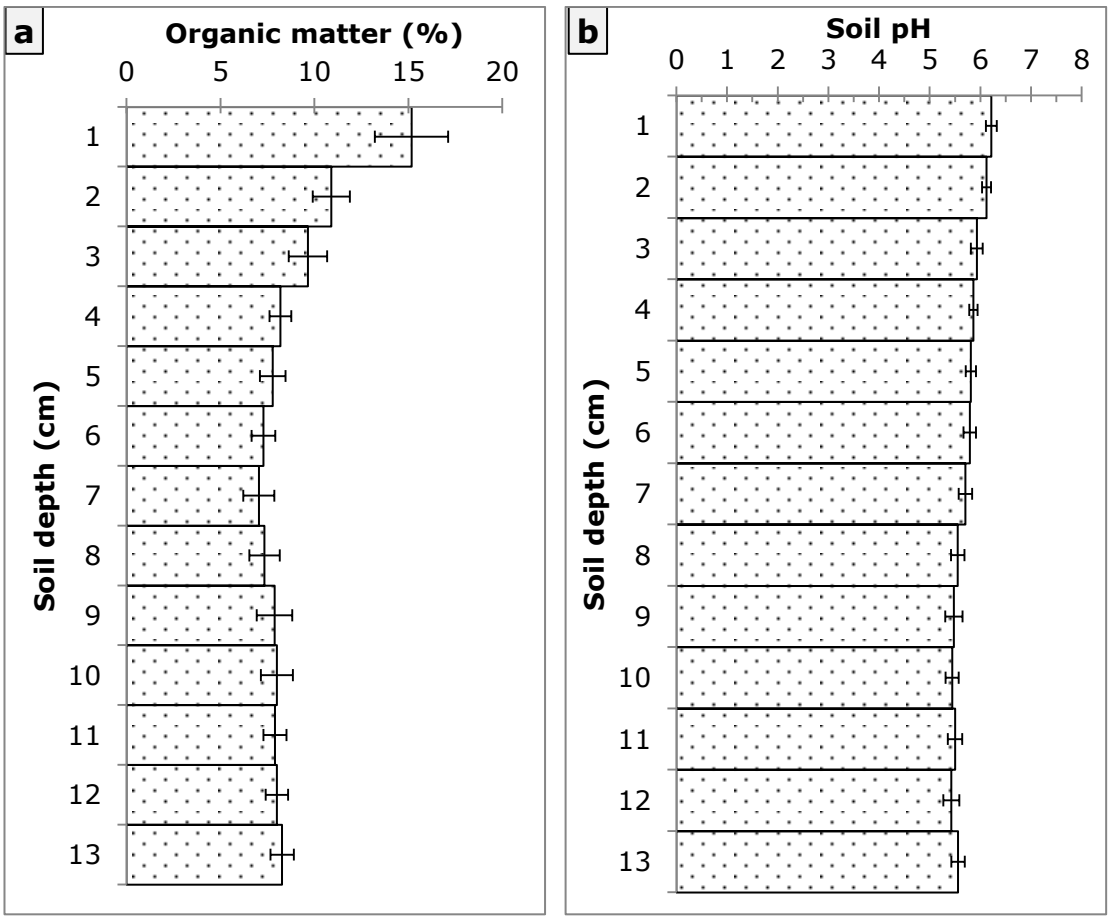
5.2.1.1 Organic matter content

Organic matter content in soil profiles was measured using loss on ignition (LOI - see section 2.4.1 for details of methods); the results are shown in Figure 5-5a.

Even in the upper part of the soil profile, the organic matter was relatively low (compared with a temperate pine forest soil) and decreased systematically to a depth of 7 cm. The maximum average organic matter content was 15.2 % in the 'litter' layer and the minimum was 7.04 – 8.01 % in the lower part of the soil cores (5 - 13 cm depth). Only the upper 3 cm had OM which was higher than

the average of the entire soil profile; the variability of OM in the upper 3 cm was also generally greater than lower down the soil core.

Figure 5-5 Depth profiles of average organic matter content (a) and pH (b) of soil collected at Wat Ban Chan forest (6 replicates, the horizontal bars show standard errors of means).



5.2.1.2 Soil pH

pH of the soil core collected at Wat Ban Chan was measured layer-by-layer (see section 2.4.2 for details of methods) as illustrated in Figure 5-5b.

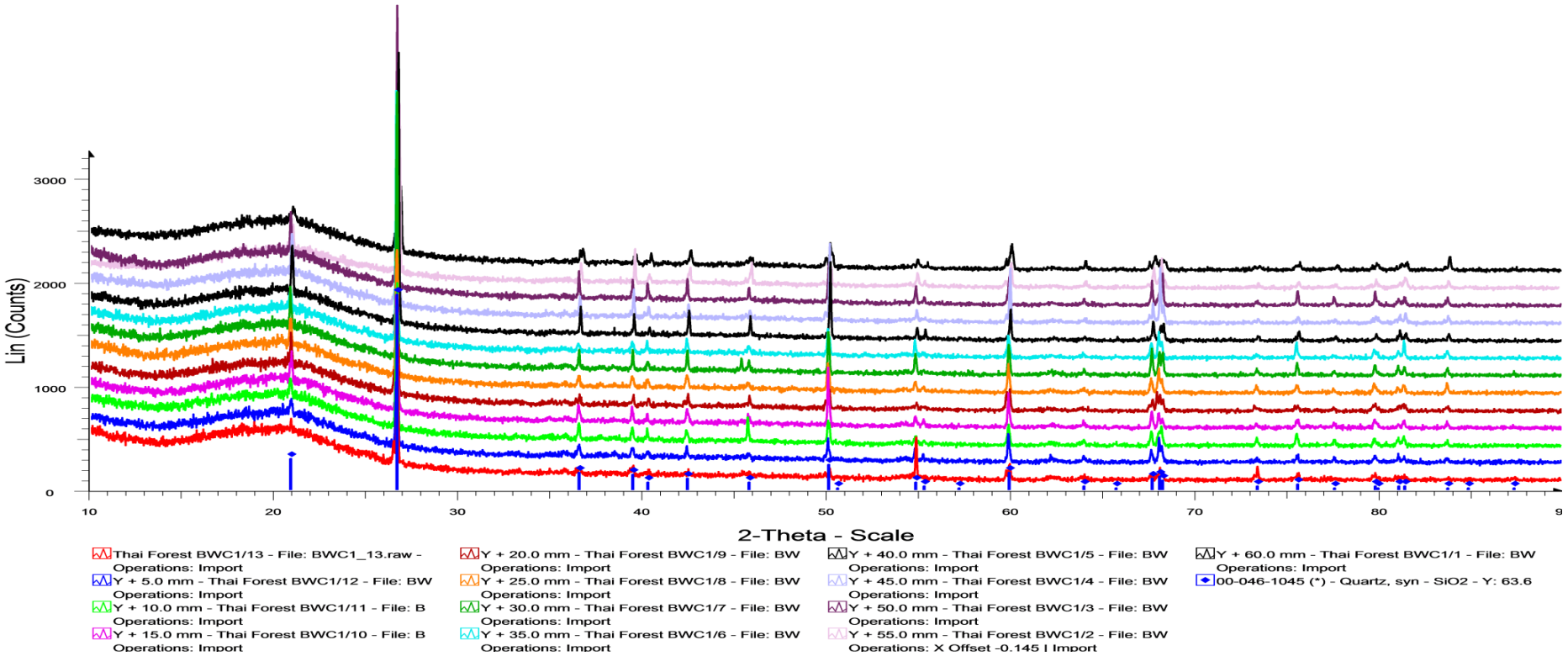
Soil pH at Wat Ban Chan was maximal in the uppermost (soil surface) layer, then slowly decreased with depth. At 9 – 13 cm depth, soil pH ranged between 5.43 – 5.56. The entire pH range in the soil cores was less than one pH unit, in contrast to the much larger pH range seen in the temperate forest soil at Boundary Plantation (Figure 3-4).

5.2.1.3 Mineralogy of soil profile

Samples from each 1 cm layer within the Wat Ban Chan soil cores were analysed to investigate changes in mineralogy down the soil profile using X-Ray Diffraction (XRD - see section 2.4.3 for details of methods). The diffraction patterns (diffractograms) of all 13 depth samples of the soil profile are shown in Figure 5-6.

The XRD results suggest that quartz was the only major crystalline phase in all soil layers. At some depths there was evidence of a second phase with reflections around the major quartz reflections. This is typical of the plagioclase group feldspars e.g. labradorite, albite, microcline ($M(AlSi)_4O_8$). Significantly, there was no indication of low-angled reflections belonging to any layered clay minerals which might be implicated in the specific sorption of caesium isotopes (Dann, pers. comm.).

Figure 5-6 Overlaid XRD diffractograms of 13 soil samples representing 1 to 13 cm depths (from uppermost to lowermost lines plotted in the figure) of the soil profile at Wat Ban Chan. The Y axis represents intensity (related to only the lowermost spectrum at 13 cm depth), the X axis is 2Theta (2Θ, degree of diffraction) of the Bragg equation.



5.2.2 Vertical distribution of total of stable caesium (^{133}Cs), potassium (^{39}K) and rubidium (^{85}Rb)

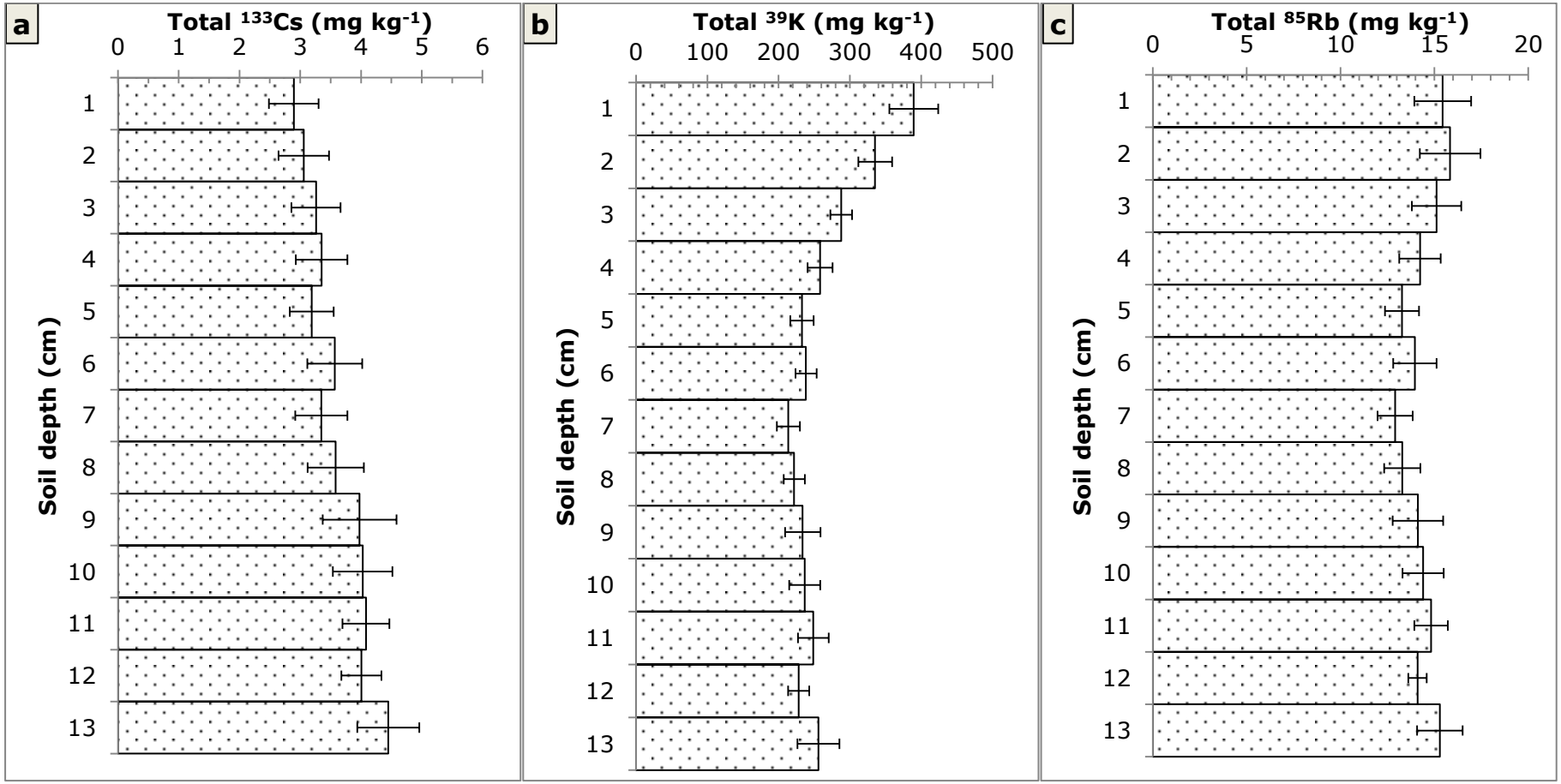
Vertical distributions of total, exchangeable and fixed concentrations of ^{133}Cs, ^{39}K and ^{85}Rb including activity concentration of ^{137}Cs were measured throughout the 13 cm soil cores collected at Wat Ban Chan; the results are presented below.

5.2.2.1 Total ^{133}Cs, ^{39}K and ^{85}Rb

Vertical distributions of average total concentrations of ^{133}Cs, ^{39}K and ^{85}Rb throughout the upper 13 cm of the Wat Ban Chan soil profile are shown in Figure 5-7.

The results illustrate that total concentrations of stable caesium, potassium and rubidium in the Thai forest soil were within narrow ranges between 2.89 – 4.45, 214 – 389 and 12.9 – 15.8 mg kg^{-1}, respectively. In the uppermost layer, total ^{133}Cs was minimal at 2.89 mg kg^{-1} whilst total ^{39}K was maximal at 389 mg kg^{-1}. Total ^{39}K and ^{85}Rb concentrations were minimal at 214 and 12.9 mg kg^{-1}, respectively, in the 7 cm depth of soil profile.

Figure 5-7 Depth profiles of average total concentrations of ^{133}Cs (a), ^{39}K (b) and ^{85}Rb (c) in soil cores collected at Wat Ban Chan (6 replicates, the horizontal bars are standard errors of means).

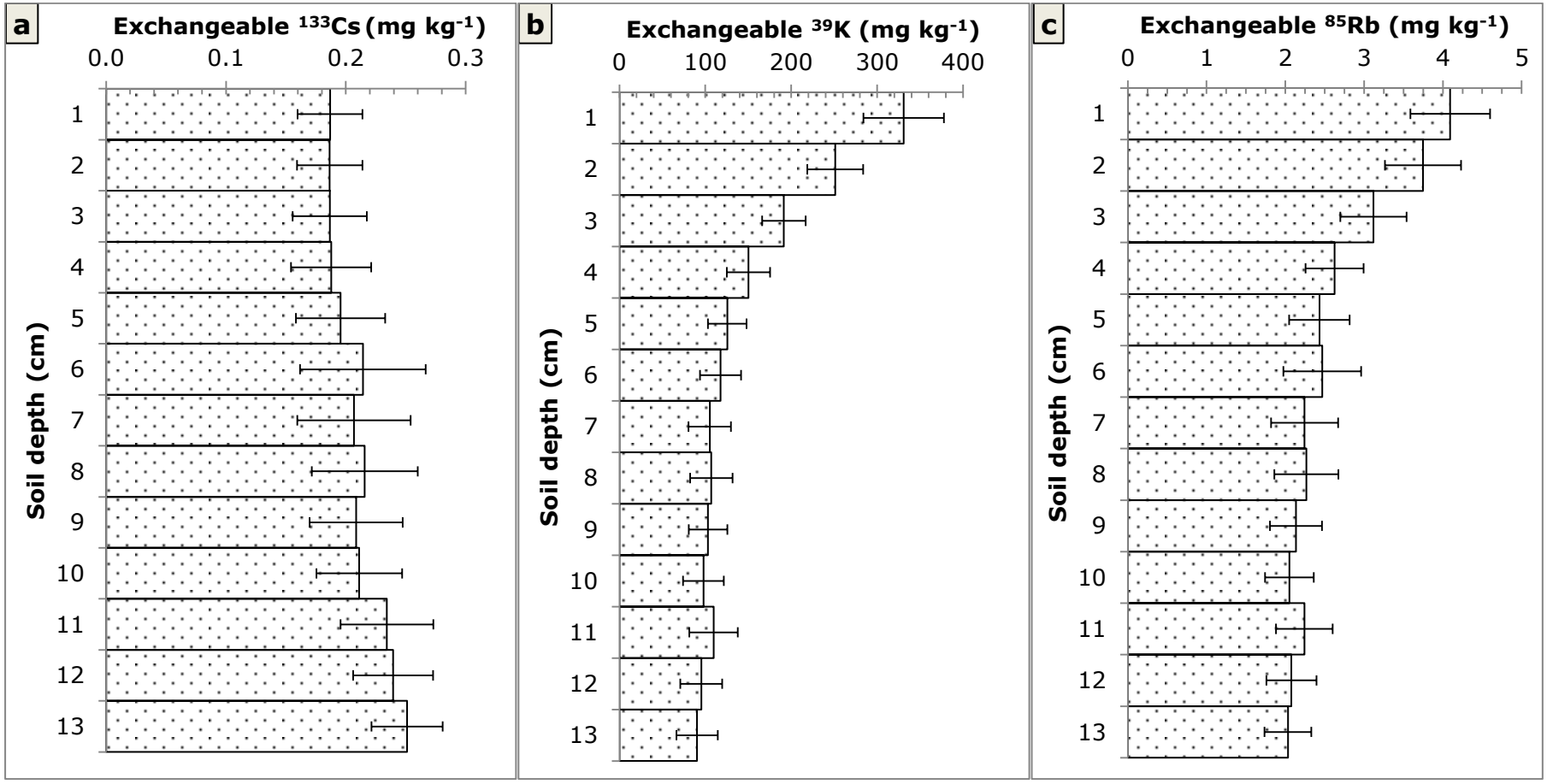


5.2.2.2 Exchangeable ^{133}Cs, ^{39}K and ^{85}Rb

Vertical distributions of exchangeable concentrations of ^{133}Cs, ^{39}K and ^{85}Rb throughout the Wat Ban Chan soil profile are shown in Figure 5-8.

The results illustrate that exchangeable ^{133}Cs was minimal at 0.19 mg kg^{-1} in the uppermost (surface) layer, in contrast to exchangeable ^{39}K and ^{85}Rb which were maximal at 331 and 4.09 mg kg^{-1}, respectively, in this layer. In bottom part of the soil core exchangeable ^{133}Cs was maximal at 0.25 mg kg^{-1} but exchangeable ^{39}K and ^{85}Rb were minimal at 90.4 and 2.03 mg kg^{-1}, respectively.

Figure 5-8 Depth profiles of average exchangeable concentrations of ^{133}Cs (a), ^{39}K (b) and ^{85}Rb (c) in soil cores collected at Wat Ban Chan (6 replicates, the horizontal bars are standard errors of means).



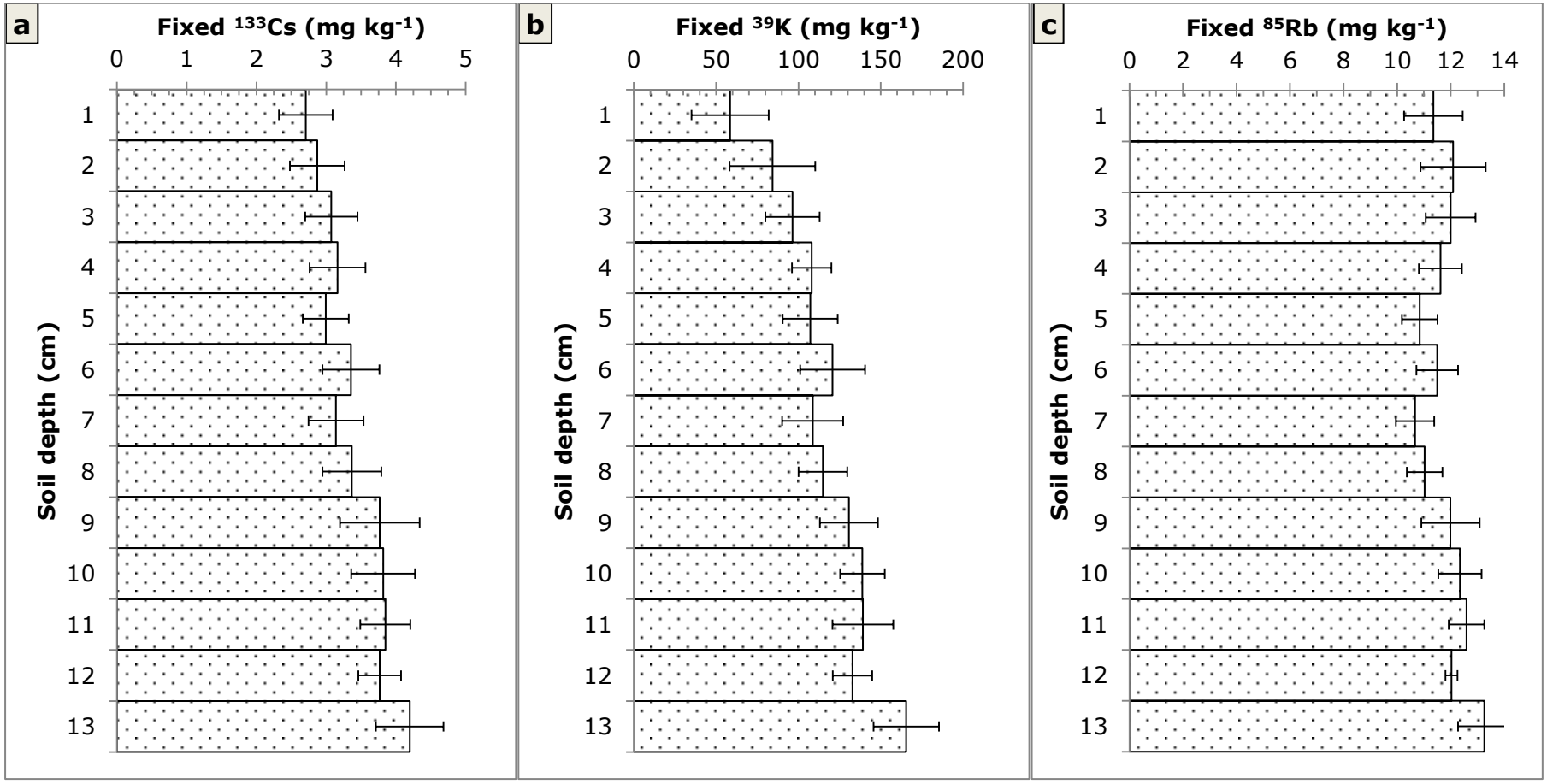
5.2.2.3 Fixed ^{133}Cs, ^{39}K and ^{85}Rb

'Unavailable' or 'fixed' concentrations of ^{133}Cs, ^{39}K and ^{85}Rb were calculated by subtracting exchangeable from total concentrations. The vertical distributions of unavailable concentrations of ^{133}Cs, ^{39}K and ^{85}Rb throughout the 13 cm of soil cores are shown in Figure 5-9.

As with the total concentrations, the fixed fraction of ^{39}K was much higher in absolute concentration units than for ^{133}Cs and ^{85}Rb throughout the soil cores.

The vertical distribution of fixed ^{133}Cs was qualitatively very similar to its total and exchangeable concentrations, with minimum and maximum fixed ^{133}Cs in the upper and lower parts of the soil core, respectively. Fixed ^{39}K also showed a qualitatively very similar distribution to fixed ^{133}Cs.

Figure 5-9 Depth profiles of average of 'unavailable' concentrations of ^{133}Cs (a), ^{39}K (b) and ^{85}Rb (c) in soil collected at Wat Ban Chan (6 replicates, the horizontal bars are standard errors of means).



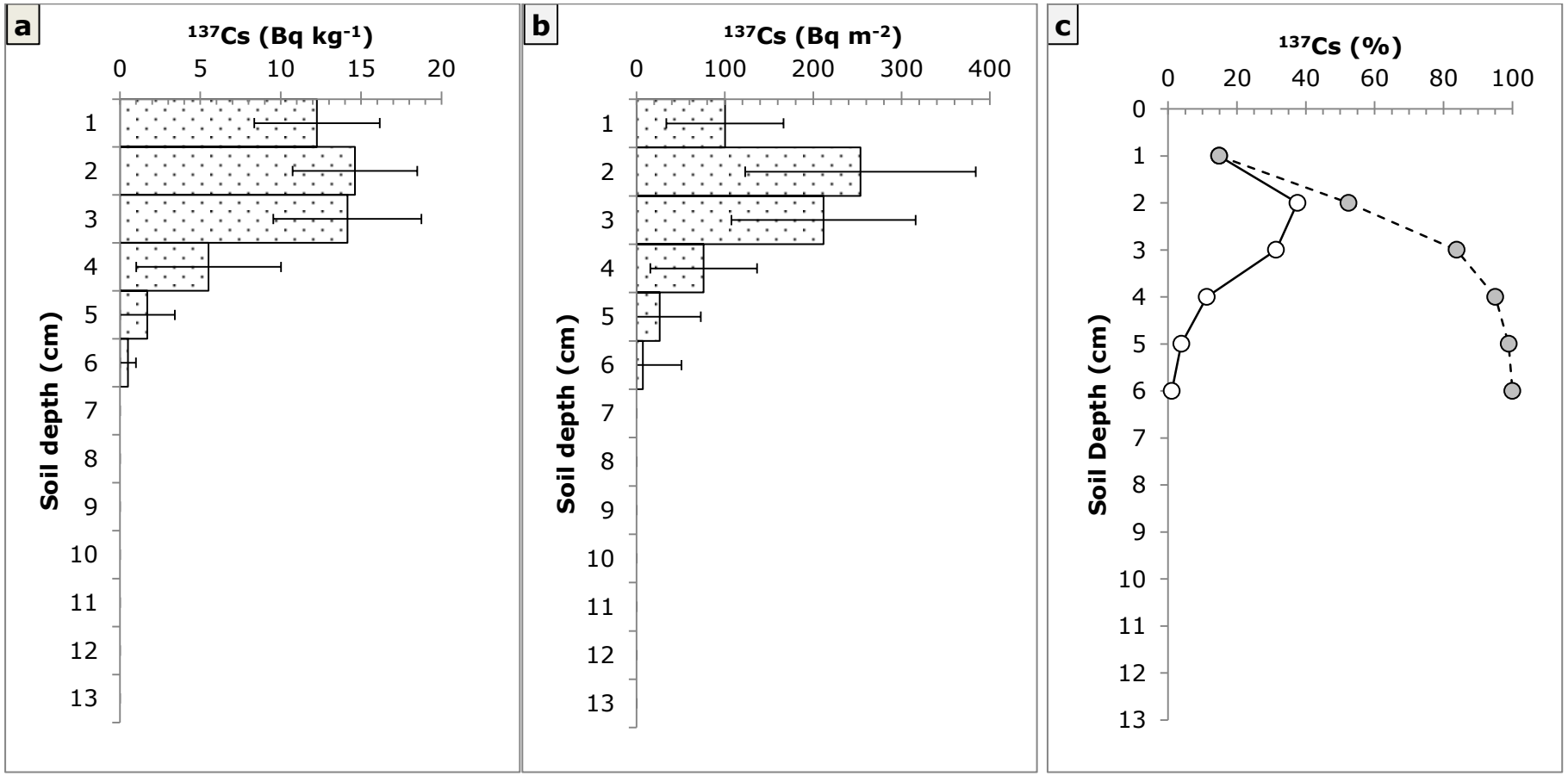
5.2.2.4 ^{137}Cs

Activity concentrations of ^{137}Cs in the soil profile were measured and decay corrected to 1963 as the assumed year of peak atmospheric deposition at Wat Ban Chan. The results are shown in Figure 5-10a. The results show accumulation of ^{137}Cs in the upper part of the soil layer (14.2 - 14.6 Bq kg^{-1} at 2 - 3 cm depth); no detectable ^{137}Cs was found in soil layers deeper than 6 cm.

The activity concentration of ^{137}Cs in each soil layer at Wat Ban Chan (Bq kg^{-1}) is shown in Figure 5-10a. ^{137}Cs activity concentrations were multiplied by the bulk density for each layer, allowing a layer-by-layer activity inventory to be constructed, as shown in Figure 5-10b. These inventories were decay corrected to 1963 and summed to provide a total soil profile inventory of 643 Bq m^{-2}.

The percentage ^{137}Cs distribution and its accumulation in soil core are shown in Figure 5-10c. It can be seen that about 50% of ^{137}Cs was distributed to a depth of 2 cm while 95% of ^{137}Cs was distributed to a depth of 4 cm. In other words, vertical migration of ^{137}Cs 53 years since deposition in 1963 has been minimal.

Figure 5-10 Depth profile of average ^{137}Cs (a), ^{137}Cs deposition inventories (b) and percentage ^{137}Cs inventory (white circle) and accumulated percentage ^{137}Cs inventory (dark circle) (c), decay corrected to 1963 of soil collected at Wat Ban Chan (6 replicates, the horizontal bars are standard errors of means).

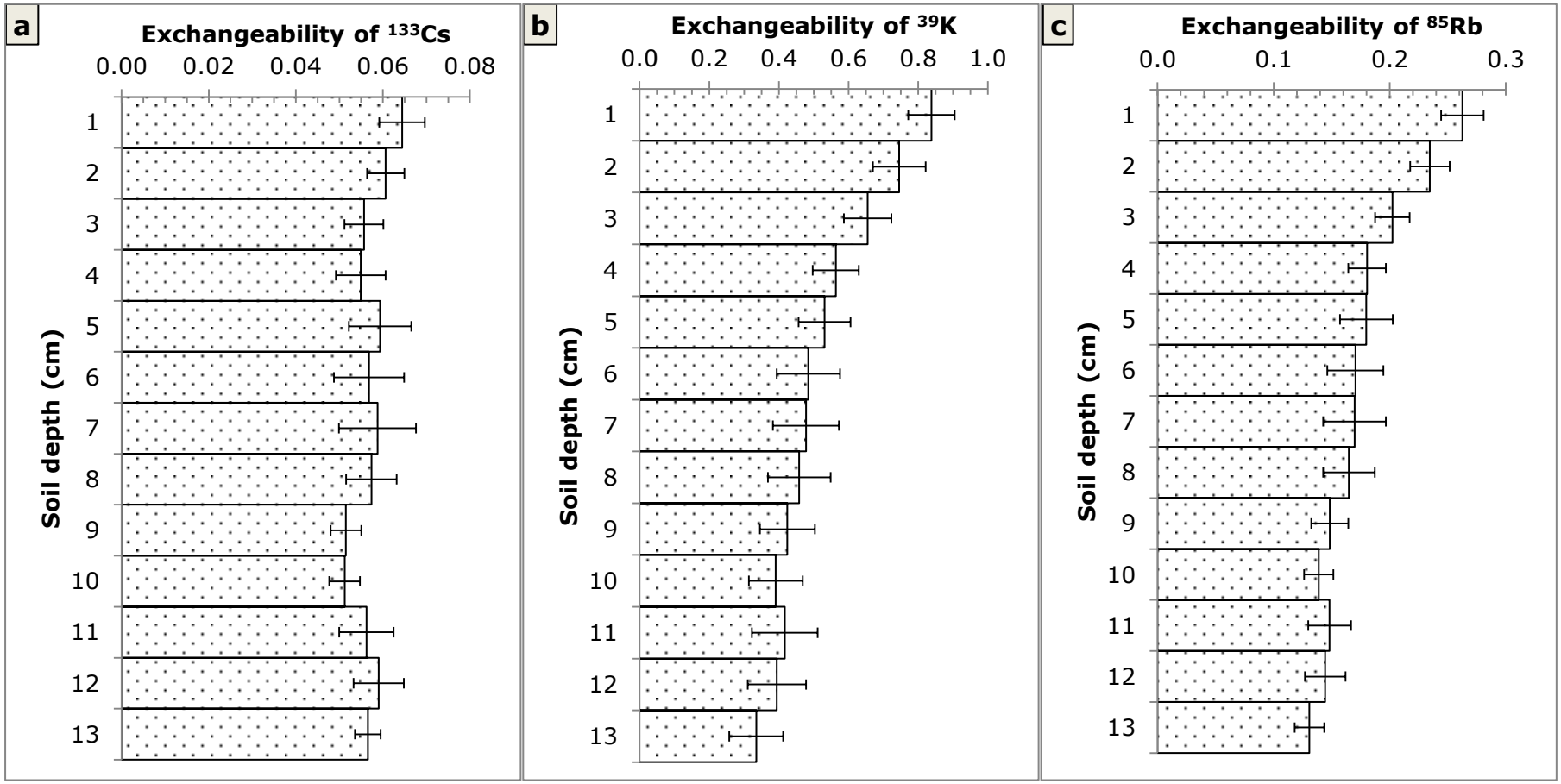


5.2.3 Exchangeable fractions of ^{133}Cs, ^{39}K and ^{85}Rb

The exchangeable fractions ('exchangeability') of ^{133}Cs, ^{39}K and ^{85}Rb within the soil profile were calculated using equation 2.2 and the results are shown in Figure 5-11.

Results suggest that exchangeability of ^{133}Cs (5.12 – 6.44 %) was least whilst that of ^{39}K (33.5 – 83.8 %) was highest for the three alkali metals. Exchangeability of ^{133}Cs was almost constant throughout the soil cores whilst exchangeabilities of ^{39}K and ^{85}Rb both decreased with soil depth. The gradients of decrease in exchangeability of ^{39}K and ^{85}Rb were steeper in the organic layer than in the deeper mineral layer.

Figure 5-11 Depth profiles of average exchangeability of ^{133}Cs (a), ^{39}K (b) and ^{85}Rb (c) in forest soil cores collected at Wat Ban Chan, Chiang Mai, Thailand (the vertical bars are standard errors of means).



5.2.4 Correlations of forest soil properties with ^{133}Cs, ^{39}K, ^{85}Rb and ^{137}Cs in the soil cores

Relationships of soil pH and organic matter with total, exchangeable and fixed concentrations of ^{133}Cs, ^{39}K, ^{85}Rb and ^{137}Cs were investigated by examining correlations between these variables.

5.2.4.1 Soil pH

Theoretically, soil pH is directly related to H^+ activity in soil solution. Since the H^+ is a strong competitor for available cation exchange sites in soils, correlations of exchangeable ^{133}Cs, ^{39}K and ^{85}Rb with soil pH were investigated. In the case of ^{137}Cs, no exchangeable concentrations were available so the correlation of total ^{137}Cs with soil pH was investigated.

- *Correlations of soil pH with exchangeable concentrations of ^{133}Cs, ^{39}K and ^{85}Rb*

Correlations between average soil pH and exchangeable concentrations of ^{133}Cs, ^{39}K and ^{85}Rb within the soil profile are shown in Figure 5-12.

Correlation patterns of soil pH with exchangeable concentrations of ^{39}K and ^{85}Rb were similar, but somewhat different for ^{133}Cs. Generally, an increase in soil pH was associated with a decrease in exchangeable ^{133}Cs but with an increase in exchangeable ^{39}K and ^{85}Rb.

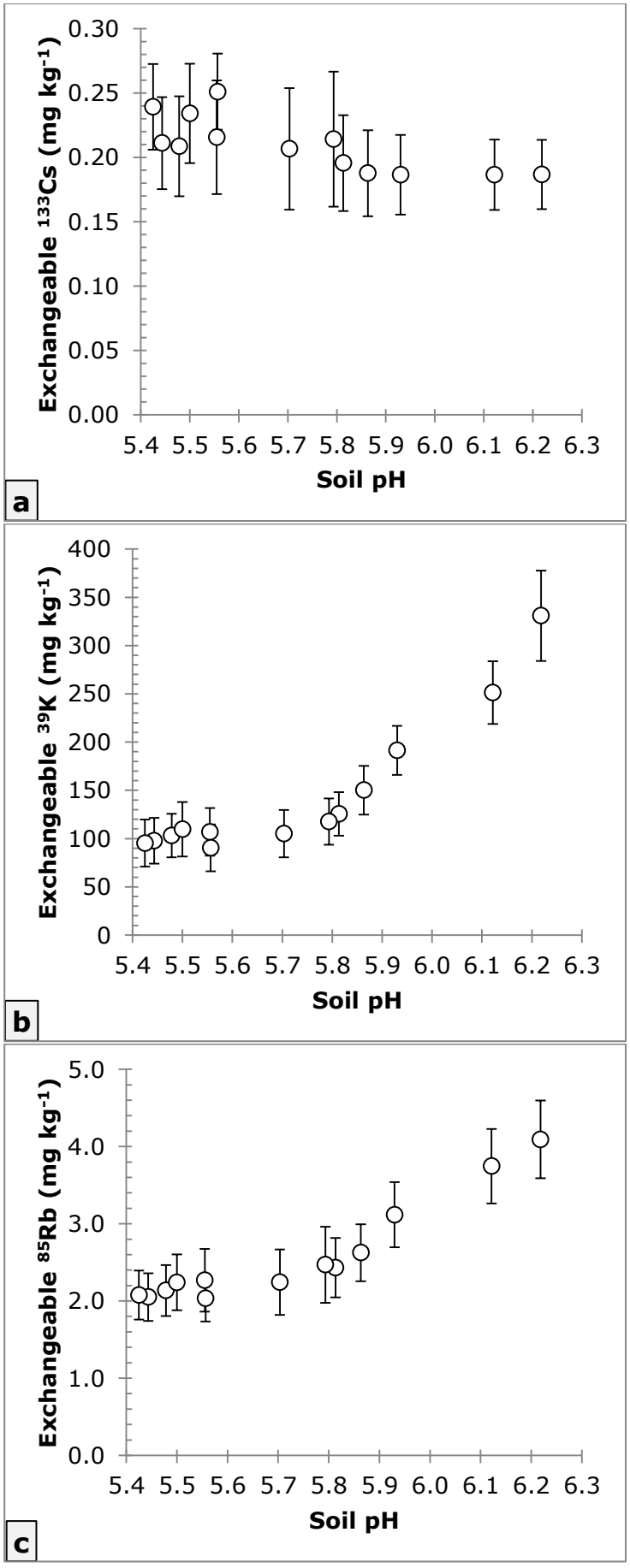


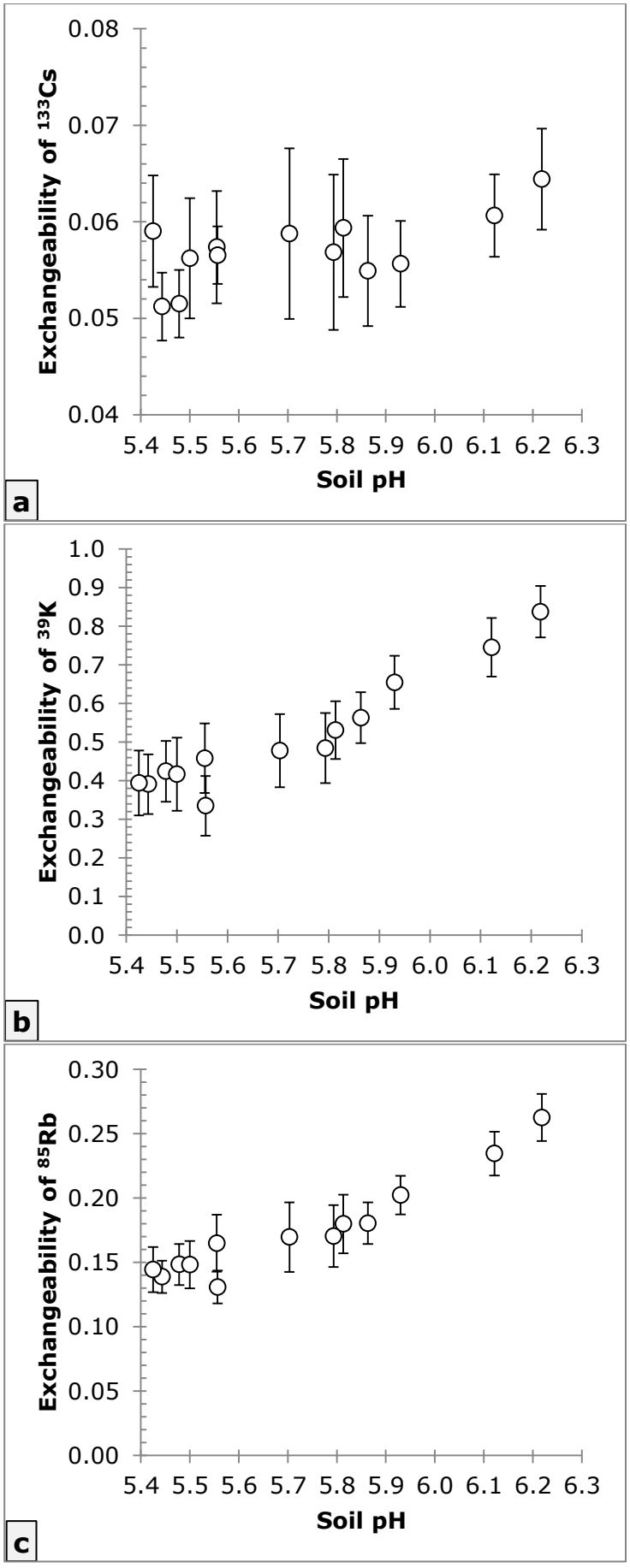
Figure 5-12 *Correlations of average soil pH with average exchangeable concentrations of ^{133}Cs (a), ^{39}K (b) and ^{85}Rb (c) in soil cores collected at Wat Ban Chan (6 replicates, the vertical bars are standard errors of means).*

- *Correlations with exchangeabilities of ^{133}Cs, ^{39}K and ^{85}Rb*

Correlations between average soil pH and exchangeable fractions of ^{133}Cs, ^{39}K and ^{85}Rb within the soil cores are shown in Figure 5-13.

As with exchangeable concentrations, exchangeable fractions of ^{39}K and ^{85}Rb were positively correlated with soil pH. However, there was little or no discernible correlation between the exchangeable fraction of ^{133}Cs and soil pH.

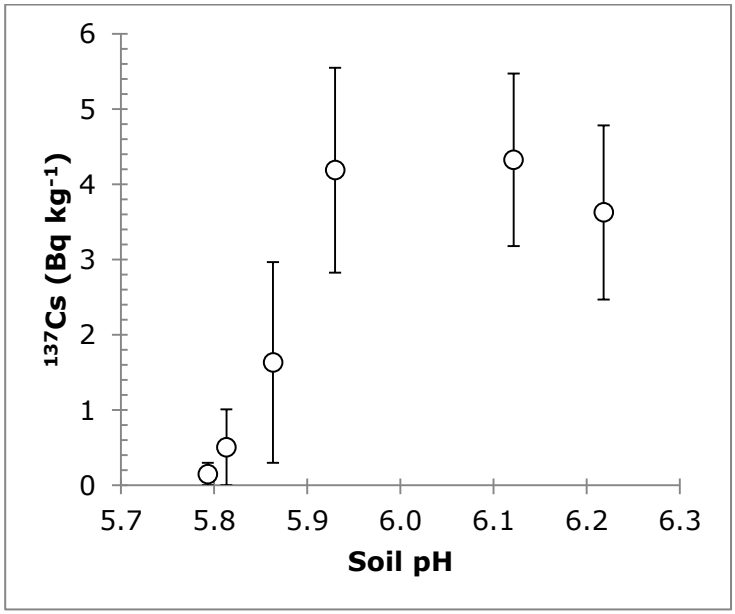
Figure 5-13 *Correlations of average soil pH with average exchangeability of ^{133}Cs (a), ^{39}K (b) and ^{85}Rb (c) of soil collected at Wat Ban Chan (6 replicates, the vertical bars are standard errors of means).*



- *Correlation of soil pH with total ^{137}Cs*

Figure 5-14 shows the relationship between soil pH and total ^{137}Cs activity concentration within the soil cores. As shown in Figure 5-10, radiocaesium from atmospheric weapons testing, deposited in 1963, has accumulated predominantly in the upper 3 cm of the soil profile in which soil pH ranged from 5.93 – 6.22.

Figure 5-14 Correlation of average soil pH with average ^{137}Cs in soil collected at Wat Ban Chan (6 replicates, the vertical bars are standard errors of means).



5.2.4.2 Organic matter

- *Correlations with total ^{133}Cs, ^{39}K and ^{85}Rb*

Correlations between soil organic matter (as measured by LOI) and total ^{133}Cs, ^{39}K and ^{85}Rb within organic and mineral layers are shown in Figure 5-15.

Correlations of organic matter with total ^{85}Rb and ^{39}K were positive and monotonic. Total ^{133}Cs decreased with increasing OM within the upper 7 cm of soil cores but increased with OM in the lower 6 cm of soil cores.

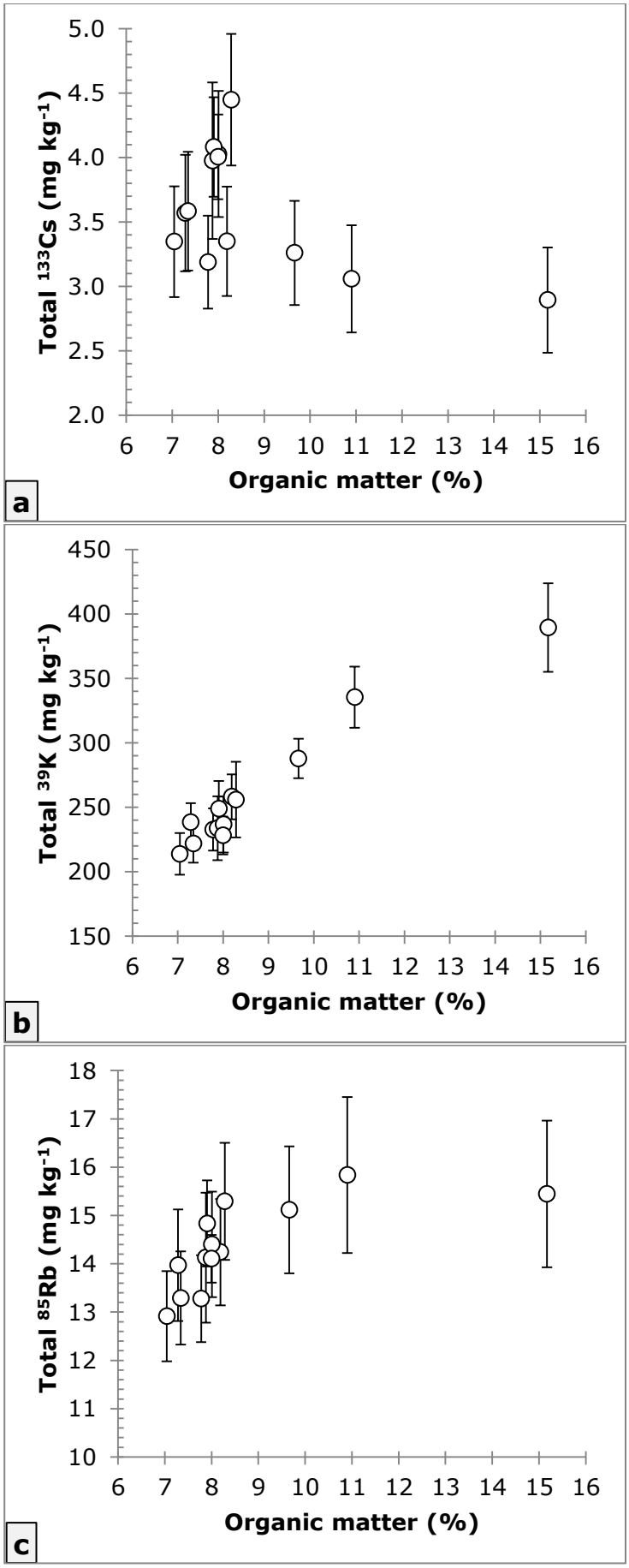
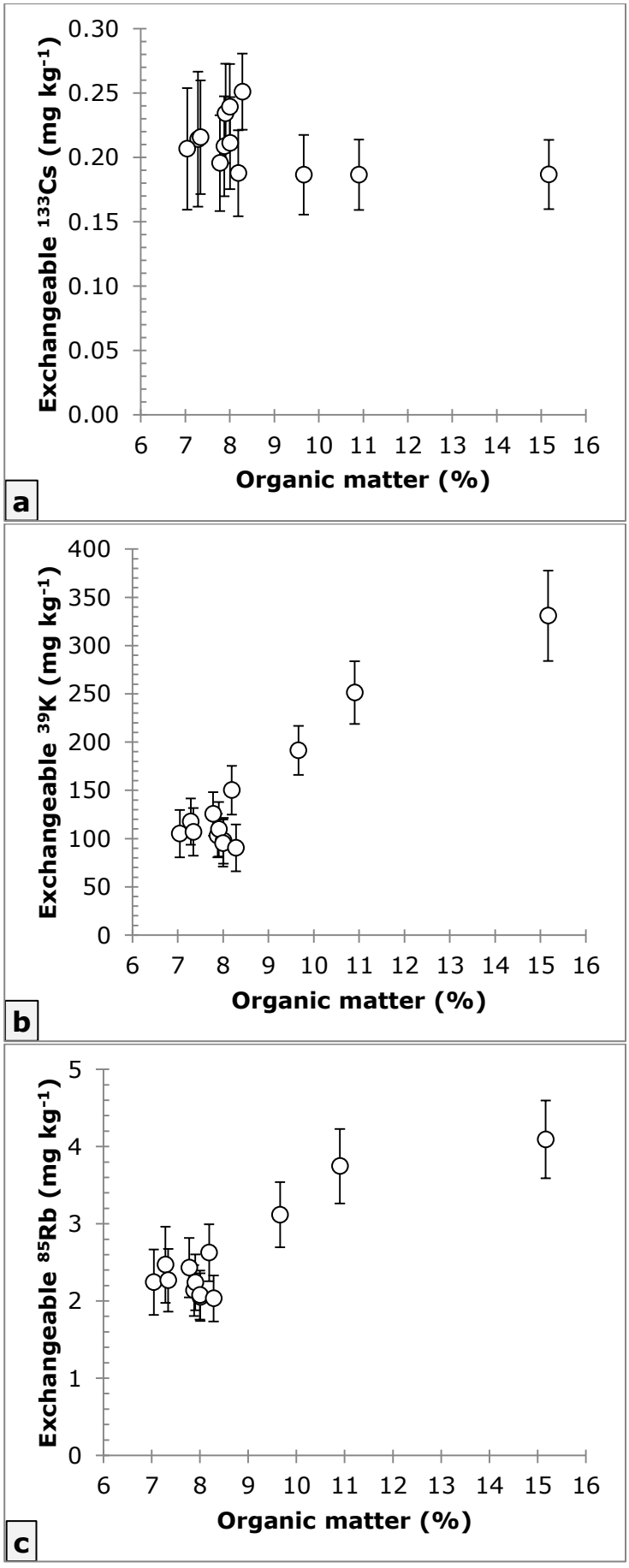


Figure 5-15 *Correlations of average organic matter with average total ^{133}Cs (a), ^{39}K (b) and ^{85}Rb (c) in soil cores collected at Wat Ban Chan (6 replicates, the vertical bars are standard errors of means).*

- *Correlations with exchangeable ^{133}Cs, ^{39}K and ^{85}Rb*

Correlations between soil organic matter (as measured by LOI) and exchangeable ^{133}Cs, ^{39}K and ^{85}Rb are shown in Figure 5-16.

Correlations of organic matter with exchangeable ^{39}K and ^{85}Rb were qualitatively similar, following a monotonically positive trend within the upper 7 cm depth but no correlation within the lower 6 cm depth. In contrast, there was little or no discernible correlation between the exchangeable concentrations of ^{133}Cs and soil organic matter.



<u>Figure 5-16</u> Correlation of average organic matter content with average exchangeable ^{133}Cs (a), ^{39}K (b) and ^{85}Rb (c) in soil cores collected at Wat Ban Chan (6 replicates, the vertical bars are standard errors of means).

- *Correlations with fixed ^{133}Cs, ^{39}K and ^{85}Rb*

Correlations between organic matter (as measured by LOI) and 'fixed' ^{133}Cs, ^{39}K and ^{85}Rb concentrations are shown in Figure 5-17.

Correlations of organic matter with fixed ^{133}Cs, ^{39}K and ^{85}Rb were qualitatively similar, following a negative trend within the upper 7 cm layers and a weakly positive trend within the lower 6 cm depths. For ^{85}Rb these trends were only weakly visible.

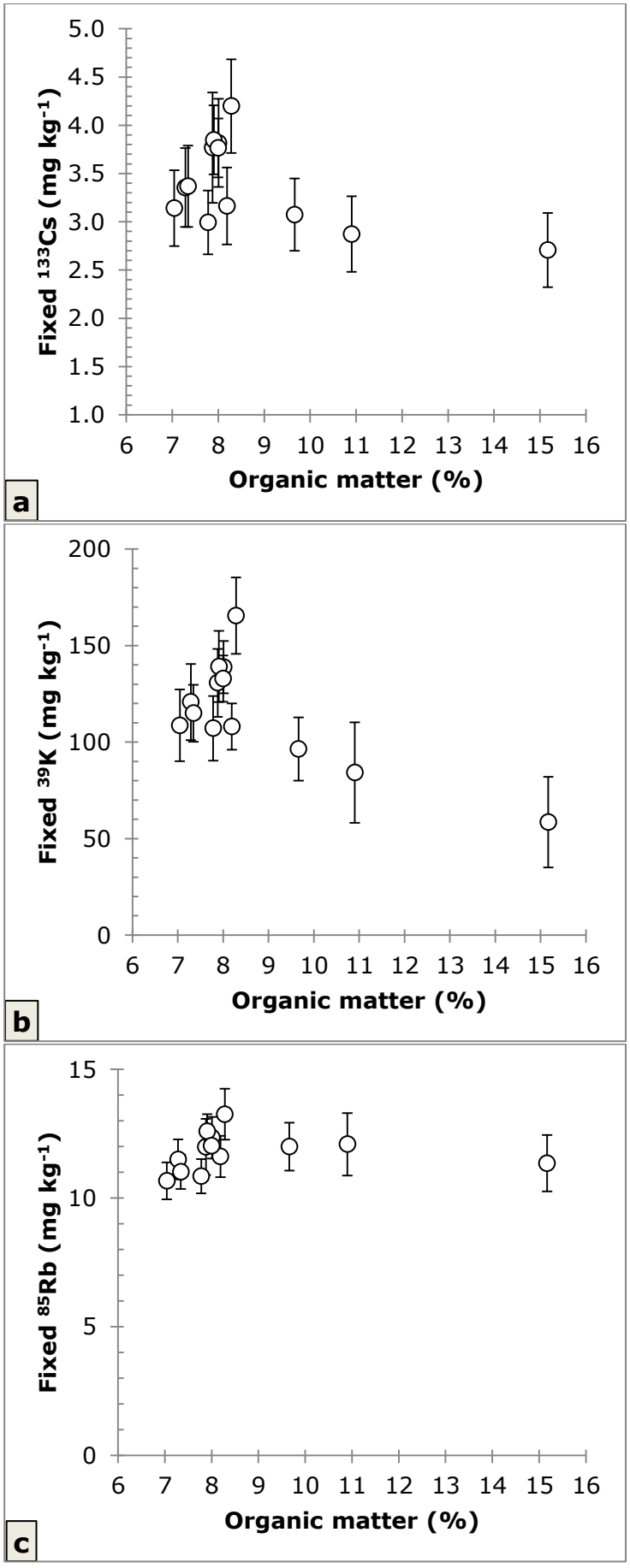


Figure 5-17 *Correlations of average soil organic matter content with average 'fixed' concentrations of ^{133}Cs (a), ^{39}K (b) and ^{85}Rb (c) in soil cores collected at Wat Ban Chan (6 replicates, the vertical bars are standard errors of means).*

- *Correlations with exchangeable factions of ^{133}Cs, ^{39}K and ^{85}Rb*

Correlations between soil organic matter (as measured by LOI) and exchangeable fractions of ^{133}Cs, ^{39}K and ^{85}Rb are shown in Figure 5-18.

The correlations for ^{85}Rb and ^{39}K were qualitatively similar, following a clear positive trend within the upper 7 cm layers and a negative trend within the lower 6 cm depths. There was a discernible positive correlation between the exchangeable fraction of ^{133}Cs and soil organic matter contents greater than 8%, in the upper 4 cm of the soil cores.

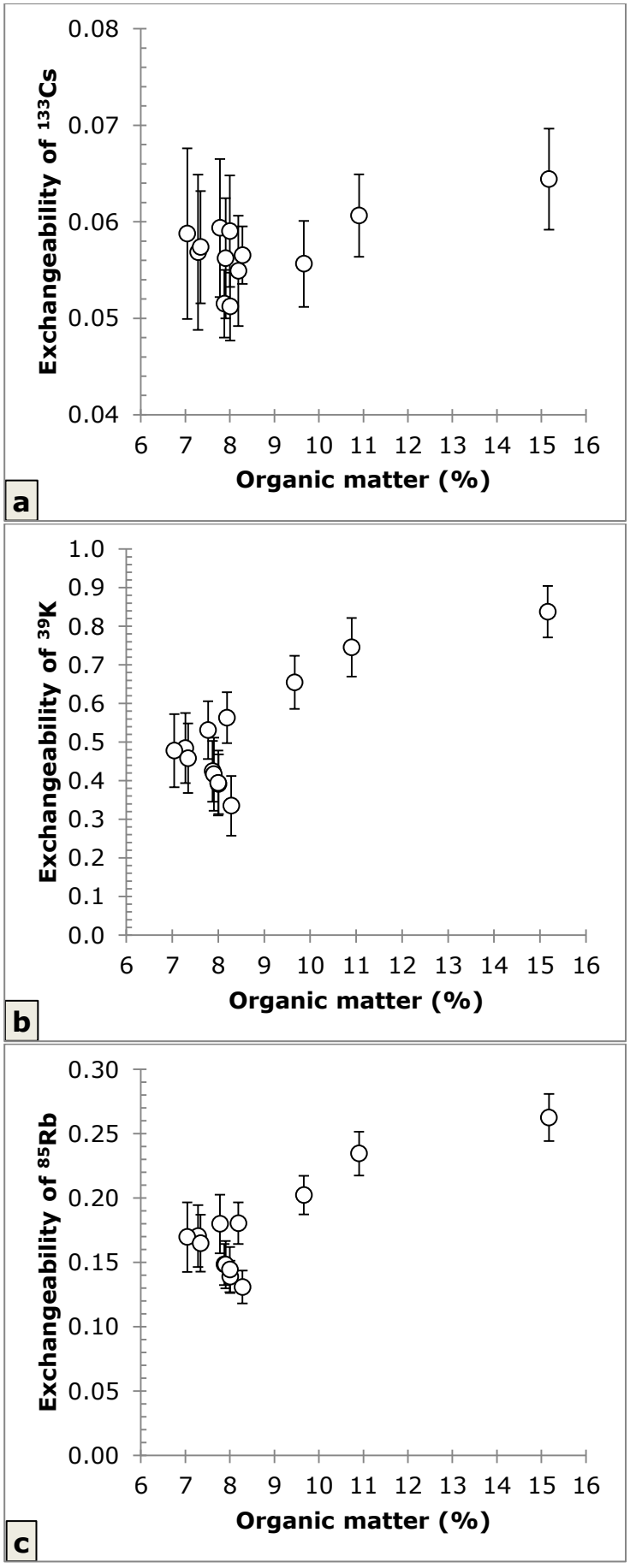


Figure 5-18 *Correlations of average organic matter content with average exchangeabilities of ^{133}Cs (a), ^{39}K (b) and ^{85}Rb (c) in soil cores collected at Wat Ban Chan (6 replicates, the vertical bars are standard errors of means).*

- *Correlation of soil organic matter with ^{137}Cs*

The relationship between soil organic matter (as measured by LOI) and total activity concentrations of ^{137}Cs is shown in Figure 5-19.

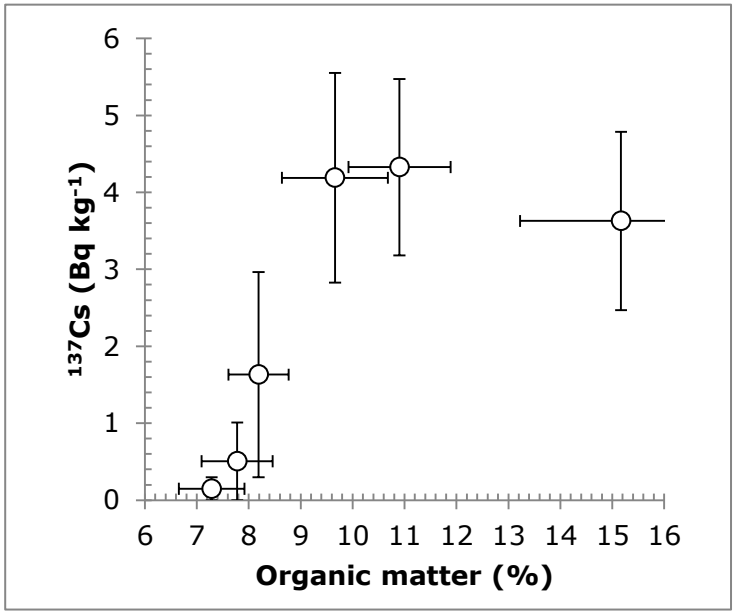


Figure 5-19 Correlations of average soil organic matter with average activity concentrations of ^{137}Cs in soil cores collected at Wat Ban Chan (6 replicates, the vertical bars are standard errors of means).

The graph shows that the ^{137}Cs accumulation (at 2 and 3 cm of 4.33 and 4.19 Bq kg^{-1}, respectively) was associated with an organic matter content of about 10 %. The overall shape of the correlation emphasises the successive decrease in ^{137}Cs activity concentrations away from the point of peak contamination, with higher organic matter contents above this point and lower organic matter contents below.

5.2.5 Correlation between fractions of ^{133}Cs and ^{137}Cs within forest soil

5.2.5.1 Total ^{133}Cs versus exchangeable and fixed ^{133}Cs

Correlations between total ^{133}Cs and exchangeable and fixed concentrations ^{133}Cs were investigated as shown in Figure 5-20a and b.

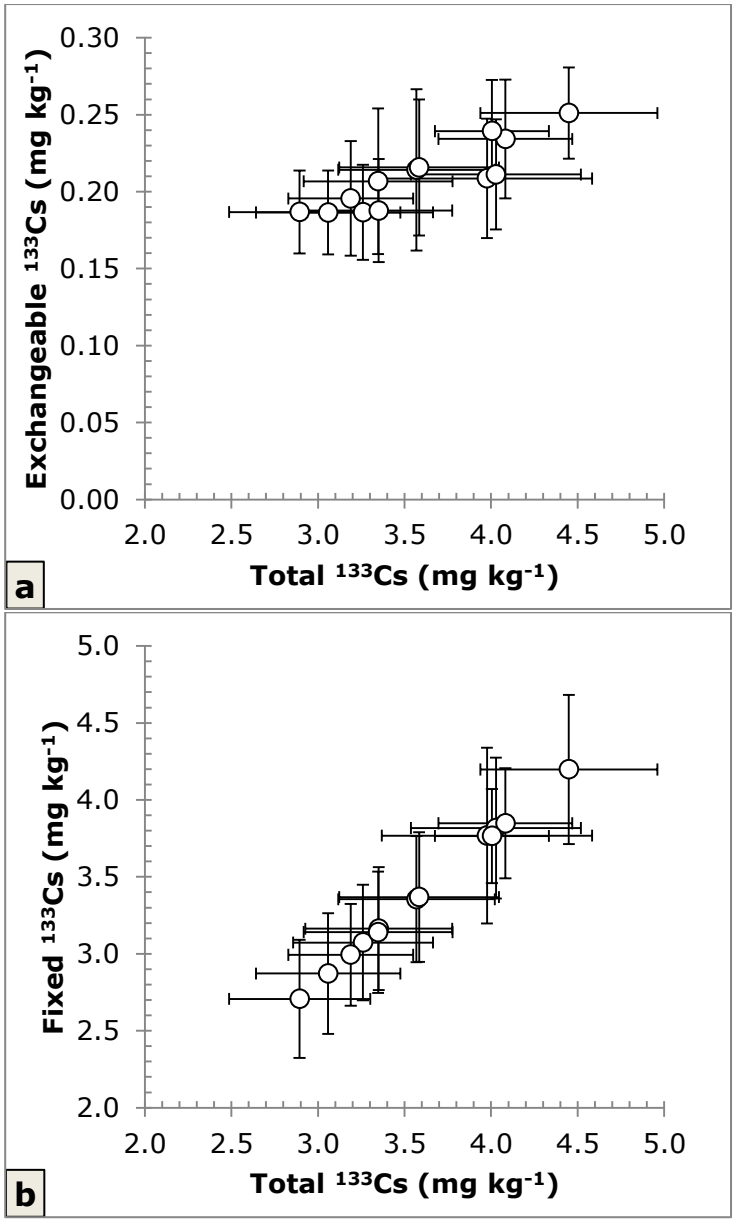


Figure 5-20 Correlations of average total ^{133}Cs concentration with average exchangeable and fixed ^{133}Cs in soil cores collected at Wat Ban Chan (6 replicates, the bars are standard errors of means).

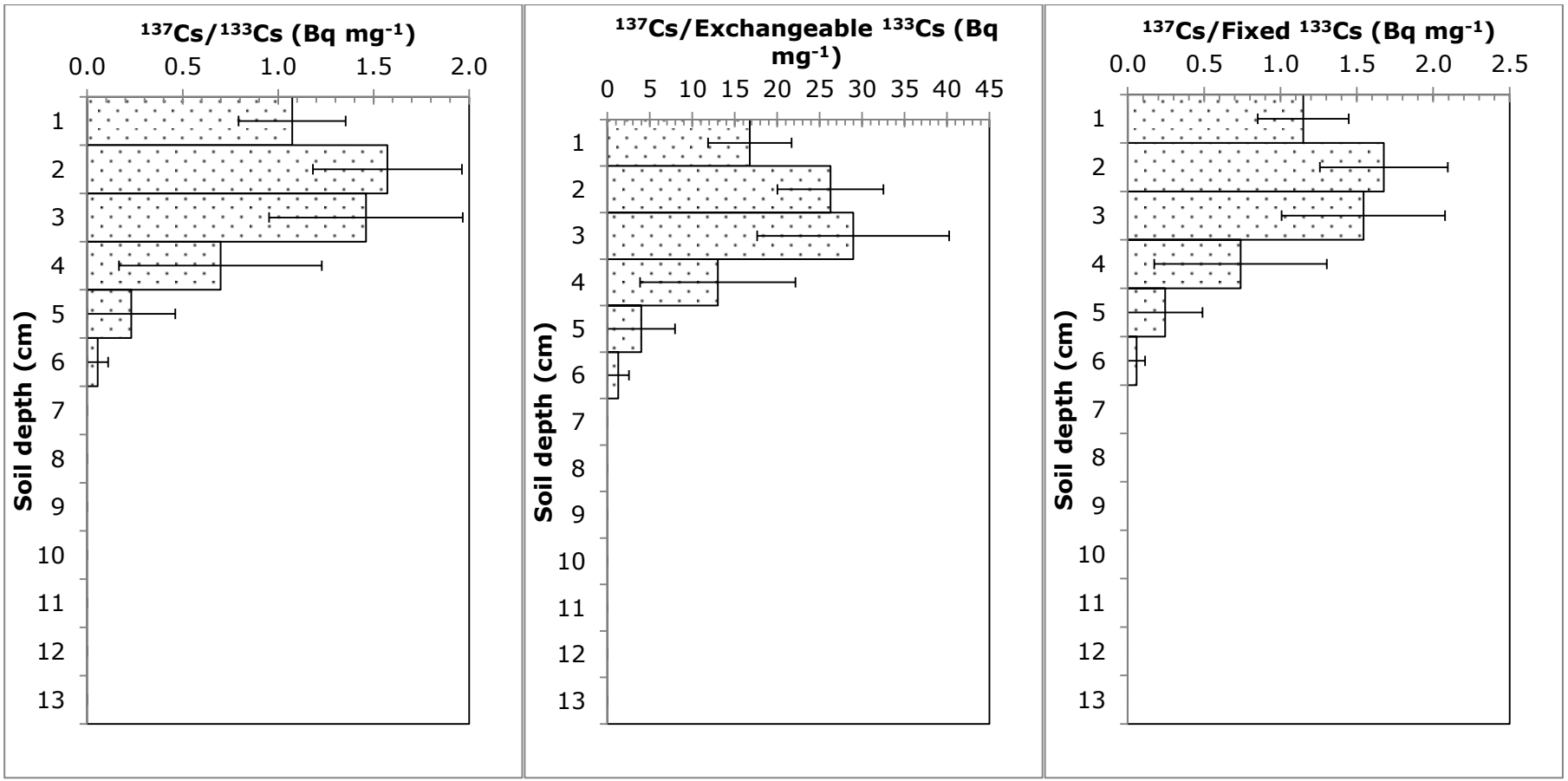
Total ^{133}Cs was strongly correlated with the 'fixed' and exchangeable fractions of ^{133}Cs throughout the soil profile.

5.2.5.2 ^{137}Cs with total, exchangeable and fixed ^{133}Cs

The isotopic ratios of ^{137}Cs with total, exchangeable and fixed fractions of ^{133}Cs are shown in Figure 5-21.

The depth profiles of each of the isotopic ratios calculated for ^{137}Cs (with total, exchangeable and fixed ^{133}Cs) broadly reflect the shape of the ^{137}Cs depth distribution previously shown in Figure 5-10, though with maximum values at 2 - 3 cm depth.

Figure 5-21 Depth profiles of average isotopic ratios of ^{137}Cs (n = 6) with average ^{133}Cs in total concentration (a, n = 6), exchangeable fraction (b, n = 6) and fixed fraction (c, n = 6) in soil cores collected at Wat Ban Chan (horizontal bars are standard errors of means).



5.2.6 Isotopic exchange of ^{133}Cs and ^{134}Cs

^{134}Cs was used to investigate the isotopic exchangeability of ^{133}Cs throughout the Wat Ban Chan (site 1) soil profile. Isotopically exchangeable ^{133}Cs (E-value) was calculated using equation 2.8. The results of data obtained from this experiment are shown in Table 5-2 and Figure 5-22 for selected soil depths (1, 3, 5, 7, 9, 11 and 13 cm) and for equilibration (shaking) times of 1 hour, 1 day and 1 week. Finally, the progression of E-values for the three equilibration (shaking) times at each soil depth is shown in Figure 5-23.

Isotopic exchangeability of ^{133}Cs with ^{134}Cs of soil collected at Wat Ban Chan was only slightly higher (103 – 112%) than the exchangeable concentrations of ^{133}Cs. Increasing the shaking time from one hour to one week increased the E-value by less than 2-fold. Longer-term shaking may increase the E-value further, although the rate of increase of the E-value was much more rapid at the beginning of the experiment (from one hour to one day) than during the following 6 days.

Isotopic exchangeability of ^{133}Cs with ^{134}Cs was lowest and highest in soil at 9 and 13 cm depths, respectively (Figure 5-23), while in the other depths the calculated E-values were rather constant.

Table 5-2 Concentrations of ^{134}Cs and exchangeable ^{133}Cs, and E-values for ^{133}Cs obtained from isotopic exchange with ^{134}Cs in selected soil samples collected at Wat Ban Chan (site 1).

Depth (cm)	^{134}Cs (Bq ml^{-1})			Exchangeable ^{133}Cs (mg kg^{-1})			E-value (mg kg^{-1}) (% of exchangeable concentration)		
	Shaking time (hours)			Shaking time (hours)			Shaking time (hours)		
	1	24	168	1	24	168	1	24	168
1	17.6	17.3	17.5	0.209	0.286	0.359	0.222 (106)	0.309 (108)	0.383 (107)
3	18.0	18.0	18.1	0.204	0.278	0.346	0.210 (103)	0.287 (103)	0.356 (103)
5	17.0	17.7	17.5	0.222	0.289	0.378	0.243 (109)	0.304 (105)	0.403 (107)
7	18.1	17.4	17.7	0.227	0.307	0.371	0.233 (103)	0.329 (107)	0.390 (105)
9	17.4	17.4	17.5	0.159	0.244	0.332	0.170 (107)	0.262 (107)	0.354 (107)
11	17.5	17.2	17.3	0.207	0.301	0.372	0.220 (106)	0.327 (109)	0.401 (108)
13	16.7	17.8	16.9	0.283	0.402	0.461	0.316 (112)	0.422 (105)	0.508 (110)

Figure 5-22 Depth profiles of average of E-values for ^{133}Cs determined for 1 hour (a), 1 day (b) and 1 week (c) in selected soil samples collected at Wat Ban Chan (site 1).

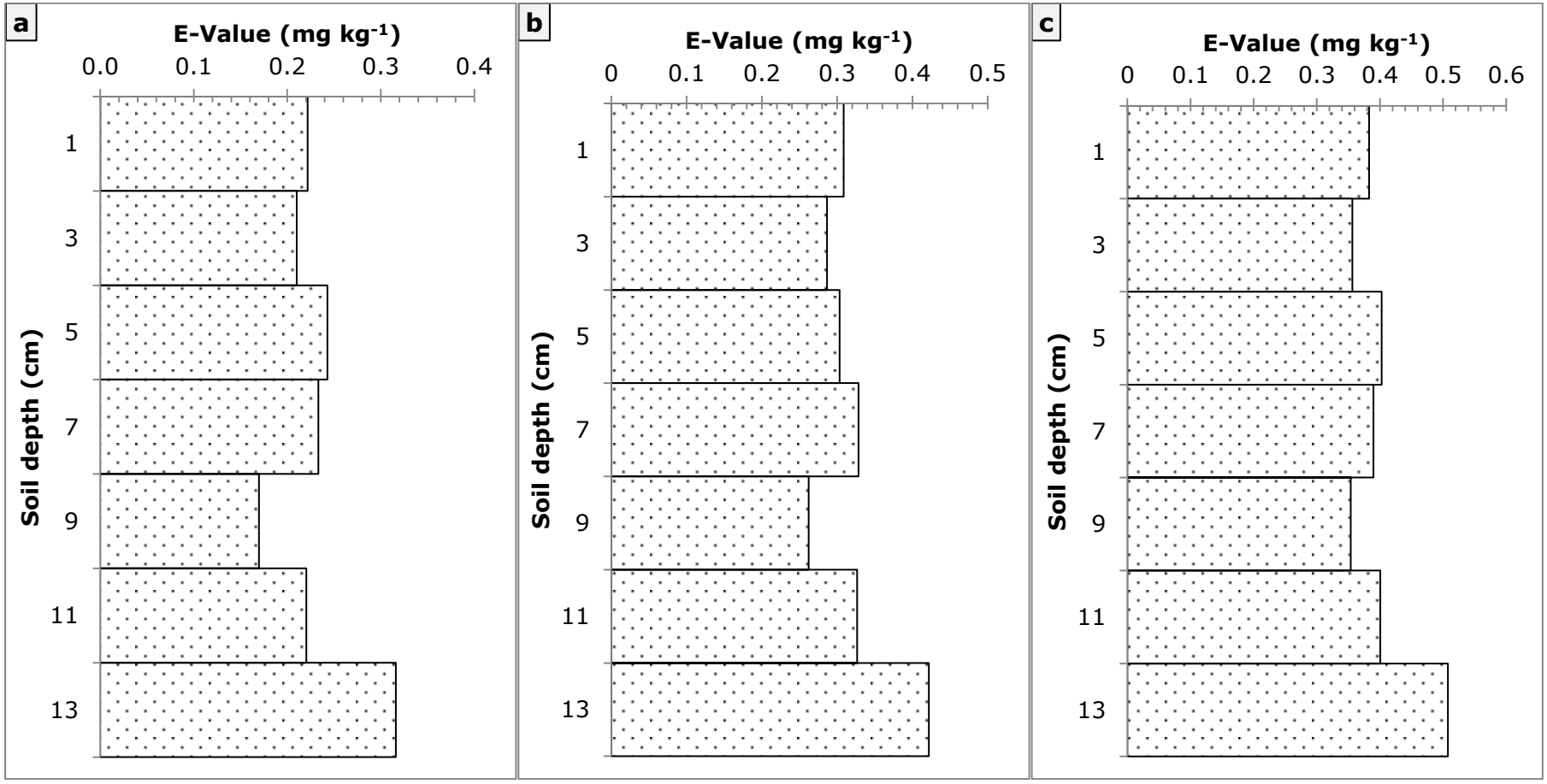
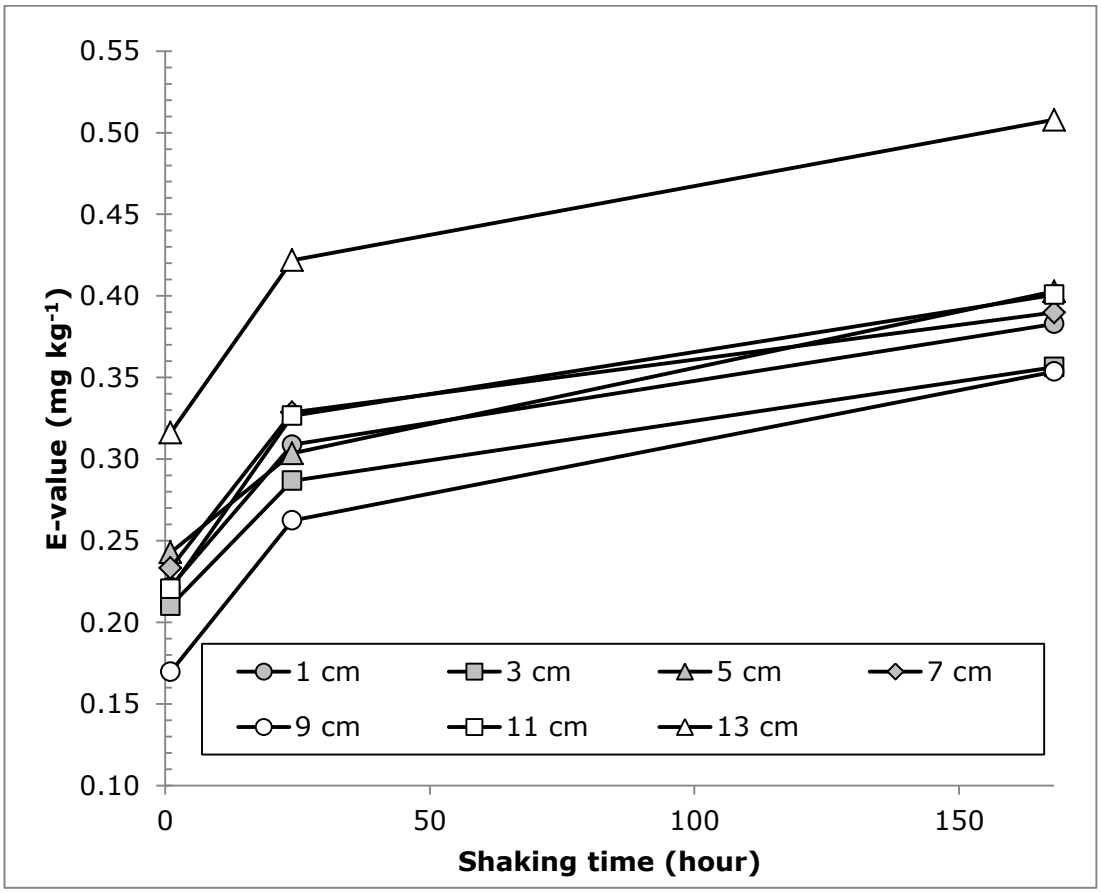


Figure 5-23 Progression of E-values with shaking time in 1, 3, 5, 7, 9, 11 and 13 cm depths of soil collected at Wat Ban Chan (site 1).

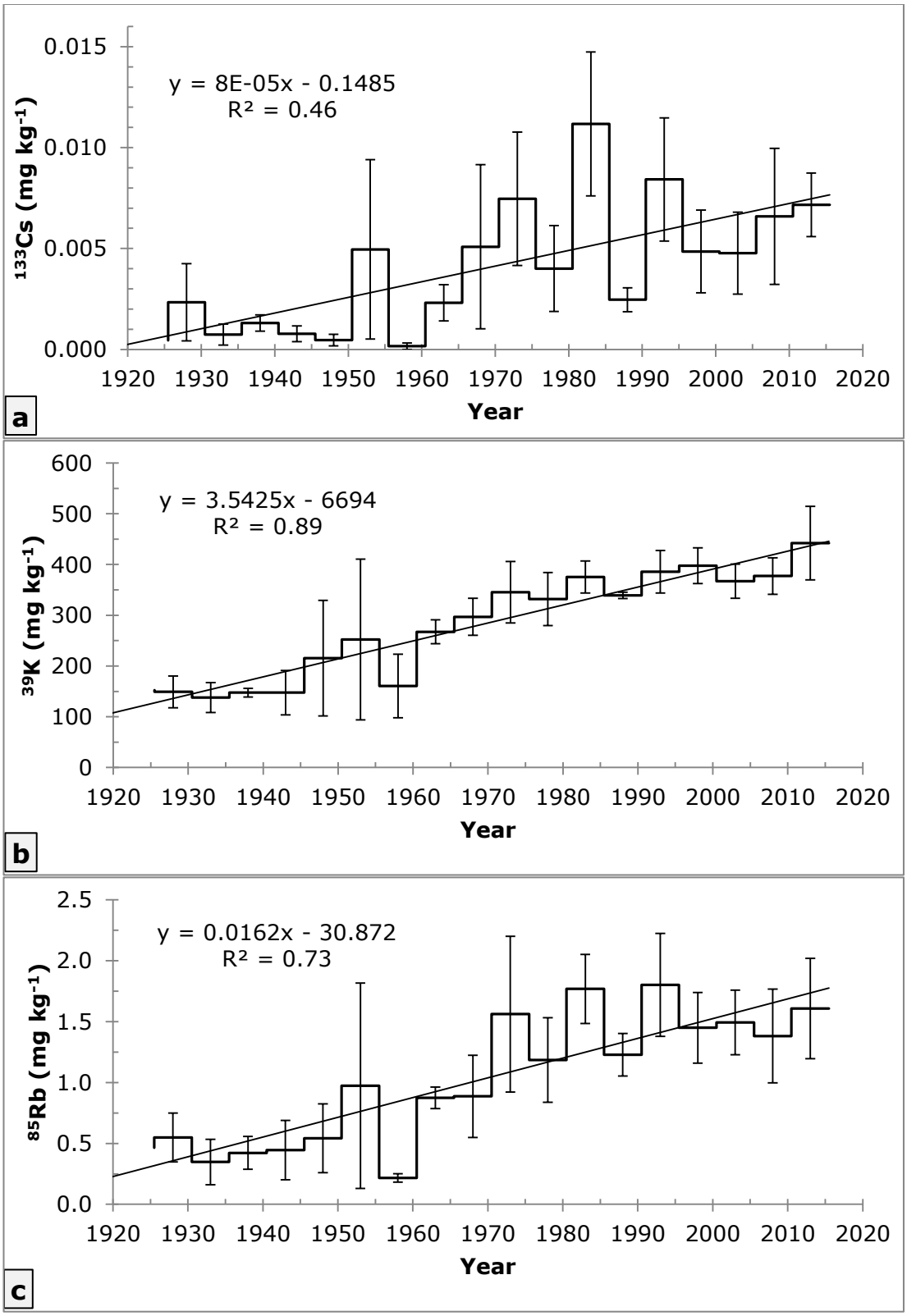


5.2.7 Accumulation of ^{133}Cs, ^{39}K and ^{85}Rb in above-ground biological compartments

5.2.7.1 ^{133}Cs, ^{39}K and ^{85}Rb concentrations in stem wood and bark of Three-needled pine

Tree cores of Three-needled pine collected at Wat Ban Chan were analysed to investigate concentrations of ^{133}Cs, ^{39}K and ^{85}Rb; the results are shown in Figure 5-24 and Table 5-3.

Figure 5-24 Concentrations of ^{133}Cs (a), ^{40}K (b) and ^{85}Rb (c) in tree rings of Three-needled pine collected at Wat Ban Chan (6 replicates, the vertical bars are standard errors of means).



Counts of tree rings of Three-needled pine collected at Wat Ban Chan suggest that the trees were planted around 1925. The distribution patterns of ^{39}K and ^{85}Rb were similar, both showing a more or less linear increase from the youngest to the oldest tree rings. The trend of ^{133}Cs concentrations in trees was for a general increase from old to young wood, though the concentrations were more variable than for ^{39}K and ^{85}Rb and the maximum ^{133}Cs concentration was in wood produced in 1980 – 1985. Overall, however, the results suggest younger tree rings of contained higher concentrations of ^{133}Cs, ^{39}K and ^{85}Rb than older rings.

The bark of Three-needled pine was analysed and the measured concentrations of ^{133}Cs, ^{39}K and ^{85}Rb are shown in Table 5-3. These data indicate substantially higher concentrations of ^{133}Cs, ^{39}K and ^{85}Rb in bark than in wood.

5.2.7.2 ^{133}Cs, ^{39}K and ^{85}Rb concentrations in needles of Three-needled pine

Fresh and dry needles were collected and analysed for ^{133}Cs, ^{39}K and ^{85}Rb; the results are shown in Table 5-3.

Table 5-3 Concentrations of ^{133}Cs, ^{39}K and ^{85}Rb in wood, bark and fresh needles collected at Wat Ban Chan (6 replicates, SEM is standard error of mean).

Sample type	^{133}Cs (mg kg^{-1})		^{39}K (mg kg^{-1})		^{85}Rb (mg kg^{-1})	
	Conc.	SEM	Conc.	SEM	Conc.	SEM
Wood	5.43×10^{-3}	1.72×10^{-3}	356	41.9	1.44	0.28
Fresh needles	2.42×10^{-2}	3.10×10^{-3}	756	331	4.00	0.21
Bark	3.01×10^{-2}	7.46×10^{-3}	513	229	4.55	0.58

^{133}Cs concentrations in fresh needles were substantially higher than in wood, but lower than in bark. ^{133}Cs concentrations in fresh needles were very low compared with ^{39}K and ^{85}Rb (4 and 2 orders of magnitude lower, respectively).

5.2.8 Comparison of ^{133}Cs, ^{39}K and ^{85}Rb in recirculation processes within forest ecosystems

5.2.8.1 Uptake of alkali metals by Three-needled pine

The relative uptake of ^{133}Cs, ^{39}K and ^{85}Rb by Three-needled pine was investigated by examining their concentration ratios and aggregated transfer factors as follows.

- *Concentration ratio (CR)*

Concentration ratios for ^{133}Cs, ^{39}K and ^{85}Rb in wood and needles of Three-needled pine were calculated using equation 1.3 (section 1.2.8.3), assuming that root absorption takes place from the uppermost 13 cm of the soil profile. The results are shown in Table 5-4.

Table 5-4 Concentration ratios (CR) of ^{133}Cs, ^{39}K and ^{85}Rb in wood (n = 6) and fresh needles (n = 6) calculated on a dry basis for wood and needles using total and exchangeable concentrations in the entire top 13 cm of the soil (n = 6).

Nuclide	*CR* (dry weight basis)			
	Total concentration		Exchangeable concentration	
	Wood	Fresh needles	Wood	Fresh needles
^{133}Cs	1.48×10^{-3}	6.59×10^{-3}	2.53×10^{-2}	1.13×10^{-1}
^{39}K	1.41	6.02	2.75	11.7
^{85}Rb	1.00×10^{-1}	2.79×10^{-1}	5.83×10^{-1}	1.62

- *Aggregated transfer factor* (T_{ag})

Aggregated transfer factors for ^{133}Cs, ^{39}K and ^{85}Rb in Three-needled pine wood and needles were calculated using equation 1.4 (section 1.2.8.3) in which the

elemental inventory within the upper 13 cm of soil profile was used as the denominator. The results are shown in Table 5-5.

Table 5-5 Aggregated transfer factors (T_{ag}) for ^{133}Cs, ^{39}K and ^{85}Rb in wood (n = 6) and fresh needles (n = 6) of Three-needled pine calculated on a dry weight basis (n = 6).

Nuclide	T_{ag} (m^2 kg^{-1} dry weight basis)			
	Total concentration		Exchangeable concentration	
	Wood	Fresh needles	Wood	Fresh needles
^{133}Cs	7.94×10^{-6}	3.54×10^{-5}	1.37×10^{-4}	6.09×10^{-4}
^{39}K	7.43×10^{-3}	3.16×10^{-2}	1.41×10^{-2}	5.98×10^{-2}
^{85}Rb	5.31×10^{-4}	1.48×10^{-3}	3.02×10^{-3}	8.41×10^{-3}

The calculated T_{ag} values for ^{133}Cs are in the range of measured T_{ag} values for pine wood and needles specified by the IAEA (2010).

For both *CR* and T_{ag} the lowest values for ^{133}Cs, ^{85}Rb and ^{39}K were found in wood and the highest values in fresh needles.

5.2.8.2 Translocation within wood of Three-needled pine

Concentration ratios of $^{39}K/^{133}Cs$, $^{85}Rb/^{133}Cs$ and $^{39}K/^{85}Rb$ in annual growth rings of wood are shown in Figure 5-25.

Concentration ratios of ^{39}K and ^{85}Rb to ^{133}Cs in wood decreased from older to younger annual rings suggesting that ^{39}K and ^{85}Rb are less mobile than ^{133}Cs towards the cambial region in wood of Three-needled pine. Moreover, the trends of $^{39}K/^{133}Cs$ and $^{85}Rb/^{133}Cs$ were very similar which suggests that ^{85}Rb behaves in a more similar manner to ^{39}K than to ^{133}Cs, as indicated by the stronger correlation between ^{39}K and ^{85}Rb than between ^{39}K and ^{133}Cs in Figure 5-26.

Figure 5-25 Concentration ratios of $^{39}K/^{133}Cs$, $^{85}Rb/^{133}Cs$ and $^{39}K/^{85}Rb$ in annual growth rings of Three-needled pine collected at Wat Ban Chan (1 replicate).

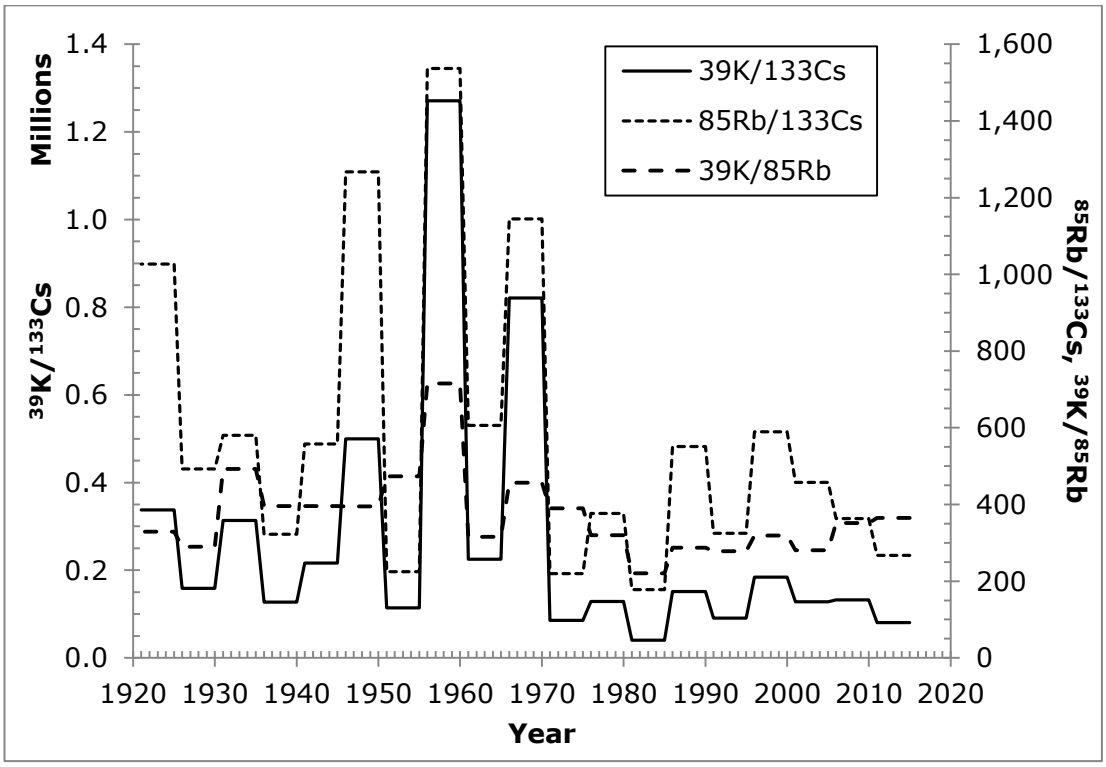
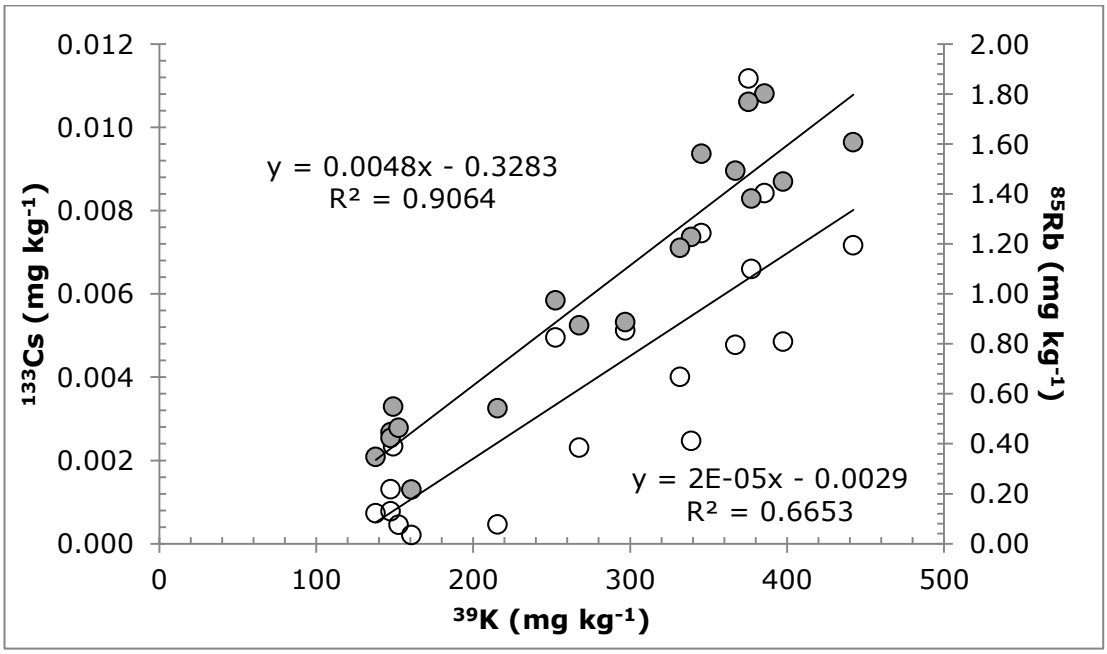


Figure 5-26 Average concentrations of ^{39}K plotted against ^{85}Rb (dark points) and ^{133}Cs (white points) in Three-needled pine cores collected at Wat Ban Chan (n = 6).



5.2.8.3 Translocation from wood to needles in Three-needled pine

The relative magnitude of translocation of ^{39}K, ^{85}Rb and ^{133}Cs from wood to needles was investigated using the following ratios.

- *Concentration ratios of $^{39}K/^{133}Cs$ $^{85}Rb/^{133}Cs$ and $^{39}K/^{85}Rb$*

Concentration ratios of $^{39}K/^{133}Cs$, $^{85}Rb/^{133}Cs$ and $^{39}K/^{85}Rb$ in tree cores and needles were calculated as shown in Table 5-6.

Table 5-6 Concentration ratios of $^{39}K/^{133}Cs$, $^{85}Rb/^{133}Cs$ and $^{39}K/^{85}Rb$ in soil (total and exchangeable concentration, n = 6), wood (n = 6), fresh needles (n = 6) and bark (n = 6) calculated on a dry basis.

Forest compartment	$^{39}K/^{133}Cs$	$^{85}Rb/^{133}Cs$	$^{39}K/^{85}Rb$
Soil - total concentration	74.8 ± 30.5	4.15 ± 1.69	17.9 ± 7.32
Soil - exchangeable concentration	690 ± 282	12.5 ± 5.11	53.9 ± 22.0
Wood	92,700 ± 20,300	451 ± 244	305 ± 154
Bark	53,300 ± 19,800	195 ± 39.8	241 ± 35.0
Fresh needles	68,000 ± 9,520	173 ± 13.4	382 ± 29.7

The concentration ratios of $^{39}K/^{133}Cs$ indicate that the proportion of exchangeable ('available') K in soil was much higher than for Cs. This indicates that K is not just a more abundant element than Cs in the forest soil, it is also a much more biologically available element than Cs.

The concentration ratios of $^{39}K/^{133}Cs$ in wood, fresh needles and bark were about 2 orders of magnitude higher than the $^{39}K/^{133}Cs$ ratios for soil in exchangeable concentration, indicating that all tree tissues take up K much more selectively than they absorb Cs.

Examining the $^{39}K/^{85}Rb$ ratios for soil, wood and fresh needles, the same trends are evident but the ratios are lower, indicating that K is a more biologically available element than Rb in the soil and that tree tissues take up K much more selectively than they absorb Rb. However, the differences between K and Rb are substantially less than the differences between K and Cs.

- *Translocation factor (f_{tr})*

Wood-to-needle translocation factors were calculated using equation 3.2 (section 3.2.8.3) to compare the degree of transfer of ^{133}Cs, ^{39}K and ^{85}Rb from wood to fresh needles. The results are shown in Table 5-7.

Table 5-7 Wood-to-needle translocation factors (f_{tr}) for ^{133}Cs, ^{39}K and ^{85}Rb in Three-needled pine calculated on a dry weight basis.

Translocation factor (f_{tr}, dry weight basis)		
^{133}Cs	^{39}K	^{85}Rb
4.45	4.25	2.78

The results suggest translocation factors of ^{133}Cs, ^{39}K and ^{85}Rb are in the same order of magnitude but wood-to-needle translocation of ^{39}K and ^{133}Cs was greater than for 85Rb (1.53 and 1.60 times respectively). It therefore appears that, once K and Cs have been taken up from the soil by Three-needled pine, the relative partitioning of these two elements between wood and needles is comparable.

5.3 DISCUSSION

Compared with the Boundary Plantation soil, the soil at Wat Ban Chan was low in organic matter even in the surface layers of the soil profile. Based on the USDA classification, only the top 1 cm of the Wat Ban Chan soil can be considered to be 'organic'. As well as having a much lower organic matter content, the Wat Ban Chan soil is much less acidic than the organic rich soil at Boundary Plantation. The geological/soil map (Figure 5-3, section 5.1.2) shows the Wat Ban Chan soil to be a red-yellow podzolic soil which, according to the results of XRD analyses, is predominantly composed of quartz particles. Surprisingly, clay minerals were not evident in the XRD diffractograms, probably a consequence of eluviation of clayey material from the upper soil. Eluviation of clays is a process which is important for tropical soils, particularly in areas of steep terrain which are typical of Wat Ban Chan and nearby areas in northern Thailand (Yoshinaga et al., 1989). Low potassium (209 – 385 mg kg^{-1} average) combined with high iron (11.6 – 16.1 g kg^{-1} average) and aluminium (16.4 – 27.5 g kg^{-1} average) concentrations in the soil at Wat Ban Chan indicate a highly weathered soil, probably an oxisol (USDA taxonomy) or a ferralsol (FAO taxonomy) given that clay minerals were undetectable by XRD.

All of the detectable ^{137}Cs in the Wat Ban Chan soil was distributed within the upper 6 cm depth, with the peak ^{137}Cs inventory (253 Bq m^{-2}, representing 37.6% of the total activity) located at 2 cm depth (section 5.2.2.4). If it is assumed that the major deposition of ^{137}Cs at this site occurred in 1963 this would imply a mean long-term vertical migration rate of 0.38 mm per year. The rate of ^{137}Cs migration is considered further using the model described in Chapter 7.

Total ^{133}Cs was strongly correlated with both its exchangeable and fixed fractions but the correlation with the fixed fraction was particularly strong, confirming that stable Cs was predominantly in an unavailable form within the soil. The exchangeable fraction of ^{133}Cs varied only slightly throughout the soil cores from 5.1 to 6.4 % of the total ^{133}Cs, with the highest exchangeability (6.4%) in the surface soil layer. Isotopic exchangeability has been proposed as a better measure of the 'available' portion of an element within soil. However, the isotopic exchangeability (E-value) of ^{133}Cs was only slightly higher (103 – 112%) than the exchangeable concentrations of ^{133}Cs (section 5.2.6). This suggests that the exchangeable fraction of Cs isotopes in soil probably provides an adequate measure of Cs lability and potential availability for biological uptake in

the short term. As with the Boundary Plantation soils, the E-Value increased more rapidly from 1 hour to 1 day than from 1 day to week (Table 5-2, section 5.2.6) suggesting that isotopic exchange of Cs with binding sites in the solid matrix is a diffusion-limited process. Longer-term diffusion of radiocaesium from interlayer sites within clay minerals has been observed several years after the Chernobyl accident (Smith et al., 1999) but isotopic exchange measurements over time periods of 1 week or less will not reveal this 'fixed' fraction.

The organic matter content of the soil of Wat Ban Chan is low in comparison with temperate forest soils, but it could still influence the distribution of ^{137}Cs and ^{133}Cs in the soil profile. Within the upper 4 cm of the Wat Ban Chan soil, where fallout ^{137}Cs was predominantly distributed, the average organic matter content was higher than in the soil core as a whole (section 5.2.1.1). The positive correlation of organic matter with the exchangeable fraction of ^{133}Cs within the upper 4 cm layer (Figure 5-18, section 5.2.4.2) was also seen within the organic layer of the Boundary Plantation soil. However, the range of organic matter content within the Wat Ban Chan soil (7.04 - 15.2%) was not enough to dramatically alter the exchangeability of ^{133}Cs, which ranged from 5.12 – 6.44%, with an average of 5.71% for the entire soil core. The non-monotonic relationship between ^{137}Cs activity concentration and soil organic matter (Figure 5-19, section 5.2.4.2) was strongly influenced by the relative vertical distributions of these two variables within the soil cores.

Within the upper 4 cm of the soil, pH ranged from 5.93 - 6.22 (average 6.09) which was only slightly higher than the pH in deeper soil layers which ranged between 5.43 – 5.86 (average 5.61). Overall, an increase in soil pH was associated with a decrease in exchangeable ^{133}Cs concentrations, although there was little discernible correlation between the exchangeable fraction of ^{133}Cs and soil pH except for a weak increase in exchangeability of ^{133}Cs with pH in the upper 4 cm (section 5.2.4.1).

Potassium and rubidium both have strong physico-chemical similarities to caesium but generally (especially potassium) occur at much higher concentrations than caesium in soils. In the Wat Ban Chan soil ^{39}K (214 – 389 mg kg^{-1}) and ^{85}Rb (12.9 – 15.8 mg kg^{-1}) were at much higher total concentrations than ^{133}Cs (2.89 – 4.45 mg kg^{-1}) (section 5.2.2.1). Depth profiles of the exchangeable fractions of ^{39}K and ^{85}Rb (Figure 5-11, section 5.2.3) show that exchangeability of ^{39}K (33.5 – 83.8%, 51.6% average) and ^{85}Rb (13.1 – 26.3%, 17.5% average) were 9.04 and 3.06 times greater than the

exchangeability of ^{133}Cs (5.12 – 6.44%, 5.71% average) in the soil at Wat Ban Chan. Within the upper 4 cm soil depth the exchangeabilities of ^{39}K and ^{85}Rb both increased with increasing organic matter content, with exchangeabilities of ^{39}K (range 56.3 – 83.8%, average 70.0%) and ^{85}Rb (range 18.0 – 26.3%, average 22.0%) being greater than the average for the entire soil core (average 51.6% of ^{39}K and 17.5% of ^{85}Rb, respectively). In contrast, the exchangeability of ^{133}Cs within the upper 4 cm layer (range 5.49 – 6.44%, average 5.89%) was not obviously different to the entire soil profile (average 5.71%). This suggests that the 'available' concentrations of potassium, especially, dominated over exchangeable ^{133}Cs in the cation exchange sites within Wat Ban Chan soil. Thus, potassium availability, as a fraction of total soil potassium, for uptake by Three-needled pine is much greater than that of caesium.

The ratios of the ^{39}K/^{133}Cs CRs in wood and needles were 92,700 and 68,000, respectively, while the ^{85}Rb/^{133}Cs CRs in wood and needles were 451 and 173, respectively. Thus, of these three alkali metals Cs is not only the least abundant, it is also the least available within the soil and the least preferred during biological uptake from the available soil pool.

Despite the availability and biological uptake of K, Rb and Cs being quantitatively very different, the patterns of distribution of all three elements in trees appear similar (section 5.2.7.1). The radial distributions of ^{39}K and ^{85}Rb concentrations across annual growth rings of Three-needled pine were particularly similar in qualitative terms, with approximately linear increases in concentration from older to younger wood. This probably reflects the demand for potassium, in particular, at the physiologically active cambial layer just beneath the bark, from which point secondary growth (trunk expansion) is initiated. The trend in ^{133}Cs across the growth rings was similar to both ^{39}K and ^{85}Rb although the variability of ^{133}Cs concentration from year-to-year was greater, resulting in a less clear pattern as shown in Figure 5-24a (section 5.2.7.1). It is likely that both ^{85}Rb and ^{133}Cs 'piggy back' on the movement of ^{39}K, since neither Rb or Cs are known to be essential for plant metabolism.

Interestingly, however, ^{133}Cs appears to be preferentially translocated from wood to needles over ^{39}K and ^{85}Rb, as shown by the translocation factors in Table 5-7 (section 5.2.8.3). f_{tr} values of 4.45, 4.25 and 2.78 for ^{133}Cs, ^{39}K and ^{85}Rb, respectively, indicate that translocation of the alkali metals from wood to needles in Three-needled pine at Wat Ban Chan was in the order ^{133}Cs > ^{39}K > ^{85}Rb. A consequence of this pattern is that Cs is more prone to be lost from the tree as needles fall from the canopy to the forest floor. Thus, as a proportion of

the total elemental inventory within the tree, litter fall is likely to be quantitatively more important for Cs than for K and Rb.

Comparison of findings at Wat Ban Chan and Boundary Plantation

Summary data from Boundary Plantation, Wat Ban Chan and Kopachi are presented in Annex 1. A very high rate of organic matter decomposition in the soil at Wat Ban Chan resulted in the accumulation of almost no litter at the soil surface. Consequently, it's the accumulation of organic matter was much lower than at Kopachi and, especially, at Boundary Plantation. The range in organic matter content and pH between the upper and lower parts of the soil core was not as great as seen at Boundary Plantation. However, the main compositions of the mineral fraction of the soils at both sites were similar. XRD results suggest that quartz was the only major crystalline phase in the soil below 2 cm depth at Wat Ban Chan and below 3 - 4 cm depth at Boundary Plantation. The surface soil layers at both sites contained amorphous, non-crystalline material. At Boundary Plantation this is likely to be organic matter while at Wat Ban Chan, where the iron and aluminium content was high, this may represent a mixture of organic matter and amorphous sesquioxides.

The soil at Wat Ban Chan was higher in ^{133}Cs and ^{85}Rb but lower in ^{39}K compared with Boundary Plantation. Within the mineral layers of soil at Wat Ban Chan the exchangeability of ^{133}Cs, ^{39}K and ^{85}Rb was higher than at Boundary Plantation which suggests these elements are more strongly fixed within the sandy subsoil at Boundary Plantation. However, within the acidic organic layer of soil at Boundary Plantation the exchangeability of ^{133}Cs, ^{39}K and ^{85}Rb increased, possibly due to displacement from non-specific binding sites by protons, and was higher than in the soil at Wat Ban Chan. The exchangeable concentration of ^{39}K in mineral soil at Wat Ban Chan was higher than in mineral soil at Boundary Plantation. The E-Values determined using ^{134}Cs were 5 – 50% lower at Boundary Plantation than at Wat Ban Chan.

At both Boundary Plantation and Wat Ban Chan ^{137}Cs originated from atmospheric nuclear weapons tests in the 1960s; ^{137}Cs was much higher at Boundary Plantation due to its location is in a higher latitude and closer to the western edge of the European continent where washout from the atmosphere was greater (UNSCEAR, 1969). At Wat Ban Chan about 85 % of ^{137}Cs was distributed in the upper 3 cm depth and all deposited ^{137}Cs was distributed within the upper 6 cm depth, while at Boundary Plantation about 60 % of ^{137}Cs

was distributed within the organic soil layers (down to 9 cm depth) and a smaller amount of ^{137}Cs leached down at least as deep as 18 cm which was the maximum depth of soil cores. The mean migration rate of ^{137}Cs at Wat Ban Chan (0.33 mm y^{-1}) was approximately five-times lower than at Boundary Plantation (1.54 mm y^{-1}).

Uptake of ^{39}K and ^{85}Rb from soil to timber by Three-needled pine at Wat Ban Chan was greater than uptake by Corsican pine at Boundary Plantation, while uptake of ^{133}Cs was greater by Corsican pine at Boundary Plantation. However, the translocation from timber of ^{133}Cs, ^{39}K and ^{85}Rb to needles of Corsican pine at Boundary Plantation was greater than translocation of the same elements in Three-needled pine at Wat Ban Chan. Uptake of ^{133}Cs, ^{39}K and ^{85}Rb from soil to needles by Three-needled pine at Wat Ban Chan was lower than soil to needle uptake by Corsican pine at Boundary Plantation.

The needles of Three-needled pine at Wat Ban Chan absorbed both ^{39}K and ^{85}Rb in preference to ^{133}Cs, as indicated by the comparative concentration ratios (*CR*) of these elements in Table 5-4 (section 5.2.8.1).

5.4 CONCLUSIONS

The soil at Wat Ban Chan is typical of similar forest soils in the tropical zone. The organic matter, even at the surface, is much lower than in temperate forest soils while the mineral content is composed almost entirely of quartz with no identifiable clay minerals which might 'fix' caesium originating from atmospheric fallout. Despite this lack of clay minerals, 53 years following deposition of nuclear weapons fallout almost all (83%) the ^{137}Cs within the soil is distributed within the upper 2 - 3 cm of the soil profile. Even though the organic matter content in the upper 2 – 3 cm of soil profile is low it probably still plays an important role in the vertical distribution of ^{137}Cs. The variation of soil pH throughout the upper 13 cm of the soil profile is less than 1 pH unit and thus is unlikely to influence the vertical distributions of ^{137}Cs and ^{133}Cs in the soil.

As a major nutrient, K is present in soils and tree tissues at much higher concentrations than Rb and especially Cs. However, the degree of translocation of K from wood to pine needles is less than that of Cs. As was seen in the Boundary Plantation soil, the vertical profile of K concentrations in the soil at Wat Ban Chan suggests that there is a substantial input of K at the soil surface in the form of tree litter. This appears to be a quantitatively less important

mechanism for Cs, but must still be operating because litter fall from Three-needled pine must carry a small but measurable flux of both ^{133}Cs and ^{137}Cs translocated from wood to needles. Rapid decomposition of organic matter in the tropical climate of northern Thailand results in a much shallower distribution of organic matter within the soil, where fallout ^{137}Cs has accumulated. Model calculations in Chapter 7 suggest that the rate of downwards migration of ^{137}Cs is slower than the rate of 'burial' of the organic matter which may indicate that organic matter decomposition is not as important a process controlling the long-term migration of ^{137}Cs in a tropical forest ecosystem as it appears to be for temperate forests such as Boundary Plantation.

CHAPTER 6: VALIDATION AND CALIBRATION OF LONG-TERM PREDICTIONS USING THE RIFE MODEL

Models to predict the distribution and transfer of radionuclides in forest ecosystems provide essential support when designing remedial and abatement strategies in radioactively contaminated areas. A number of models have been developed to forecast the migration behaviour of radionuclides in forests, especially radiocaesium and strontium which present the most hazardous human exposures when compared with other radionuclides. To investigate the readiness of existing models to assist in managing European forests contaminated by Chernobyl fallout, a Forest Working Group was established within the International Atomic Energy Agency's BIOMASS programme with the aim to compare, test and validate 10 participating forest models (IAEA, 2002). The results of the IAEA's BIOMASS inter-comparison exercise showed the high uncertainty between the predictions of radiocaesium behaviour by different models even for a well-defined source term (Chernobyl) over a relatively short time scale (10 years). This highlights the need for improved model testing and calibration over the longer term which, to date, have not been carried out (Shaw et al., 2005; Yoshida et al., 2004).

6.1 OBJECTIVES

To test and, if necessary, calibrate the RIFE model using long-term (>50 years after atmospheric weapons deposition) data on radiocaesium distributions in forests at Boundary Plantation (UK) and Wat Ban Chan (Thailand). RIFE1, one of three models in the RIFE model package, was selected to be tested and calibrated.

6.2 RIFE1 MODEL

The RIFE (Radionuclides in Forest Ecosystems) model was developed to forecast radiocaesium contamination in forest ecosystems following the Chernobyl accident. It was calibrated using data obtained in several western European

countries and Belarus up to 1996 and was one of the models successfully used in the IAEA's BIOMASS inter-comparison exercise (Shaw et al., 2005).

The RIFE model package comprises three models which differ in their structure depending on the purpose of users (Shaw and Belli, 1999). RIFE1 is possibly the most flexible model in the RIFE model package since it provides a compromise between the complexity of structure and sufficiently detailed information for decision making. It is a simple dynamic model for the prediction of radionuclides circulating in forest ecosystems, comprising 5 compartments. Transfer of radionuclides between compartments is calculated using a series of 7 transfer half times which are assumed to be constant with time following a contamination event. RIFE1 has been calibrated using data from 8 sites within the SEMINAT network (Belli, 2000) and has most recently been used to make predictions of radiocaesium dynamics in forests in the Fukushima prefecture from 2011 to 2031 (Hashimoto et al., 2013). The structure of RIFE1 is shown in Figure 6-1.

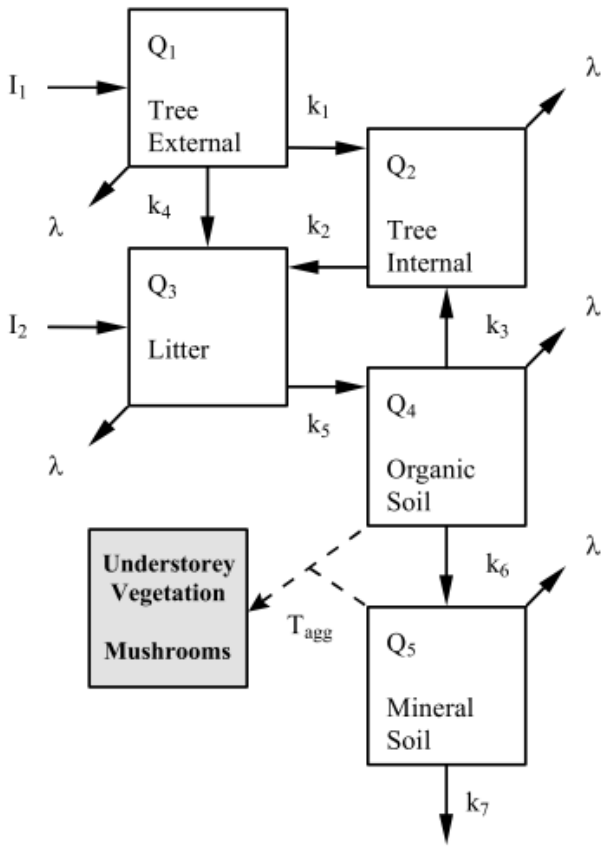


Figure 6-1 Structure diagram of RIFE1 (Shaw and Belli, 1999).

6.3 PARAMETERS USED FOR RIFE MODEL CALCULATIONS

The RIFE model uses specific rate constants and parameters to calculate radionuclide cycling in forest ecosystems. However, some of these parameters are assumed to be the same at each site and default values can be applied. The full list of rate constants and parameters is shown in Table 6-7 (section 6.4).

Some of the parameters are available for Boundary Plantation and Wat Ban Chan (eg. standing biomass, soil characteristics). Other specific parameters needed to calibrate the model for Boundary Plantation and Wat Ban Chan have been estimated; these are shown in Table 6-9 (section 6.5) which concludes this chapter.

6.3.1 Density of standing biomass calculation

In order to calculate inventories of caesium and other elements in standing biomass within a forest, the standing biomass must first be evaluated. Measurements were made in the field of the spatial density and the average circumference and height of trees from which estimates can be made of standing biomass.

The standing biomass is calculated as follows:

$$SB = TN \times MS \qquad (6.1)$$

Where SB = Standing biomass per area (kg m^{-2})

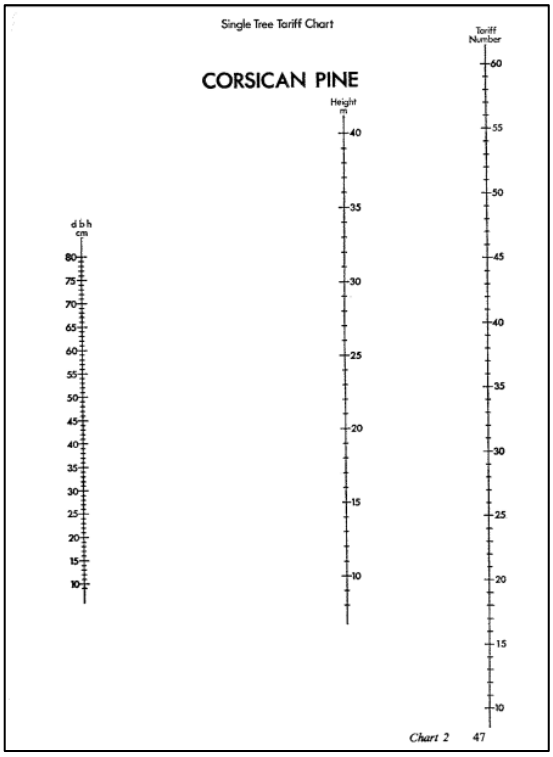
TN = Average number of standing trees per unit area (m^{-2})

MS = Average mass of single standing trees (kg)

The average number of standing trees per unit area was estimated by counting pine trees in 6 replicate areas of 50 × 50 m surrounding or adjacent to the soil sampling sites. The average masses of timber, needles and branches were calculated using the methods described below.

6.3.1.1 Biomass density of timber

The standing volume of single trees of Corsican pine (*Pinus nigra*) at Boundary Plantation was estimated using forest mensuration tables (Hamilton, 1996). Timber height and diameter at breast height (dbh) of pine trees were used with a single tree tariff chart to find the tariff number. The tariff number and dbh were then used to look up the 'over bark' volume (m^3). The tariff chart and tariff table for Corsican pine are shown in Figure 6-2 and Table 6-1, respectively.



<u>Figure 6-2</u> Single tree tariff chart for Corsican pine (Hamilton, 1996); dbh (diameter at breast height, cm) and height of tree (m) are used to estimate the tariff number, shown in Table 6-1.

Finally, the timber volume of Corsican pine at Boundary Plantation was converted to a dry mass using an assumed dry density of 500 kg m^{-3} and summarised in Table 6.2.

Table 6-1 Tariff table (Hamilton, 1996); dbh (diameter at breast height, cm) and tariff number are used to estimate the 'over bark' volume of timber (m^3).

Tariff Table, *contd.*

	VOLUME IN CUBIC METRES OVERBARK											
dbh cm	Tariff Number											dbh cm
	50	51	52	53	54	55	56	57	58	59	60	
21	0.49	0.50	0.51	0.52	0.53	0.54	0.55	0.56	0.57	0.58	0.59	21
22	0.54	0.55	0.56	0.57	0.58	0.60	0.61	0.62	0.63	0.64	0.65	22
23	0.60	0.61	0.62	0.63	0.64	0.66	0.67	0.68	0.69	0.70	0.72	23
24	0.66	0.67	0.68	0.69	0.71	0.72	0.73	0.75	0.76	0.77	0.79	24
25	0.72	0.73	0.74	0.76	0.77	0.79	0.80	0.82	0.83	0.84	0.86	25
26	0.78	0.79	0.81	0.83	0.84	0.86	0.87	0.89	0.90	0.92	0.93	26
27	0.84	0.86	0.88	0.89	0.91	0.93	0.94	0.96	0.98	1.00	1.01	27
28	0.91	0.93	0.95	0.97	0.98	1.00	1.02	1.04	1.06	1.08	1.09	28
29	0.98	1.00	1.02	1.04	1.06	1.08	1.10	1.12	1.14	1.16	1.18	29
30	1.05	1.08	1.10	1.12	1.14	1.16	1.18	1.20	1.22	1.24	1.27	30
31	1.13	1.15	1.18	1.20	1.22	1.24	1.27	1.29	1.31	1.33	1.36	31
32	1.21	1.23	1.26	1.28	1.30	1.33	1.35	1.38	1.40	1.43	1.45	32
33	1.29	1.31	1.34	1.37	1.39	1.42	1.44	1.47	1.49	1.52	1.55	33
34	1.37	1.40	1.43	1.45	1.48	1.51	1.54	1.56	1.59	1.62	1.64	34
35	1.46	1.49	1.51	1.54	1.57	1.60	1.63	1.66	1.69	1.72	1.75	35
36	1.54	1.57	1.61	1.64	1.67	1.70	1.73	1.76	1.79	1.82	1.85	36
37	1.63	1.67	1.70	1.73	1.76	1.80	1.83	1.86	1.89	1.93	1.96	37
38	1.73	1.76	1.80	1.83	1.86	1.90	1.93	1.97	2.00	2.04	2.07	38
39	1.82	1.86	1.89	1.93	1.97	2.00	2.04	2.08	2.11	2.15	2.19	39
40	1.92	1.96	2.00	2.03	2.07	2.11	2.15	2.19	2.23	2.26	2.30	40

The biomass of single trees of Three-needled pine at Wat Ban Chan was estimated using a biomass equation proposed by Nongnuang (2012) as follows.

$$W_S = 0.0503(D^2H)^{0.8775} \qquad (6.2)$$

When W_S = Biomass of single timber (kg)

D = Diameter of timber at breast height (cm)

H = Height of Three-needled pine (m)

The standing biomasses of Corsican pine at Boundary Plantation and Three-needled pine at Wat Ban Chan were calculated using equation 6.1. These values are summarised in Table 6-2.

6.3.1.2 Biomass density of needles and branches

Biomass of needles and branches of Corsican pine at Boundary Plantation were calculated using the geometric mean of biomass fractions estimated for coniferous needles and branch compartments in temperate forests in the SEMINAT study (Belli, 2000).

For Three-needled pine, a stratified clipping technique was applied to create allometric equations (equations 6.3 and 6.4) to calculate the biomass of needles and branches (Nongnuang, 2012).

$$W_B = 0.0012 \times (D^2 \times H)^{1.0996} \quad (6.3)$$

$$W_L = 0.4536 \times (W_B)^{0.7933} \quad (6.4)$$

When W_B = Biomass of branch (kg)

W_L = Biomass of needles (kg)

D = Diameter of timber at breast height (cm)

H = Height of tree (m)

The standing biomass of needles and branches of Corsican pine at Boundary Plantation and Three-needled pine at Wat Ban Chan are summarised in Table 6-2.

Table 6-2 Calculated parameters and standing biomass of Corsican pine at Boundary Plantation and Three-needled pine at Wat Ban Chan.

Pine species and site	Density of standing trees (m^{-2})	Single timber volume (m^3)	Standing biomass of timber (kg m^{-2})	Biomass of branches (kg m^{-2})	Biomass of needles (kg m^{-2})	Total standing biomass (kg m^{-2})
Corsican pine at Boundary Plantation	4.06×10^{-2}	1.29 ± 0.10	26.2 ± 2.09	3.28 ± 0.20	1.61 ± 0.13	34.1 ± 2.72
Three-needled pine at Wat Ban Chan	2.52×10^{-2}	-	15.9 ± 3.18	4.27 ± 1.06	0.655 ± 0.141	20.9 ± 3.35

6.3.2 Initial deposition of ^{137}Cs

Ideally, the initial total deposition of ^{137}Cs would be calculated from summation of ^{137}Cs in forest soil and standing tree inventories. Unfortunately, the activity of ^{137}Cs in standing tree inventories at Boundary Plantation and Wat Ban Chan were undetectable using high efficiency gamma counting. Data published by Cawse and Horrill (1986) provide an estimate for the total ^{137}Cs deposition at Boundary Plantation. No deposition data are available in the literature for Wat Ban Chan.

6.3.2.1 Deposition of ^{137}Cs in pine wood and needles

^{137}Cs activity concentrations (Bq kg^{-1}) in pine wood and needles were calculated using equation 1.4 (section 1.2.8.3); the suggested T_{ag} values for pine wood and needles are 0.0017 and 0.12 m^2 kg^{-1}, respectively (IAEA, 2010). The calculated ^{137}Cs activity concentrations in wood and needles at Boundary Plantation and Wat Ban Chan are summarised in Table 6-3.

Table 6-3 Calculated ^{137}Cs activity concentrations in pine wood and needles at Boundary Plantation and Wat Ban Chan

Site (sampling year)	^{137}Cs (Bq kg^{-1})	
	Wood (tree internal)	Needle
Boundary Plantation (2015)	2.53	14.88
Wat Ban Chan (2016)	0.32	1.90

Calculated ^{137}Cs activity concentrations in pine wood and needles at Boundary Plantation and Wat Ban Chan at the sampling time were converted to their activity concentrations at 1963 using equation 2.7 (section 2.4.6.4).

Finally, ^{137}Cs activity inventories at 1963 in standing biomass are calculated using equation 6.5. The results are summarised in Table 6-4.

$$I_0 = A_i \times B_i \qquad (6.5)$$

Where I_0 = Initial deposition of ^{137}Cs in aboveground inventory (Bq m^{-2})

A_i = Activity concentration of aboveground inventory at 1963 (Bq kg^{-1})

B_i = Biomass of aboveground inventory (kg m^{-2})

6.3.2.2 Deposition of ^{137}Cs in soil

- *Boundary Plantation*

Data on the deposition of ^{137}Cs throughout Great Britain are available from a survey carried out in 1977 (Cawse and Horrill, 1986). The two survey points closest to Boundary Plantation were Medon Vale (woodland) and Perlethorpe (grassland), as shown in Figure 6-3. The Ordnance Survey coordinates and the measured ^{137}Cs deposition densities in soil are shown in Table 6-4. It was suggested by Cawse and Horrill (1986) that there was no significant difference in areal deposition of ^{137}Cs between grassland and woodland sites.

Table 6-4 Deposition of ^{137}Cs in soil at Medon Vale (woodland) and Perlethorpe (grassland) in 1977 (Cawse and Horrill, 1986)

Site	Grid Reference	^{137}Cs (Bq m^{-2})			% Retention
		0-15 cm	15-30 cm	0-30 cm	Top 15 cm
Medon Vale	SK592705	1,665	550	2,220	74.6
Perlethorpe	SK640710	1,295	370	1,665	>78.4

Deposition of ^{137}Cs down to 30 cm depth of the soil profile at Medon Vale and Perlethorpe in 1977 were 2,220 and 1,665 Bq m^{-2}, respectively. These values were corrected to an assumed initial deposition date in 1963 using equation 2.7

(section 2.4.6.4) which marks the peak of deposition from nuclear weapons testing (Cambray, 1989).

After decay correction, the calculated initial deposition densities of ^{137}Cs at Medon Vale and Perlethorpe in 1963 were 2,289 and 3,051 Bq m^{-2}, respectively.

Figure 6-3 Survey points at Medon Vale (SK592705) and Perlethorpe (SK640710) (1.79 km and 4.47 km away from Boundary Plantation, respectively) which were sampled for ^{137}Cs deposition in 1977 (Cawse and Horrill, 1986).



However, deposition of ^{137}Cs calculated using data from this study from 18 cm soil profiles collected at Boundary Plantation indicated a total deposition to the soil of 4,800 Bq m^{-2} in 1963 (section 3.2.2.4). The estimated initial total deposition of ^{137}Cs is summarised in Table 6-5.

- *Wat Ban Chan*

Initial deposition of ^{137}Cs in soil at Wat Ban Chan in 1963 was calculated using equation 2.7 (section 2.4.6.4; 643 Bq m^{-2} of ^{137}Cs deposition in soil in 1963 is calculated in section 5.2.2.4). The estimated initial total deposition of ^{137}Cs is summarised in Table 6-5.

6.3.2.3 Summarised calculated initial deposition of ^{137}Cs

Estimates for the initial deposition of ^{137}Cs at Boundary Plantation (1963) and Wat Ban Chan (1963) are summarised in Table 6-5.

Table 6-5 Summarised estimates of initial deposition of ^{137}Cs at Boundary Plantation (1963) and Wat Ban Chan (1963) in forest soil and aboveground biomass.

Site	Initial deposition of ^{137}Cs at 1963 (Bq m^{-2})		
	Forest soil	Aboveground	Total
Boundary Plantation	4,800 ± 253	244	5,044
Wat Ban Chan	643 ± 119	26.3	669

Total deposition of ^{137}Cs at 1963 at Boundary Plantation (5,044 Bq m^{-2}) and Wat Ban Chan (669 Bq m^{-2}) were used to validate the RIFE model in section 6.4

6.4 VALIDATION OF THE RIFE MODEL

The suitability of the RIFE model for making 50 year predictions of ^{137}Cs contamination in forest compartments (soil layers and trees) at both Boundary Plantation and Wat Ban Chan was tested by comparing calculated distributions with the actual distributions measured at both sites in 2015 and 2016, respectively. Deposition and activity concentrations of ^{137}Cs in forest compartments at Boundary Plantation in 2015 and Wat Ban Chan in 2016 are summarised in Table 6-6.

Table 6-6 Summarised estimates of total deposition and activity concentrations of ^{137}Cs at Boundary Plantation (2015) and Wat Ban Chan (2016) in forest soil and aboveground biomass.

Site (sampling year)	Deposition/activity concentration of ^{137}Cs								
	Forest soil				Aboveground				
	Organic layer		Mineral layer		Tree internal		Litter		Needles
	Bq kg^{-1}	Bq m^{-2}	Bq kg^{-1}	Bq m^{-2}	Bq kg^{-1}	Bq m^{-2}	Bq kg^{-1}	Bq m^{-2}	Bq kg^{-1}
Boundary Plantation (2015)	25.5	928	4.80	523	2.53	74.7	11.5	37.4	14.9
Wat Ban Chan (2016)	4.27	64.4	0.58	95.6	0.37	7.78	3.63	30.3	1.90

This 'validation' exercise was carried out using the total deposition of ^{137}Cs estimated for 1963 (section 6.3.2), the current biomass data described in section 6.3.1 and the physical characteristics of the soil layers described in sections 3.2.1 and 5.2.1. The half times of ^{137}Cs transfer between forest compartments were originally estimated for the 7 'SEMINAT' forest sites in Europe (Novaggio, Tarvisio, Weinsberger, Kobernausser, Round Wood, Clogheen and Shanagarry) (Belli, 2000) as shown in Table 6-8. The ^{137}Cs distributions in forest compartments (litter, organic soil, mineral soil, 'tree internal' (wood and needles)) were calculated using half-lives for the SEMINAT forest sites, plus the average half-lives of all sites. Finally, the calculated distributions were compared to the experimentally measured data.

Table 6-7 Parameter values used for validation of RIFE model calculations.

Factor/Parameter	Boundary Plantation	Wat Ban Chan
Deposition		
Specific initial deposition parameters		
Initial deposition density (Bq/m^2)	5,044	669
Interception fraction :Tree	0.75	0.75
Interception fraction :Litter	0.25	0.25
Soil		
Specific soil layer thickness		
Thickness of Litter layer (m)	0.02	0.01
Thickness of Organic soil (m)	0.07	0.01
Thickness of Mineral soil (m)	0.09	0.11
Specific soil layer bulk density		
Bulk density of Litter layer (kg/m^3)	162	811
Bulk density of Organic soil (kg/m^3)	520	1,509
Bulk density of Mineral soil (kg/m^3)	1,210	1,498
Tree		
Specific tree biomass and growth parameters		
Age of tree at contamination (years)	0	0
Current biomass density of trees (kg/m^2)	26.2	20.9
Expect yield of trees at maturity (kg/m^2)	27.0	21.0
Estimated growth rate of trees ($year^{-1}$)	0.1	0.1

Table 6-7 Parameter values used for validation of RIFE model calculation (continued).

Factor/Parameter	Boundary Plantation	Wat Ban Chan
Tree (continued)		
Specific tree root distribution in soil		
Fraction of tree root in organic soil	0.7	0.7
Fraction of tree root in mineral soil	0.3	0.3
Fungi		
Specific Mushroom T_{ag} value		
Mushroom T_{ag} value (m^2/kg)	0.393	0.393
Specific Mycelium distribution in soil		
Fraction of Mycelium in Litter layer	0.3	0.3
Fraction of Mycelium in Organic horizon	0.5	0.5
Fraction of Mycelium in Mineral horizon	0.2	0.2
Understorey		
Specific Understorey T_{ag} value		
Understorey T_{ag} value (m^2/kg)	0.054	0.054
Specific Understorey Root distribution in soil		
Fraction of Root in Litter layer	0.3	0.3
Fraction of Root in Organic horizon	0.4	0.4
Fraction of Root in Mineral horizon	0.3	0.3

6.4.1 Boundary Plantation

RIFE model calculations for Boundary Plantation used an initial ^{137}Cs deposition of 5,044 Bq m^{-2} in 1963. Standing biomass (section 6.3.1), bulk density and thickness of soil layers, age and growth rate of Corsican pine were all specified parameters. The activity concentrations (Bq kg^{-1}) and inventories (Bq m^{-2}) of ^{137}Cs in litter, organic and mineral soil, tree internal and needle (only Bq kg^{-1}) were calculated up to 52 years after initial deposition (2015) using parameters from the 7 SEMINAT forest sites as shown in Figure 6-4. The percentage inventory distribution of ^{137}Cs in forest compartments was also calculated, as shown in Figure 6-5.

6.4.1.1 Activity concentrations and inventories of ^{137}Cs

The measured ^{137}Cs in litter (37.4 Bq m^{-2} and 11.5 Bq kg^{-1}), tree internal (74.7 Bq m^{-2} and 2.53 Bq kg^{-1}) and needles (14.9 Bq kg^{-1}) at Boundary Plantation were all within the ranges of values predicted using parameters from the 7 SEMINAT forest sites (9.48 - 102 Bq m^{-2} and 2.93 – 31.5 Bq kg^{-1} in litter; 34.4 - 225 Bq m^{-2} and 1.34 – 8.79 Bq kg^{-1} in tree internal tissues; and 5.87 – 38.4 Bq kg^{-1} in needles) as shown in Figure 6-4. Moreover, measured ^{137}Cs in litter, tree internal and needles at Boundary Plantation was close to the values predicted using the parameter averages from the 7 calibration sites (49.6 Bq m^{-2} and 15.3 Bq kg^{-1} in litter; 116 Bq m^{-2} and 4.53 Bq kg^{-1} in tree internal; and 19.8 Bq kg^{-1} in needles).

However, there was considerable divergence between the measured and predicted ^{137}Cs in organic and mineral soil layers. ^{137}Cs measured in organic soil (928 Bq m^{-2} and 25.5 Bq kg^{-1}) exceeded the range predicted (78.1 - 695 Bq m^{-2} and 2.14 – 19.1 Bq kg^{-1}) whilst ^{137}Cs measured in mineral soil (523 Bq m^{-2} and 4.80 Bq kg^{-1}) was below the range predicted (617 – 1,380 Bq m^{-2} and 5.66 – 12.6 Bq kg^{-1}). This suggests that the RIFE model parameters obtained by calibration for Chernobyl deposition to forest sites in Europe under- and over-forecast ^{137}Cs in organic and mineral soil layers, respectively. Clearly, the rate of migration from organic to mineral soil layers has been much slower over 50 years than was anticipated based on post-Chernobyl measurements of ^{137}Cs in organic soil in the 1990s.

6.4.1.2 Percentage inventory distributions

Consideration of the inventory distribution of ^{137}Cs on a percentage basis is useful when comparing the distribution of ^{137}Cs in ecological compartments of forests which have received different initial deposition loads.

The measured percentage distributions of ^{137}Cs in litter and tree internal (2.39 and 4.78%, respectively) at Boundary Plantation were in the range of RIFE-calculated data using parameters from the 7 SEMINAT forest sites (0.74 – 6.59% in litter and 2.20 – 14.4% in tree internal). Furthermore, they were close to the percentage distributions predicted using the parameter averages from the SEMINAT forest sites (3.21 and 7.54%, respectively). However, consistent with the predicted concentrations and budgets of ^{137}Cs in the Boundary Plantation soil, the percentage inventory distributions for ^{137}Cs were under- and over-predicted by the RIFE model in organic and mineral soil layers, respectively.

Table 6-8 Specific compartmental half times (years) obtained by calibration at the SEMINAT forest sites (Belli, 2000).

Forest site	Compartmental half times (years)						
	Foliar absorption (k1)	leaching/Leaf loss (k2)	Tree root absorption (k3)	Weathering : Tree external-Litter (k4)	Leaching		
					Litter-Organic soil (k5)	Organic-Mineral soil (k6)	Mineral-Sub soil (k7)
Clogheen	1×10^6	2.31	5.78	0.45	1.16	6.93	693
Kobernausser	1×10^6	5.06	13.86	0.45	2.31	3.47	1386
Novaggio	1×10^6	3.85	69.31	0.45	2.95	19.8	1019
Round Wood	1×10^6	2.31	6.93	0.45	0.28	23.1	693
Shanagarry	1×10^6	2.31	10.66	0.45	1.73	5.78	693
Tarvisio	1×10^6	2.27	19.8	0.45	0.46	4.23	133
Weinsberger	1×10^6	5.06	69.31	0.45	3.71	9.9	1386

Figure 6-4 *^{137}Cs in Bq m^{-2} (a) and Bq kg^{-1} (b) in forest compartments (tree internal, litter, organic and mineral soil, needle (only Bq kg^{-1}) at Boundary Plantation calculated using parameters obtained for the SEMINAT forest sites in Europe. Their measured distributions of ^{137}Cs (Bq m^{-2} and Bq kg^{-1}) are shown for Boundary Plantation. Measured data of ^{137}Cs at Boundary Plantation is added to compare.*

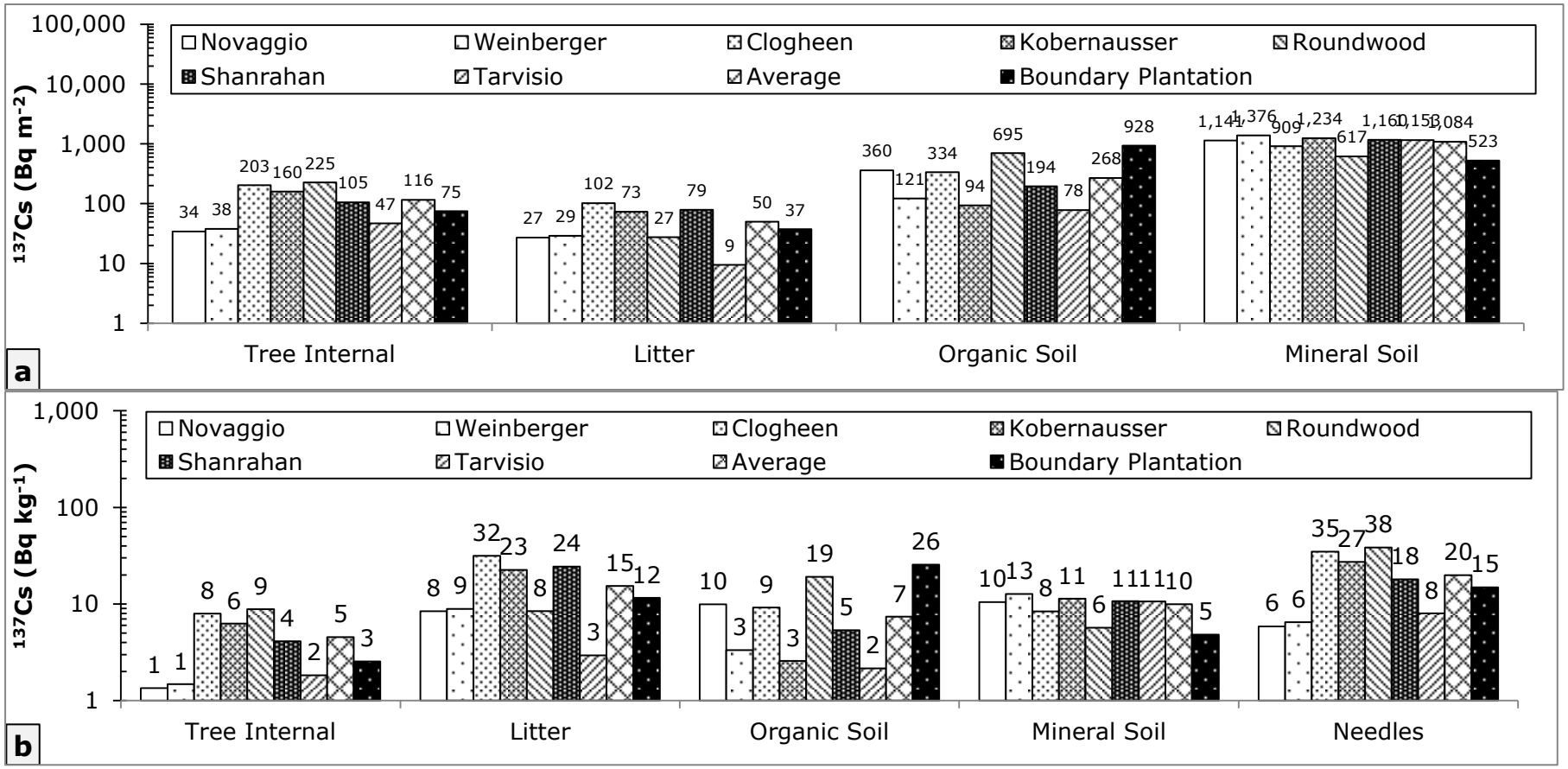
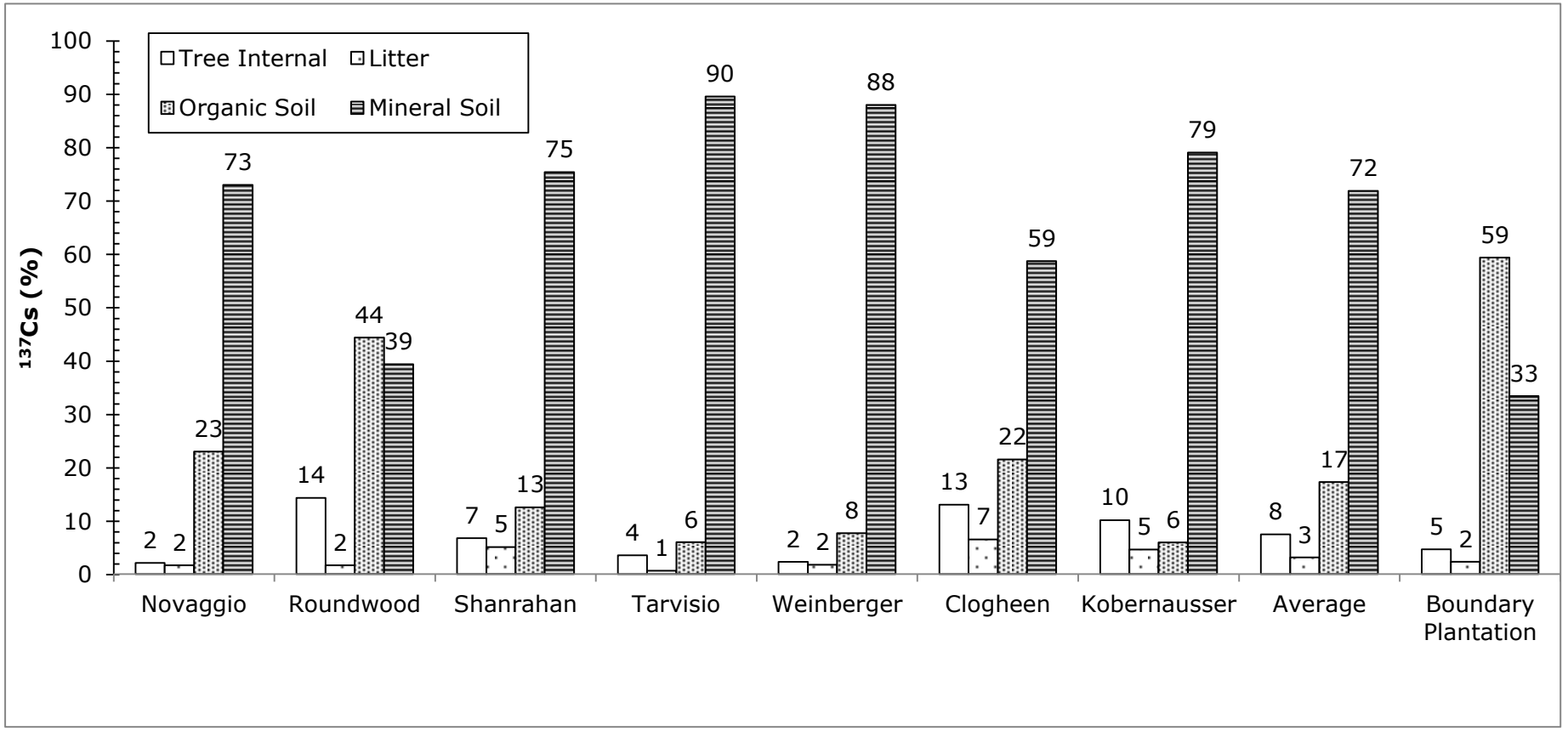


Figure 6-5 *Percentage inventory distributions of ^{137}Cs in forest compartments (tree internal, litter, organic and mineral soil) at Boundary Plantation calculated using parameters obtained for the SEMINAT forest sites in Europe. Their measured distributions of ^{137}Cs are shown for Boundary Plantation. Measured data of ^{137}Cs at Boundary Plantation is added to compare.*



6.4.2 Wat Ban Chan

Because the RIFE model was written to represent Cs behaviour in temperate forests, the model structure includes discrete compartments for forest floor litter and an organic soil layer. However, these compartments are absent in tropical forest soils such as those at Wat Ban Chan, where the surface of the soil has an obvious mineral content with very sparse traces of litter on the forest floor. When applying RIFE to Wat Ban Chan, therefore, the 'litter' and 'organic soil' compartments in the model were used to represent the 0 - 1 and 1 - 2 cm soil layers, respectively.

RIFE model calculations for Wat Ban Chan used an initial ^{137}Cs deposition of 669 Bq m^{-2} (in 1963). Standing biomass (section 6.3.1), bulk density and thickness of soil layers, age and growth rate of Three-needled pine were all specified parameters. The activity concentrations (Bq kg^{-1}) and inventories (Bq m^{-2}) of ^{137}Cs in 'litter', 'organic' and mineral soil, tree internal and needle (only Bq kg^{-1}) were calculated up to 53 years after initial deposition (2016) using parameters from the 7 SEMINAT forest sites as shown in Figure 6-6. The percentage inventory distribution of ^{137}Cs in forest compartments was also calculated, as shown in Figure 6-7.

6.4.2.1 Activity concentrations and inventories of ^{137}Cs

The measured ^{137}Cs in tree internal (7.78 Bq m^{-2} and 0.37 Bq kg^{-1}), organic soil (64.4 Bq m^{-2} and 4.27 Bq kg^{-1}), mineral soil (95.6 Bq m^{-2} and 0.58 Bq kg^{-1}) and needle (1.90 Bq kg^{-1}) compartments at Wat Ban Chan were within the range of predicted values using the parameters from the 7 SEMINAT forest sites (4.23 – 28.0 Bq m^{-2} and 0.21- 1.39 Bq kg^{-1} in tree internal, 9.64 – 86.2 Bq m^{-2} and 0.64 – 5.72 Bq kg^{-1} in organic soil, 77.4 - 172 Bq m^{-2} and 0.47 – 1.05 Bq kg^{-1} in mineral soil and 0.92 – 6.09 Bq kg^{-1} in needles) as shown in Figure 6-6. Moreover, the measured and predicted ^{137}Cs in tree internal, organic soil, mineral soil and needle compartments at Wat Ban Chan were of the same order of magnitude when predictions were made using the parameter averages from the SEMINAT forest sites (14.4 Bq m^{-2} and 0.72 Bq kg^{-1} in tree internal, 32.92 Bq m^{-2} and 2.18 Bq kg^{-1} in organic soil, 135 Bq m^{-2} and 0.82 Bq kg^{-1} in mineral soil and 3.14 Bq kg^{-1} in needles).

However, the measured ^{137}Cs in the litter compartment (30.3 Bq m^{-2} and 3.63 Bq kg^{-1}) was higher than the range predicted (1.17 – 12.7 Bq m^{-2} and 0.14 –

1.57 Bq kg^{-1}) which indicates that the RIFE model under-predicts ^{137}Cs in 'litter' at Wat Ban Chan when calibrated with parameters obtained for forest sites in Europe. However, it must be borne in mind that the use of the 'litter' compartment for the Wat Ban Chan soil is somewhat artificial, since no clearly definable litter layer exists at the site.

6.4.2.2 Percentage inventory distributions

The measured percentage distributions of ^{137}Cs in tree internal (3.93%), organic soil (32.5%) and mineral soil (48.3%) at Wat Ban Chan were in the range of predicted values obtained using parameters for the SEMINAT forest sites (2.17 – 14.4% in tree internal, 6.00 – 44.2% in organic soil and 39.7 – 89.6% in mineral soil). Furthermore, measured percentage distributions of ^{137}Cs were close to the predicted values using parameter averages for the SEMINAT forest sites (7.53% in tree internal, 17.1% in organic soil and 72.2% in mineral soil) as well. However, the percentage of ^{137}Cs in litter (15.3%) was above the predicted range (0.74 – 6.59%).

Figure 6-6 *^{137}Cs in Bq m^{-2} (a) and Bq kg^{-1} (b) in forest compartments (tree internal, litter, organic and mineral soil) at Wat Ban Chan calculated using parameters obtained for the SEMINAT forest sites in Europe. Their measured distributions of ^{137}Cs (Bq m^{-2} and Bq kg^{-1}) are shown for Wat Ban Chan. Measured data of ^{137}Cs at Wat Ban Chan is added to compare.*

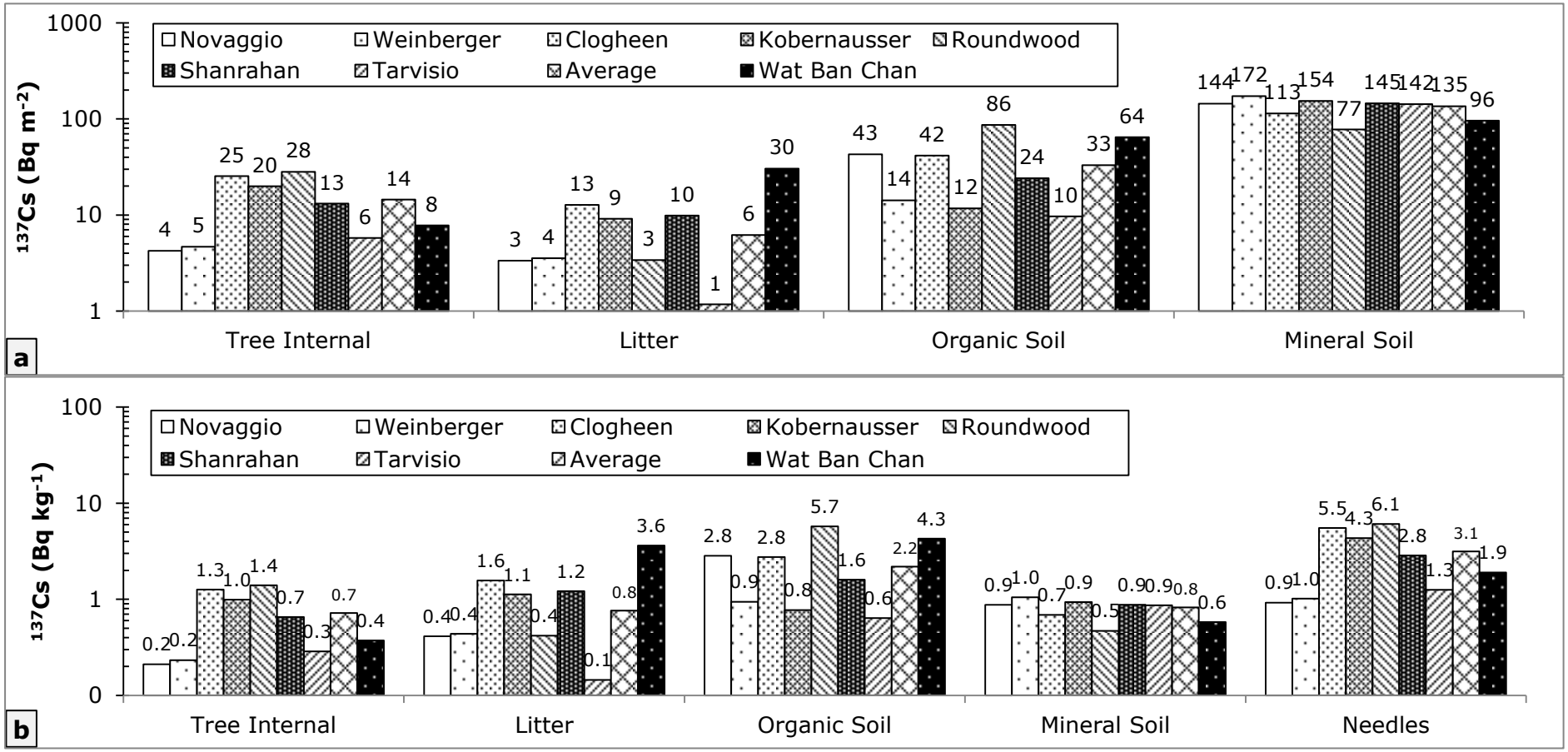
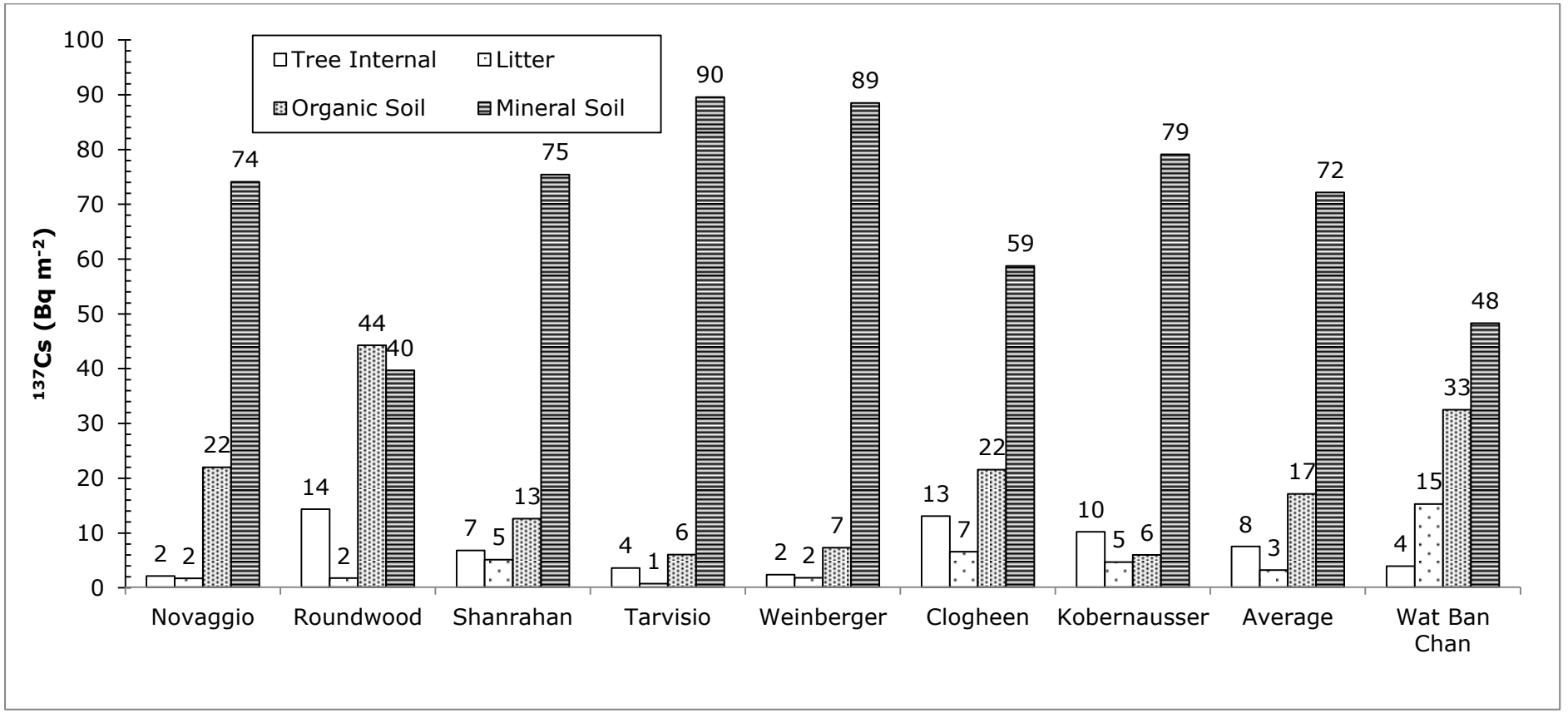


Figure 6-7 Percentage inventory distributions of ^{137}Cs in forest compartments (tree internal, litter, organic and mineral soil) at Wat Ban Chan calculated using parameters obtained for the SEMINAT forest sites in Europe. Their measured distributions of ^{137}Cs are shown for Wat Ban Chan. Measured data of ^{137}Cs at Wat Ban Chan is added to compare.



6.5 CALIBRATION OF RIFE MODEL

Calibration of the RIFE model is carried out by adjusting the half-lives of individual compartments and other parameters (eg. standing biomass of trees, thickness and bulk density of soil layers) to 'tune' predictions for Cs distributions in specific forest ecosystems for which initial deposition activities and times can be determined. However, to calibrate the RIFE model using data for Boundary Plantation and Wat Ban Chan, only the parameters k3, k5, k6 and k7 (see Figure 6-1) were adjusted to improve the predictions of ^{137}Cs in litter, organic and mineral soil, and tree internal tissue. 'Tree external' ^{137}Cs is assumed to be unimportant in the long term whilst data for understorey and fungi were not available at the study sites. A summary of the RIFE compartmental half-times after calibration is shown in Table 6-9.

6.5.1 Boundary Plantation

The model validation described in section 6.4.1 was used as a guide to facilitate adjustment of model parameters to predict ^{137}Cs inventories in the Boundary Plantation forest, which can be summarised as follows.

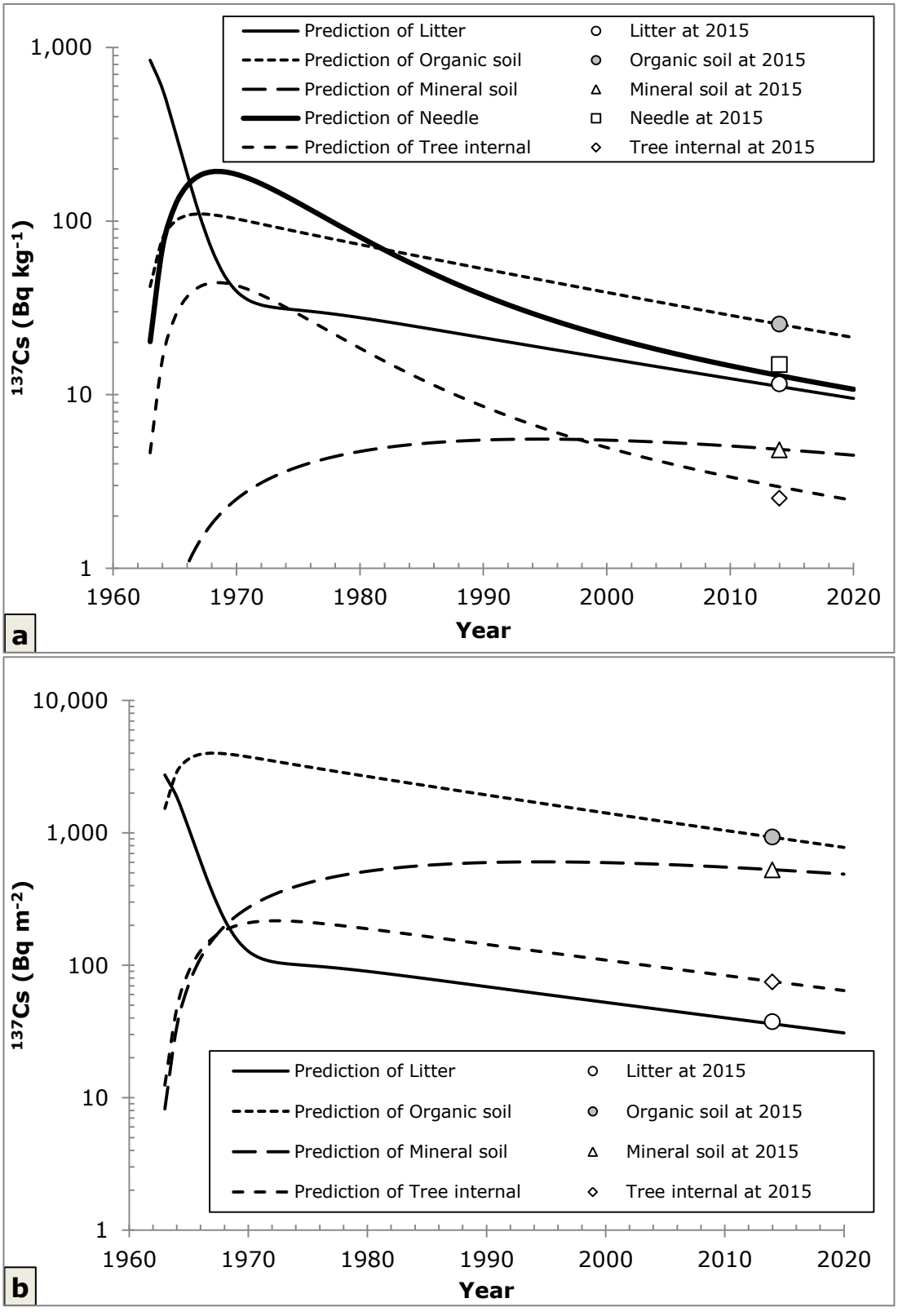
Field data from Boundary Plantation show that the majority of ^{137}Cs (59.4%) is distributed in the organic soil, which is substantially higher than the average percentage inventory (17.4%) predicted using the calibration based on the SEMINAT parameters. The percentage distributions of ^{137}Cs in litter and tree internal tissues (2.39 and 4.78%, respectively) were slightly lower than the average values (3.21 and 7.54%, respectively) predicted using the SEMINAT parameter set. This suggested the compartmental half-times should be adjusted to decrease ^{137}Cs migration from organic soil, but to increase turnover in litter and tree internal tissues.

Within the mineral soil at Boundary Plantation the measured inventory of ^{137}Cs (33.4%) was lower than the average predicted value (71.9%); therefore, the turnover of ^{137}Cs in the mineral soil had to be adjusted by changing the leaching half-times from both the organic and mineral soil layers (k6 and k7, respectively).

A higher total inventory of ^{137}Cs (Bq m^{-2} in 18 cm of the soil profile and tree internal tissues) was measured at Boundary Plantation than was predicted using

SEMINAT parameter averages, suggesting that adjustment was needed to decrease leaching out of the mineral soil layer. Following appropriate adjustment of compartmental half-times, the calculated curves of ^{137}Cs distributions in forest compartments at Boundary Plantation (in Bq kg^{-1} and Bq m^{-2}) are shown in Figure 6-8, with measured distributions in 2015 plotted as points.

Figure 6-8 Calculated curves of ^{137}Cs distributions in forest compartments at Boundary Plantation (in Bq kg^{-1} and Bq m^{-2}) after calibration using Boundary Plantation data, with measured distributions in 2015 plotted as points.



6.5.2 Wat Ban Chan

The model validation described in section 6.4.2 was used as a guide to facilitate adjustment of model parameters to predict ^{137}Cs inventories in the Wat Ban Chan forest, which can be summarised as follows.

Field data from Wat Ban Chan show that approximately half of the ^{137}Cs inventory (48.3%) was distributed in the mineral soil, with the remaining half distributed between the organic soil, litter and tree internal tissues. The measured ^{137}Cs within the mineral soil was substantially lower than the average value (72.2%) predicted using the SEMINAT parameters. Measured ^{137}Cs distributed in litter and organic soil compartments at Wat Ban Chan (15.3 and 32.5% respectively) were greater than the average values (3.2 and 17.1%, respectively) predicted using the SEMINAT parameters. In general, measured retention of ^{137}Cs in organic soil compartments (ie. 'litter' plus organic soil layer) was higher than predicted, suggesting that half-time parameters for Wat Ban Chan should be adjusted to increase the predicted retention of ^{137}Cs in organic soil after 50 years.

Measured ^{137}Cs in tree internal tissues at Wat Ban Chan (3.93%) was approximately half the average value predicted using the SEMINAT parameters (7.93%) so the tree root adsorption half-time was adjusted to decrease ^{137}Cs in tree internal tissues.

The total measured inventory of ^{137}Cs (Bq m^{-2}) at Wat Ban Chan (calculated for 13 cm soil depth plus tree internal tissues) was slightly higher than the average predicted inventory suggesting that adjustment of half-times was needed to decrease leaching from the mineral soil, thus decreasing loss from the system overall. Following appropriate adjustment of compartmental half-times, the calculated curves of ^{137}Cs distributions in forest compartments at Wat Ban Chan (in Bq kg^{-1} and Bq m^{-2}) are shown in Figure 6-9, with measured distributions in 2016 plotted as points.

Figure 6-9 Calculated curves of ^{137}Cs distributions in forest compartments at Wat Ban Chan (Bq kg^{-1} and Bq m^{-2}) after calibration using Wat Ban Chan data, with measured distributions in 2016 plotted as points.

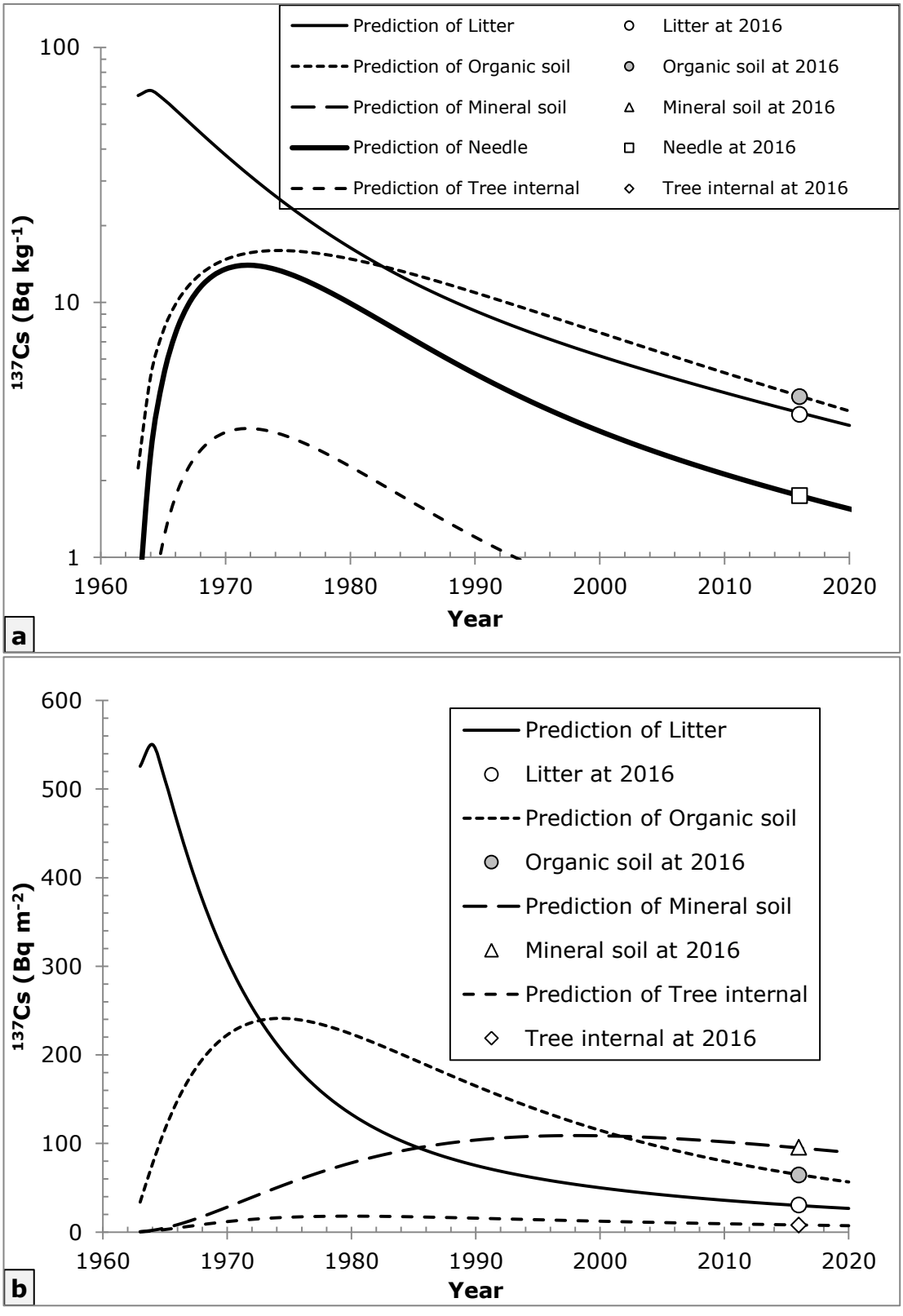


Table 6-9 Half-times (years) after calibration of the RIFE model using data from Boundary Plantation and Wat Ban Chan.

Compartmental half times (years)	Boundary Plantation	Wat Ban Chan
Foliar absorption (k1)	1×10^6	1×10^6
Foliar leaching/Leaf loss (k2)	2.31	2.31
Tree root absorption (k3)	25	21.5
Weathering :Tree external-Litter (k4)	0.45	0.45
Leaching :Litter-Organic soil (k5)	1.1	8
Leaching :Organic-Mineral soil (k6)	58.8	24
Leaching :Mineral-Sub soil (k7)	500	9,000

6.6 CONCLUSIONS

The RIFE model was originally calibrated using data on ^{137}Cs distributions in seven temperate coniferous forest sites which formed the SEMINAT network in the 1990s (Belli, 2000). Using these calibrations, RIFE calculations were made for Boundary Plantation and Wat Ban Chan to determine the accuracy with which ^{137}Cs distributions at both sites could be 'predicted' 50 years after deposition of nuclear weapons fallout. The results of these validation calculations were surprisingly good, although the model consistently under-predicted the percentage of the total ^{137}Cs inventory which is retained in the organic soil layer. As a consequence, the model over-predicted the percentage of the total ^{137}Cs inventory which is retained in the mineral soil layer.

Further calibrations of the RIFE model were made using data from Boundary Plantation and Wat Ban Chan, collected 52 and 53 years, respectively, after peak nuclear weapons deposition in 1963. Although these calibrations are based on single time points they can be expected to be more applicable for long-term predictions than the SEMINAT calibrations, which were based on measurements made around 10 years after the Chernobyl accident in 1986.

The substantial under-estimation of long-term ^{137}Cs accumulation in the organic soil layer within forest soils raises an intriguing question as to the relationship between organic matter accumulation and ^{137}Cs retention. This question is addressed in the next chapter.

The findings of this study support the use of RIFE as a predictive tool for radiocaesium contamination in temperate coniferous forests, for which the model was originally written and calibrated. With the addition of the calibration data supplied here the RIFE model could also be applied with some confidence to tropical and sub-tropical evergreen forests. RIFE has already been used to make forecasts of the 20-year fate of radiocaesium in coniferous forests in the Fukushima prefecture following the Fukushima accident in 2011 (Hashimoto et al., 2013). This part of Japan lies in the northern temperate zone but has a humid monsoonal climate which is distinct to the oceanic climate of Western Europe. It is an open question whether the level of uncertainty in predictions of simple compartment models such as RIFE is more dependent on soil, tree species or climatic factors.

CHAPTER 7: MODELLING ^{137}Cs MIGRATION IN FOREST SOILS

Measurements of 'unsupported' ^{210}Pb activities have most often been used for dating lake sediments or peat bog accumulations. Throughout the development of this method it has not generally been considered that ^{210}Pb dating can be applied to forest soils due to the effect of organic decomposition and consequent reduction of soil depth within the organic layer on the forest floor (Kaste et al., 2011).

Previous studies which modelled the vertical movement of organic matter using ^{210}Pb and ^{137}Cs in soil were carried out with organic-rich soils in Germany (Dörr and Münnich, 2016) with the conclusion that ^{210}Pb is bound tightly with organic matter, therefore its migration rate in the soil directly depends on the downward movement of organic matter. However, vertical migration of ^{137}Cs in organic soils is expected to be faster than lead and depends both on the turnover and downward movement of soil organic matter, including chemical exchange between solid organic and solution phases in the soil.

This modelling study aims to investigate the relationship between depth profiles of ^{210}Pb and ^{137}Cs with the year of deposition of leaf litter on the organic-rich soil at Boundary Plantation (Sherwood Forest, UK) and the organic-poor soil at Wat Ban Chan in Thailand. The soil properties at Boundary Plantation and Wat Ban Chan are presented in section 3.2.1 and 5.2.1, respectively.

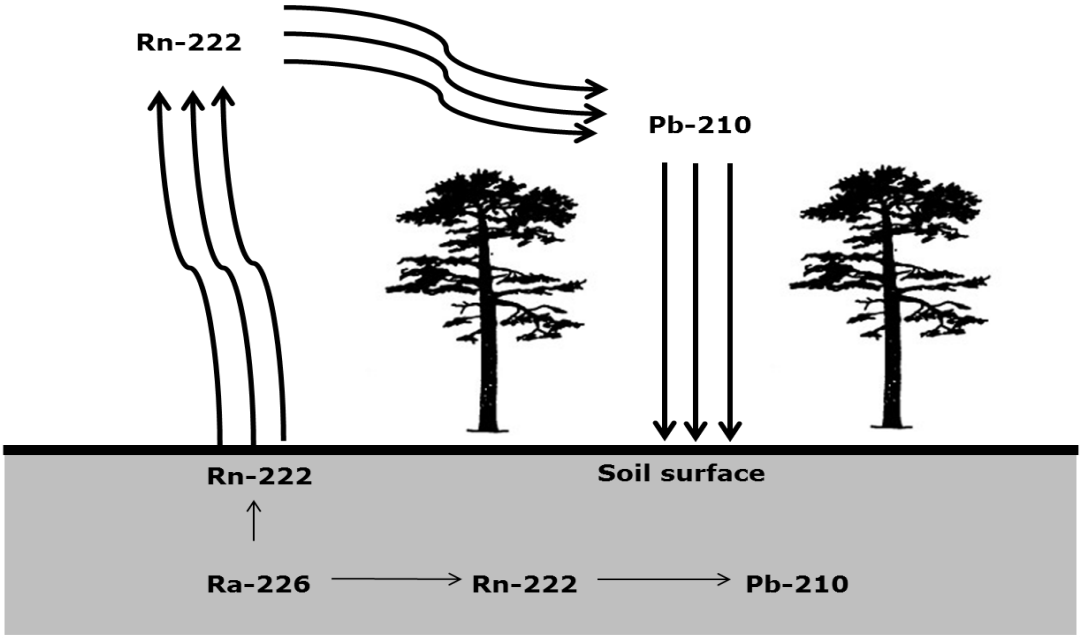
7.1 APPLICATION OF ^{210}Pb DATING TECHNIQUE

^{210}Pb dating provides a method to investigate the age of undisturbed, young (less than 150 – 200 years) sediments and peat profiles (Appleby and Oldfield, 1978). It has been applied in a wide range of environmental research (e.g. Baskaran et al., 2014; MacKenzie et al., 2011; Putyrskaya et al., 2015) though not commonly to estimate the age of organic matter accumulations on the forest floor beneath tree canopies.

^{210}Pb is a naturally occurring isotope in the ^{238}U decay series. ^{222}Rn, a radioactive gas within the decay series, can escape from the Earth's crust into the atmosphere where it decays to ^{210}Pb which then deposits onto the ground

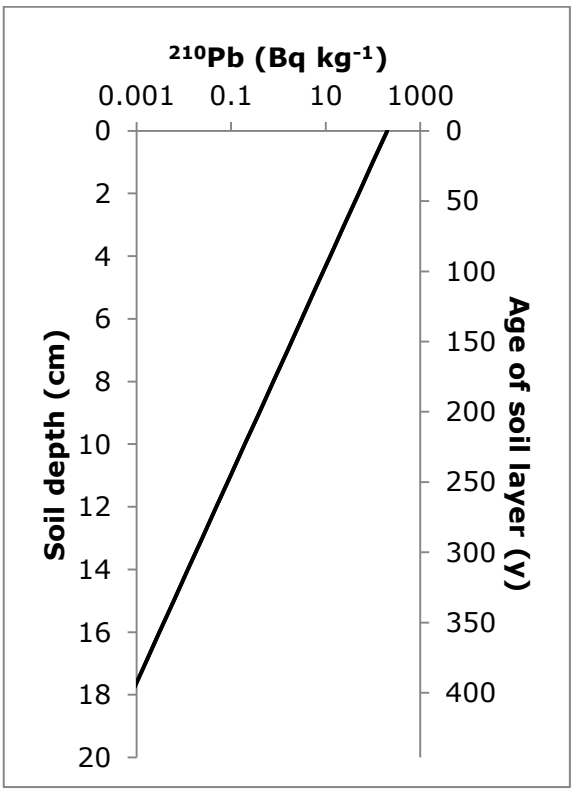
surface through atmospheric precipitation. This source of ^{210}Pb is known as 'unsupported' ^{210}Pb since it is not resupplied by the decay of ^{238}U decay series radionuclides in the soil itself. It can be assumed that the supply of natural fallout of unsupported ^{210}Pb onto the surfaces of sediments, peats or soils occurs at a constant rate. Therefore, the age of sediment or peat at specific depths can be calculated using the assumed rate of unsupported ^{210}Pb precipitation and the physical (radioactive) decay rate of ^{210}Pb. Figure 7-1 shows the pathway of ^{210}Pb: ^{222}Rn gas derived by decay of ^{226}Ra (a ^{238}U daughter) then diffuses through the Earth's crust into the atmosphere where it decays to ^{210}Pb which finally precipitates onto the soil surface.

Figure 7-1 Environmental pathway of ^{210}Pb derived by decay of ^{238}U to ^{222}Rn which diffuses from the Earth's crust into the atmosphere. Here it decays to ^{210}Pb and then deposits on the soil (applied from Appleby and Oldfield, 1978).



The dates of soil layers can be obtained by the correlations of ^{210}Pb with soil depth, as shown in Figure 7-2.

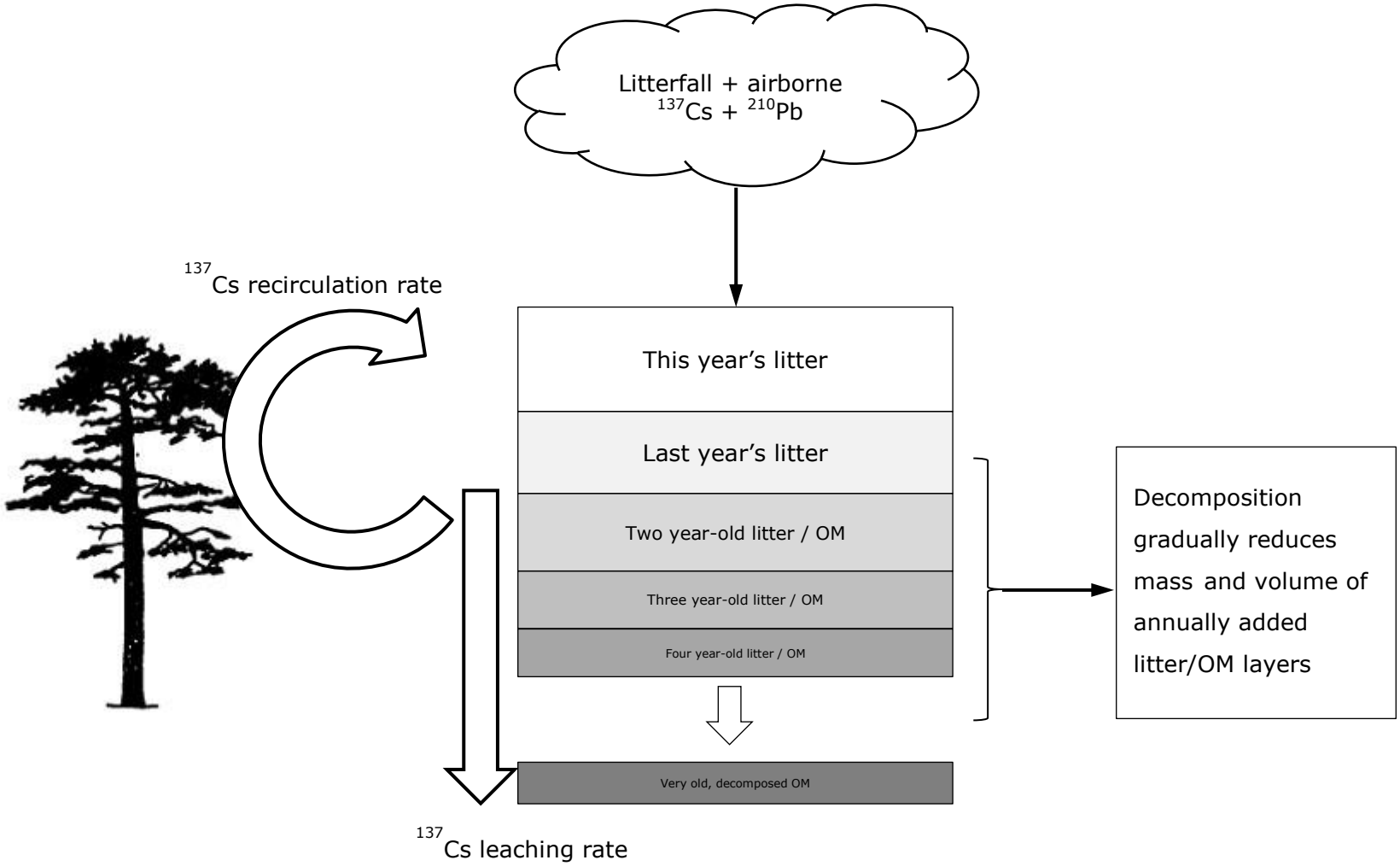
Figure 7-2 Ideal correlation of ^{210}Pb with soil depth, and the corresponding ages of soil layers.



7.2 CONCEPT OF MODELLING

The model describes the relationship between the depth of organic matter accumulating in the upper part of the forest soil profile and the year of litterfall, to better understand the migration of fallout ^{137}Cs. It is assumed that rates of litterfall, ^{210}Pb deposition and organic matter decomposition are constant. Decomposition of litter gradually reduces the mass and volume of annually added litter/OM layers. Therefore, the activity concentration of fallout ^{137}Cs and annually precipitated ^{210}Pb increase with time in a given unit of organic soil as the soil's mass and volume are reduced. However, the activity is simultaneously reduced by radioactive decay (half-lives of 22.3 and 30.2 years, respectively, for

Figure 7-3 Conceptual diagram of model



^{210}Pb and ^{137}Cs). Additionally ^{137}Cs is able to recirculate within the litter fall to the forest floor. The conceptual diagram of the model is shown in Figure 7-3.

7.3 MODEL DESCRIPTION

The model was scripted using OpenModel (www.openmodel.info); model equations are summarised as follows. Descriptions of model parameters are given in Table 7-1.

7.3.1 Adjusting depth of soil due to organic decomposition

Decomposition of soil organic matter reduces the depth of each annual soil layer, using an exponential function between depth of annual soil (litter/organic matter) layer and time since litter fall. The depth of each annual soil layer is given by equation 7.1.

$$AnnualDeltaZ(j) = LitterRate*(a + b*exp(c*(t-j))) \quad (7.1)$$

Where AnnualDeltaZ is the depth of annual soil layer (cm)

LitterRate is the rate of litter fall (kg m^{-2} y^{-1})

a, b and c are exponential parameters of organic matter decomposition

t is time since litter deposition (y)

j is annual layer of soil

7.3.2 Input of ^{137}Cs and ^{210}Pb

The rate of unsupported ^{210}Pb deposition was assumed to be constant every year. Fallout ^{137}Cs was added as a single event representing peak nuclear weapons deposition in 1963 whilst recirculated ^{137}Cs was constantly input every year to represent litter fall from the tree canopy to the forest floor. Equations of activities of inputted ^{137}Cs and ^{210}Pb were created in a two dimensional array (1

= ^{137}Cs, 2 = ^{210}Pb) as shown in equations 7.2, 7.3 and 7.4. Their activities were simultaneously corrected by their decays as shown in equations 7.5 and 7.6.

$$AnnualActivity(1,t) = CsSource1 \quad (7.2)$$

$$AnnualActivity(1,t) = CsSource2 \quad (7.3)$$

$$AnnualActivity(2,t) = PbSource \quad (7.4)$$

$$AnnualActivity(1,j).rate = -CsRate*AnnualActivity(1,j) \quad (7.5)$$

$$AnnualActivity(2,j).rate = -PbRate*AnnualActivity(2,j) \quad (7.6)$$

Where PbSource is the input rate of unsupported ^{210}Pb (Bq m^{-2}y^{-1})

CsSource2 is the input of fallout ^{137}Cs (Bq m^{-2})

CsSource1 is the input of recirculated ^{137}Cs (Bq m^{-2})

AnnualActivity(1,t) is annual activity of ^{137}Cs (Bq m^{-2})

AnnualActivity(2,t) is annual activity of ^{210}Pb (Bq m^{-2})

CsRate is the decay constant of ^{137}Cs (y^{-1})

PbRate is the decay constant of ^{210}Pb (y^{-1})

7.3.3 Binning annual activities of ^{137}Cs and ^{210}Pb into soil profile

In order to present the annual soil layer as a conventional activity soil profile measured from the soil surface, the annual layers were 'binned' using the following procedures.

- Initialise to zero:

Activities of ^{137}Cs and ^{210}Pb were initialised to zero using equation 7.7:

$$SoilProfile(i,j) = 0 \quad (7.7)$$

Where SoilProfile(i,j) represents activities of ^{137}Cs (i = 1) and ^{210}Pb (i = 2) in the soil profile in the j^{th} layer (Bq m^{-2})

- Specify position of the soil 'bin' layer in soil profile:

Top and bottom positions of the soil 'bin' layer were specified using equations 7.8 and 7.9.

$$h2 = (j-1)*SoilDeltaZ \quad (7.8)$$

$$h1 = h2 + SoilDeltaZ \quad (7.9)$$

Where SoilDeltaZ is the depth of soil layer (cm)

h1 is the position of the bottom of the soil 'bin' layer - measured from the top of the profile (cm)

h2 is the position of the top of the soil 'bin' layer - measured from the top of the profile (cm)

- Specify lower and upper boundaries of the annual layer:

Lower and upper boundaries of the annual layer were specified using equations 7.10 and 7.11.

$$hlower = MaxDepth - Zlower(k) \quad (7.10)$$

$$hupper = MaxDepth - Zupper(k) \quad (7.11)$$

Where hlower is the lower boundary of the annual layer - measured from the top of the profile (cm)

hupper is the upper boundary of the annual layer - measured from the top of the profile (cm)

MaxDepth is the position at top of soil profile (cm)

Zlower(k) is the position of the base of the annual layer, measured from the bottom (cm)

Zupper(k) is the position of the top of the annual layer, measured from the bottom (cm)

k is the annual layer

- calculate the fraction of the k^{th} annual layer in the j^{th} soil bin:

The fractions of annual layer in the soil 'bin' layer (1 cm) were calculated using equation 7.12.

if (hlower>=h2) and (hlower<=h1) and (hupper>=h2) and (hupper<=h1) // The annual layer is fully contained within the soil 'bin' layer

f = 1

elseif (hlower>=h2) and (hlower<=h1) // Base of the annual layer is in the soil bin but the top of the annual layer is not.

f = (hlower - h2)/(hlower - hupper)

elseif (hupper>=h2) and (hupper<=h1) // Top of the annual layer is in the soil bin but the base is not.

f = (h1 - hupper)/(hlower - hupper)

else // No any part of the annual layer is in the soil bin.

f = 0 *(7.12)*

Where f is fraction of the annual layer

- Bin the fraction 'f' of the annual activity layer into the soil profile:

Activities of ^{137}Cs and ^{210}Pb of annual layer were converted to their activities in soil profile using equation 7.13.

$$SoilProfile(i,j) = SoilProfile(i,j) + f*AnnualActivity(i,k) \quad (7.13)$$

Where AnnualActivity(i,k) is the activity of ^{137}Cs (i = 1) and ^{210}Pb (i = 2) in soil 'bin' k^{th} layer (Bq m^{-2})

SoilProfile(i,j) is the activity of ^{137}Cs (i = 1) and ^{210}Pb (i = 2) in soil 'bin' profile j^{th} layer (Bq m^{-2})

Full script of model is shown in Annex 2.

7.4 MODEL PARAMETERISATION

The model was fitted to data of ^{210}Pb distributions in 18 and 13 cm depth soil profiles at Boundary Plantation and Wat Ban Chan, collected in 2014 – 2015 and 2016, respectively. The adjusted parameters of both forest soil profiles are shown in Table 7-1.

Table 7-1 Symbols, descriptions and values of model parameters at Boundary Plantation and Wat Ban Chan (are the specific parameters for Boundary Plantation and Wat Ban Chan)*

Symbol	Description	Unit	Value	
			Boundary Plantation	Wat Ban Chan
*a	Organic decomposition (1)	-	4.90	3.31447
*b	Organic decomposition (2)	-	16.50	16.85
*c	Organic decomposition (3)	-	-0.0780	-0.0988
CsRate	Decay constant of ^{137}Cs	y^{-1}	0.02232	0.02232
CsSource1	Recirculated ^{137}Cs	Bq m^{-2} y^{-1}	13	4.1
CsSource2	Single deposited ^{137}Cs	Bq m^{-2}	500	175
Cst	Yearth of ^{137}Cs deposition	-	1	1
*LitterRate	Rate of litterfall	kg m^{-2} y^{-1}	0.016	0.006
PbRate	Decay constant of ^{210}Pb	y^{-1}	0.03060	0.03060
*Pbsource	Source of ^{210}Pb	Bq m^{-2} y^{-1}	96	61

7.5 MODEL RESULTS

The model results of unsupported ^{210}Pb (Bq m^{-2}) in both forest soils were calculated and then compared with the observed data for 2015 and 2016 at Boundary Plantation and Wat Ban Chan, respectively. Results of comparisons are shown in Figure 7-4 and Figure 7-5.

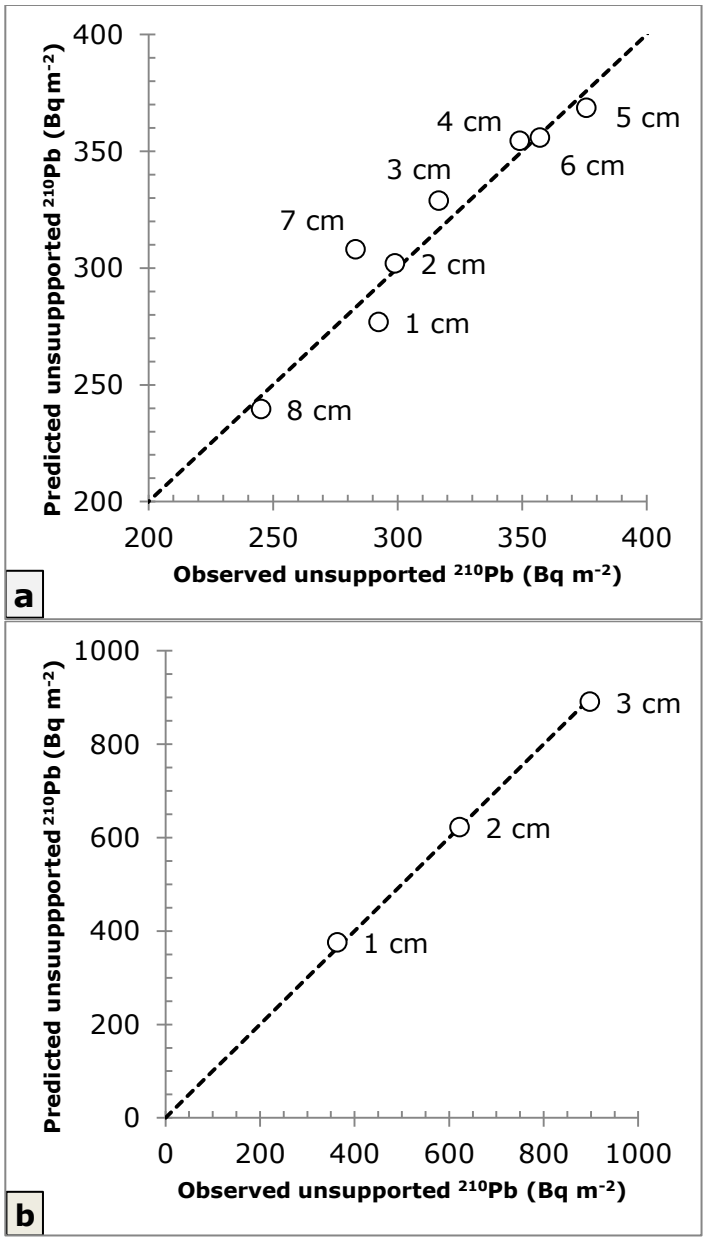
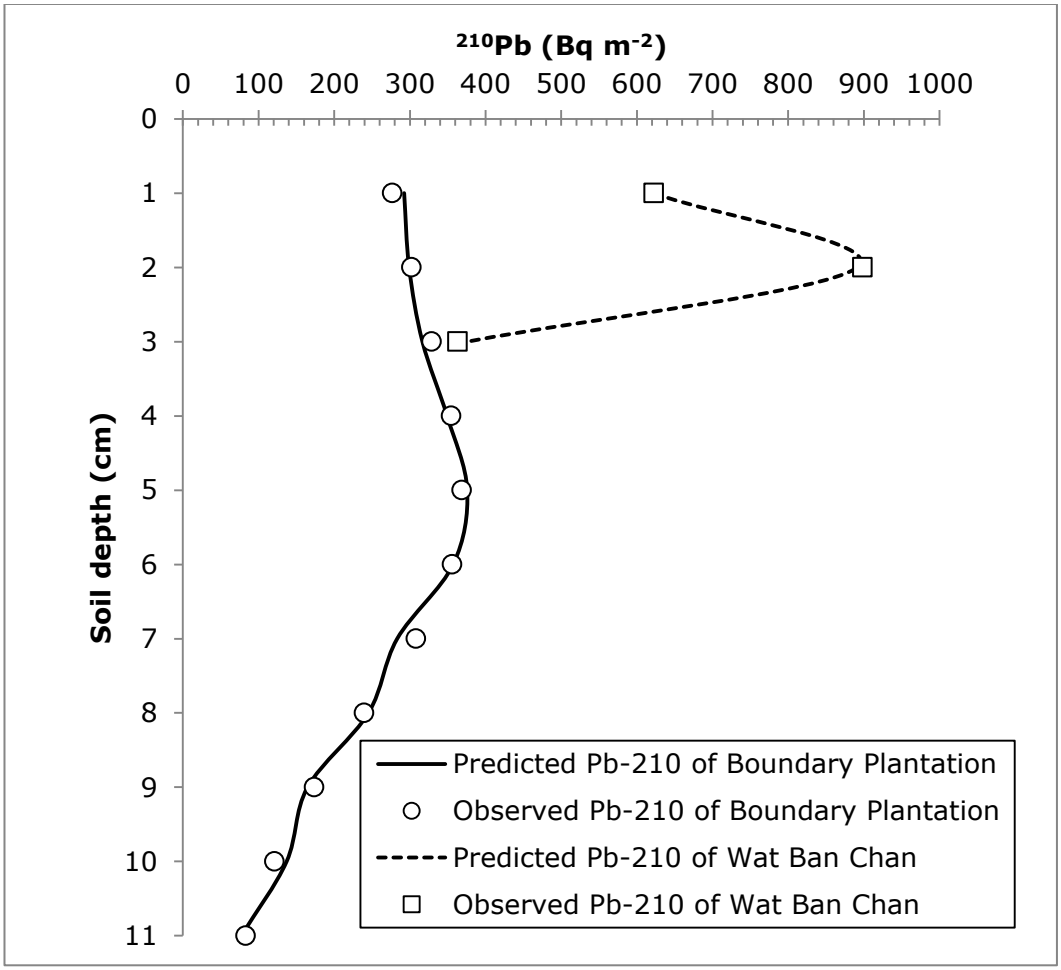


Figure 7-4 Scatter plots between observed and predicted values of unsupported ^{210}Pb in soil profiles at Boundary Plantation (a, 8 cm depths) and Wat Ban Chan (b, 3 cm depths), the dashed line represents unity.

Figure 7-5 Graph of predicted unsupported ^{210}Pb (Bq m^{-2}) overlaid with observed ^{210}Pb (Bq m^{-2}) in soil profiles at Boundary Plantation (a, 8 cm depths) and Wat Ban Chan (b, 3 cm depths).



After fitting to observed ^{210}Pb data, the estimated parameters were then adjusted for ^{137}Cs calculation. The estimated parameters of ^{137}Cs (CsSource1 for recirculated ^{137}Cs and CsSource2 for single deposited ^{137}Cs) are shown in Table 7-1 and the results of ^{137}Cs calculations are shown in Figure 7-6 and Figure 7-7.

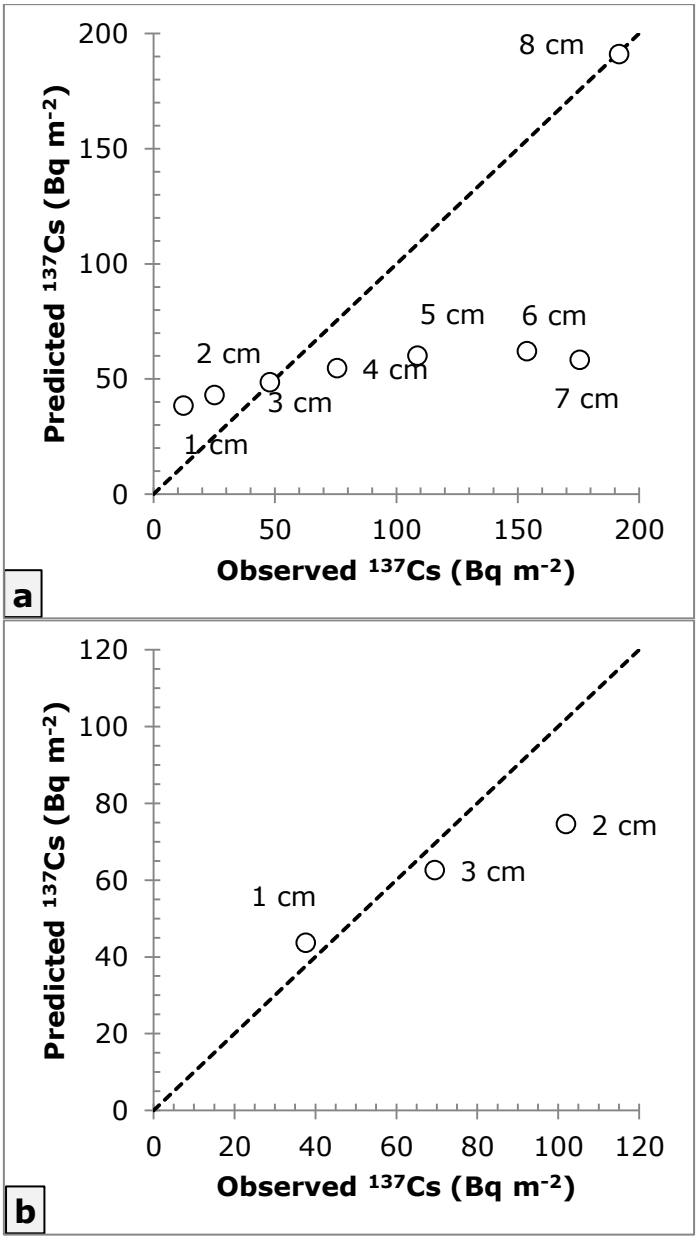
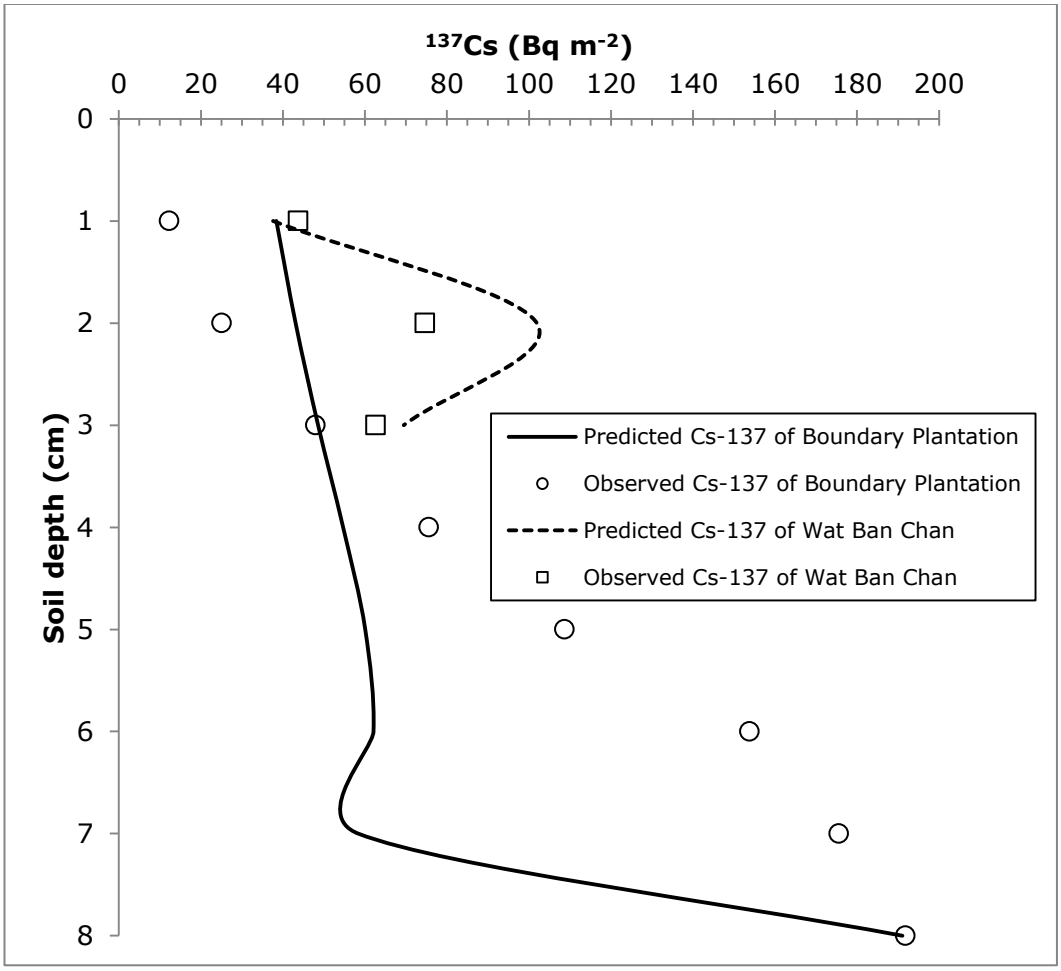


Figure 7-6 Scatter plots between observed and predicted activities of ^{137}Cs in soil profiles at Boundary Plantation (a, 8 cm depths) and Wat Ban Chan (b, 3 cm depths), the dashed line represents unity.

The modelled radiocaesium distributions agree quite poorly with observations. It appears that the recirculated Cs is underestimated. Model calculation of ^{137}Cs activity in the soil at Wat Ban Chan also suggests inconsistent observed data.

Figure 7-7 Graph of predicted ^{137}Cs (Bq m^{-2}) overlaid with observed ^{137}Cs (Bq m^{-2}) in soil profiles at Boundary Plantation (a, 8 cm depths) and Wat Ban Chan (b, 3 cm depths).



The Nash-Sutcliffe model efficiency coefficient (NSE) (Nash and Sutcliffe, 1970) was used to quantify how well the model calculations predicted the outcome variables. The comparison of predicted and observed data for ^{210}Pb and ^{137}Cs at Boundary Plantation and ^{137}Cs at Wat Ban Chan were also analysed by testing whether the slope and intercept of the best fitted line were significantly different from 1 and 0, respectively (t-test). These statistical analyses were carried out using 7 and 3 data points for ^{210}Pb at Boundary Plantation and Wat Ban Chan, and 8 and 3 data points for ^{137}Cs data at Boundary Plantation and Wat Ban Chan, respectively. Results of the statistical analyses are shown in Table 7-2.

Table 7-2 Summary statistics for model calculations of ^{210}Pb and ^{137}Cs at Boundary Plantation (n = 11 and 8 for ^{210}Pb and ^{137}Cs) and Wat Ban Chan (n = 3 for both ^{210}Pb and ^{137}Cs).

Method of statistical analysis	Boundary Plantation		Wat Ban Chan	
	^{210}Pb	^{137}Cs	^{210}Pb	^{137}Cs
Nash-Sutcliffe index (NSE, deviation from grand mean)	0.96720	0.23035	0.99856	0.59967
Slope best line	0.9711	0.4745	0.9636	0.4808
Intercept best line	11.084	22.653	24.591	26.821
P (hypothesis slope NS different to 1.0)	0.6619	0.8595	0.1338	0.1620
P (hypothesis intercept NS different to 0.0)	0.7018	0.3680	0.1316	0.1927

The Nash-Sutcliffe index (NSE) represents the proportion of the observed variation about the mean accounted for by the model, calculated using equation 7.14. NSE can vary between -∞ to 1; the model calculation is perfect if it is 1.

$$NSE = 1 - \frac{\Sigma(Observed - Model)^2}{\Sigma(Observed - Mean)^2} \qquad (7.14)$$

Where NSE is Nash-Sutcliffe index (NSE) calculated based on mean

Observed is observed data

Model is model data

Mean is the mean of the observation data

The Nash index of ^{210}Pb and ^{137}Cs at Boundary Plantation and Wat Ban Chan are close to 1.0 and evaluated to be acceptable (N. Moriasi et al., 2007).

The slope and intercept of the best linear relationship between the model-calculated and observed data ideally are not significantly different to 1 and 0 respectively. This was the case for both sites and isotopes (Table 7-2).

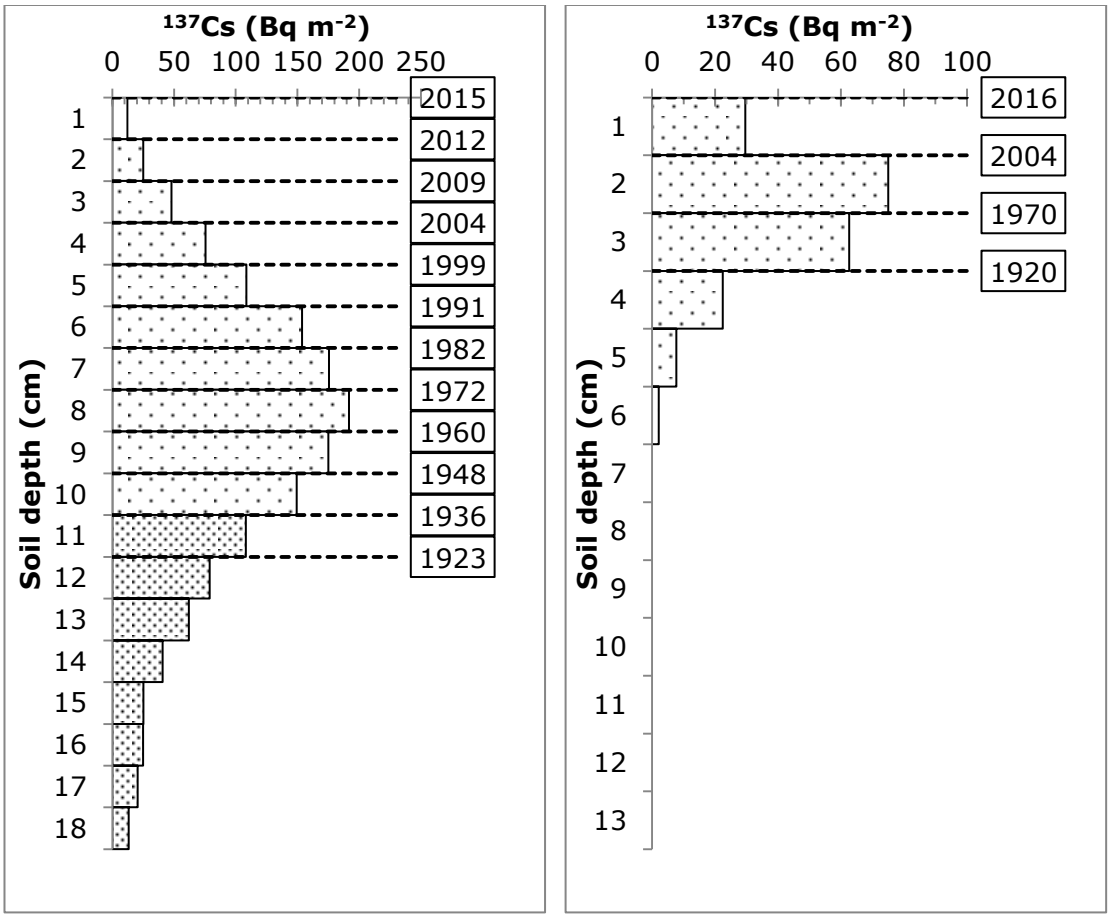
7.6 DISCUSSION

The fitted parameters for both forest sites showed model calculations of unsupported ^{210}Pb that are consistent with the observed data. However, only Boundary Plantation has enough data to make a useful interpretation of the model fits.

Statistical analysis of ^{210}Pb data at Boundary Plantation suggests the accuracy of this model calculation is acceptable. However, the model calculation of ^{137}Cs at Boundary Plantation and Wat Ban Chan are not accurate, particularly within the upper 7 and 2 cm layers at Boundary Plantation and Wat Ban Chan respectively where the activity of ^{137}Cs depends on recirculated ^{137}Cs. This model assumes a constant rate of recirculation of ^{137}Cs whilst the accumulation and loss of ^{137}Cs from tree canopies is actually time dependent (IAEA, 2010).

The hypothesis that organic matter decomposition is the key process controlling the longevity of ^{137}Cs in the forest ecosystem, mentioned in Chapters 3 and 5, was tested in this Chapter. The model calculations of ^{210}Pb in Figure 7-4 and ^{137}Cs in Figure 7-6 suggest that, during 2015 and 2016, fallout ^{137}Cs deposited in 1963 had migrated to 8 and 3 cm at Boundary Plantation and Wat Ban Chan, respectively as conclude in Fig 7-8. This calculation is consistent with the observed data for ^{137}Cs at Boundary Plantation but at Wat Ban Chan the model calculation is about 1 cm below the observed data.

Figure 7-8 Depth profiles of ^{137}Cs deposition inventories (Bq m^{-2}) of soil collected at Boundary Plantation (a, 18 cm, at 2015) and Wat Ban Chan (b, 13 cm, at 2016), the dash lines are the year of model calculation.



7.7 CONCLUSION

A model of annual input of unsupported ^{210}Pb and litterfall with organic matter decomposition in soil is useful to investigate ^{137}Cs migration in soil. Statistical analysis showed that ^{210}Pb calculations provided an accurate prediction of the relationship between soil depth and the year of litter deposition. The accuracy of ^{137}Cs calculations in the layers above fallout ^{137}Cs distribution is not acceptable. However, this deficiency can be addressed using the appropriate recirculation rate of ^{137}Cs which is a time-dependent parameter. Finally, the model suggests that at forest site with thick organic layer as Boundary Plantation fallout ^{137}Cs migrated within the organic depth therefore the rate of 'burial' of the organic matter is the same as the rate of downwards migration of ^{137}Cs, while at site

with no organic layer as Wat Ban Chan ^{137}Cs is migrated into mineral depth therefore its migration is not depend on the rate of 'burial' of the organic matter.

CHAPTER 8: GENERAL CONCLUSIONS

Despite the diversity of characteristics of the forests at Boundary Plantation, Chernobyl and Wat Ban Chan (soil structure, pine species, acute or chronic deposition, temperate or tropical zone) the long-term migration of ^{137}Cs in all three forest ecosystems is dominated by the accumulation of ^{137}Cs within the shallow surface layers of the forest soil.

No indication of clay minerals was found in the forest soils at Boundary Plantation and Wat Ban Chan, so the organic matter content in the soil appears to play an important role in the vertical distribution of ^{137}Cs. At Boundary Plantation, ^{137}Cs accumulated in the middle of the organic layer where organic matter is highly decomposed. At Wat Ban Chan, where the accumulation of organic matter was much less than in a temperate forest, ^{137}Cs was still dominantly distributed in the upper 4 cm of the soil where organic matter content was highest. At Boundary Plantation it was found that the soil organic matter content is associated with an increase in the exchangeability of native ^{133}Cs in the soil.

Using ^{210}Pb to model organic matter accumulation in the soil indicated that, at Boundary Plantation, nuclear weapons fallout ^{137}Cs deposited in 1963 is mainly located within organic matter which was added to the soil surface as litter around 1963. This indicates that ^{137}Cs 'migration' has actually been controlled by the accumulation and decomposition of organic matter on the forest floor. Progressive humification of litter added to the soil surface leads to increasing concentrations of ^{137}Cs in the deeper parts of the soil organic horizon. This could be the most plausible mechanism to explain the slow migration of ^{137}Cs deposited in 1963 to a 'peak activity' depth of only 6 cm in 2015.

Soil pH also appears to play a key role in controlling the mobility of Cs isotopes in organic-rich soil. Within Boundary Plantation's soil, the highest ^{137}Cs activity concentrations are held within the most acidic layers of the soil organic horizons which have the highest exchangeable ^{133}Cs concentrations. However, since the pH range throughout the soil cores sampled at Wat Ban Chan is less than one pH unit, this is unlikely to have influenced the vertical distributions of ^{137}Cs and ^{133}Cs at this site.

As a major nutrient, K (and, to a lesser extent, Rb) is a strong competitor of Cs in the elemental cycle within forest ecosystems. K was found to be present in

the exchangeable fraction in both temperate and tropical forest soils at much higher concentrations than Rb and especially Cs. In Three-needled pine at Wat Ban Chan, wood to needle transfer of ^{133}Cs was slightly higher than for ^{39}K and ^{85}Rb. However, the overall degree of uptake and translocation from soil to needles is in the order of $^{39}K > {}^{85}Rb > {}^{133}Cs$.

The forest site at Kopachi within the Chernobyl Exclusion Zone received ^{137}Cs in a very different form to the global weapons fallout deposited in the British Isles and Thailand. Sites close to the Chernobyl reactor, such as Kopachi, were contaminated with uranium oxide fuel particles which carried very high activities of radionuclides, including ^{137}Cs. The accumulation of ^{137}Cs in the very shallow surface organic matter in the soil at Kopachi may be due mainly to the initial physico-chemical form of the deposit.

Despite the initially less soluble form of ^{137}Cs deposited at Kopachi, transfer factors for ^{137}Cs uptake into trees were higher at Kopachi compared with those for ^{133}Cs at Boundary Plantation and Wat Ban Chan. This confirms that ^{137}Cs at Kopachi is more exchangeable and mobile than ^{133}Cs at Boundary Plantation and Wat Ban Chan and also indicates that equilibration between ^{133}Cs and ^{137}Cs within Kopachi approximately 30 years after initial contamination of ^{137}Cs has not been achieved.

Acute deposition of very high activities of ^{137}Cs and other short-lived radionuclides has affected the growth of Scots pine in the 'Red Forest' and the 'North Trace', both areas where tree death was observed in 1986. Surviving Scots pine trees show a transient decrease in growth rate for several years after 1986, and then show signs of accelerated growth possibly due to a reduction in competition from other surrounding trees. This is an acknowledged phenomenon known as 'growth release' which is observed after catastrophic events such as storms, major pollution episodes such as 'acid rain' or after thinning.

The chronic deposition of ^{137}Cs from global weapons fallout has had no impact on the growth of Corsican pine and Three-needled pine at Boundary Plantation and Wat Ban Chan, respectively. However, the long-term (>50 years) accumulation of ^{137}Cs in the surface organic horizons of the soils at both these sites is much greater than would have been predicted using existing models which have been calibrated with data up to 10 – 15 years after the Chernobyl accident. If it is assumed that trees are not harvested from the forest, the life time of ^{137}Cs in the forest ecosystem is almost solely dependent on its radioactive half-life. This

is why, long-term data are essential to calibrate and validate existing models, and perhaps to improve model structure to improve their longer-term predictive abilities. This is important for the long-term quantification of radiation dose which humans receive from forest ecosystem pathways as well as providing a firmer basis to explore and evaluate any proposed remedial and abatement strategies.

As an example, when calibrated with Chernobyl data up to circa 1996, the RIFE model consistently under- and over-predicted the percentage of the total ^{137}Cs inventory which is retained in the organic and mineral soil layers, respectively, after 50 years. However, the model results for litter, tree internal and needle were surprisingly accurate.

Calibrations of the RIFE model were made using data for nuclear weapons-derived ^{137}Cs deposited in 1963 at Boundary Plantation and Wat Ban Chan, collected 52 and 53 years, respectively, after peak nuclear weapons deposition. Although these calibrations are based on single time points in 2015 and 2016, respectively, they can be expected to be more applicable for long-term predictions than the earlier calibrations, which were based on measurements made approximately 10 years after the Chernobyl accident in 1986. The findings of this study support the use of RIFE as a predictive tool for radiocaesium contamination in temperate coniferous forests, for which the model was originally written and calibrated. With the addition of the calibration data supplied here, the RIFE model could also be applied with some confidence to tropical and sub-tropical evergreen forests.

Reductions in uncertainties of RIFE model calculations can be made by improving calibrations for the rate of radiocaesium migration within the forest soil's organic layers. As observed at the beginning of this chapter, a key observation in this study has been the accumulation of ^{137}Cs over a period of 50 years in the organic matter on the forest floor in both temperate and tropical pine forests. The model of annual inputs of unsupported ^{210}Pb and litterfall in conjunction with organic matter decomposition in soil suggests that the longevity of ^{137}Cs in the forest ecosystem is controlled by decomposition of organic matter even in forests site with such diversity in the net accumulation of soil organic layers as Boundary Plantation and Wat Ban Chan.

FUTURE STUDIES

Fixation of ^{137}Cs by clay minerals in soil is well-studied and it is known that illite plays a major role in immobilisation of Cs in soils. The observation that ^{137}Cs is retained in humified organic soil layers at Boundary Plantation and Wat Ban Chan, with no indication of the presence of clay minerals, suggests the mechanism for this retention should be investigated further.

Aspects of this retention which should be researched are:

- Strength of binding of Cs by organic matter at different stages of humification.
- Possible presence of very small concentrations of clay minerals, eg. as 'dust' deposited from the atmosphere, which may be sufficient to immobilise Cs.
- The role of biological recycling of Cs by macro-, meso- and microorganisms in the forest soil.

Deeper study of the mechanism and rates of organic matter accumulation and decomposition at different forest sites would help to understand the significance of these processes on the migration of ^{137}Cs. Global weapons fallout originating from 1963 is still clearly measurable and could be investigated at a wider range of forest types than this study has been able to address.

Investigation of the activities of ^{210}Pb in the soil profile has been shown in this study to improve our understanding of the migration of ^{137}Cs in forest soil. Additional work using this method would help us to investigate organic matter migration and decomposition and their contribution to the migration of ^{137}Cs in forest soils.

ANNEX 1 COMPARISON OF FINDINGS OF BOUNDARY PLANTATION, KOPACHI AND WAT BAN CHAN

Summary data from Boundary Plantation, Wat Ban Chan and Kopachi are presented in Table A1 below.

Table A1 Summary comparison of findings from Wat Ban Chan, Boundary Plantation and Kopachi.

Subject		Wat Ban Chan	Boundary Plantation	Kopachi
Climate forest zone		tropical	temperate	temperate
Soil type		red-yellow podzolic	Sandy, high organic matter	Sandy, high organic matter
Organic layer (identified based on USDA, 1999; FAO, 1998)		no	0 - 9 cm	0 - 2 cm
Calculated initial deposition of ^{137}Cs		643 Bq m^{-2} at 1963	4,800 Bq m^{-2} at 1963	3.28 MBq m^{-2} at 1986
Vertical migration rate of ^{137}Cs		0.38 cm/y	1.54 cm/y	0.07 cm/y
Total ^{133}Cs (mg kg^{-1})	Max	4.45	0.61	-
	Min	2.89	0.16	-
	Average	3.60	0.49	-
Total ^{39}K (mg kg^{-1})	Max	385	866	-
	Min	209	237	-
	Average	255	344	-
Total ^{85}Rb (mg kg^{-1})	Max	15.8	7.37	-
	Min	12.9	2.24	-
	Average	14.4	5.04	-
Exchangeable ^{133}Cs (mg kg^{-1})	Max	0.25	0.06	-
	Min	0.19	0.02	-
	Average	0.21	0.04	-
Exchangeable ^{39}K (mg kg^{-1})	Max	331	609	-
	Min	90.4	36.4	-
	Average	144	171	-
Exchangeable ^{85}Rb (mg kg^{-1})	Max	4.09	0.97	-
	Min	2.03	0.50	-
	Average	2.58	0.60	-

Table A1 (continued)

Subject		Wat Ban Chan	Boundary Plantation	Kopachi
Exchangeability of ^{133}Cs	Max	0.06	0.14	-
	Min	0.05	0.04	-
	Average	0.06	0.09	-
Exchangeability of ^{39}K	Max	0.86	0.74	-
	Min	0.36	0.14	-
	Average	0.54	0.39	-
Exchangeability of ^{85}Rb	Max	0.26	0.49	-
	Min	0.13	0.07	-
	Average	0.18	0.18	-
Isotopic exchangeability (E-value) of ^{134}Cs (mg kg^{-1}) 1 hour shaking	1 cm	0.222	0.025	-
	3 cm	0.210	0.065	-
	5 cm	0.243	0.107	-
	7 cm	0.233	0.115	-
	9 cm	0.170	0.076	-
	11 cm	0.220	0.057	-
	13 cm	0.316	0.052	-
	15 cm	-	0.054	-
	17 cm	-	0.030	-
Isotopic exchangeability (E-value) of ^{134}Cs (mg kg^{-1}) 1 day shaking	1 cm	0.309	0.027	-
	3 cm	0.287	0.074	-
	5 cm	0.304	0.136	-
	7 cm	0.329	0.142	-
	9 cm	0.262	0.089	-
	11 cm	0.327	0.067	-
	13 cm	0.422	0.062	-
	15 cm	-	0.067	-
	17 cm	-	0.044	-
Isotopic exchangeability (E-value) of ^{134}Cs (mg kg^{-1}) 1 week shaking	1 cm	0.383	0.021	-
	3 cm	0.356	0.079	-
	5 cm	0.403	0.140	-
	7 cm	0.390	0.156	-
	9 cm	0.354	0.099	-
	11 cm	0.401	0.081	-
	13 cm	0.508	0.079	-
	15 cm	-	0.086	-
	17 cm	-	0.055	-
^{133}Cs wood (mg kg^{-1})		$5.43*10^{-3}$	$1.16*10^{-3}$	$2 – 10*10^{2}$ (^{137}Cs, Bq/kg)
^{39}K wood (mg kg^{-1})		356 mg/kg	261 mg/kg	-
^{85}Rb wood (mg kg^{-1})		1.44 mg/kg	$3.14*10^{-1}$ mg/kg	-
^{133}Cs fresh needle (mg kg^{-1})		$2.42*10^{-2}$ mg/kg	$1.20*10^{-2}$ mg/kg	$2.21*10^{4}$ (^{137}Cs, Bq/kg)
^{39}K fresh needle(mg kg^{-1})		756 mg/kg	7620 mg/kg	-

Table A1 (continued)

Subject		Wat Ban Chan	Boundary Plantation	Kopachi
^{85}Rb fresh needle (mg kg^{-1})		4.00 mg/kg	8.12 mg/kg	-
^{133}Cs dry needle (mg kg^{-1})		-	1.18*10^{-2} mg/kg	-
^{39}K dry needle (mg kg^{-1})		-	1060 mg/kg	-
^{85}Rb dry needle (mg kg^{-1})		-	1.13 mg/kg	-
^{133}Cs bark (mg kg^{-1})		3.01*10^{-2} mg/kg	5.00*10^{-3} mg/kg	-
^{39}K bark (mg kg^{-1})		513 mg/kg	700 mg/kg	-
^{85}Rb bark (mg kg^{-1})		4.55 mg/kg	1.25 mg/kg	-
^{133}Cs rainwater (mg kg^{-1})		-	3.00*10^{-5} mg/kg	-
^{39}K rainwater (mg kg^{-1})		-	5.21 mg/kg	-
^{85}Rb rainwater (mg kg^{-1})		-	5.94*10^{-3} mg/kg	-
Concentration ratio of ^{133}Cs (CR)	Wood	1.48 x 10^{-3},	2.24 x 10^{-3}	
	needle	6.59 x 10^{-3}	2.32 x 10^{-2}	
Concentration ratio of ^{39}K (CR)	Wood	1.41	7.47*10^{-1}	
	needle	6.02	21.8	-
Concentration ratio of ^{85}Rb (CR)	Wood	1.00 x 10^{-1}	8.03 x 10^{-2}	
	needle	2.79 x 10^{-1}	2.08	-
Aggregated transfer factor of ^{133}Cs (T_{ag})	Wood	7.94 x 10^{-6}	1.34 x 10^{-5}	1.74 x 10^{-3} (^{137}Cs)
	needle	3.54 x 10^{-5}	1.39 x 10^{-4}	1.31 x 10^{-2} - (^{137}Cs)
Aggregated transfer factor of ^{39}K (T_{ag})	Wood	7.43 x 10^{-3}	6.42 x 10^{-3}	
	needle	3.16 x 10^{-2}	1.87 x 10^{-1}	-
Aggregated transfer factor of ^{85}Rb (T_{ag})	Wood	5.31*10^{-4}	3.37 x 10^{-4}	
	needle	1.48 x 10^{-3}	8.72 x 10^{-3}	-
Concentration ratio ^{39}K/^{133}Cs in organic soil		74.8	473	-
Concentration ratio ^{39}K/^{133}Cs in wood		9.27 x 10^{4}	2.25 x 10^{5}	-
Concentration ratio ^{39}K/^{133}Cs in bark		5.33 x 10^{4}	1.39 x 10^{5}	-
Concentration ratio ^{39}K/^{133}Cs in fresh needle		6.80 x 10^{4}	9.51 x 10^{5}	-
Concentration ratio ^{39}K/^{133}Cs in dry needle		-	1.04 x 10^{5}	-
Concentration ratio ^{39}K/^{133}Cs in rainwater		-	1.84 x 10^{5}	-

Table A1 (continued)

Subject	Wat Ban Chan	Boundary Plantation	Kopachi
Concentration ratio $^{39}K/^{133}Cs$ in litter	-	1.00×10^4	-
Concentration ratio $^{85}Rb/^{133}Cs$ in organic soil	4.15	10.8	-
Concentration ratio $^{85}Rb/^{133}Cs$ in wood	451	270.81	-
Concentration ratio $^{85}Rb/^{133}Cs$ in bark	195	249	-
Concentration ratio $^{85}Rb/^{133}Cs$ in fresh needle	173	914	-
Concentration ratio $^{85}Rb/^{133}Cs$ in dry needle	-	98.7	-
Concentration ratio $^{85}Rb/^{133}Cs$ in rainwater	-	209	-
Concentration ratio $^{85}Rb/^{133}Cs$ in litter	-	19.8	-
Concentration ratio $^{85}Rb/^{133}Cs$ in litter	-	19.8	-
Concentration ratio $^{39}K/^{85}Rb$ in organic soil	17.9	43.8	-
Concentration ratio $^{39}K/^{85}Rb$ in wood	305	832	-
Concentration ratio $^{39}K/^{85}Rb$ in bark	241	559	-
Concentration ratio $^{39}K/^{85}Rb$ in fresh needle	382	1060	-
Concentration ratio $^{39}K/^{85}Rb$ in dry needle	-	1070	-
Concentration ratio $^{39}K/^{85}Rb$ in rainwater	-	853	-
Concentration ratio $^{39}K/^{85}Rb$ in litter	-	448	-
Translocation factor of ^{133}Cs wood to needle (f_{tr})	4.45	10.4	-
Translocation factor of ^{39}K wood to needle (f_{tr})	4.25	29.2	-
Translocation factor of ^{85}Rb wood to needle (f_{tr})	2.78	25.9	-

ANNEX 2 MODEL SCRIPT OF ^{137}Cs MIGRATION IN FOREST SOILS

```
AnnualDeltaZ(t) = litterRate
for j=1,Nlayer
  if t>=j
    AnnualDeltaZ(j) = litterRate*(a + b*exp(c*(t-j)) + d*exp(e*(t-j)))
    if j>1
      Zlower(j) = Zupper(j-1)
    else
      Zlower(j) = 0
    endif
    Zupper(j) = Zlower(j) + AnnualDeltaZ(j)
    MaxDepth = Zupper(j)
  endif
endfor

  AnnualActivity(2,t) = PbSource
  AnnualActivity(1,t) = CsSource1 //add recirculated Cs

if t=Cst
  AnnualActivity(1,t) = CsSource2
endif

for j=1,Nlayer
```

```
  AnnualActivity(1,j).rate = -(1-CsRate)*AnnualActivity(1,j)
  AnnualActivity(2,j).rate = -(1-PbRate)*AnnualActivity(2,j)
endfor

for j=1,Nsoillayer
  for i=1,2
    SoilActivity(i,j) = 0
  endfor
endfor

for j=1,NSoilLayer
  z1 = (j-1)*SoilDeltaZ
  z2 = z1 + SoilDeltaZ

  for k=1,Nlayer
    if (Zlower(k)>=z1) and (Zlower(k)<=z2) and (Zupper(k)>=z1) and
(Zupper(k)<=z2)
      f = 1
    elseif (Zlower(k)>=z1) and (Zlower(k)<=z2)
      f = (z2 - Zlower(k))/(Zupper(k) - Zlower(k))
    elseif (Zupper(k)>=z1) and (Zupper(k)<=z2)
      f = (Zupper(k) - z1)/(Zupper(k) - Zlower(k))
    else
      f = 0
    endif
```

```
    for i=1,2
      SoilActivity(i,j) =  SoilActivity(i,j) + f*AnnualActivity(i,k)
    endfor
  endfor
endfor

for j=1,Nprofile // initialise to zero
  for i=1,2
    SoilProfile(i,j) = 0
  endfor
endfor

for j=1,NProfile
  h2 = (j-1)*SoilDeltaZ
  h1 = h2 + SoilDeltaZ

  for k=1,Nlayer
    hlower = MaxDepth - Zlower(k)
    hupper = MaxDepth - Zupper(k)
    if (hlower>=h2) and (hlower<=h1) and (hupper>=h2) and (hupper<=h1)
      f = 1
    elseif (hlower>=h2) and (hlower<=h1)
      f = (hlower - h2)/(hlower - hupper)
    elseif (hupper>=h2) and (hupper<=h1)
      f = (h1 - hupper)/(hlower - hupper)
    else
```

```
      f = 0
    endif


    for i=1,2
      SoilProfile(i,j) =  SoilProfile(i,j) + f*AnnualActivity(i,k)
    endfor
  endfor
endfor
for i = 1,NProfile
PbProfile(i) = SoilProfile(2,i)
CsProfile(i) = SoilProfile(1,i)
endfor
```

REFERENCES

ABSALOM, J. P., YOUNG, S. D., CROUT, N. M. J., SANCHEZ, A., WRIGHT, S. M., SMOLDERS, E., NISBET, A. F. & GILLETT, A. G. 2001. Predicting the transfer of radiocaesium from organic soils to plants using soil characteristics. *Journal of Environmental Radioactivity,* 52**,** 31-43.

AHMED, I. A. M.,YOUNG, S. D. and CROUT, N. M. J. (2006). Time-dependent sorption of Cd2+ on CaX zeolite: Experimental observations and model predictions. Geochimica et Cosmochimica Acta 70 (19): 4850-4861.

AMBROSE, K, HOUGH, E, SMITH, N J P and WARRINGTON, G. 2014. Lithostratigraphy of the Sherwood Sandstone Group of England, Wales and south-west Scotland. British Geological Survey Research Report, RR/14/01.

APPLEBY, P. G. & OLDFIELD, F. 1978. The calculation of lead-210 dates assuming a constant rate of supply of unsupported ^{210}Pb to the sediment. *CATENA,* 5**,** 1-8.

BASKARAN, M., NIX, J., KUYPER, C. & KARUNAKARA, N. 2014. Problems with the dating of sediment core using excess ^{210}Pb in a freshwater system impacted by large scale watershed changes. *Journal of Environmental Radioactivity,* 138**,** 355-363.

BELLI, M. 2000. *Long term dynamics of radionuclides in semi-natural environments — Derivation of parameters and modelling,* Rome, Agenzia Nazionale per la Protezione dell'Ambiente.

BOULYGA, S. F., ZORIY, M., KETTERER, M. E. & SABINE BECKER, J. 2003. Depth profiling of Pu, ^{241}Am and ^{137}Cs in soils from southern Belarus measured by ICP-MS and [small alpha] and [gamma] spectrometry. *Journal of Environmental Monitoring,* 5**,** 661-666.

BUNZL, K. & KRACKE, W. 1988. Cumulative deposition of ^{137}Cs, ^{238}Pu, $^{239+240}$Pu and ^{241}Am from global fallout in soils from forest, grassland and arable land in Bavaria (FRG). *Journal of Environmental Radioactivity,* 8**,** 1-14.

CAMBRAY, R. S. P., K.; LEWIS, G.N.J.; CARPENTER, R.C.; 1989. Radioactive fallout in air and rain: results to the end of 1987. United Kingdom: UKAEA Harwell Lab. (UK). Environmental and Medical Science Division.

CAWSE, P. A. & HORRILL, A. D. 1986. A survey of caesium-137 and plutonium in British soils in 1977. United Kingdom: United Kingdom Atomic Energy Authority

CHESSER, R. K., BONDARKOV, M., BAKER, R. J., WICKLIFFE, J. K. & RODGERS, B. E. 2004. Reconstruction of radioactive plume characteristics along Chernobyl's Western Trace. *Journal of Environmental Radioactivity,* 71**,** 147-157.

COMANS, R. N. J., HILTON, J., VOITSEKHOVITCH, O., LAPTEV, G., POPOV, V., MADRUGA, M. J., BULGAKOV, A., SMITH, J. T., MOVCHAN, N. & KONOPLEV, A. 1998. A comparative study of radiocesium mobility measurements in soils and sediments from the catchment of a small

upland oligotrophic lake (Devoke Water, U.K.)1. *Water Research,* 32**,** 2846-2855.

COOK, L. L., INOUYE, R. S., MCGONIGLE, T. P. & WHITE, G. J. 2007. The distribution of stable cesium in soils and plants of the eastern Snake River Plain in southern Idaho. *Journal of Arid Environments,* 69**,** 40-64.

CREMERS A, ELSEN A, PRETER PD, MAES A (1988). Quantitative analysis of radiocaesium retention in soils. Nature 335: 247.

ENDO, I., OHTE, N., ISEDA, K., TANOI, K., HIROSE, A., KOBAYASHI, N. I., MURAKAMI, M., TOKUCHI, N. & OHASHI, M. 2015. Estimation of radioactive 137-cesium transportation by litterfall, stemflow and throughfall in the forests of Fukushima. *Journal of Environmental Radioactivity,* 149**,** 176-185.

ESLAVA-GOMES, A. & BROWN, J. 2013. Determination of root uptake to vegetables grown in soil contaminated for twenty-five years. Health Protection Agency.

FAO. 1998. *World reference base for soil resources* [Online]. Rome Food and Agriculture Organisation of United Nations,. Available: http://www.fao.org/docrep/W8594E/w8594e0b.htm#organic%20soil%20material 2017].

FOREGS (2005) Geochemical atlas of Europe. http://weppi.gtk.fi/publ/foregsatlas/

GIANNAKOPOULOU, F., HAIDOUTI, C., CHRONOPOULOU, A. & GASPARATOS, D. 2007. Sorption behavior of cesium on various soils under different pH levels. *Journal of Hazardous Materials,* 149**,** 553-556.

GUILLEN J, BAEZA A, SALAS A, MUNOZ-MUNOZ JG, MUNOZ-SERRANO A (2017). Factors Influencing the Soil to Plant Transfer of Radiocaesium. In: Gupta DK, Walther C (ed)^(eds). *Impact of Cesium on Plants and the Environment*, edn. Cham: Springer International Publishing. p^pp 19-33.

HAMILTON, G. J. 1996. Forestry Commission Booklet 39 Forest Mensuration. London: HMSO.

HAMON, R.E., PARKER, D.R., LOMBI, E., 2008. Chapter 6 Advances in Isotopic Dilution Techniques in Trace Element Research: A Review of Methodologies, Benefits, and Limitations, in: Agronomy, B.-A. in (Ed.), Academic Press, pp. 289–343.

HARB, S., SALAHEL DIN, K. & ABBADY, A. 2009. Study of Efficiency Calibrations of HPGe Detectors for Radioactivity Measurements of Environmental Samples. *Third Environmental Physics Conference (EPC-2008).* Egypt.

HASHIMOTO S, UGAWA S, NANKO K, SHICHI K (2012). The total amounts of radioactively contaminated materials in forests in Fukushima, Japan. *Scientific reports* **2:** 416.

HASHIMOTO, S., MATSUURA, T., NANKO, K., LINKOV, I., SHAW, G. & KANEKO, S. 2013. Predicted spatio-temporal dynamics of radiocesium deposited onto forests following the Fukushima nuclear accident. *Sci Rep,* 3**,** 2564.

HUS, M., KOŠUTIĆ, K. & LULIĆ, S. 2001. Radioactive contamination of wood and its products. *Journal of Environmental Radioactivity,* 55**,** 179-186.

IAEA. 1996. The atlas of cesium-137 contamination of Europe after the Chernobyl accident. The radiological consequences of the Chernobyl accident, 18-22 Mar 1996 1996 Minsk (Belarus). IAEA, 1192.

IAEA 2002. *Modelling the migration and accumulation of radionuclides in forest ecosystems,* Vienna, International Atomic Energy Agency.

IAEA 2003. *Assessing Radiation Doses to the Public from Radionuclides in Timber And Wood Products*, International Atomic Energy Agency.

IAEA 2006. *Environmental Consequences of the Chernobyl Accident and their Remediation: Twenty Years of Experience,* Vienna, INTERNATIONAL ATOMIC ENERGY AGENCY.

IAEA 2010. *Handbook of Parameter Values for the Prediction of Radionuclide Transfer in Terrestrial and Freshwater Environments,* Vienna, INTERNATIONAL ATOMIC ENERGY AGENCY.

IAEA (2013). The International Nuclear and Radioecology Event Scale: Incident and Emergency Center.

IAEA (2015). *The Fukushima Daiichi Accident*. edn. INTERNATIONAL ATOMIC ENERGY AGENCY: Vienna.

ISRAELACHVILI, J. N. 2011. 7 - Repulsive Steric Forces, Total Intermolecular Pair Potentials, and Liquid Structure. *Intermolecular and Surface Forces (Third Edition).* San Diego: Academic Press.

KARADENIZ, Ö. & YAPRAK, G. 2007. Dynamic equilibrium of radiocesium with stable cesium within the soil–mushroom system in Turkish pine forest. *Environmental Pollution,* 148**,** 316-324.

KARAVAEVA, Y. N., KULIKOV, N. V., MOLCHANOVA, I. V., POZOLOTINA, V. N. & YUSHKOV, P. I. 1994. Accumulation and distribution of long-living radionuclides in the forest ecosystems of the Kyshtym accident zone. *Science of The Total Environment,* 157**,** 147-151.

KASTE, J. M., BOSTICK, B. C., HEIMSATH, A. M., STEINNES, E. & FRIEDLAND, A. J. 2011. Using atmospheric fallout to date organic horizon layers and quantify metal dynamics during decomposition. Geochimica et Cosmochimica Acta, 75, 1642-1661.

KIDD PS, Proctor J (2001). Why plants grow poorly on very acid soils: are ecologists missing the obvious? *Journal of Experimental Botany* **52**(357)**:** 791-799.

KIRCHNER, G., STREBL, F., BOSSEW, P., EHLKEN, S. & GERZABEK, M. H. 2009. Vertical migration of radionuclides in undisturbed grassland soils. *Journal of Environmental Radioactivity,* 100**,** 716-720.

KONOPLEVA, I., KLEMT, E., KONOPLEV, A. & ZIBOLD, G. 2009. Migration and bioavailability of ^{137}Cs in forest soil of southern Germany. *Journal of Environmental Radioactivity,* 100**,** 315-321.

KRSTIC, D., DJALOVIC, I., NIKEZIC, D., and BJELIC, D. (2012). Aluminium in Acid Soils: Chemistry, Toxicity and Impact on Maize Plants, Food Production - Approaches, Challenges and Tasks, Prof. Anna Aladjadjiyan (Ed.), InTech, DOI: 10.5772/33077. Available from: https://www.intechopen.com/books/food-production-approaches-challenges-and-tasks/aluminium-in-acid-soils-chemistry-toxicity-and-impact-on-maize-plants

LOFFREDO, N., ONDA, Y., HURTEVENT, P. & COPPIN, F. 2015. Equation to predict the ^{137}Cs leaching dynamic from evergreen canopies after a radio-cesium deposit. *Journal of Environmental Radioactivity,* 147**,** 100-107.

MACKENZIE, A. B., HARDIE, S. M. L., FARMER, J. G., EADES, L. J. & PULFORD, I. D. 2011. Analytical and sampling constraints in ^{210}Pb dating. *Science of The Total Environment,* 409**,** 1298-1304.

MADRUGA MJ, CREMERS A, BULGAKOV A, ZHIRNOV V, BOBOVNIKOVA T, LAPTEV G, et al. (1996). Radiocesium sorption-desorption behavior in soils and sediments. In: The radiological consequences of the Chernobyl accident, p 1192. Luxembourg.

METZGER, R. L., VAN RIPER, K. & POUQUETTE, P. 2016. A Monte Carlo approach to food density corrections in gamma spectroscopy. *Journal of Radioanalytical and Nuclear Chemistry,* 307**,** 1595-1598.

Midwood, Andrew J. (2007) Stable Isotope Methods for Estimating the Labile Metal Content of Soils. Pp. 149-159, in Willey, N. (Ed.) Phytoremediation - Methods and Reviews. Springer.

MORIASI, D., ARNOLD, J., VAN LIEW, M., BINGNER, R., HARMEL, R. & VEITH, T. 2007. Model Evaluation Guidelines for Systematic Quantification of Accuracy in Watershed Simulations. *Transactions of the ASABE,* 50**,** 885.

NASH, J. E. & SUTCLIFFE, J. V. 1970. River flow forecasting through conceptual models part I — A discussion of principles. *Journal of Hydrology,* 10**,** 282-290.

NONGNUANG, S. 2012. Biomass Carbon Stocks of Trees in Pine Plantations at Boa Kaew Watershed Management Station, Chiang Mai Provience. *Thai Journal of Forestry,* 31**,** 1-15.

PAYNE, T. E. & EDIS, R. 2012. Chapter 3 - Mobility of Radionuclides in Tropical Soils and Groundwater. *In:* JOHN, R. T. (ed.) *Radioactivity in the Environment.* Elsevier.

PRÖHL, G., TWINING, J. R. & CRAWFORD, J. 2012. Chapter 7 - Radiological Consequences Modelling. *In:* JOHN, R. T. (ed.) *Radioactivity in the Environment.* Elsevier.

PUMPANEN, J., OHASHI, M., ENDO, I., HARI, P., BÄCK, J., KULMALA, M. & OHTE, N. 2016. ^{137}Cs distributions in soil and trees in forest ecosystems after the radioactive fallout – Comparison study between southern Finland and Fukushima, Japan. *Journal of Environmental Radioactivity,* 161**,** 73-81.

PUTYRSKAYA, V., KLEMT, E., RÖLLIN, S., ASTNER, M. & SAHLI, H. 2015. Dating of sediments from four Swiss prealpine lakes with ^{210}Pb determined by gamma-spectrometry: progress and problems. *Journal of Environmental Radioactivity,* 145**,** 78-94.

Rawlins, B G, McGrath, S P, Scheib, A J, Breward, N, Cave, M, Lister, T R, Ingham, M, Gowing, C and Carter, S. 2012. The advanced soil geochemical atlas of England and Wales. British Geological Survey, Keyworth. www.bgs.ac.uk/gbase/advsoilatlasEW.html

ROWELL, D. L. 1994. *Soil science : methods and applications / David L. Rowell,* Harlow, Essex : New York, Longman Scientific & Technical ; Wiley.

RÜHM, W., YOSHIDA, S., MURAMATSU, Y., STEINER, M. & WIRTH, E. 1999. Distribution patterns for stable ^{133}Cs and their implications with respect to

the long-term fate of radioactive ^{134}Cs and ^{137}Cs in a semi-natural ecosystem. *Journal of Environmental Radioactivity,* 45**,** 253-270.

SAWAI, H., RAHMAN, I. M. M., LU, C., TSUKAGOSHI, Y., BEGUM, Z. A., MAKI, T. & HASEGAWA, H. 2015. Temporal variations of accumulated cesium in natural soils after an uncharacteristic external exposure. *Microchemical Journal,* 118**,** 158-165.

SHAW, G. 2007. Radionuclides in forest ecosystems. *In:* SHAW, G. (ed.) *Radioactivity in the Terrestrial Environment.* Elsevier.

SHAW, G. & BELL, J. N. B. 1991. Competitive effects of potassium and ammonium on caesium uptake kinetics in wheat. *Journal of Environmental Radioactivity,* 13**,** 283-296.

SHAW, G. & BELLI, M. 1999. The RIFE Models of Radionuclide Fluxes in European Forests. *In:* LINKOV, I. & SCHELL, W. (eds.) *Contaminated Forests.* Springer Netherlands.

SHAW, G., VENTER, A., AVILA, R., BERGMAN, R., BULGAKOV, A., CALMON, P., FESENKO, S., FRISSEL, M., GOOR, F., KONOPLEV, A., LINKOV, I., MAMIKHIN, S., MOBERG, L., ORLOV, A., RANTAVAARA, A., SPIRIDONOV, S. & THIRY, Y. 2005. Radionuclide migration in forest ecosystems – results of a model validation study. *Journal of Environmental Radioactivity,* 84**,** 285-296.

SHCHEGLOV, A. I., TSVETNOVA, O. B. & KLIÄSHTORIN, A. L. 2001. *Biogeochemical migration of technogenic radionuclides in forest ecosystems: by the materials of a multiyear study in the areas severely contaminated due to the Chernobyl accident*, Nauka.

SMITH, J., BERESFORD, N.A. 2005. Chernobyl: Catatrophe and Consequences. Chichester, UK: Springer Praxis publishers.

SNYDER, D. C., DELMORE, J. E., TRANTER, T., MANN, N. R., ABBOTT, M. L. & OLSON, J. E. 2012. Radioactive cesium isotope ratios as a tool for determining dispersal and re-dispersal mechanisms downwind from the Nevada Nuclear Security Site. *Journal of Environmental Radioactivity,* 110**,** 46-52.

SÖDERLUND, M., HAKANEN, M. & LEHTO, J. 2016. Sorption of cesium on boreal forest soil I: the effect of grain size, organic matter and mineralogy. *Journal of Radioanalytical and Nuclear Chemistry,* 309**,** 637-645.

SPARKS, D. L. 2001. Dynamics of K in Soils and Their Role in Management of K Nutrition. *In:* INSTITUTE, I. P. (ed.) *Nutrient management for sustainable crop production in India.* New Delhi, India.

TAGAMI, K., TWINING, J. R. & WASSERMAN, M. A. V. 2012. Chapter 5 - Terrestrial Radioecology in Tropical Systems. *In:* JOHN, R. T. (ed.) *Radioactivity in the Environment.* Elsevier.

TATE RLI (1997). Clay, Controlling the Environment. *Soil Science* **162**(7)**:** 528-529.

THAMMAVECH, T., VEERAPASPONG, T. 2007. Soil-to-Plant transfer of Radiocaesium in Thailand. *Kaetsart J. (Nat. Sci.),* 41**,** 8.

THE NORWEGIAN RADIATION PROTECTION AUTHORITY 2007. The Kyshtym accident, 29th September 1957. *NRPA Bulletin,* 8.07.

UCHIDA, S. & TAGAMI, K. 2007a. Soil-to-plant transfer factors of fallout ^{137}Cs and native ^{133}Cs in various crops collected in Japan. *Journal of Radioanalytical and Nuclear Chemistry,* 273**,** 205-210.

UCHIDA, S. & TAGAMI, K. 2007b. Soil-to-plant transfer factors of naturally occurring radionuclides and stable elements for long-term dose assessment. *Waste Management Conference & Exhibition.* Tucson, Arizona USA.

UKSO. 2006. *Forest Research BioSoil data* [Online]. Forest research. Available: http://www.ukso.org/forestbiosoil/home.html 2017].

UNSCEAR (1969) Report of the United Nations Scientific Committee on the Effects of Atomic Radiation, general assembly official records: twenty-fourth session, supplement no. 13 (A/7613). United Nations, New York.

UNSCEAR 2000. Sources and Effects of Ionising Radiation *Report to General Assembly with Scientific Annexes.* New York: UNSCEAR 2000.

USDA 1977. Soil Taxonomy, A Basic System of Soil Classification for Making and Interpreting Soil Surveys. *Soil Science,* 123**,** 270.

USDA. 1998. *Soil Quality Information Sheet* [Online]. USDA Natural Resources Conservation Service. Available: https://www.nrcs.usda.gov/Internet/FSE_DOCUMENTS/nrcs142p2_052208.pdf 2017].

USDA. 1999. *Agriculture Handbook* [Online]. Washington, DC: United States Department of Agriculture, Natural Resources Conservation Service, U.S. Government Printing Office. Available: http://www.nrcs.usda.gov/Internet/FSE_DOCUMENTS/nrcs142p2_051232.pdf [Accessed 30 June 2014].

VAN BERGEIJK, K. E., NOORDIJK, H., LEMBRECHTS, J. & FRISSEL, M. J. 1992. Influence of pH, soil type and soil organic matter content on soil-to-plant transfer of radiocesium and -strontium as analyzed by a nonparametric method. *Journal of Environmental Radioactivity,* 15**,** 265-276.

VANDEBROEK L, VAN HEES M, DELVAUX B, SPAARGAREN O, THIRY Y (2012). Relevance of Radiocaesium Interception Potential (RIP) on a worldwide scale to assess soil vulnerability to 137Cs contamination. Journal of Environmental Radioactivity 104(Supplement C): 87-93.

VARSKOG, P., NÆUMANN, R. & STEINNES, E. 1994. Mobility and plant availability of radioactive Cs in natural soil in relation to stable Cs, other alkali elements and soil fertility. *Journal of Environmental Radioactivity,* 22**,** 43-53.

WYTTENBACH, A., BAJO, S., BUCHER, J., FURRER, V., SCHLEPPI, P. & TOBLER, L. 1995. The concentrations of K, Rb and Cs in spruce needles (Picea abies Karst.) and in the associated soils. *Zeitschrift für Pflanzenernährung und Bodenkunde,* 158**,** 499-504.

YOSHIDA, S., MURAMATSU, Y., DVORNIK, A. M., ZHUCHENKO, T. A. & LINKOV, I. 2004. Equilibrium of radiocesium with stable cesium within the biological cycle of contaminated forest ecosystems. *Journal of Environmental Radioactivity,* 75**,** 301-313.

YOSHIDA, S., MURAMATSU, Y., STEINER, M., BELLI, M., PASQUALE, A., RAFFERTY, B., RÜHM, W., RANTAVAARA, A., LINKOV, I., DVORNIK, A. & ZHUCHENKO, T. 2002. Stable elements - as a key to predict radionuclide transport in forest ecosystems. *Radioprotection,* 37**,** C1-391 - C1-396.

YOSHINAGA, N., KATO, Y. & NAKAI, M. 1989. Mineralogy of red- and yellow-colored soils from Thailand. *Soil Science and Plant Nutrition,* 35**,** 181-205.